

Springer Protocols


Methods in Molecular Biology 505

# The Nuclear Receptor Superfamily

Methods and Protocols

Edited by

Iain J. McEwan

 Humana Press

# METHODS IN MOLECULAR BIOLOGY™

*Series Editor*  
**John M. Walker**  
School of Life Sciences  
University of Hertfordshire  
Hatfield, Hertfordshire, AL10 9AB, UK

For other titles published in this series, go to  
[www.springer.com/series/7651](http://www.springer.com/series/7651)

**METHODS IN MOLECULAR BIOLOGY™**

# **The Nuclear Receptor Superfamily**

**Methods and Protocols**

Edited by

**Iain J. McEwan**

*University of Aberdeen, Aberdeen, UK*

 **Humana Press**

*Editor*

Iain J. McEwan  
School of Medical Sciences  
University of Aberdeen  
Aberdeen, Scotland  
UK

ISSN 1064-3745

ISBN: 978-1-60327-574-3

DOI: 10.1007/978-1-60327-575-0

e-ISSN: 1940-6029

e-ISBN: 978-1-60327-575-0

Library of Congress Control Number: 2008932576

© Humana Press, a part of Springer Science+Business Media, LLC 2009

All rights reserved. This work may not be translated or copied in whole or in part without the written permission of the publisher (Humana Press, c/o Springer Science + Business Media, LLC, 233 Spring Street, New York, NY 10013, USA), except for brief excerpts in connection with reviews or scholarly analysis. Use in connection with any form of information storage and retrieval, electronic adaptation, computer software, or by similar or dissimilar methodology now known or hereafter developed is forbidden.

The use in this publication of trade names, trademarks, service marks, and similar terms, even if they are not identified as such, is not to be taken as an expression of opinion as to whether or not they are subject to proprietary rights.

*Cover illustration:* Figure 1, Chapter 15, “Methods for Identifying and Studying Genetic Alterations in Hormone-Dependent Cancers,” Outi R. Saramäk, Kati K. Waltering, and Tapio Visakorpi

Printed on acid-free paper

springer.com

---

## Preface

It is just over 20 years since the first steroid receptor cDNAs were cloned, a development that led to the concept of a superfamily of ligand-activated transcription factors: The nuclear receptors. Nuclear receptors share a common architecture at the protein level, but a remarkable diversity is observed in terms of natural ligands and xenobiotics that bind to and regulate receptor function. Natural ligands for nuclear receptors are generally lipophilic in nature and include steroid hormones, bile acids, fatty acids, thyroid hormones, certain vitamins, and prostaglandins. A significant proportion of the family members have been described as *orphans*, as the natural ligand, if it exists, remains to be identified. Nuclear receptors act principally to directly control patterns of gene expression and play vital roles during development and in the regulation of metabolic and reproductive functions in the adult organism. Since the original cloning experiments, considerable progress has been made in our understanding of the structure, mechanisms of action, and biology of this important family of proteins. The aims of this volume of *Methods in Molecular Biology* are to describe a range of molecular, structural, and cell biological protocols currently used to investigate the structure–function of nuclear receptors, together with experimental approaches that may lead to new therapeutic strategies for treating nuclear receptor-associated diseases.

This volume will be of great benefit and use to those starting out in the nuclear receptor research field (life sciences graduate students and postdoctoral fellows) as well as to more established researchers who wish to apply different methods to a particular receptor/research problem. The volume will also be of use to medical students and clinicians undertaking research in this ever-growing field of study.

Aberdeen, UK

***I.J. McEwan***

---

# Contents

<i>Preface</i> . . . . .	v
<i>Contributors</i> . . . . .	ix
PART I: INTRODUCTION	
1 Nuclear Receptors: One Big Family . . . . . <i>Iain J. McEwan</i>	3
PART II: LIGAND BINDING AND NUCLEAR RECEPTOR TURNOVER	
2 Methods for Measuring Ligand Dissociation and Nuclear Receptor Turnover in Whole Cells . . . . . <i>Elizabeth M. Wilson</i>	21
3 Flow Cytometry as a Tool for Measurement of Steroid Hormone Receptor Protein Expression in Leukocytes . . . . . <i>Cherie L. Butts and Esther M. Sternberg</i>	35
4 X-Ray Crystallography of Agonist/Antagonist-Bound Receptors . . . . . <i>Ashley C.W. Pike</i>	51
PART III: NUCLEAR LOCALIZATION AND DNA BINDING	
5 FRAP and FRET Methods to Study Nuclear Receptors in Living Cells. . . . . <i>Martin E. van Royen, Christoffel Dinant, Pascal Farla, Jan Trapman, and Adriaan B. Houtsmuller</i>	69
6 Receptor-DNA Interactions: EMSA and Footprinting . . . . . <i>Jason T. Read, Helen Cheng, Stephen C. Hendy, Colleen C. Nelson, and Paul S. Rennie</i>	97
7 Chromatin Immunoprecipitation (ChIP) Methodology and Readouts . . . . . <i>Charles E. Massie and Ian G. Mills</i>	123
PART IV: NUCLEAR RECEPTOR – CO-REGULATORY PROTEIN INTERACTIONS	
8 Yeast-Based Reporter Assays for the Functional Characterization of Cochaperone Interactions with Steroid Hormone Receptors . . . . . <i>Heather A. Balsiger and Marc B. Cox</i>	141
9 High Throughput Analysis of Nuclear Receptor–Cofactor Interactions . . . . . <i>Michael L. Goodson, Behnom Farboud, and Martin L. Privalsky</i>	157
10 Binding Affinity and Kinetic Analysis of Nuclear Receptor/Co-Regulator Interactions Using Surface Plasmon Resonance . . . . . <i>Derek N. Lavery</i>	171
11 Using RNA Interference to Study Protein Function. . . . . <i>Carol D. Curtis and Ann M. Nardulli</i>	187
12 Using Intrinsic Fluorescence Emission Spectroscopy to Study Steroid Receptor and Coactivator Protein Conformation Dynamics . . . . . <i>Kate Watt and Iain J. McEwan</i>	205

PART V: PATHOPHYSIOLOGICAL ANALYSIS OF NUCLEAR RECEPTOR FUNCTION

13	Development of Phosphorylation Site-Specific Antibodies to Nuclear Receptors. . . . .	221
	<i>Inés Pineda Torra, Julia A. Staverosky, Susan Ha, Susan K. Logan, and Michael J. Garabedian</i>	
14	Tissue-Selective Knockouts of Steroid Receptors: A Novel Paradigm in the Study of Steroid Action . . . . .	237
	<i>Karel De Gendt and Guido Verhoeven</i>	
15	Methods for Identifying and Studying Genetic Alterations in Hormone-Dependent Cancers. . . . .	263
	<i>Outi R. Saramäki, Kati K. Waltering, and Tapio Visakorpi</i>	
	<i>Index</i> . . . . .	279

---

## Contributors

- HEATHER A. BALSIGER • *Department of Biological Sciences, Border Biomedical Research Center, University of Texas at El Paso, El Paso, TX, USA*
- CHERIE L. BUTTS • *Section on Neuroendocrine Immunology & Behavior, National Institute of Mental Health/NIH, Bethesda, MD, USA*
- HELEN CHENG • *Department of Urologic Sciences, Prostate Center, Vancouver General Hospital, University of British Columbia, Vancouver, BC, Canada*
- MARC B. COX • *Department of Biological Sciences, Border Biomedical Research Center, University of Texas at El Paso, El Paso, TX, USA*
- CAROL D. CURTIS • *Department of Molecular and Integrative Physiology, University of Illinois, Urbana, IL, USA*
- KAREL DE GENDT • *Laboratory for Experimental Medicine and Endocrinology, Catholic University of Leuven, Leuven, Belgium*
- CHRISTOFFEL DINANT • *Department of Pathology, Josephine Nefkens Institute, Erasmus MC, Rotterdam, The Netherlands*
- BEHNOM FARBOUD • *Section of Microbiology, Division of Biological Sciences, University of California at Davis, Davis, CA, USA*
- PASCAL FARLA • *Department of Pathology, Josephine Nefkens Institute, Erasmus MC, Rotterdam, The Netherlands*
- MICHAEL J. GARABEDIAN • *Departments of Microbiology and Urology, NYU School of Medicine, New York, NY, USA*
- MICHAEL L. GOODSON • *Section of Microbiology, Division of Biological Sciences, University of California at Davis, Davis, CA, USA*
- SUSAN HA • *Departments of Urology and Pharmacology, NYU School of Medicine, New York, NY, USA*
- STEPHEN C. HENDY • *Department of Urologic Sciences, Prostate Center, Vancouver General Hospital, University of British Columbia, Vancouver, BC, Canada*
- ADRIAAN B. HOUTSMULLER • *Department of Pathology, Josephine Nefkens Institute, Erasmus MC, Rotterdam, The Netherlands*
- DEREK N. LAVERY • *Institute of Medical Sciences, University of Aberdeen, Aberdeen, UK*
- SUSAN K. LOGAN • *Departments of Urology and Pharmacology, NYU School of Medicine, New York, NY, USA*
- CHARLES E. MASSIE • *Uro-Oncology Research Group, Cancer Research UK, Cambridge Research Institute, Li Ka Shing Centre, Cambridge, UK*
- IAIN J. MCEWAN • *School of Medical Sciences, University of Aberdeen, Aberdeen, Scotland, UK*
- IAN G. MILLS • *Uro-Oncology Research Group, Cancer Research UK, Cambridge Research Institute, Li Ka Shing Centre, Cambridge, UK*
- ANN M. NARDULLI • *Department of Molecular and Integrative Physiology, University of Illinois, Urbana, IL, USA*



- COLLEEN C. NELSON • *Department of Urologic Sciences, Prostate Center, Vancouver General Hospital, University of British Columbia, Vancouver, BC, Canada*
- ASHLEY C.W. PIKE • *Structural Genomics Consortium, University of Oxford, Headington, Oxford, UK*
- MARTIN L. PRIVALSKY • *Section of Microbiology, Division of Biological Sciences, University of California at Davis, Davis, CA, USA*
- JASON T. READ • *Department of Urologic Sciences, Prostate Center, Vancouver General Hospital, University of British Columbia, Vancouver, BC, Canada*
- PAUL S. RENNIE • *Department of Urologic Sciences, Prostate Center, Vancouver General Hospital, University of British Columbia, Vancouver, BC, Canada*
- OUTI R. SARAMÄKI • *Institute of Medical Technology, University of Tampere and Tampere University Hospital, Tampere, Finland*
- JULIA A. STAVEROSKY • *Department of Pharmacology, NYU School of Medicine, New York, NY, USA*
- ESTHER M. STERNBERG • *Section on Neuroendocrine Immunology & Behavior, National Institute of Mental Health/NIH, Bethesda, MD, USA*
- INÉS PINEDA TORRA • *Department of Microbiology, NYU School of Medicine, New York, NY, USA*
- JAN TRAPMAN • *Department of Pathology, Josephine Nefkens Institute, Erasmus MC, Rotterdam, The Netherlands*
- MARTIN E. VAN ROYEN • *Department of Pathology, Josephine Nefkens Institute, Erasmus MC, Rotterdam, The Netherlands*
- GUIDO VERHOEVEN • *Laboratory for Experimental Medicine and Endocrinology, Catholic University of Leuven, Leuven, Belgium*
- TAPIO VISAKORPI • *Institute of Medical Technology, University of Tampere and Tampere University Hospital, Tampere, Finland*
- KATI K. WALTERING • *Institute of Medical Technology, University of Tampere and Tampere University Hospital, Tampere, Finland*
- KATE WATT • *School of Medical Sciences, University of Aberdeen, Aberdeen, Scotland, UK*
- ELIZABETH M. WILSON • *Laboratories for Reproductive Biology, Department of Pediatrics and Department of Biochemistry and Biophysics, Lineberger Comprehensive Cancer Center, University of North Carolina, Chapel Hill, NC, USA*

# Chapter 1

## Nuclear Receptors: One Big Family

Iain J. McEwan

### Abstract

It is just over 20 years since the first steroid receptor cDNAs were cloned, a development that led to the birth of a superfamily of ligand activated transcription factors: the nuclear receptors. Natural ligands for nuclear receptors are generally lipophilic in nature and include steroid hormones, bile acids, fatty acids, thyroid hormones, certain vitamins and prostaglandins. These molecules act as sensors of the extracellular and intracellular environment and play crucial roles controlling development, differentiation, metabolic homeostasis, and reproduction. Since the original cloning experiments considerable progress has been made in our understanding of the structure, mechanisms of action and biology of this important family of proteins.

**Key words:** Steroid hormones, Glucocorticoid receptors, Estrogen receptors, Retinoic acid receptors, Orphan receptors, Gene regulation, Phosphorylation, Acetylation, Sumoylation, Hormone resistance.

---

### 1. Introduction

A human adult has been estimated to comprise  $10^{14}$  cells that go into making of the different organs and cell layers in the body. The ability of humans and other multicellular animals to develop, grow, and reproduce is dependent on the ability of different specialized cells in the body to communicate and function together. It is perhaps not surprising then that a large number of biomolecules can act as signals. Some such as growth hormones and cytokines act at the cell surface, while a diverse group of small lipophilic molecules can enter cells and bind to intracellular receptor proteins to effect a response, typically, directly at the level of gene regulation. **Figure 1** illustrates a selection of such signals and the nuclear receptors to which they bind (*see Note 1*).

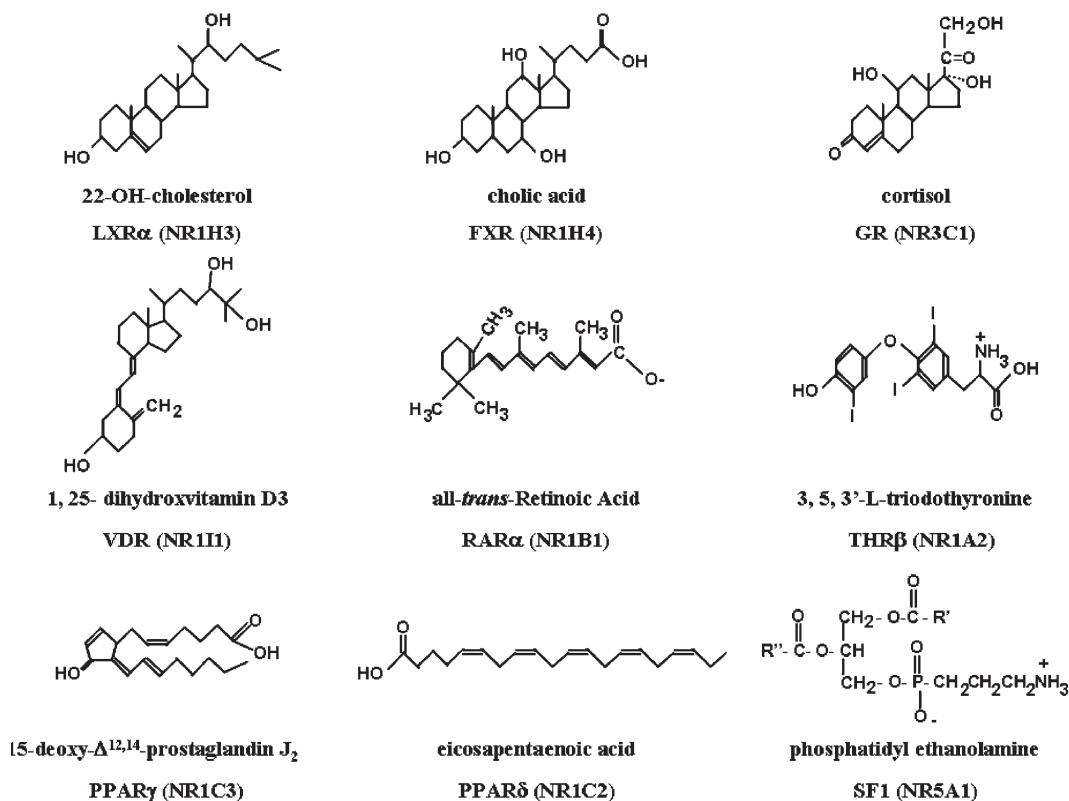


Fig. 1. Ligands for nuclear receptors. A diverse range of natural chemicals, as well as pharmaceutical agents, can act as ligands for members of the nuclear receptor superfamily. These include metabolites of cholesterol (steroid hormones, bile acids), amino acids (thyroid hormone), and fatty acid and lipid metabolites (prostaglandins, phosphatidyl choline). *FXR* farnesyl X receptor, *GR* glucocorticoid receptor, *LXR* liver X receptor, *PPAR* peroxisome proliferators-activated receptor, *RAR* retinoic acid receptor, *SF-1* steroidogenic factor-1, *THR* throid hormone receptor, *VDR* vitamin D<sub>3</sub> receptor.

This group of molecules includes cholesterol and cholesterol derivatives such as steroid hormones and bile acids, amino acid derivatives such as thyroid hormones and melatonin, vitamins such as retinoic acid and vitamin D<sub>3</sub>, and lipid and fatty acid metabolites such as eicosapentaenoic acid and leukatrienes. Although different biosynthetic pathways are involved in the production of this diverse group of signaling molecules and they show distinct chemical properties, they act by common mechanisms involving members of the nuclear receptor superfamily (1).

## 2. Nuclear Receptor Domain Organization and Evolution

In humans, 48 members of the family have been identified, with a significant proportion now having a recognized or putative ligand and the others collectively referred to as orphan receptors.

Members of the nuclear receptor superfamily share a common protein structure, consisting of a  $\alpha$ -helical globular domain at the C-terminus responsible for ligand-binding and dimerization, and this is linked via a hinge region to a second helical globular domain, responsible for specific DNA-binding and dimerization, and a structurally variable and plastic N-terminal domain responsible in some cases for transcriptional regulation (**Fig. 2**). Members of the nuclear receptor superfamily have been identified in all metazoans, but are absent in plants and yeast. Analysis of the amino acid sequence of the ligand (LBD) or DNA-binding domains (DBD) has led to the classification of six subfamilies (2). Isolation of steroid receptor-like sequences from the sea lamprey (3) and a mollusc (4) has revealed that this subfamily of receptors are ancient and evolved from an ancestral protein with estrogen-like activity. It appears that the superfamily arose from two separate gene duplication and diversification events and that ligand

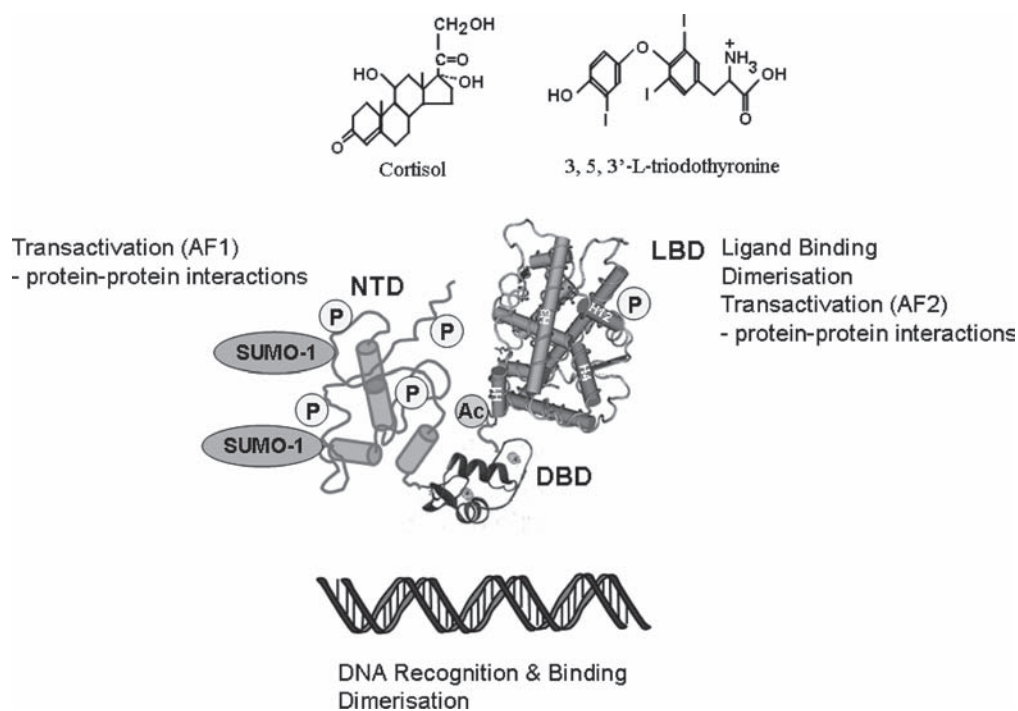


Fig. 2. Domain organisation of nuclear receptors. The receptor proteins consist of a ligand-binding domain (LBD) in the C-terminus, linked by a hinge domain to the DNA-binding domain (DBD). The DBD is then followed by the N-terminal domain. The LBD mediates specific ligand binding, dimerization, and transactivation through the activation function (AF) 2 region. The DBD is necessary and sufficient for sequence specific DNA binding. The NTD is structurally flexible and varies in length and sequence; regions within the NTD, termed AF1 are important for transactivation. Nuclear receptors are subject to decoration with various posttranslational modifications, including phosphorylation (P), acetylation (Ac), and sumoylation (SUMO-1). The structure depicted for a nuclear receptor is a model only: the 3-D structures are available for the isolated LBD and DBD regions (see **Fig. 3**), but no high-resolution structures are available for the isolated NTD, a two-domain protein or whole receptor.

binding is an acquired property occurring more than once during evolution (2). It is quite likely that the ancestral protein was an orphan receptor, and it has been speculated that the family arose from the fusion of two genes coding for proteins related to the “DBD” and “LBD” of nuclear receptors (5).

---

### 3. Nuclear Receptor Structures

#### 3.1. Ligand-Binding Domain

X-ray crystallography structures are available for the LBD from at least one member of nearly every subfamily of nuclear receptors and have revealed some interesting properties regarding hormone binding, identification of natural ligands, and activation of orphan receptors that are thought to function independent of ligand-binding. The canonical fold of the LBD consists of 12  $\alpha$ -helices and 2–3  $\beta$ -strands forming a short sheet structure (Fig. 3A) (6–8). Structures are available with no ligand bound or with agonist or antagonists occupying the ligand-binding pocket, and numerous cocomplexes have now been studied with peptides derived from coregulatory proteins (see later) bound to the surface of the LBD (Fig. 3B) (6–8).

Activation of nuclear receptors is thought to involve the rearrangement of helix 12 and the formation of hydrophobic groove on the surface of the LBD made up of residues from helices 3–5: this surface together with charged residues in helix 12 and the top of helix 3 defines the AF-2 transactivation domain. The amino acid motif, LxxLL, found in coactivator proteins (9) has been shown to sit into this groove with the leucine residues making hydrophobic contacts with residues in the bottom of the LBD groove and the coactivator peptide held in place by a charge clamp mechanism involving a glutamic acid in helix 12 and a lysine residue in helix 3 (10, 11). Agonists permit the correct orientation of helix 12 and are buried within the ligand-binding pocket, where a combination of hydrophobic interactions and specific hydrogen bonding networks, involving residues in helices 3, 5, and 11, ensure ligand-binding selectivity. Interestingly, but again perhaps not so surprising given the range of molecules that have been found to act as ligands for members of the nuclear receptor superfamily, the ligand pocket can vary dramatically in volume from 450 to 700  $\text{\AA}^3$  to greater than 1,600  $\text{\AA}^3$  for the xenobiotic-binding receptor, pregnane X receptor (PXR, NR1I2) (8). Variations in the canonical fold of the LBD have been observed for the SF-1 (steroidogenic factor 1, NR5A1)/LRH-1 (NR5A2) family of receptors, where a fourth layer of  $\alpha$ -helices was found (Fig. 3B). Interestingly, the ligand-binding pocket of these receptors was found bound with phosphatidylethanolamine,

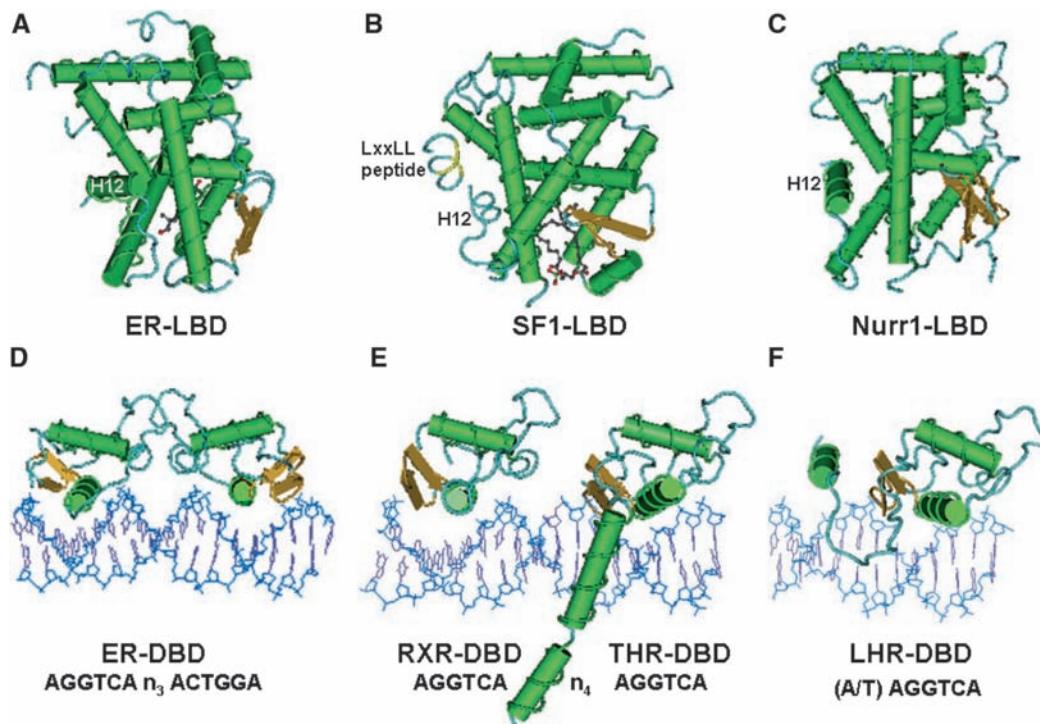


Fig. 3. Structural analysis of the isolated LBD and DBD. **A–C** crystal structures for the LBD of the ER $\alpha$  (pdb 1ERE (46)), SF-1 (pdb 1YOW (47)), and Nurr1 (pdb 1OVL (48)). Helix 12 which undergoes conformational changes upon binding of agonists or antagonists is indicated as a bound coregulatory peptide (containing a LxxLL motif, where L is leucine) to the surface of SF1. The presence of ligand in the structures for ER and SF1 is shown as a *ball-and-stick* molecule. **D–F** Structures of the DBD of a member of subfamily 3 (ER: pdb 1HCQ (49)), which bind DNA as homodimers; subfamily 1 (THR: pdb 2NLL (19)), which form heterodimers with RXR; and subfamily 5 (LRH: pdb 2A66 (50)), which binds as a monomer. The architecture of consensus DNA half-sites (inverted repeats, direct repeats, and single sites) bound by the different receptors is shown: n, represents any nucleotide (see Color Plates).

leading to the suggestion that phospho-lipids maybe the natural ligand for these receptors (8 and references therein).

In addition to binding ligand and coregulatory proteins, the LBD also has a surface involved in dimerization. This region maps generally to helix 9 and helix 10, but can also include residues in helices 7 and 8 and the loops between helices 8 and 9 and 9 and 10, and involves clusters of hydrophobic amino acids surrounded by charged or polar residues. Although a similar dimerization interface has been characterized for members of subfamily 3, the steroid receptors that form homo-dimers and members of subfamily 1 that form heterodimers with retinoid X receptor (RXR, NR2B1), differences have also been observed (12–14). For example, the crystal structure of a dimer of the progesterone receptor (PR, NR3C3) LBD appears to involve helices 11 and 12 (13).

The structure of the orphan receptor Nur-related protein 1 (Nurr1, NR4A2) has been particularly informative. Nurr1



is involved in neuronal development and dopaminergic neurone activity, and the crystal structure revealed the absence of a “ligand-binding pocket”; the space is occupied by bulky amino acid side chains, which leave no space for an exogenous ligand (reviewed in *ref.* 8). This raises the question of how this receptor is activated. Interestingly, the structure revealed that the AF2 transactivation surface is disrupted, with helix 12 in an inactive conformation (**Fig. 3C**), the charge clamp reversed and the presence of charged residues in the normally hydrophobic groove on the LBD surface. It has been speculated that other surfaces on the LBD may act as binding sites for coregulatory proteins. The presence of a second peptide bound to LBDs of SF-1 and the farnesoid receptor (FXR, NR1H4) (8), and the estrogen receptor (ER $\alpha$ , NR3A1) (15) would support this argument.

### **3.2. DNA-Binding Domain**

Nuclear receptors typically regulate gene expression through binding to DNA response elements associated with target genes (see later). The response elements comprise six nucleotide (5'AGAACA3' or 5'AGGTCA3') half-sites that are arranged as monomeric, inverted or direct repeats (**Fig. 3D–F**). The DBD contains eight conserved residues that coordinately bind to Zn ions. The binding of Zn is important for protein folding and specific DNA binding. Structural information from NMR spectroscopy and X-ray crystallography studies is available for members of subfamilies I, II, III, and V. Strikingly, the DBD of different family members are structurally very similar, made up of two  $\alpha$ -helices that fold perpendicular to each other and form a compact globular conformation (**Fig. 3D–F**). The first Zn-module forms a “recognition helix” that sits in the major groove of the DNA double helix; three residues, termed the P-box, make specific amino acid-nucleotide contacts. For the steroid receptor subfamily that bind inverted repeats as homo-dimers, five amino acids in the second Zn-module, termed the D-box, are involved in protein–protein interactions (**Fig. 3D**) (reviewed in *ref.* 16).

Members of subfamily I, which includes the thyroid hormone (TR $\alpha$ , NR1A1), retinoic acid (RAR $\alpha$ , NR1B1), and liver X (LXR $\alpha$ , NR1H3) receptors, bind to direct repeats as heterodimers with another nuclear receptor, RXR. Biochemical, mutational, and structural studies have shown that RXR usually occupies the 5' half site and makes specific protein–protein interactions with distinct regions of the partner receptor determined by the spacing of the half-sites (17–19). For example, RXR-TR binds preferentially to sequences with a spacer of four nucleotides (**Fig. 3E**), while RXR-RAR binds half-sites separated by one or five nucleotides. Therefore, specific DNA binding and response element selection depends in part on both receptor-DNA and RXR-receptor interactions. In addition, the structure for RXR-TR revealed a C-terminal extension (CTE) that also contributes to DNA-binding,

by making minor groove contacts and also protein–protein interactions with RXR (**Fig. 3E**) (19).

Members of subfamily IV and V, for example liver receptor homologue (LRH-1, NR5A2), again have the same overall globular fold for the core DBD, but bind to single half-sites with the CTE making contacts with adjacent 5' major groove (**Fig. 3F**). Another variation on the DNA binding and dimerization theme is exemplified by members of subfamily II (e.g., HNF4), which bind to direct repeats as homodimers. Therefore, although the DBD is highly conserved at the level of both primary amino acid sequence and tertiary structure, DNA response element is selectively achieved by a combination of protein–DNA and specific protein–protein interactions between the receptor monomers. Significantly, recent studies have suggested that DNA binding may have a more active role in receptor function, than simply tethering the receptor to DNA. DNA binding may, therefore, act as an allosteric regulator of receptor function by modulating the structure of the NTD and receptor–protein interactions (reviewed in **refs. 20, 21**).

### 3.3. NTD

The NTD of nuclear receptor varies dramatically in terms of both length and amino acid sequence and in contrast to both the DBD and LBD shows little if any sequence homology between different nuclear receptors. Members of the steroid receptor subfamily tend to have long NTD of several hundred amino acids and have sequences termed AF1 that are important for transactivation and protein–protein interactions (21 and references therein). Work from Wilson and coworkers correlated the NTD length with the importance of AF1 vs. AF2 for receptor-dependent transactivation (22).

The other striking feature of the NTD, in comparison to the DBD and LBD, is the apparent lack of a stable structure. Analysis by circular dichroism or NMR spectroscopy of secondary structure content of the NTD and/or AF1 of the androgen (AR, NR3C4), ER, glucocorticoid (GR, NR3C1), peroxisome proliferator activated (PPAR $\alpha$ , NR1C1) and PR receptors revealed these domains lack stable secondary structure, but have the propensity to form  $\alpha$ -helix in hydrophobic environment or in the presence of a natural osmolyte trimethyl amine N-oxide (TMAO) (21, 23, 24). TMAO and related chemical chaperones are thought to stabilize proteins in a native folded conformation. Strikingly, a  $\alpha$ -helical conformation of the AR, ER $\alpha$ , GR, and PR NTD/AF1 was stabilized by specific protein–protein interactions (reviewed in **refs. 21, 24**).

Interestingly, the presence of the DBD and/or binding to a DNA response element was found to modulate the structure of the AR, GR, and PR NTDs (21 and references therein). In the case of the PR, the binding of a coregulatory protein to the DBD



resulted in structural folding of the NTD (25). These studies further emphasize the potential allosteric role DNA-binding may play in nuclear receptor function and also highlight the possibility of intradomain communication (20). Current models for the folding of the NTD couple function (i.e., protein–protein interactions) with induced protein-folding (21, 24).

---

## 4. Nuclear Receptor Mechanisms of Action

### 4.1. Regulation of Target Genes

The availability of gene microarray technology has dramatically increased the information available on potential hormone-regulated genes or gene networks in target cells. And when combined with chromatin immunoprecipitation (ChIP) assays, it can lead directly to the identification of nuclear receptor-regulated genes and a global identification of natural DNA hormone response elements (HRE). ChIP-chip analysis for the AR (26–28), ER (29–31), and GR (32) has revealed some interesting findings. The two main features to emerge from these studies are (1) the significant divergence of receptor-binding sites from the 15 bp canonical HRE sequence, characterized by *in vitro* studies, and (2) the presence of composite receptor-binding sites and the binding sites for other transcription factors, including AP-1, ETS proteins, Foxo1 (forkhead), GATA-2, HNF-4, and Sp1. Significantly, comparison of GRE across four mammalian species demonstrated significant conservation for individual binding sites, which otherwise showed considerable variation (32).

Studies with AR (26, 28), ER (29, 30), and GR (32) highlighted the presence of binding sites for these receptors at considerable distances (>10 kb), either upstream or downstream, from the transcription start sites. However, other studies analyzing AR (27) and ER (31)-binding emphasized the interaction of the receptor with sequences within the promoter adjacent (within 1.5 kb upstream) to the hormone regulated gene. The differences reported in the studies to-date may simply reflect individual experimental protocols or more interestingly may highlight cell-type and/or receptor specificity for a given hormone response.

Once bound to promoter or enhancer elements, nuclear receptors activate transcription via AF1 and/or AF2 by recruitment of: (1) proteins or protein complexes with enzymatic activities that permit the opening up of the chromatin structure; and (2) components of the general transcription machinery resulting in the formation of the preinitiation complex (reviewed in refs. 33, 34). Nuclear receptor coactivators with enzymatic activity include the CREB-binding protein (CBP), P/CAF (p300/CBP associated factor) and Tip60 (all histone acetyl transferases), E6-AP and ubc9

(E2 and E3 ubiquitin/SUMO-1 conjugating enzymes), CDK7 (TFIIH) (kinase) and CARM1, JMJD2C and LSD1 (demethylases). Different members of the nuclear receptor superfamily have also been reported to bind directly to several general transcription factors, including TATA-binding protein (TBP), TFIIB and TFIIF and to RNA polymerase II (21 and references therein). Elegant studies from Gannon and coworkers illustrated that the assembly and disassembly of protein complexes in response to a hormone signal follows a cyclical pattern on a target gene promoter for the ER (35). A limited number of other studies would support this view and suggest that this may be a common theme in nuclear receptor-dependent transcriptional activation.

In addition to activating transcription, nuclear receptors can also repress specific gene expression. Different mechanisms may be employed, but again the recruitment of protein complexes, this time composed of corepressors with distinct enzymatic activities that can modify chromatin structure to switch off genes have been described (34).

#### **4.2. Posttranslational Modifications**

Nuclear receptors are subject to a number of post-translational modifications that decorate the protein and modulate receptor action in the absence and presence of ligand (Fig. 2). The modifications include phosphorylation, acetylation, sumoylation, ubiquitination and possibly glycosylation and may act in concert or be mutually exclusive (36–39). The functional and structural consequences of these different modifications for different receptors are just beginning to be revealed. Probably most is known about receptor phosphorylation, which is typically on serine and threonine residues, but can also occur on tyrosine. The recent availability of phosphor-specific antibodies together with improvements in identifying phosphorylated residues through mass-spectrometry peptide finger-printing have greatly enhanced our understanding of the role phosphorylation can play in receptor function. Phosphorylation of members of the steroid receptor subfamily occurs predominantly, but not exclusively, in the NTD and has been found to regulate nuclear localisation, protein-protein interactions and receptor turnover (for reviews *see refs.* 37, 39). For example, ER $\alpha$  is phosphorylated on serine 118 in response to epidermal growth factor, which enhances receptor-coactivator interactions. Phosphorylation of the GR by MAP kinases or cyclin-dependent kinase on serines 203 and 211 has been shown to regulate the nuclear localization of the receptor (37, 39 and references therein). Interestingly, serine 16 in the ER $\beta$ -NTD has been found to be either phosphorylated or modified by O-linked- $\beta$ -N-acetylglucosamine (O-GlcNAc): the phosphorylated receptor is thought to be more active (36). Of particular significance was the observation that this modification may alter the structure of the ER $\beta$ -NTD: a phosphorylated

peptide was found to be more extended, while O-GlcNAc modification resulted in the adoption of a type II  $\beta$ -turn (36). This is an area of active investigation and it is likely to reveal further functional consequences of phosphorylation and the kinases and signaling pathways that lead to receptor-specific modification.

Acetylation occurs on lysine residues and alters the charge on the receptor protein. Acetylation of a conserved KLKK motif in the AR, by the HAT enzymes Tip60, p300, and P/CAF, is associated with augmentation of the hormone response (reviewed in refs. 37, 38). Further, acetylation of the AR was associated with reduced cell-death (apoptosis) in prostate cells and recruitment of coactivator complexes. Significantly, a functional link has also been established between receptor phosphorylation and acetylation (37, 38). This opens up possibilities for coordinately regulating receptor activity in response to different environmental cues.

Steroid receptors have also been shown to be sumoylated, which may act in a receptor and target gene-specific manner to regulate the hormone response. The AR is sumoylated on lysines 386 and 520, in the NTD, by Ubc9 and the E3 ligases PIAS1 and PIASx $\alpha$ , which represses AR-dependent transactivation at certain promoters (37, 38). In contrast, sumoylation of ER $\alpha$  on lysines 266 and 268 in the hinge region, which are also subject to acetylation, has been found to enhance the activity of the receptor (37, 38). Thus posttranslational modification of nuclear receptors can provide fine tuning of the receptor-response by modulating function or possibly receptor folding and stability. A further level of control of the receptor response that is only now beginning to be fully appreciated and studied is the posttranslational modification of coregulatory proteins (39, 40).

Thus the cellular response to a particular hormone is going to depend on the integration of various levels of control. These will include the expression and levels of receptor protein, the binding of ligand, the binding to DNA target sequences by the receptor, posttranslational modification of the receptor, and the expression and posttranslational modification status of coregulatory proteins.

---

## 5. Nuclear Receptors and Disease

The ability to manipulate the expression of nuclear receptors either globally or in a cell-specific manner in transgenic mice has dramatically increased our understanding of the critical roles

nuclear receptors play during development and in a wide range of physiological processes. Such studies have also helped researchers gain a better knowledge of how defects in receptor signaling can have profound effects on health and lead to a number of chronic diseases. Nuclear receptors have also proved valuable drug targets for the pharmacology industry in the search for therapies for conditions as diverse as hormone sensitive cancers, inflammation, cardiovascular disease, and metabolic syndrome. Currently, a major goal of this research is to develop small molecules that will exhibit tissue-specific responses in regulating members of the nuclear receptor superfamily.

Point mutations in the receptors for androgens, vitamin D, and thyroid hormones are the underlying pathology in syndromes with variable phenotypes that result from end organ resistance to the hormone. In the case of the AR mutations impairing hormone or DNA binding or downstream signaling by the receptor have been associated with disruption of male development and/or fertility (41, 42). Mutations in the TR $\beta$  (NR1A2), which is expressed in the hypothalamus and pituitary, map to hot spots in the LBD and result in general resistance to thyroid hormone through a dominant-negative mechanism (43). The symptoms of general resistance to thyroid hormone include growth and cognitive defects.

More recently, considerable attention has been paid to the PPARs, which are involved in a range of activities associated with adipocyte differentiation, glucose and lipid homeostasis, and metabolic disease. PPAR $\alpha$  (NR1C1) is activated by fibrate drugs and has antiinflammatory and antiproliferative effects in macrophages, which is thought to explain the antiatherogenic actions of these drugs (44). The other class of drugs, the thiazolidinediones, which are insulin-sensitizing agents used in the treatment of type 2 diabetes, are potent agonists for PPAR $\gamma$  (NR1C3). Point mutations in the PPAR $\gamma$  LBD have been identified that lead to insulin resistance and lipodystrophy, emphasising the role of the receptor in insulin sensitization and the reduction of blood glucose levels (43, 45).

In addition to causing defects in reproductive development and metabolic processes changes in nuclear receptor levels have been associated with neurological disorders. Polymorphisms in a noncoding exon of the *Nurr1* receptor gene, which we saw above acts in the absence of a bound ligand, have been correlated with a familial form of Parkinson's disease, schizophrenia, and manic depression (43). Therefore, the combined use of animal models and clinical studies is yielding valuable data that are leading to a better understanding of the diverse physiological functions of members of the nuclear receptor superfamily during development and later in adult life.

---

## 6. Conclusions and Future Perspectives

The first steroid receptors were cloned over 20 years ago and the intervening period has seen the birth of the nuclear receptor superfamily and tremendous progress in our understanding of the structure–function relationships of these vital ligand-regulated transcription factors and their biological actions. This has included the functional analysis of the isolated receptor domains (NTD, DBD, and LBD), the solving at atomic resolution of the structure of the DBD and LBD, the identification of binding partners, and a clearer appreciation of the role of mutations in nuclear receptors resulting in a wide range of pathological states. However, despite the progress made, a number of questions remain unanswered:

- (1) What is structure of an intact member of the nuclear receptor superfamily, or a two-domain polypeptide, possibly bound to DNA or peptides derived from coregulatory proteins?
- (2) What are the gene networks that underlie the tissue/cell-specific nuclear receptor response?
- (3) How are different signaling pathways integrated in a cell-specific manner?

In conclusion, it is assured there will be further dramatic developments as researchers strive to understand the biology and physiological actions of nuclear receptors, the structural and biochemical basis for receptor function, and the impact genetic alterations have on receptor-signaling in disease. In this volume of *Methods in Molecular Biology* leading laboratories in the field describe step-by-step protocols for a range of key biochemical, genetic, and structural tools that will help answer the above questions on nuclear receptor structure and function. Methods for studying ligand binding and receptor expression levels and turnover in whole cells are described by Wilson and Butt and Sternberg. The use of X-ray crystallography to analyze the structure of the LBD with agonist or antagonists bound is discussed by Pike. The ability of nuclear receptor to directly regulate gene expression depends on localization to the nucleus and specific DNA binding. Houtsmuller and coworkers describe the use of FRAP/FLIP approaches for studying and visualizing receptor-DNA binding dynamics in whole cells. Rennie and coworkers consider methods for investigating the molecular aspects of receptor-DNA complexes in vitro and these approaches are complemented by Massie and Mills detailed discussion of ChIP-on-chip methodology to identify receptor-regulated genes and DNA-binding sites in target cells. The study of receptor-co-regulatory proteins continues to be a major area of nuclear receptor research. Methods for screening for binding partners and for quantifying specific

receptor-target protein interactions are discussed by Pravinsky and coworkers and Lavery, respectively. Baisiger and Cox, focussing on steroid receptor cochaperone interactions, describe the use of a yeast reporter gene assay as a model system for investigating receptor action, while Curtis and Nardulli describe protocols for using siRNA technology to knock-down coregulatory protein levels and assay the consequences for nuclear receptor-signaling, and Watt and McEwan describe how measuring tryptophan fluorescence emission spectra can provide information on the folding of nuclear receptors and co-regulatory proteins. Increasingly the pathophysiological actions of nuclear receptors action are being addressed. Understanding the role of phosphorylation on receptor function, through the use of phosphospecific antibodies, is the topic of Garabedian and coworkers. De Gendt and Verhoeven discuss some of the recent advances in tissue selective gene targeting and knock-out strategies for generating mouse models of receptor function in vivo. The volume ends with Visakarpi and coworkers considering protocols for identifying and studying genetic alterations in hormone-dependent cancers. The techniques described in this volume can be applied to the investigation of different members of the superfamily and together with the continued development of new approaches will provide important insights into understand the structure and mechanisms of action of these diverse and essential signaling proteins.

---

## 7. Notes

1. The Nuclear Receptor Signaling Atlas (NURSA, <http://www.nursa.org>) is a valuable web-based resource for researchers in the nuclear receptor field. This site has information on each member of the superfamily, links to published literature and experimental data on nuclear receptor expression levels in the mouse and a range of microarray and qPCR studies on receptor regulated gene networks.

## References

1. Evans, R. M. (1988) The Steroid and Thyroid Hormone Receptor Superfamily. *Science*. **240**, 889–895.
2. Escriva, H., Bertrand, S., and Laudet, V. (2004) The Evolution of the Nuclear Receptor Superfamily. *Essays Biochem.* **40**, 11–26.
3. Thornton, J. W. (2001) Evolution of Vertebrate Steroid Receptors from an Ancestral Estrogen Receptor by Ligand Exploitation and Serial Genome Expansions. *Proc. Natl. Acad. Sci. USA.* **98**, 5671–5676.
4. Thornton, J. W., Need, E., and Crews, D. (2003) Resurrecting the Ancestral Steroid Receptor: Ancient Origin of Estrogen Signaling. *Science*. **301**, 1714–1717.
5. Barnett, P., Tabak, H. F., and Hettema, E. H. (2000) Nuclear Receptors Arose from



- Pre-Existing Protein Modules during Evolution. *Trends Biochem. Sci.* **25**, 227–228.
6. Egea, P. F., Klaholz, B. P., and Moras, D. (2000) Ligand-Protein Interactions in Nuclear Receptors of Hormones. *FEBS Lett.* **476**, 62–67.
  7. Pike, A. C., Brzozowski, A. M., and Hubbard, R. E. (2000) A Structural Biologist's View of the Oestrogen Receptor. *J. Steroid Biochem. Mol. Biol.* **74**, 261–268.
  8. Ingraham, H. A., and Redinbo, M. R. (2005) Orphan Nuclear Receptors Adopted by Crystallography. *Curr. Opin. Struct. Biol.* **15**, 708–715.
  9. Heery, D. M., Kalkhoven, E., Hoare, S., and Parker, M. G. (1997) A Signature Motif in Transcriptional Co-Activators Mediates Binding to Nuclear Receptors. *Nature.* **387**, 733–736.
  10. Darimont, B. D., Wagner, R. L., Apriletti, J. W., Stallcup, M. R., Kushner, P. J., Baxter, J. D., Fletterick, R. J., and Yamamoto, K. R. (1998) Structure and Specificity of Nuclear Receptor-Coactivator Interactions. *Genes Dev.* **12**, 3343–3356.
  11. McInerney, E. M., Rose, D. W., Flynn, S. E., Westin, S., Mullen, T. M., Krones, A., Inostroza, J., Torchia, J., Nolte, R. T., Assa-Munt, N., Milburn, M. V., Glass, C. K., and Rosenfeld, M. G. (1998) Determinants of Coactivator LXXLL Motif Specificity in Nuclear Receptor Transcriptional Activation. *Genes Dev.* **12**, 3357–3368.
  12. Nolte, R. T., Wisely, G. B., Westin, S., Cobb, J. E., Lambert, M. H., Kurokawa, R., Rosenfeld, M. G., Willson, T. M., Glass, C. K., and Milburn, M. V. (1998) Ligand Binding and Co-Activator Assembly of the Peroxisome Proliferator-Activated Receptor-Gamma. *Nature.* **395**, 137–143.
  13. Tanenbaum, D. M., Wang, Y., Williams, S. P., and Sigler, P. B. (1998) Crystallographic Comparison of the Estrogen and Progesterone Receptor's Ligand Binding Domains. *Proc. Natl. Acad. Sci. USA.* **95**, 5998–6003.
  14. Bourguet, W., Vivat, V., Wurtz, J. M., Chambon, P., Gronemeyer, H., and Moras, D. (2000) Crystal Structure of a Heterodimeric Complex of RAR and RXR Ligand-Binding Domains. *Mol. Cell.* **5**, 289–298.
  15. Kong, E. H., Heldring, N., Gustafsson, J. A., Treuter, E., Hubbard, R. E., and Pike, A. C. (2005) Delineation of a Unique Protein-Protein Interaction Site on the Surface of the Estrogen Receptor. *Proc. Natl. Acad. Sci. USA.* **102**, 3593–3598.
  16. Claessens, F., and Gewirth, D. T. (2004) DNA Recognition by Nuclear Receptors. *Essays Biochem.* **40**, 59–72.
  17. Perlmann, T., Rangarajan, P. N., Umesono, K., and Evans, R. M. (1993) Determinants for Selective RAR and TR Recognition of Direct Repeat HREs. *Genes Dev.* **7**, 1411–1422.
  18. Kurokawa, R., Yu, V. C., Naar, A., Kyakumoto, S., Han, Z., Silverman, S., Rosenfeld, M. G., and Glass, C. K. (1993) Differential Orientations of the DNA-Binding Domain and Carboxy-Terminal Dimerization Interface Regulate Binding Site Selection by Nuclear Receptor Heterodimers. *Genes Dev.* **7**, 1423–1435.
  19. Rastinejad, F., Perlmann, T., Evans, R. M., and Sigler, P. B. (1995) Structural Determinants of Nuclear Receptor Assembly on DNA Direct Repeats. *Nature.* **375**, 203–211.
  20. Lefstin, J. A., and Yamamoto, K. R. (1998) Allosteric Effects of DNA on Transcriptional Regulators. *Nature.* **392**, 885–888.
  21. Lavery, D. N., and McEwan, I. J. (2005) Structure and Function of Steroid Receptor AF1 Transactivation Domains: Induction of Active Conformations. *Biochem. J.* **391**, 449–464.
  22. He, B., Gampe, R. T., Jr, Kole, A. J., Hnat, A. T., Stanley, T. B., An, G., Stewart, E. L., Kalman, R. I., Minges, J. T., and Wilson, E. M. (2004) Structural Basis for Androgen Receptor Interdomain and Coactivator Interactions Suggests a Transition in Nuclear Receptor Activation Function Dominance. *Mol. Cell.* **16**, 425–438.
  23. Hi, R., Osada, S., Yumoto, N., and Osumi, T. (1999) Characterization of the Amino-Terminal Activation Domain of Peroxisome Proliferator-Activated Receptor Alpha. Importance of Alpha-Helical Structure in the Transactivating Function. *J. Biol. Chem.* **274**, 35152–35158.
  24. Kumar, R., and Thompson, E. B. (2003) Transactivation Functions of the N-Terminal Domains of Nuclear Hormone Receptors: Protein Folding and Coactivator Interactions. *Mol. Endocrinol.* **17**, 1–10.
  25. Wardell, S. E., Kwok, S. C., Sherman, L., Hodges, R. S., and Edwards, D. P. (2005) Regulation of the Amino-Terminal Transcription Activation Domain of Progesterone Receptor by a Cofactor-Induced Protein Folding Mechanism. *Mol. Cell. Biol.* **25**, 8792–8808.
  26. Bolton, E. C., So, A. Y., Chaivorapol, C., Haqq, C. M., Li, H., and Yamamoto, K. R. (2007) Cell- and Gene-Specific Regulation of Primary Target Genes by the Androgen Receptor. *Genes Dev.* **21**, 2005–2017.

27. Massie, C. E., Adryan, B., Barbosa-Morais, N. L., Lynch, A. G., Tran, M. G., Neal, D. E., and Mills, I. G. (2007) New Androgen Receptor Genomic Targets show an Interaction with the ETS1 Transcription Factor. *EMBO Rep.* **8**, 871–878.
28. Wang, Q., Li, W., Liu, X. S., Carroll, J. S., Janne, O. A., Keeton, E. K., Chinnaiyan, A. M., Pienta, K. J., and Brown, M. (2007) A Hierarchical Network of Transcription Factors Governs Androgen Receptor-Dependent Prostate Cancer Growth. *Mol. Cell.* **27**, 380–392.
29. Carroll, J. S., Liu, X. S., Brodsky, A. S., Li, W., Meyer, C. A., Szary, A. J., Eeckhoutte, J., Shao, W., Hestermann, E. V., Geistlinger, T. R., Fox, E. A., Silver, P. A., and Brown, M. (2005) Chromosome-Wide Mapping of Estrogen Receptor Binding Reveals Long-Range Regulation Requiring the Forkhead Protein FoxA1. *Cell.* **122**, 33–43.
30. Carroll, J. S., Meyer, C. A., Song, J., Li, W., Geistlinger, T. R., Eeckhoutte, J., Brodsky, A. S., Keeton, E. K., Fertuck, K. C., Hall, G. F., Wang, Q., Bekiranov, S., Sementchenko, V., Fox, E. A., Silver, P. A., Gingeras, T. R., Liu, X. S., and Brown, M. (2006) Genome-Wide Analysis of Estrogen Receptor Binding Sites. *Nat. Genet.* **38**, 1289–1297.
31. Kininis, M., Chen, B. S., Diehl, A. G., Isaacs, G. D., Zhang, T., Siepel, A. C., Clark, A. G., and Kraus, W. L. (2007) Genomic Analyses of Transcription Factor Binding, Histone Acetylation, and Gene Expression Reveal Mechanistically Distinct Classes of Estrogen-Regulated Promoters. *Mol. Cell. Biol.* **27**, 5090–5104.
32. So, A. Y., Chaivorapol, C., Bolton, E. C., Li, H., and Yamamoto, K. R. (2007) Determinants of Cell- and Gene-Specific Transcriptional Regulation by the Glucocorticoid Receptor. *PLoS Genet.* **3**, e94.
33. Acevedo, M. L., and Kraus, W. L. (2004) Transcriptional Activation by Nuclear Receptors. *Essays Biochem.* **40**, 73–88.
34. Rosenfeld, M. G., Luniyak, V. V., and Glass, C. K. (2006) Sensors and Signals: A coactivator/corepressor/epigenetic Code for Integrating Signal-Dependent Programs of Transcriptional Response. *Genes Dev.* **20**, 1405–1428.
35. Metivier, R., Penot, G., Hubner, M. R., Reid, G., Brand, H., Kos, M., and Gannon, F. (2003) Estrogen Receptor-Alpha Directs Ordered, Cyclical, and Combinatorial Recruitment of Cofactors on a Natural Target Promoter. *Cell.* **115**, 751–763.
36. Chen, Y. X., Du, J. T., Zhou, L. X., Liu, X. H., Zhao, Y. F., Nakanishi, H., and Li, Y. M. (2006) Alternative O-GlcNAcylation/O-Phosphorylation of Ser16 Induce Different Conformational Disturbances to the N Terminus of Murine Estrogen Receptor Beta. *Chem. Biol.* **13**, 937–944.
37. Faus, H., and Haendler, B. (2006) Post-Translational Modifications of Steroid Receptors. *Biomed. Pharmacother.* **60**, 520–528.
38. Popov, V. M., Wang, C., Shirley, L. A., Rosenberg, A., Li, S., Nevalainen, M., Fu, M., and Pestell, R. G. (2007) The Functional Significance of Nuclear Receptor Acetylation. *Steroids.* **72**, 221–230.
39. Weigel, N. L., and Moore, N. L. (2007) Kinases and Protein Phosphorylation as Regulators of Steroid Hormone Action. *Nucl. Recept. Signal.* **5**, e005.
40. Li, S., and Shang, Y. (2007) Regulation of SRC Family Coactivators by Post-Translational Modifications. *Cell. Signal.* **19**, 1101–1112.
41. Gottlieb, B., Beitel, L. K., Wu, J., Elhaji, Y. A., and Trifiro, M. (2004) Nuclear Receptors and Disease: Androgen Receptor. *Essays Biochem.* **40**, 121–136.
42. Hughes, I. A., and Deeb, A. (2006) Androgen Resistance. *Best Pract. Res. Clin. Endocrinol. Metab.* **20**, 577–598.
43. Gurnell, M., and Chatterjee, V. K. (2004) Nuclear Receptors in Disease: Thyroid Receptor Beta, Peroxisome-Proliferator-Activated Receptor Gamma and Orphan Receptors. *Essays Biochem.* **40**, 169–189.
44. Lefebvre, P., Chinetti, G., Fruchart, J. C., and Staels, B. (2006) Sorting Out the Roles of PPAR Alpha in Energy Metabolism and Vascular Homeostasis. *J. Clin. Invest.* **116**, 571–580.
45. Semple, R. K., Chatterjee, V. K., and O'Rahilly, S. (2006) PPAR Gamma and Human Metabolic Disease. *J. Clin. Invest.* **116**, 581–589.
46. Brzozowski, A. M., Pike, A. C., Dauter, Z., Hubbard, R. E., Bonn, T., Engstrom, O., Ohman, L., Greene, G. L., Gustafsson, J. A., and Carlquist, M. (1997) Molecular Basis of Agonism and Antagonism in the Oestrogen Receptor. *Nature.* **389**, 753–758.
47. Krylova, I. N., Sablin, E. P., Moore, J., Xu, R. X., Waitt, G. M., MacKay, J. A., Juzumiene, D., Bynum, J. M., Madauss, K., Montana, V., Lebedeva, L., Suzawa, M., Williams, J. D., Williams, S. P., Guy, R. K., Thornton, J. W., Fletterick, R. J., Willson, T. M., and Ingraham, H. A. (2005) Structural Analyses Reveal Phosphatidyl Inositols as Ligands for



- the NR5 Orphan Receptors SF-1 and LRH-1. *Cell*. **120**, 343–355.
48. Wang, Z., Benoit, G., Liu, J., Prasad, S., Aarnisalo, P., Liu, X., Xu, H., Walker, N. P., and Perlmann, T. (2003) Structure and Function of Nurr1 Identifies a Class of Ligand-Independent Nuclear Receptors. *Nature*. **423**, 555–560.
49. Schwabe, J. W., Chapman, L., Finch, J. T., and Rhodes, D. (1993) The Crystal Structure of the Estrogen Receptor DNA-Binding Domain Bound to DNA: How Receptors Discriminate between their Response Elements. *Cell*. **75**, 567–578.
50. Solomon, I. H., Hager, J. M., Safi, R., McDonnell, D. P., Redinbo, M. R., and Ortlund, E. A. (2005) Crystal Structure of the Human LRH-1 DBD-DNA Complex Reveals Ftz-F1 Domain Positioning is Required for Receptor Activity. *J. Mol. Biol.* **354**, 1091–1102.

# Chapter 2

## Methods for Measuring Ligand Dissociation and Nuclear Receptor Turnover in Whole Cells

Elizabeth M. Wilson

### Abstract

Understanding the molecular mechanisms of steroid hormone action requires assays that measure rates of ligand dissociation and receptor degradation. Ligand dissociation is a pseudo-first order reaction of a high affinity [<sup>3</sup>H]-labeled ligand. Receptor turnover as described here is the rate of degradation of a radiolabeled receptor. The methods make use of transient expression of a nuclear receptor in cultured cells and are applicable to all nuclear receptors. Rates of ligand dissociation and receptor degradation provided the first insight into the interdomain interactions of the androgen receptor and the molecular basis for the phenotypic effects of naturally occurring androgen receptor loss-of-function germline mutations and gain-of-function somatic mutations, and for the potency differences between the biologically active androgens, testosterone, and dihydrotestosterone.

**Key words:** Nuclear receptors, Ligand dissociation, Receptor turnover, Androgen receptor, Receptor degradation.

---

### 1. Introduction

Steroid receptors are ligand-activated transcription factors that regulate gene transcription throughout growth and development. The principal initiating event in steroid receptor action is the binding of a high affinity hormone, which increases receptor occupancy in the nucleus and binding to hormone response element DNA. Steroid receptor action is influenced by the kinetics of ligand binding and by the changes in receptor turnover. The focus of this chapter is to describe methods for measuring the dissociation rates of high affinity [<sup>3</sup>H]-labeled ligands and the rates

of degradation of [<sup>35</sup>S]methionine-labeled receptors. Methods are described for the androgen receptor (AR) but are applicable to other nuclear receptors.

Before cloning of the AR complementary DNA (cDNA), early methods for measuring AR androgen binding affinity and dissociation rates made use of tissue cytosol preparations from rats that were castrated to remove the endogenous source of androgen (1). The studies were complicated by the resulting low concentration of androgen that increases AR susceptibility to proteolytic degradation during extraction and storage (2). AR dissociation kinetics assayed in cytosol fractions required long incubation times at 4°C for androgen dissociation half-times greater than 20 h. With the cloning of the human (3–5) and rat (6) AR cDNAs, ligand binding and receptor degradation assays were simplified by the use of transient receptor expression in cultured cells.

Monkey kidney COS cells are useful for ligand dissociation and receptor degradation assays because high receptor levels can be achieved by transient transfection of expression plasmids containing receptor cDNAs. Cells are incubated with a high affinity, high specific activity radiolabeled natural or synthetic androgen, and the dissociation is monitored in a time-dependent manner after the addition of an excess of unlabeled chase ligand to prevent rebinding of the labeled hormone. Ligand dissociation rates are pseudo-first order and are not influenced by the free ligand concentration as long as rebinding of the labeled hormone is blocked. Receptor degradation assays make use of the same transient expression methods in COS cells and measure the decline in [<sup>35</sup>S]methionine-labeled receptor over time in the presence of excess unlabeled methionine. Receptor degradation can be influenced by many factors, the most important of which for the AR is high affinity androgen binding that stabilizes the AR.

Rates of ligand dissociation and receptor degradation provided the first insights into the androgen-dependent AR NH<sub>2</sub> and carboxyl-terminal (N/C) interaction between the AR NH<sub>2</sub>-terminal FXXLF motif and activation function 2 (AF2) in the ligand-binding domain (7–9). The AR N/C interaction slows the dissociation rate of bound androgen and stabilizes AR against degradation (8–10). There is a direct relationship between the rate of ligand dissociation and androgen potency in vivo (11, 12). Dihydrotestosterone (DHT), the most potent naturally occurring androgen, dissociates three times slower (half-time ~3 h at 37°C) than testosterone (T, half-time ~1 h at 37°C) (13). The slower dissociation rate of DHT results from the twofold higher affinity of AF2 for the AR FXXLF motif when DHT is bound compared with T (13). The AR N/C interaction induced by androgen and anabolic steroids stabilizes AR against degradation (8, 11, 14), whereas AR antagonists dissociate more rapidly (half-time ~5 min at 37°C) and do not induce the AR N/C interaction or stabilize

AR (12). Naturally occurring loss-of-function AR gene mutations in the ligand-binding domain that cause the androgen insensitivity syndrome, and gain-of-function mutations in prostate cancer, alter the rates of dissociation of bound androgen and AR degradation without altering equilibrium androgen-binding affinity (15–18). Methods outlined below, therefore, provide insight into the molecular mechanisms of steroid receptor action.

---

## 2. Materials

### **2.1. COS Cell Culture and Transfection: Reagents and Buffers**

1. Monkey kidney COS-1 cells (American Type Culture Collection, Rockville, MD).
2. Dulbecco's Modified Eagle's Medium (DMEM) with phenol red, L-glutamine and sodium pyruvate (Gibco/Invitrogen, Grand Island, NY).
3. Bovine calf serum (BCS) (Hyclone, Logan UT or Thermo Fisher Scientific, Waltham, MA), 55 mL added to 500 mL medium.
4. Penicillin and streptomycin (Cellgro/Mediatech, Herndon, VA or Gibco/Invitrogen): 100× stock, 10,000 IU/mL, 5.5 mL added to 500 mL media.
5. L-glutamine (Gibco/Invitrogen): 200 mM, 100× stock, 5.5 mL added to 500 mL media.
6. 2 M Hepes, pH 7.2 (Fisher Scientific, Fair Lawn, New Jersey), 238.3 g Hepes powder added to 500 mL sterile water, pH to 7.2 with 5 N NaOH, sterile filter, store at 4°C, add 5.5 mL to 500 mL media.
7. COS cell DMEM with phenol red and 10% BCS, 20 mM Hepes, pH 7.2 and penicillin/streptomycin: 500 mL DMEM containing phenol red, 55 mL BCS, 5.5 mL 2 M Hepes, pH 7.2, 5.5 mL 100× L-glutamine and 5.5 mL 100× penicillin/streptomycin.
8. DMEM with high glucose (4.5 g/l D-glucose) without phenol red or sodium pyruvate (Gibco/Invitrogen, Grand Island, NY).
9. COS cell serum free DMEM without phenol red, to 500 mL DMEM without phenol red add 5.5 mL 2 M Hepes, pH 7.2, 5.5 mL 100× L-glutamine and 5.5 mL 100× penicillin/streptomycin.
10. L-methionine-free, L-cystine-free DMEM with high glucose and 20 mM Hepes, pH 7.2 without L-glutamine or sodium pyruvate (Gibco/Invitrogen, Grand Island, NY): 5.5 mL

2 M Hepes, pH 7.2, 5.5 mL 100× L-glutamine and 5.5 mL 100× penicillin/streptomycin.

11. Trypsin (0.5%) and ethylenediamine tetraacetic acid (EDTA, 0.53 mM) in Hank's Balanced Salts Solution (Cellgro/Mediatech, Herndon, VA or Gibco/Invitrogen).
12. DEAE dextran (Sigma, St. Louis, MO), 0.25 g in 50 mL sterile H<sub>2</sub>O, sterile filter using 150 mL bottle top filter (0.22 μm, Corning, Inc., Corning, NY), prepare fresh.

**2.2. Reagents for  
Ligand Dissociation  
and Receptor  
Degradation Assays**

1. Chloroquine stock (Sigma, St. Louis, MO): 50 mg to 10.5 mL sterile water and sterile filter using a 10 mL syringe and Acrodisc syringe filter (0.2 μm, Pall Life Sciences, Ann Arbor, MI); Chloroquine solution, prepare fresh by adding 1 mL chloroquine stock (5 mg/mL) to 100 mL DMEM medium containing 10% BCS and additives.
2. 2× Tris buffered saline (TBS): 32.72 g NaCl, 0.92 g KCl, 0.588 g CaCl<sub>2</sub>·2H<sub>2</sub>O, 0.4 g MgCl<sub>2</sub>·6H<sub>2</sub>O, 0.512 g NaH<sub>2</sub>PO<sub>4</sub>·H<sub>2</sub>O and 12.12 g Tris, pH 7.4 made up to 2 l H<sub>2</sub>O and sterile filter. For 1.08 TBS, combine 270 mL 2×TBS with 230 mL sterile distilled H<sub>2</sub>O.
3. Phosphate buffer saline (PBS) (Gibco/Invitrogen, Grand island, NY).
4. Steroids, unlabeled T and DHT (Steraloids, Inc., Newport, RI), methyltrienolone (R1881), [<sup>3</sup>H]R1881, [<sup>3</sup>H]DHT and [<sup>3</sup>H]T (PerkinElmer, Waltham, MA).
5. NEG-772 Easytag Express Protein Labeling mix, L-[<sup>35</sup>S] methionine, 1175 Ci/mmol, 11.08 mCi/mL (PerkinElmer Life and Analytical Sciences, Boston, MA).
6. Protein A-agarose immunoprecipitation reagent (Santa Cruz Biotechnology, Santa Cruz, CA), prepare by hydrating 1 g agarose beads/5 mL PBS overnight at 4°C. Wash with 10 mL PBS twice and once with 10 mL IP lysis buffer. Prepare 5% suspension according to bead volume, aliquot 200 μl to each tube and aspirate.
7. Immunoprecipitation (IP) lysis buffer: 0.15 M NaCl, 0.5% NP-40, 50 mM NaF, 50 mM Tris-HCl, pH 7.5, 1 mM dithiothreitol, 1 mM phenylmethylsulfonyl fluoride, and protease inhibitor cocktail (Roche).
8. 2× ligand dissociation (LD)-sodium dodecylsulfate (SDS) sample buffer: 4% SDS, 20% glycerol, and 20 mM Tris-HCl, pH 6.8. Prepare by combining 20 mL SDS upper gel buffer containing 0.5 M Tris, pH 6.8 and 0.4% SDS, with 200 mL 10% SDS, 100 mL glycerol and 180 mL of dH<sub>2</sub>O to a final volume of 500 mL.

9. 2× IP-SDS sample buffer: 3.3% SDS, 10% glycerol, 10 mM 2-mercaptoethanol and 0.12 M Tris, pH 6.8.
10. Six well tissue culture plates, 100 × 20 mm<sup>2</sup> polystyrene sterile dishes (Corning, Inc., Corning NY), 15 mL Falcon tube (Corning Inc., Corning, NY), disposable cell lifters, sterile (Fisher Scientific, Pittsburg, PA).
11. Antibodies for AR immunoprecipitation include polyclonal AR32 anti-peptide antibody (rabbit polyclonal, 0.4 μg/mL) (19) and AR52 anti-peptide antibody (rabbit polyclonal, 0.4 μg/mL) (4). For tagged fusion proteins, anti-Flag M2 affinity gel (Sigma, mouse monoclonal, 15 μl resin/500 μg protein) and anti-HA Affinity Matirx (Roche, rat polyclonal, 15 μl resin/500 μg protein) (20) or receptor-specific commercial antibodies may be used.

---

### 3. Methods

#### 3.1. Ligand Dissociation Assay

##### 3.1.1. COS Cell Culture

COS cells (*see Note 1*) are propagated in DMEM supplemented with 10% BCS, L-glutamine, penicillin, and streptomycin. Cells are passaged twice each week at 1:12 dilution or  $3 \times 10^6$ /T150 tissue culture flask. Cells are harvested by washing the flask with 8–10 mL PBS, aspirating, adding 2 mL trypsin-EDTA solution/flask and incubating at 37°C for 7–10 min using the minimum time required to release the cells. DMEM containing serum is added to inactivate the trypsin and cells are collected, centrifuged, counted using a hemocytometer and plated at  $4 \times 10^5$ /well of 6-well plates.

##### 3.1.2. Experimental Design

Multiple time points are required to measure rates of ligand dissociation. Selection of the time points is based on the expected dissociation rate, the bound ligand, and whether a wild-type or mutant receptor is assayed. Faster dissociation rates require shorter incubation times. For each time point, 2 wells are set in 6-well culture plates for total binding of the [<sup>3</sup>H]-labeled ligand. The first (0 time) and last time points have an additional third well that contains the [<sup>3</sup>H]-ligand plus a 100-fold excess unlabeled ligand to assess nonspecific binding. The dissociation rate of bound androgen from AR is typically assayed using 5 nM [<sup>3</sup>H] R1881, a high affinity radiolabeled synthetic androgen, 3 nM [<sup>3</sup>H]DHT or 5 nM [<sup>3</sup>H]T (*see Note 2*) in the absence and presence of a 100-fold excess of unlabeled ligand. Cells in culture are incubated with the radiolabeled ligand for 2 h at 37°C. After incubation, the 0 time point wells are washed with PBS and 0.5 mL LD-SDS sample buffer is added. For the remaining wells, ligand dissociation is initiated by the addition of a 50,000-fold excess of unlabeled androgen (*see Note 3*). For experiments with [<sup>3</sup>H]

DHT, unlabeled R1881 is used as the chase ligand because of the greater water solubility of R1881 compared with DHT. Typical dissociation rate time points for full-length wild-type AR are 0, 15, 30, 45, 60, and 90 min for [<sup>3</sup>H]T, and 0, 0.5, 1, 1.5, 2, and 2.5 h for [<sup>3</sup>H]DHT and [<sup>3</sup>H]R1881. AR deletions and mutations within the AR NH<sub>2</sub>-terminal FXXLF motif or ligand-binding domain may require shorter time points if the AR N/C interaction is disrupted and the androgen dissociation rate is faster.

### 3.1.3. Transient Transfection of COS Cells Using DEAE Dextran

#### Day 1

Plate  $4 \times 10^5$  COS cells/well in 6-well plates with 3 mL/well DMEM containing 10% BCS. Three wells are required for the 0 and last time points and 2 wells for the intervening time points.

#### Day 2

1. Cell density should be ~50% confluence. In a 15 mL Falcon tube for groups of 5 or less (or 50 mL tube for > 5 wells), combine (per well) 0.95 mL 1.08× TBS, 2 μg pCMVhAR expression vector DNA (or 3 μg DNA/well for low expressing plasmids) and 0.11 mL DEAE-dextran (*see Note 4*) and vortex. Scale up as needed according to the number of wells. DNA aliquots can be set 3 days in advance and stored at -20°C.
2. Aspirate the media, vortex the DNA solution, add 1 mL/well and place the cells at 37°C for 30 min.
3. Aspirate the DNA solution and add 2 mL chloroquine solution/well and incubate for 3 h at 37°C.
4. Aspirate the media and glycerol shock by adding 1 mL/well 15% glycerol in DMEM containing 10% BCS and incubate for precisely 4 min at room temperature.
5. Aspirate the glycerol shock solution, wash carefully with 3 mL PBS/well, add 3 mL DMEM containing 10% BCS and incubate overnight at 37°C.

#### Day 3

Cells remain at 37°C in the same DMEM with serum.

### 3.1.4. Binding of Ligand and Measuring Dissociation Rate

#### Day 4

1. Prepare the labeling solutions in serum free, phenol red free DMEM (*see Note 5*) by estimating the total volume, based on the total number of wells  $\times$  0.625 mL (to use 0.6 mL/well) and prepare 5 nM [<sup>3</sup>H]R1881, 3 nM [<sup>3</sup>H]DHT, or 5 nM [<sup>3</sup>H]T. Appropriate safety measures and adherence to local and national rules should be followed when working with ionizing radiation sources and discarding waste materials. For nonspecific binding controls, remove from the [<sup>3</sup>H]-labeling solution a volume equal to the number of wells to contain 100-fold excess unlabeled ligand  $\times$  0.625 mL and add unlabeled ligand to 500 nM (equivalent to a 100-fold excess of

[<sup>3</sup>H]-ligand). Take 0.1 mL of the hot and hot + cold labeling solutions to determine the total radioactivity in a scintillation counter.

2. Label the plates according to the selected time points.
3. Aspirate the media but do not wash the cells, add 0.6 mL labeling solution to the side of the wells, being careful not to detach the cells and incubate for 2 h at 37°C (*see Note 6*). Toward the end of the incubation, prepare the 0.35 mM unlabeled chase solution (7× stock) in serum free, phenol red free DMEM, enough to add 0.1 mL/well for all time points except 0 time.
4. To begin the ligand dissociation assay, remove the plates from the incubator and as quickly as possible, aspirate the labeling media only from the 0 time point samples into a radioactive waste flask, carefully wash the 0 time cells with 3 mL PBS/well, completely aspirate the PBS, and add 0.5 mL 1× LD-SDS sample buffer. Delay the actual harvest of the 0 time samples until the end of the entire experiment.
5. To begin the dissociation, quickly and carefully add 0.1 mL of 0.35 mM unlabeled ligand chase solution to the labeling medium of the remaining wells (50 μM unlabeled ligand final concentration). The plates are returned to the 37°C tissue culture cell incubator, spread out as a single layer on the shelf, and the time is recorded. Subsequent time points are relative to this initial time. It is important to work quickly, processing the wells at the appropriate times and returning the plates to the 37°C incubator. At the indicated times, plates are removed from the incubator and cells are carefully washed one time with 3 mL PBS/well, aspirate twice to dryness and add 0.5 mL 1× LD-SDS sample buffer. Plates are returned to the 37°C incubator. Once all wells are processed, the plates are placed on a rocking shaker for ~15 min at room temperature. All samples are subsequently transferred to scintillation counting vials using a 1 mL pipettman and 4 mL scintillation fluid is added and radioactivity determined.
6. Calculations: Radioactivity in the 0 time nonspecific binding controls is subtracted from the average of the 0 time total binding samples. The last time point nonspecific binding control is subtracted from the average of all other time points. The total fmol bound [<sup>3</sup>H]-label is determined based on the cpm/fmol of the starting labeling solutions. These data are plotted on a semi-log scale as fmol bound relative to time. The half-time of dissociation is the time required to reduce specific binding by 50%.

Examples of measurements of [<sup>3</sup>H]R1881 dissociation rates from full-length wild-type AR and the effect of naturally occurring



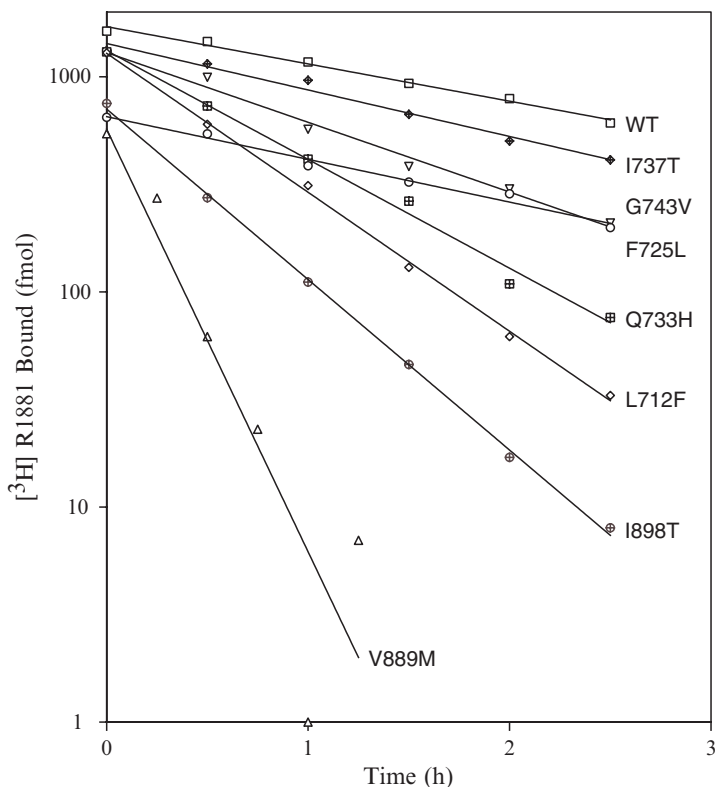


Fig. 1. Dissociation rate measurements of [ $^3\text{H}$ ]R1881 from full-length wild-type and mutant AR. Dissociation rates of [ $^3\text{H}$ ]R1881 were determined at 37°C in whole cell cultures as described in the text by expressing wild-type pCMVhAR and the indicated pCMVhAR mutants in COS cells. The naturally occurring mutations that cause partial or complete androgen insensitivity recreated in pCMVhAR increase the androgen dissociation rate, even though the equilibrium binding affinity is similar to wild-type AR (17).

mutations in or near the AF2 site of the ligand-binding domain that cause partial or complete androgen insensitivity are shown in [Fig. 1](#).

### 3.2. Receptor Degradation Assay

#### Day 1

COS cells are plated in 6 mL DMEM containing 10% BCS at  $2 \times 10^6$  cells/10 cm dish.

#### Day 2

1. Cell density should be ~50% confluence. In a 15 mL Falcon tube combine (per dish) 2.85 mL of 1× TBS, 2–10  $\mu\text{g}$  of pCMVhAR expression vector DNA and 0.33 mL of 5 mg/mL DEAE-dextran solution and vortex. Scale up as needed according to the number of dishes. DNA aliquots can be prepared 3 days in advance and stored at  $-20^\circ\text{C}$ .
2. Aspirate the media, vortex the DNA solution, and add 3 mL/dish. Place cells at 37°C for 30 min.

3. Aspirate the DNA solution and add 6 mL chloroquine solution/dish and incubate for 3 h at 37°C. Chloroquine is prepared by adding 1 mL of 5 mg/mL chloroquine stock to 100 mL DMEM containing 10% BCS and additives.
4. Aspirate the media and glycerol stock by adding 3 mL of 15% glycerol in DMEM containing 10% BCS and incubate for 4 min at room temperature timing carefully.
5. Aspirate the media, wash carefully with 8 mL PBS/dish, add 6 mL DMEM containing 10% BCS and incubate overnight at 37°C.

### Day 3

Exchange the media to 6 mL serum free, phenol red medium in the absence and presence of test reagents such as hormones and growth factors.

### Day 4

1. Exchange the media to 4 mL methionine-free, cystine-free, serum-free medium containing the test reagents such as hormones and growth factors and incubate for 20 min at 37°C.
2. In a chemical fume hood add 100  $\mu$ L/plate of 8.0  $\mu$ Ci/ $\mu$ L [<sup>35</sup>S]methionine diluted stock prepared in methionine-free, serum-free medium for a final concentration of 60–80  $\mu$ Ci [<sup>35</sup>S]methionine/4 mL per 10 cm dish. Place the cells in an unsealed plexiglass box in the 37°C tissue culture cell incubator and incubate for 20–30 min.
3. At each time point, place the cells to be harvested on ice in the fume hood, aspirate the media using an [<sup>35</sup>S] waste container, wash twice with 8 mL cold PBS and harvest by scraping into 1 mL cold PBS. Pellet the cells at 4,000  $\times g$  for 1 min at 4°C. To all remaining plates, replace the 8 mL serum-free, phenol-red medium with and without hormone additives at room temperature and return to the plexiglass box at 37°C.
4. Extract each cell pellet in 1 mL IP lysis buffer and shear the DNA using a 1 mL pipette several times up and down. Tumble for 15 min at 4°C and sediment at 18,000  $\times g$  for 20 min at 4°C.
5. Determine the protein concentration and transfer equal amounts of supernatant protein to a microfuge tube containing the antibody of choice and 10  $\mu$ L washed packed protein A-agarose from a 5% suspension. Tumble at 4°C for 2 h or incubate overnight in a 4°C cold room with the samples tumbling and packed on ice. Antibodies useful for immunoprecipitation are those described in **Subheading 2.2, item 11**.
6. Sediment at 1,000  $\times g$  for 2 min at 4°C. Wash the pellets twice with 0.5 mL of IP lysis buffer, each time carefully removing the supernatant and avoiding loss of the agarose resin.

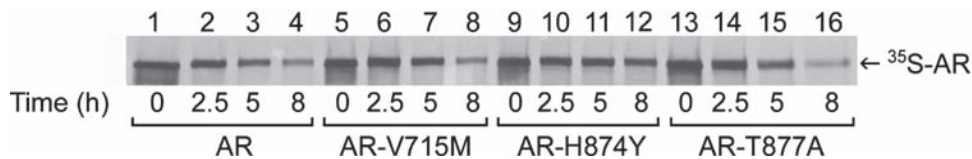


Fig. 2. Increased AR stabilization by naturally occurring mutations in prostate cancer. Wild-type pCMVhAR and pCMVhAR with the indicated AR mutations identified in prostate cancer specimens and cell lines were expressed in COS cells and degradation rates determined at 37°C by incubation with [<sup>35</sup>S]methionine as described in the text. Degradation rates were determined for full-length wild-type AR,  $t_{1/2} = 1.8$  h; AR-V715M,  $t_{1/2} = 2.8$  h; CWR22 prostate cancer xenograph AR-H874Y,  $t_{1/2} = 3.2$  h; and LNCaP cell line AR-T877A,  $t_{1/2} = 2.0$  h (17).

7. Add 50  $\mu$ l of 2 $\times$  IP-SDS sample buffer, boil for 8 min, sediment the agarose beads and apply the supernatant to a 10% acrylamide gel containing SDS and separate by electrophoresis for  $\sim$ 3 h at 160 V.
8. Dry the gel or transfer to a nitrocellulose membrane overnight and quantitate using a phosphoimager.

An example of an AR degradation study performed as described above is shown in Fig. 2. AR is stabilized to a greater extent by bound testosterone when naturally occurring mutations that arise in prostate cancer are introduced into full-length AR.

#### 4. Notes

1. *Cell lines*: The choice of cell lines for ligand binding, dissociation, and receptor degradation assays is important. Accurate measurements of [<sup>3</sup>H]-ligand dissociation and receptor degradation require high receptor expression levels. Cell lines that express the SV40 T antigen amplify the plasmid copy number to produce high receptor expression. Examples of useful cell lines are monkey kidney COS cells and human embryonic kidney HEK-293 cells. Monkey kidney CV-1 cells do not express the SV40 T-antigen and thus transient receptor expression levels are lower. CV1 cells are useful for nuclear receptor transcription assays using luciferase reporter vectors, but not for ligand dissociation or receptor degradation assays. To measure androgen dissociation rates from endogenous AR in cell lines such as human foreskin fibroblasts or prostate cancer cell lines, the number of cells used for each time point may be increased by using 6-well plates, 6 or 10 cm dishes depending on the receptor level.
2. *Radiolabeled ligand*: A radiolabeled ligand is required to determine the ligand dissociation rate. This limits the applicability of

the method to ligands that are available in radiolabeled form. Dissociation rates of the common AR antagonists, hydroxyflutamide and casodex, have not been determined because they are not readily available in radiolabeled form. Results with the high affinity [ $^3\text{H}$ ]-labeled AR antagonist RU-56187 indicate that AR antagonists dissociate with much faster rates than agonists (12).

3. *Ligand solubility*: To measure the dissociation rate of a bound radiolabeled ligand, it is necessary to block rebinding of the [ $^3\text{H}$ ]-labeled ligand. This is done by adding a large excess of a high affinity unlabeled ligand. The unlabeled chase ligand must have sufficient solubility in the  $50\ \mu\text{M}$  range. DHT has relatively low water solubility of  $\sim 25\ \mu\text{M}$  compared with  $250\ \mu\text{M}$  T and  $1\text{--}2\ \text{mM}$  R1881. The unlabeled chase ligand must also bind with high affinity to block rebinding of the [ $^3\text{H}$ ]-labeled ligand. Because the ligand dissociation reaction is pseudo-first order and thus independent of the high affinity unlabeled chase ligand, the more soluble R1881 is used as the unlabeled chase ligand with [ $^3\text{H}$ ]DHT to avoid the complications of low water solubility of unlabeled DHT (13). Methods such as sample dilution are not applicable as the assays described are performed in whole cells in culture. With sufficient levels of specific binding, low levels of nonspecific binding, and efficient handling of the plates during the assay, dissociation rates can be determined with relatively high accuracy and precision.
4. *Transfection method*: DEAE dextran is used to transfect COS or HEK-293 cells because it is a reproducible and inexpensive procedure. Lipid-based methods such as Effectene (Qiagen, Germany) and FuGENE 6 transfection reagent (Roche Applied Science, Indianapolis, IN) may be used with greater efficiency but are more expensive and not necessary. DNAs are routinely aliquoted 3 days before the experiment into Falcon tubes and stored at  $-20^\circ\text{C}$  without loss of activity or aliquoted the same day of the experiment. Samples stored for 1 week or more at  $-20^\circ\text{C}$  should not be used.
5. *Phenol red*: Because of its estrogen-like activity, phenol red is typically avoided when cells are treated with androgen. However, we have not detected an effect of phenol red on AR transcriptional activity. The medium is also typically serum free during androgen treatments, although the amount of androgen in normal serum may be low. If cells require serum, charcoal stripped serum may be used with minimal AR transcriptional activity. For studies with the estrogen receptor, phenol red should be avoided and multiple treatments of serum with charcoal may be required to minimize serum activation of the estrogen receptor.

6. *Precautions for labeling transfected cells:* Two days after transfection, COS cells only weakly adhere to the plates. Care must be taken with the PBS washes and media additions to avoid cell loss. Media and PBS should be added to the side of the well to minimize cell detachment that contributes to poor reproducibility. Because the reactions are timed, plates must be removed from the incubator and the time points processed rapidly. A 37°C heating block might be used in the tissue culture hood to better maintain 37°C. However, we routinely perform the assay by minimizing the time the cells are out of the incubator.

All procedures involving [<sup>35</sup>S]-labeling should be performed with cells placed in an unsealed plexiglass box. All washing and harvesting of cells is performed in a fume hood to minimize exposure to possible volatile [<sup>35</sup>S]-labeled material. Addition of HEPES buffer to DMEM helps to maintain the pH while the plates are in the 37°C tissue culture incubator. The plexiglass box is not sealed so that equilibrium with the 5% CO<sub>2</sub> environment is maintained.

Occasionally the 0 time points result in lower levels of labeling compared with early times after the addition of the chase. This may be due to intracellular stores of [<sup>35</sup>S]methionine and may be remedied by shortening the labeling time, including additional short time points after the start of the chase, and amending the chase media with 2 mM unlabeled methionine. It is important to immunoprecipitate equal amounts of protein from the different test samples particularly when different hormone treatments are used on the cells. The medium should be changed on all plates at each time point to minimize reincorporation of [<sup>35</sup>S]methionine.

## References

1. Wilson, E. M., and French, F. S. (1976) Binding properties of androgen receptors: evidence for identical receptors in rat testis, epididymis, and prostate. *J. Biol. Chem.* **251**, 5620–5629.
2. Wilson, E. M., and French, F. S. (1979) Effects of proteases and protease inhibitors on the 4.5S and 8S androgen receptor. *J. Biol. Chem.* **254**, 6310–6319.
3. Lubahn, D. B., Joseph, D. R., Sullivan, P. M., Willard, H. F., French, F. S., and Wilson, E. M. (1988) Cloning of human androgen receptor cDNA and localization to the X chromosome. *Science* **240**, 327–330.
4. Lubahn, D. B., Joseph, D. R., Sar, M., Tan, J. A., Higgs, H. N., Larson, R. E., French, F. S., and Wilson, E. M. (1988) The human androgen receptor: complementary DNA cloning, sequence analysis and gene expression in prostate. *Mol. Endocrinol.* **2**, 1265–1275.
5. Chang, C. S., Kokontis, J., and Liao, S. T. (1988) Molecular cloning of human and rat complementary DNA encoding androgen receptors. *Science* **240**, 324–326.
6. Tan, J. A., Joseph, D. R., Quarmby, V. E., Lubahn, D. B., Sar, M., French, F. S., and Wilson, E. M. (1988) The rat androgen receptor: primary structure, autoregulation of its messenger RNA and immunocytochemical localization of the receptor protein. *Mol. Endocrinol.* **2**, 1276–1285.
7. Langley, E., Zhou, Z. X., and Wilson, E. M. (1995) Evidence for an antiparallel orientation of the ligand activated human andro-

- gen receptor dimer. *J. Biol. Chem.* **270**, 29983–29990.
8. Langley, E., Kempainen, J. A., and Wilson, E. M. (1998) Intermolecular NH<sub>2</sub>-/carboxyl-terminal interactions in androgen receptor dimerization revealed by mutations that cause androgen insensitivity. *J. Biol. Chem.* **273**, 92–101.
  9. He, B., Kempainen, J. A., and Wilson, E. M. (2000) FXXLF and WXXLF sequences mediate the NH<sub>2</sub>-terminal interaction with the ligand binding domain of the androgen receptor. *J. Biol. Chem.* **275**, 22986–22994.
  10. He, B., Bowen, N. T., Minges, J. T., and Wilson, E. M. (2001) Androgen-induced NH<sub>2</sub>- and carboxyl-terminal interaction inhibits p160 coactivator recruitment by activation function 2. *J. Biol. Chem.* **276**, 42293–42301.
  11. Zhou, Z. X., Lane, M. V., Kempainen, J. A., French, F. S., and Wilson, E. M. (1995) Specificity of ligand dependent androgen receptor stabilization: receptor domain interactions influence ligand dissociation and receptor stability. *Mol. Endocrinol.* **9**, 208–218.
  12. Kempainen, J. A., Langley, E., Wong, C. I., Bobseine, K., Kelce, W. R., and Wilson, E. M. (1999) Distinguishing androgen receptor agonists and antagonists: distinct mechanisms of activation by medroxyprogesterone acetate and dihydrotestosterone. *Mol. Endocrinol.* **13**, 440–454.
  13. Askew, E. B., Gampe, R. T., Stanley, T. B., Faggart, J. L., and Wilson, E. M. (2007) Modulation of androgen receptor activation function 2 by testosterone and dihydrotestosterone. *J. Biol. Chem.* **282**, 25801–25816.
  14. Kempainen, J. A., Lane, M. V., Sar, M., and Wilson, E. M. (1992) Androgen receptor phosphorylation, turnover, nuclear transport and transcriptional activation: specificity for steroids and antihormones. *J. Biol. Chem.* **267**, 968–974.
  15. He, B., Kempainen, J. A., Voegel, J. J., Gronemeyer, H., and Wilson, E. M. (1999) Activation function 2 in the human androgen receptor ligand binding domain mediates interdomain communication with the NH<sub>2</sub>-terminal domain. *J. Biol. Chem.* **274**, 37219–37225.
  16. Quigley, C. A., Tan, J. A., He, B., Zhou, Z. X., Mebarki, F., Morel, Y., Forest, M., Chatelain, P., Ritzen, E. M., French, F. S., and Wilson, E. M. (2004) Partial androgen insensitivity with phenotypic variation caused by androgen receptor mutations that disrupt activation function 2 and the NH<sub>2</sub>- and carboxyl-terminal interaction. *Mech. Ageing Dev.* **125**, 683–695.
  17. He, B., Gampe, R. T., Hnat, A. T., Faggart, J. L., Minges, J. T., French, F. S., and Wilson, E. M. (2006) Probing the functional link between androgen receptor coactivator and ligand binding sites in prostate cancer and androgen insensitivity. *J. Biol. Chem.* **281**, 6648–6663.
  18. Quigley, C. A., De Bellis, A., Marschke, K. B., El-Awady, M. K., Wilson, E. M., and French, F. S. (1995) Androgen receptor defects: historical, clinical and molecular perspectives. *Endocrine Reviews* **16**, 271–321.
  19. Quarmby, V. E., Yarbrough, W. G., Lubahn, D. B., French, F. S., and Wilson, E. M. (1990) Autologous down regulation of androgen receptor messenger ribonucleic acid. *Mol. Endocrinol.* **4**, 22–28.
  20. Bai, S., and Wilson, E. M. (2008) EGF dependent phosphorylation and ubiquitinylation of MAGE-11 regulates its interaction with the androgen receptor. *Mol. Cell. Biol.* **28**, in press

# Chapter 3

## Flow Cytometry as a Tool for Measurement of Steroid Hormone Receptor Protein Expression in Leukocytes

Cherie L. Butts and Esther M. Sternberg

### Abstract

Measurement of protein expression in live, intact cells using flow cytometry (FC) has been employed for several decades in the areas of immunology, cell biology, and molecular biology. More recently, this technique has found appreciation in applied scientific fields, including cancer biology and endocrinology, to serve as a tool for identifying cells more likely to respond to specific treatments. FC, also referred to as fluorescence-activated cell sorting (FACS), is an antibody-based method that provides the user with an ability to identify proteins expressed on surfaces of cells as well as in the cytoplasm, including steroid hormone receptors. This technique is most useful for examining specific cell types in a heterogeneous population and therefore can be used to identify cells more likely to respond to treatments based on expression of the appropriate receptor. Isolation of purified subpopulations for further manipulation and investigation of functional capacity is also possible using a cell sorter, which uses similar technology to isolate cells for use by the researcher. This is especially important for studying responses of less abundant cell populations in tissues that express high levels of a target protein or receptor of interest. Furthermore, FACS analysis is clinically useful to identify and isolate responsive cell populations, which may be less appreciable in whole tissues because of the diluting effects of surrounding, nonresponding cell types. Immune cells are commonly utilized as a source of cell populations in the FC technique and have previously been shown to express steroid hormone receptors and respond to steroid hormone treatment. Here, we demonstrate that FC is a useful tool for identifying immune cells expressing steroid hormone receptor protein. This method can also be easily expanded to include other, nonimmune cell populations to address specific research questions related to steroid hormone receptor biology.

**Key words:** Flow cytometry, Steroid hormone receptors, Leukocytes.

---

### 1. Introduction

Flow cytometry was first developed by researchers at Stanford University who set out to create a system for identifying and isolating live cells that could be used for further culturing and manipulation



(1). This method creatively uses fluorescently-tagged antibodies to identify cells expressing a protein or receptor of interest (information on fluorochromes currently available for use is described and reviewed in **ref.** (2)). This method may also be similarly used with green fluorescent protein (GFP)-tagged antibodies. Samples are analyzed in a flow cytometer using lasers that can detect an array of information about cell. Detectors aimed directly in line with a single laser beam (forward scatter, FSC) determine its cell size while detectors aimed perpendicular to the laser beam (side scatter, SSC) assess granularity within the cytoplasm of cells (3–5). Fluorescent detectors within the flow cytometer are used to determine amount of fluorescence emitted by cells, which indicates level of protein expression. Currently, approximately 12 fluorochromes can be analyzed at one time.

Flow cytometry is particularly valuable as it can determine not only whether a cell is expressing the protein of interest but also indicates the amount of protein expressed by a single cell on the basis of intensity of fluorescence. In addition, flow cytometry can be used to study expression of proteins on the surface of cells as well as those localized within the cytoplasm, which can be achieved using a simple permeabilization step. Given the powerful tool of flow cytometry, it is possible to determine specific cell populations within a tissue expressing such intracellular proteins as steroid hormone receptors to determine cells most relevant and more likely to respond to steroid hormone treatment. Previous studies by our group and others indicated usefulness of this technique in analyzing steroid hormone receptor expression in patient samples, cell lines, and murine models (6–10). Another advantage to this technique is that expression of proteins can be correlated with degree of activation, maturation, or differentiation of given cell types (11). Finally, if complex mixtures of cells are present, flow cytometry can be used to sort subpopulations of cells and identify steroid hormone receptors expressed by specific cell types for further investigation. We describe here a detailed method for assessing expression of steroid hormone receptor protein in immune cells collected from rats using flow cytometry and demonstrate the feasibility of looking at other cell populations using this method.

---

## 2. Materials

### 2.1. Isolation of Cells

1. *Conditioned medium*: RPMI 1640 (Mediatech; Herndon, VA) containing 10% charcoal-stripped serum (CSS) (Biomeda; Foster City, CA) (*see* [Note 1](#)); 2% L-glutamine



and 2% penicillin–streptomycin (both from Sigma; St. Louis, MO).

2. *Cultured Cell Collection*: Polypropylene tubes (15 mL, Corning brand; Fisher Scientific; Morris Plains, NJ), conditioned medium, phosphate-buffered saline (1× PBS).
3. *Tissue Collection*: Polypropylene tubes (15 mL, Corning brand; Fisher Scientific; Morris Plains, NJ), conditioned medium, 1× PBS.
4. *Tissue Dissection*: scalpel, forceps, stainless steel surgical blade (10, Feather brand; Fisher Scientific; Morris Plains, NJ), polystyrene tissue culture dish (60 × 15 mm style; BD Biosciences; San Diego, CA), 1× PBS.
5. *Tissue Digestion*: deoxyribonuclease I from bovine pancreas, type IV (Sigma), collagenase from *Clostridium histolyticum*, type IV (Sigma), hyaluronidase from sheep testes, type IV (Sigma).
6. *Cell Filtration*: Polypropylene tubes (50 mL, Corning brand; Fisher Scientific), cell strainer (70 μm; BD Biosciences; San Diego, CA), 1× PBS.
7. *Immune Cell Isolation (removal of unwanted or nonimmune cell populations)*: BioWhittaker ACK Lysing Buffer (Cambrex; Walkersville, MD) to remove erythrocytes or Ficoll-Hypaque solution (Sigma-Aldrich, St. Louis, MO) to remove erythrocytes and granulocytes.

## 2.2. Sample Preparation for Flow Cytometer

1. Polystyrene tubes (5 mL) (Falcon brand; BD Biosciences; San Diego, CA)
2. *FACS Buffer*: 1× PBS, 2% CSS and 0.2% sodium azide.
3. *Primary Antibodies*: purified anti-rat glucocorticoid receptor (GR, recognizes and binds to amino acid residues 346–367) (reconstituted in PBS to 100 μg/mL, diluted 1:5,000); purified anti-rat progesterone receptor (PR, recognizes and binds to amino acid residues 533–547) (reconstituted in PBS to 100 μg/mL; diluted 1:5,000); and purified anti-rat androgen receptor (AR, recognizes and binds to amino acid residues 321–572) (reconstituted in PBS to 100 μg/mL; diluted 1:5,000) – all purchased from Affinity Bioreagents (Golden, CO); phycoerythrin (PE)-conjugated anti-rat CD45 expressed by leukocyte (immune cell) populations (0.1 mg/mL; BD Biosciences; San Diego, CA). Isotype control antibodies included the following: purified mouse IgG (PR control) (0.1 mg/mL; diluted 1:5,000) (BD Biosciences); purified rabbit IgG (GR and AR control) (1 mg/mL; diluted 1:10000) (R&D Systems; Minneapolis, MN); PE-conjugated mouse IgG1 (CD45 control) (0.1 mg/mL) (BD Biosciences).

4. *Secondary Antibodies*: fluorescein isothiocyanate (FITC)-conjugated goat anti-rabbit antibody (for GR and AR); fluorescein isothiocyanate (FITC)-conjugated goat anti-mouse antibody (for PR).
5. Cytotfix/Cytoperm solution and wash buffer (BD Biosciences, San Diego, CA).
6. Rat serum (Sigma) to prevent nonspecific binding of antibodies within the cytoplasm of cells.
7. Paraformaldehyde solution (4%) to generate fixed cells if cells cannot be examined within 24–48 h of collection and staining with antibodies.

### **2.3. Data Collection and Analysis**

1. BD FACSCalibur cytometer (BD Biosciences), with computer interface (Macintosh or PC).
2. Isotonic saline for FACSCalibur sheath reservoir and 10% bleach in deionized water for FACSCalibur waste reservoir.
3. *Data retrieval software (any of the following)*: BD CellQuest (BD Biosciences), BD CellQuest Pro (BD Biosciences), or FlowJo (Tree Star, Inc.; Ashland, OR).
4. *Highlighting of specific cell populations using a color coding system*: Paint-A-Gate software (BD Bioscience), which provides figures readily available for use in presentations.
5. *Statistical analysis software*: A number of different statistical packages, including basic functions included in Microsoft Excel, can be used to analyze data following acquisition in the flow cytometer.

---

## **3. Methods**

### **3.1. Generating Single-Cell Suspensions**

Live cells obtained from culture techniques or isolated from tissues can be easily prepared for analysis of protein expression using flow cytometry. Frozen tissues can also be considered for this method but should be allowed to grow overnight (at least 24 h) in tissue culture conditions to ensure nonviable cells are removed from the sample. Lymphoid organs, such as bone marrow and spleen, provide a plentiful source of immune cells. Other tissues, such as liver and kidney, can also be used for analysis of immune cells, although they have markedly reduced populations of immune cells. In addition, immune cells can be readily isolated from peripheral blood but require measures to remove erythrocytes in order to eliminate this unwanted cell population. The following includes detailed information on generating a single cell suspension to prepare for use in a flow cytometer. For cells that have

been cultured, these can be collected and counted as dictated in **Steps 3–6**:

1. Collect tissue from animals and place in separate 15-mL polypropylene tubes with 5 mL conditioned medium in each tube.
2. Transfer tissue to 15 mm culture dish (BD Biosciences) for dissection using scalpel and forceps. For spleen, continual application of pressure to tissue using forceps alone is sufficient to generate a single cell suspension. For other lymphoid tissues and non-lymphoid tissues, use of a scalpel with a surgical steel blade (#10) can generate smaller pieces of tissue. Supplementing the sample with 1× PBS (up to an additional 2 mL) to culture dish will further promote a single-cell suspension. If necessary, digestion with DNase I, collagenase, and hyaluronidase (all from Sigma) for at least 1 h at 37°C may be necessary to further break up tissue. Prior to enzymatic digestion, centrifuge sample for 5 min (900 × *g*) at 25°C to pellet cells. Remove supernatant by decanting, and resuspend pellet in enzymes to ensure maximal digestion. After digestion step, add 5 mL of conditioned medium to each tube to neutralize enzyme activity.
3. Following dissection and digestion of tissue or collection of cells from culturing conditions, it is important to filter sample to ensure a uniformly single-cell suspension and to remove any clumps or tissue debris that could potentially clog the flow cytometer. Transfer sample into a 50-mL polypropylene tube with a 70 μm cell strainer (BD Biosciences) placed in the tube opening (*see Note 2*). Mix sample (pipetting up and down to loosen clumps of cells), and slowly pour sample over cell strainer. To remove remaining debris, fill tube to 40 mL total volume using 1× PBS. Discard cell strainer.
4. For removal of only erythrocytes (retains polymorphonuclear and mononuclear immune cell populations), centrifuge samples for 5 min (900 × *g*) to pellet cells. Resuspend cell pellet in ACK Lysing Buffer for 10 min at 37°C. Centrifuge cells for 5 min (900 × *g*) at 25°C to pellet cells, and remove supernatant by decanting. Resuspend pellet in 10 mL conditioned media, depending on the concentration of cells, to prepare for cell counts (*see Note 3*).
5. For removal of erythrocytes and granulocytes (retains mononuclear immune cell populations), place 10 mL of Ficoll-Hypaque solution in empty 50-mL polypropylene tube for each sample. *Very* slowly add sample to the tube, ensuring the Ficoll layer is not disturbed (*see Note 4*). Samples should be carefully placed into centrifuge (not disturbing Ficoll layer) and centrifuged 30 min (900 × *g*) at 4°C. Samples should then be carefully removed from centrifuge, and the layer containing

immune cells (cloudy region just above Ficoll layer) can be collected and transferred to empty 50-mL tube (*see Note 5*). 1× PBS should be added to tube to fill to a total volume of 50 mL to neutralize effects of Ficoll contaminant in the collected cell suspension. Centrifuge samples for 10 min ( $900 \times g$ ) at 4°C to pellet cells. Remove supernatant by decanting, and resuspend cells in 10 mL conditioned media, depending on concentration of cells, to prepare for cell counts.

6. Cells should be counted (using trypan blue for verifying cell viability) to determine numbers of viable cells available for analysis of protein expression using flow cytometry (*see Note 3*). A range of cell numbers is expected, depending on tissue type. Lymphoid tissues (i.e., spleen) will yield higher numbers ( $\sim 2.0 \times 10^8$ ), whereas non-lymphoid tissues (i.e., liver) will likely have fewer total leukocyte numbers ( $\sim 4.0 \times 10^7$ ).

### **3.2. Labeling of Samples for Use in Flow Cytometer**

1. Flow cytometry entails the use of fluorochrome-conjugated antibodies (*see Note 6*). Therefore, it is recommended that researcher conduct this portion of the experiment in a room with very little light or with limited exposure to light. Using lighted biosafety cabinet during addition of antibodies is acceptable as exposure is minimal.
2. Determine the number of polystyrene tubes required for experiment. This should include a tube containing cells only to measure autofluorescence (no antibodies); a tube containing directly-conjugated isotype control antibodies, if primary antibody is conjugated with fluorochrome; if secondary antibody is conjugated, separate tubes containing sample with primary antibody as well as sample with primary and secondary fluorochrome-conjugated antibody should be prepared to serve as proper controls. For multiple fluorochrome-conjugated antibodies used in a single sample (i.e., FITC and PE antibodies together), tubes containing isotype control antibodies with directly-conjugated fluorochromes should be prepared with samples requiring both directly-conjugated fluorochromes and those requiring secondary antibodies. Remaining tubes should account for specific proteins or receptor of interest for analysis. An example is provided in [Table 1](#) (*see Note 11*).
3. For each polystyrene tube, transfer  $1.0 \times 10^6$  cells of sample. If cell suspension contains less than  $1.0 \times 10^6$  cells/mL, centrifuge sample for 5 min ( $900 \times g$ ) at 4°C to pellet cells. Remove supernatant by decanting, and resuspend cell pellet in FACS buffer at  $1.0 \times 10^6$  cells/mL (*see Note 7*).
4. After samples have been transferred to polystyrene tubes, add 2 mL FACS buffer to each tube to wash cells. Centrifuge tubes for 5 min ( $900 \times g$ ) at 4°C to pellet cells.

**Table 1**  
**Sample list for steroid hormone receptor labeling**  
**of immune cells using flow cytometry**

Tube no.	Fluorochrome I (FITC)	Fluorochrome II (PE)	Comments
1	None	None	Autofluorescence sample
2		Mouse IgG	Isotype control for CD45
3		CD45	Expressed on surface of leukocytes
4	Purified mouse IgG	CD45	Control for primary antibody
5	Purified mouse IgG/ FITC Goat anti-mouse IgG	CD45	Isotype control for PR
6	Purified PR/FITC goat anti-mouse IgG	CD45	Identifies cells expressing PR
7	Purified rabbit IgG	CD45	Control for primary antibody
8	Purified rabbit IgG/ FITC goat anti-mouse IgG	CD45	Isotype control for GR and AR
9	Purified GR/FITC goat anti-mouse IgG	CD45	Identifies cells expressing GR
10	Purified AR/FITC goat anti-mouse IgG	CD45	Identifies cells expressing AR

The following serves as an example of tubes and the appropriate antibodies to be added for cell labeling. This list includes a tube to measure autofluorescence (no antibodies added) as well as isotype controls and tubes to receive antibodies specific to the steroid hormone receptor of interest

- Remove supernatant by decanting, resuspend pellet in 2 mL FACS buffer (second wash step), and centrifuge tubes 5 min ( $900 \times g$ ) at  $4^{\circ}\text{C}$  to pellet cells.
- Remove supernatant by decanting, and vortex tubes (gently) to loosen cell pellet (*see Note 8*).
- Using separate pipette tips, add  $10\ \mu\text{L}$  PE-conjugated isotype control (mouse IgG) or anti-rat CD45 antibodies to appropriate

tubes (*see* **Table 1**). Thoroughly mix antibody with sample by pipetting up and down. Although this protocol includes information for isolating leukocyte populations, other markers for specific immune cell populations or other cell types can also be used to identify expression of steroid hormone receptors in cells.

8. Place all tubes (including tube containing sample for measuring autofluorescence) on ice (4°C) for 20 min in a dimly lit room to provide ample time for antibody to bind to CD45<sup>+</sup> cells (expressed by leukocyte populations).
9. Remove tubes from ice, add 2 mL FACS buffer to each tube to wash away excess antibody. Centrifuge tubes for 5 min (900 × *g*) at 4°C to pellet cells.
10. Remove supernatant by decanting. Loosen cell pellet by gently vortexing to prepare for intracellular labeling of steroid hormone receptors. Cells labeled only for determining expression of cell surface molecules or not receiving antibodies (autofluorescence) can remain on ice during intracellular labeling portion of the experiment.
11. Add 0.25 mL CytoFix/CytoPerm solution (BD Biosciences) to each tube for intracellular staining of steroid hormone receptors (*see* **Table 1**), and mix with resuspended cells. This solution will permeabilize and fix cells (*see* **Note 9**). Place tubes on ice for 15 min.
12. Remove cells from ice. Wash cells by adding 2 mL CytoFix/CytoPerm wash buffer (BD Biosciences) to each tube.
13. Centrifuge tubes for 5 min (900 × *g*) at 4°C to pellet cells. Remove supernatant by decanting. Loosen cell pellet by gently vortexing to prepare for intracellular labeling of steroid hormone receptors.
14. Using separate pipette tips, add 10 μl of rat serum to each tube. Serum provides a blocking mechanism that will inhibit nonspecific binding of antibodies to other intracellular proteins. Mix serum with cells by thoroughly pipetting up and down. Place tubes on ice for 10 min.
15. Using separate pipette tips, add 10 μl of purified isotype control (mouse IgG, rabbit IgG) or anti-rat steroid hormone receptor (PR, GR, AR) antibody to appropriate tube (*see* **Note 10**). Mix antibody with cells by thoroughly pipetting up and down. Place tubes on ice for 10 min (*see* **Note 11**).
16. Using separate pipette tips, add 10 μl of FITC-conjugated goat anti-mouse or anti-rabbit antibody to appropriate tubes (secondary antibody). Mix antibody with cells by thoroughly pipetting up and down. Place tubes on ice for 10 min.
17. Remove cells from ice. Wash cells by adding 2 mL FACS buffer. Centrifuge tubes for 5 min (900 × *g*) at 4°C to pellet

cells. Remove supernatant by decanting. Loosen cell pellet by gently vortexing.

18. If cells will be analyzed in flow cytometer within 48 h, add 1.0 mL FACS buffer to each tube. Cover with aluminum foil to prevent exposure to light.
19. If cells will be analyzed more than 48 h from time of staining, it is recommended to resuspend all samples in 1.0 mL of a 4% paraformaldehyde solution to fix cells. Although samples undergoing intracellular staining for steroid hormone receptor expression have been fixed with CytoFix/CytoPerm solution, resuspending all samples in 4% paraformaldehyde solution will provide consistency with analysis.

### **3.3. Acquisition of Steroid Hormone Receptor Expression Data Using Flow Cytometer**

1. Turn on FACSCalibur (BDBiosciences) and computer that will receive data from flow cytometer (*see Note 12*). The flow cytometer valve should be set to “Standby.” For most units, the flow cytometer must be turned on prior to the computer to ensure the computer recognizes it is connected to the instrument (*see Note 13*). The researcher should verify which equipment should be turned on first.
2. Check the sheath-fluid reservoir to ensure it contains a sufficient amount of isotonic saline and the waste reservoir to ensure waste has been removed and contains no more than 75 mL of a 10% bleach solution.
3. Launch CellQuest software on computer interface to begin acquisition of samples.
4. Choose the Dot Plot option under Plots menu (displays two parameters of information on a single frame); Select Acquisition. The X parameter should be FSC (Forward Scatter), and the Y parameter should be SSC (Side Scatter). Repeat this process to generate another dot plot on the screen. Choose FL2 (displays PE fluorescence) for X parameter and FL1 (displays FITC fluorescence) for Y parameter. If only one parameter of information is needed, the user may choose to select the Histogram option under Plots menu (displays a single parameter of information on frame). Choose parameter of information to display on the Y-axis.
5. Choose the Connect to Cytometer option under the Acquire menu to connect computer to the flow cytometer. An Acquisition Control box will appear on the Desktop.
6. Choose the Acquisition and Storage option under Acquire menu to select total number of cells to be collected for each sample by the flow cytometer.
7. Choose the Counters option under Acquire menu to see number of cells being collected as the machine acquires data.



8. Choose the Parameter Description option under Acquire menu to create a folder containing data files for each sample and provide specific information associated with the particular sample.
9. Choose the Detectors/Amps option under Cytometer menu to change settings on machine. This will require use of samples of a known size, intracellular granularity, and positive expression of protein of interest to compare with samples for each experiment.
10. Move sample arm of the flow cytometer to remove tube containing deionized water ( $\text{dH}_2\text{O}$ ). Gently vortex Autofluorescence Sample (contains no antibodies) to resuspend cells and generate a single-cell suspension. Place Autofluorescence Sample on flow cytometer stage, and reposition sample arm to ensure the machine acquires the data on sample. The Autofluorescence Sample provides the user with an opportunity to determine the most appropriate settings to account for sample-specific differences in flow cytometer readings.
11. Turn valve on flow cytometer to the Run position, and click on the Acquire button within Acquire Control box on the Desktop to begin collecting data. For Autofluorescence sample, the Setup box should be selected to provide an opportunity to change settings in the Detectors/Amps fields.
12. After settings are determined and saved, remove check mark from Setup box to begin collecting data to be saved on the file created for each sample. It may be useful to create a gate around a group of cells using a Polygon tool (found in the Tool Palette of flow cytometer software) to select a specific set of cells to be analyzed. For example, cells of a larger size or cells positive for expression of a specified parameter may be sufficient for purposes of the experiment). The user may also choose to select total number of cells for collection, based on gated population by indicating this within the Acquisition & Storage option under Acquire menu.
13. Rate of cell collection (Low, Med, Hi) by the flow cytometer may vary based on number of cells in each tube. No more than 1,500 events/second should be collected to prevent clogging machine (*see* [Note 15](#)).
14. Once the indicated number of events (cells) has been collected, the Autofluorescence Sample may be removed and replaced with next sample. Proceed with subsequent samples until a file has been generated for each sample collection.
15. Be sure to clean the machine with a tube containing the appropriate cleaning solution (10% bleach or other solution)

for at least 5 min. Return tube containing dH<sub>2</sub>O water to the stage of flow cytometer.

### 3.4. Data Analysis

1. Data analysis can be performed with a number of different software platforms currently available for use with flow cytometry data, including CellQuest and CellQuest Pro (BD Biosciences) and FlowJo (Tree Star, Inc.). In addition, Paint-A-Gate (BD Biosciences) allows the user to select specific cell populations using different colors to more prominently feature groups of cells (**Fig. 1**).
2. The selected software package allows the user to open files generated from a flow cytometer for subsequent analysis. Some software packages may require conversion of files prior to analysis. This, supplied application is usually with the flow cytometry software package.

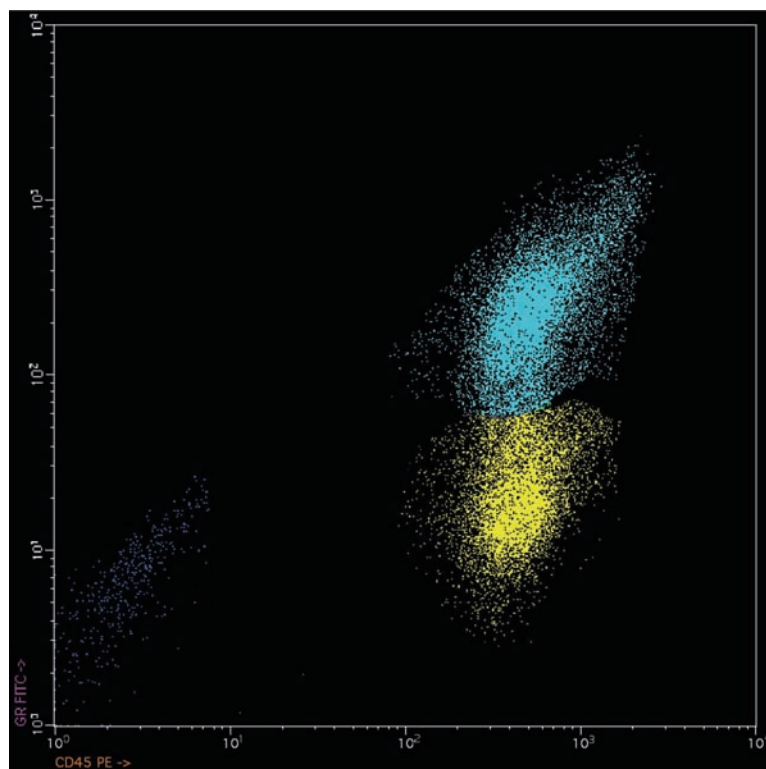


Fig. 1. Flow cytometer events displayed in a color-coded fashion. Paint-A-Gate software (BD Biosciences) allows the user to display groups of cells using a coloring system. In this dot-plot example, a population of immune cells (CD45<sup>+</sup>) collected from rat spleen is subdivided into cells expressing glucocorticoid receptor (CD45<sup>+</sup> GR<sup>+</sup>, *light blue*), not expressing GR (CD45<sup>+</sup> GR<sup>-</sup>, *yellow*), and nonimmune cells (CD45<sup>-</sup>, *dark blue*) (see *Color Plates*).

3. Data can be generated into dot plot or histogram formats for viewing (Figs. 2 and 3). There are also options to choose a contour plot or density plot, depending on needs of the researcher (see Note 14).
4. Each software package will provide flow cytometer-generated statistics on the collected data, which is easily accessible by selecting information under Stats menu. Information includes data on quadrants within a dot plot. Statistics include percentiles, raw numbers, and mean fluorescent intensity values for a sample (Fig. 4).

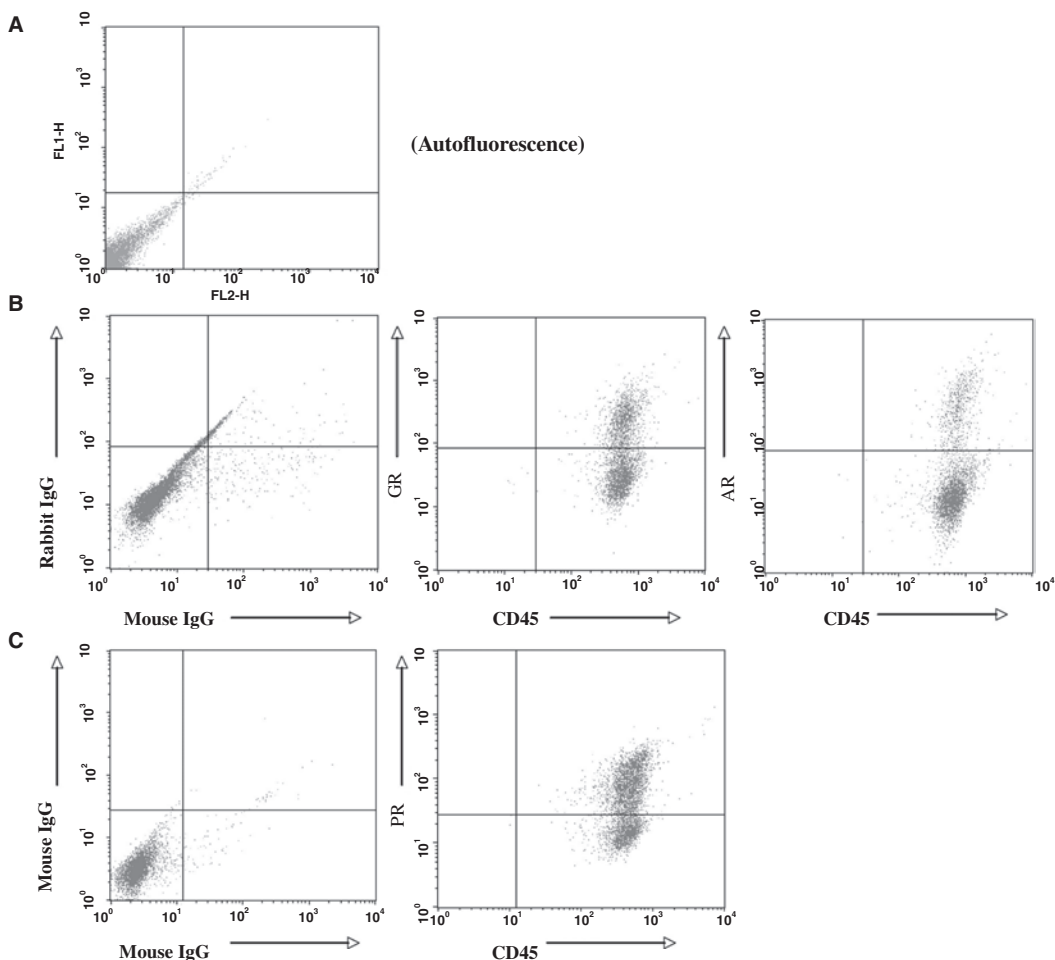


Fig. 2. Steroid hormone receptor expression in leukocytes displayed in dot-plot format expression by CD45<sup>+</sup> leukocytes obtained from rat spleen was analyzed using Cellquest Pro (BD Biosciences). Dot-plots exhibit two parameters: (A) Autofluorescence sample (no antibodies added); (B) expression of GR and AR by CD45<sup>+</sup> cells and the appropriate isotype control (Rabbit IgG); and (C) expression of PR by CD45<sup>+</sup> cells and isotype control (Mouse IgG). Cross-hatch lines (to determine positive and negative cells) were established on the basis of isotype controls. Upper right-hand quadrant represents cells expressing both CD45 and steroid hormone receptor of interest.

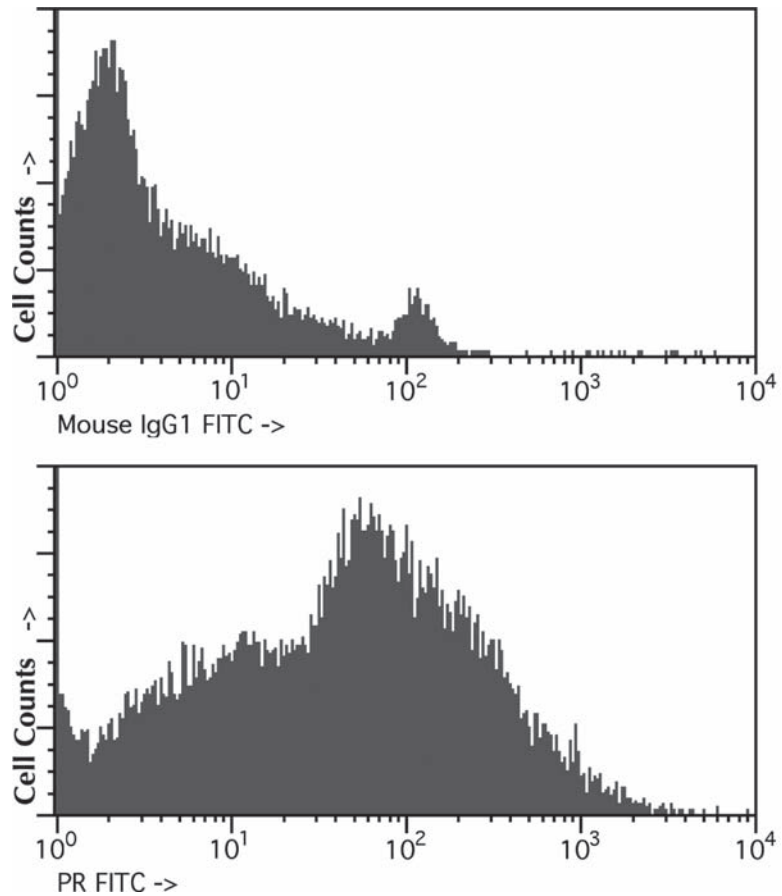


Fig. 3. Steroid hormone receptor expression in leukocytes displayed in histogram format. In this example, expression of the receptor for the steroid hormone progesterone (PR) by CD45<sup>+</sup> leukocytes obtained from rat spleen is shown using CellQuest Pro (BD Biosciences). Histograms exhibit a single parameter. PR expression is compared with the isotype control antibody (Mouse IgG), which provides information on background measure of fluorescence.

Total Events: 20000

Quad	Events	% Gated	% Total	X Mean	Y Mean
UL	1	0.01	0.01	24.36	85.05
UR	4094	29.74	20.47	400.97	776.75
LL	100	0.73	0.50	13.52	29.00
LR	9573	69.53	47.87	200.54	30.87

Fig. 4. Statistical information automatically generated by flow cytometry software provides different information about cells. In this example, quadrant statistics is provided for Fig. 3.2b. Quadrant statistics gives information generated from dot-plots, including percentiles for each quadrant (representing positive and negative expression of parameters); mean fluorescence intensity (representing average amount of receptor expressed by individual cells); and raw numbers of events (cells) collected for each quadrant. Shown is information generated from the sample analyzing CD45 and GR expression. Fluorescence intensity can only approximate receptor number and indicate cells expressing more or less of a receptor or protein of interest, unless sample with cells expressing known receptor number is used for comparison.

5. After data from software has been collected, values generated can undergo statistical analysis using any standard statistical package. For example, FlowJo has a feature to allow the user to transfer data into Microsoft Excel.

---

## 4. Notes

1. Charcoal-stripped serum (CSS) is used as some components of sera have demonstrated hormone-mimicking properties. CSS prevents unwanted changes in cellular activity that could potentially skew results of the experiment.
2. Cell strainer may need to be moistened using  $1\times$  PBS prior to addition of sample to ensure even distribution and maximal filtration across unit.
3. If cell collection results in high cell number yield, it will be important to dilute samples prior to obtaining cell counts. For this, a small portion ( $\sim 50\mu\text{l}$ ) can be collected from a well-mixed sample and added in PBS to make the appropriate dilution (i.e., 1:20 dilution factor) prior to obtaining cell counts and determining cell viability.
4. To ensure Ficoll layer is not disturbed, it might be useful to tilt 50-mL tube at an angle (approximately  $30\text{--}45^\circ$ ) prior to adding sample. If Ficoll layer is disturbed during addition of sample, it will likely reduce viability as Ficoll is toxic to cells.
5. To facilitate collection from tubes after Ficoll separation, it may be necessary to remove approximately 10–15 mL of supernatant (contains dead cells and tissue debris) before collecting leukocytes in cloudy region just above Ficoll layer.
6. One of the major limitations of flow cytometry is antibodies recognizing a protein or receptor of interest must be available for use. Without an appropriate antibody that is specific to the protein, it is not possible to utilize this method to measure protein expression.
7. If  $1 \times 10^6$  cells/tube are not available due to the number of tubes required for appropriate analysis or a low cell yield, the researcher may use as few as  $0.5 \times 10^6$  cells but no less than  $0.25 \times 10^6$  cells per tube to ensure sufficient numbers of cells for analysis.
8. Another common practice to loosen cell pellet prior to addition of antibodies is to grinch (scrape tube across grate of biosafety cabinet) instead of using a vortex.

9. To permeabilize cells for intracellular staining, use of 0.3% saponin in 1× PBS can be substituted for the CytoFix/CytoPerm solution.
10. For this protocol, only one steroid hormone receptor is analyzed for each tube. It is possible to analyze multiple steroid hormone receptors expressed by an individual cell but will likely result in problems with nonspecific binding due to multiple antibodies being introduced into the cytoplasmic region of cell. It is, therefore, highly recommended that the researcher analyze only one intracellular protein at a time in a single sample.
11. It would be useful to include a sample that does not express the steroid hormone receptor of interest (serves as a negative control) and a sample that is known to express the steroid hormone protein of interest (serves as a positive control) for each experiment.
12. There are a variety of flow cytometry instruments available from BD Biosciences, including FACScan, FACSAria, FACSCanto, and several other instruments that can be selected based on the needs of the researcher. In addition, there are other companies, including Beckman-Coulter, that offer a variety of flow cytometer instruments.
13. In the event the computer does not recognize the flow cytometer, restart both the computer and flow cytometer in the appropriate order.
14. If the fluorochrome is not stably coupled to the antibody, it will not be possible to identify fluorescence and measure amount of receptor expressed by cells. This could result in the generation of falsely negative data. Background fluorescence is sometimes higher in fixed cells, which occurs with use of the CytoFix/CytoPerm solution for intracellular staining of steroid hormone receptors. Therefore, titration of antibody to find optimal concentration for each sample may be necessary. It will be important to evaluate data generated from the flow cytometer and analyzed by software to gauge appropriate concentration for each experiment.
15. FACSCalibur may require lines to be flushed if no events are being acquired by the flow cytometer. This may be due to the machine being clogged by clumps of cells or air bubbles that have formed. Other problems preventing the flow cytometer from acquiring events include a cracked sample tube (transfer cells to new tube); sheath reservoir too low or not properly capped (check fluid amount and placement of sheath cap); or waste reservoir being full (remove waste fluid).

---

## Acknowledgments

This work was supported by the Intramural Research Program of the National Institute of Mental Health (NIMH)/NIH and a biodefense grant from the National Institute of Allergy & Infectious Diseases (NIAID)/NIH Intramural Research Program.

## References

1. Herzenberg LA, Sweet RG, Herzenberg LA. Fluorescence-activated cell sorting. *Sci Am* 1976;234(3):108–17.
2. Herzenberg LA, Parks D, Sahaf B, Perez O, Roederer M, Herzenberg LA. The history and future of the fluorescence activated cell sorter and flow cytometry: a view from Stanford. *Clin Chem* 2002;48(10):1819–27.
3. McCoy JP, Jr. Basic principles of flow cytometry. *Hematol Oncol Clin North Am* 2002;16(2):229–43.
4. McCoy JP, Jr., Carey JL, Krause JR. Quality control in flow cytometry for diagnostic pathology. I. Cell surface phenotyping and general laboratory procedures. *Am J Clin Pathol* 1990;93(4 Suppl 1):S27–37.
5. McCoy JP, Jr., Overton WR. A survey of current practices in clinical flow cytometry. *Am J Clin Pathol* 1996;106(1):82–6.
6. Berki T, Kumanovics G, Kumanovics A, Falus A, Ujhelyi E, Nemeth P. Production and flow cytometric application of a monoclonal anti-glucocorticoid receptor antibody. *J Immunol Methods* 1998;214(1–2):19–27.
7. Marchetti D, Van NT, Gametchu B, et al. Flow cytometric analysis of glucocorticoid receptor using monoclonal antibody and fluoresceinated ligand probes. *Cancer Res* 1989;49(4):863–9.
8. Butts CL, Shukair SA, Duncan KM, et al. Progesterone inhibits mature rat dendritic cells in a receptor-mediated fashion. *Int Immunol* 2007;19(3):287–96.
9. Butts CL, Shukair SA, Duncan KM, Harris CW, Belyavskaya E, Sternberg EM. Effects of dexamethasone on rat dendritic cell function. *Horm Metab Res* 2007;39(6):404–12.
10. Butts CL, Shukair SA, Duncan KM, Harris CW, Belyavskaya E, Sternberg EM. Evaluation of steroid hormone receptor protein expression in intact cells using flow cytometry. *Nucl Recept Signal* 2007;5:e007.
11. Boldizsar F, Palinkas L, Czompoly T, Bartis D, Nemeth P, Berki T. Low glucocorticoid receptor (GR), high Dig2 and low Bcl-2 expression in double positive thymocytes of BALB/c mice indicates their endogenous glucocorticoid hormone exposure. *Immunobiology* 2006;211(10):785–96.



# Chapter 4

## X-Ray Crystallography of Agonist/Antagonist-Bound Receptors

Ashley C.W. Pike

### Abstract

Crystallographic analysis of the ligand-binding domains of nuclear hormone receptors (NR) has provided a unique insight into the molecular events that underlie the ligand-mediated control of their transcriptional activity. The technique relies on preparing milligram quantities of protein, growing three-dimensional crystals of the desired protein–ligand complex, collecting X-ray diffraction data, and subsequently interpreting the derived electron density maps to reveal the structure of the complex.

**Key words:** Estrogen receptor, Protein purification, Crystallization, Crystal structure, Carboxymethylation.

---

### 1. Introduction

Attempts to crystallize intact nuclear receptors have been hindered by both interdomain flexibility and the unstructured nature of certain regions of the receptor in the absence of interaction partners. Instead a “divide and conquer” approach focussing on isolated ligand-binding domains (LBDs) has yielded a multitude of NR structures in the presence of different classes of ligand (agonists, partial agonists, antagonists, etc.) as well as with a range of coactivator/corepressor peptide fragments (1, 2). Such structural information has provided a better understanding of the relationship between the chemical structure of the ligand and the resultant conformation of the ligand-bound receptor and allowed the design of receptor-specific ligands acting either as agonists, antagonists, or selective receptor modulators (1).

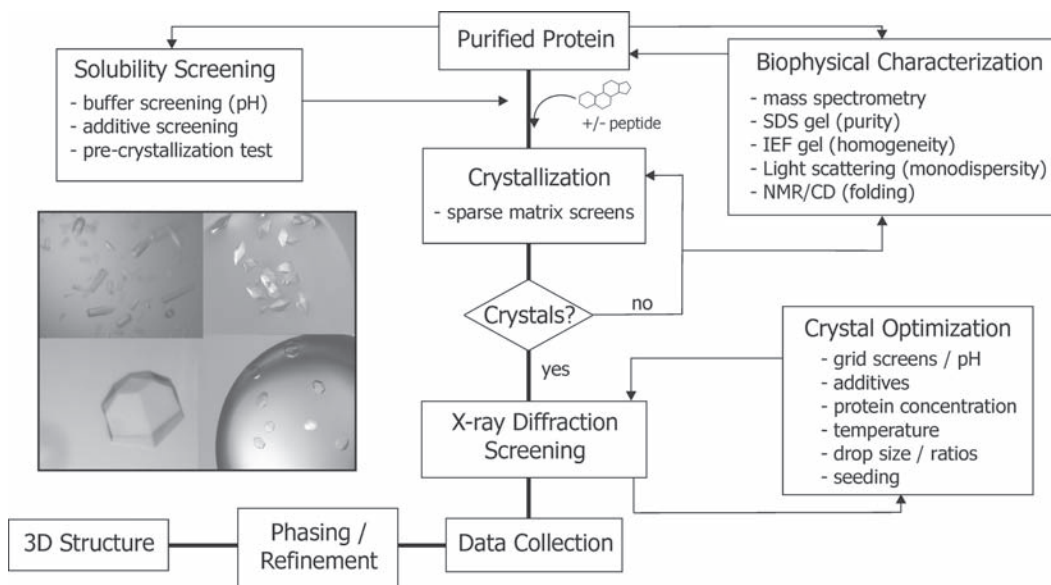


Fig. 1. From protein to 3D structure. A flowchart highlighting the different steps in the crystallization/structure solution process is shown. Inset: Representative examples of various ER-LBD ligand cocrystals.

The structure determination process is not a trivial undertaking, and it should be stressed at the outset that success is by no means guaranteed. The technique relies on obtaining single crystals suitable for diffraction analysis, and the resolution of a specific protein–ligand complex may prove impossible. Particular ligands may be sufficiently destabilizing or result in a population of conformational states that prevent or hinder successful crystallization.

Here, the preparation of the liganded estrogen receptor alpha LBD (ER $\alpha$ LBD) is described along with a protocol for setting up sitting-drop, vapor diffusion crystallization trials. Because of the more generic nature of the subsequent steps in the structure solution process (crystal optimization, data collection and reduction, phasing, refinement), the reader is referred to several excellent handbooks (3–5) and detailed protocols (6) for further practical information. An overview of the process is shown in Fig. 1.

## 2. Materials

### 2.1. Expression

1. Luria-Bertani (LB) medium: 10 g tryptone, 5 g yeast extract, 5 g NaCl per liter of distilled water. Autoclave in 1 L baffled shake flasks stoppered with foam bungs at 120°C for 20 min.

2. Ampicillin stock (100 mg/mL): 100 mg ampicillin/mL of sterile water. Filter sterilize solution through 0.2  $\mu$ m filter. Aliquot and store at  $-20^{\circ}\text{C}$ .
3. 1 M isopropyl- $\beta$ -D-thiogalactopyranoside (IPTG) stock. Dissolve IPTG in sterile water. Filter, sterilize, aliquot, and store at  $-20^{\circ}\text{C}$ .

## 2.2. Purification

1. Low/medium pressure chromatographic FPLC system (such as AKTA-FPLC).  
Columns/media: Ni-Sepharose Fast Flow resin; XK-16 column; Superdex S75 16/60 gel filtration column; MonoQ 5/5 or 10/10 ion exchange column (all from GE Healthcare).
2. Sonication buffer (SB): 25 mM Tris-HCl pH 8.0, 10% (v/v) glycerol, 10 mM  $\beta$ -mercaptoethanol ( $\beta$ -ME), 10 mM imidazole, 1 COMPLETE™ EDTA-free protease-inhibitor cocktail tablet per 50 mL SB (Roche Diagnostics), 1 mM AEBSE.
3. Ni-NTA running buffer#1 (NTA-RB1): 25 mM Tris-HCl pH 8.0, 10% (v/v) glycerol, 10 mM  $\beta$ -ME, 10 mM imidazole, 0.3 M NaCl.
4. Ni-NTA wash buffer (NTA-WB): 25 mM Tris-HCl pH 8.0, 10% (v/v) glycerol, 10 mM  $\beta$ -ME, 100 mM imidazole, 0.3 M NaCl.
5. IAA-1 buffer: 10 mM solution of iodoacetic acid (IAA) in 25 mM Tris-HCl pH 8.1. Solutions of IAA are light-sensitive and should be protected accordingly.
6. E2-ligand solution: 25 mM Tris 8.1, 100  $\mu$ M beta-estradiol (*light sensitive*) (see [Note 1](#)).
7. Ni-NTA elution buffer (NTA-EB): 25 mM Tris 8.1, 0.4 M imidazole.
8. Thrombin stock (0.03 U/ $\mu$ L): Dissolve bovine thrombin (Roche Diagnostics – 30 units) in 1 mL water. Store aliquots (50  $\mu$ L) at  $-20^{\circ}\text{C}$ . Thaw on ice and use as required.
9. Ni-NTA running buffer#2 (NTA-RB2): 25 mM Tris-HCl pH 8.0, 5 mM  $\beta$ -ME, 75 mM imidazole, 0.3 M NaCl.
10. Gel filtration running buffer (GF-RB): 25 mM Tris-HCl pH 8.0, 2 mM dithiothreitol (DTT), 0.1 M NaCl. Filter buffer through 0.2  $\mu$ m filter and degas.
11. IAA-2 solution (10 $\times$ ): 0.2 M solution of iodoacetic acid (IAA) in 250 mM Tris-HCl pH 8.0 (light sensitive). The high Tris concentration is required to buffer the IAA solution (quite acidic) and prevent precipitation of ER-LBD after addition.
12. Mono Q ion exchange buffers: IEX-A, 25 mM Tris-HCl pH 8.0, 2 mM DTT; IEX-B: as IEX-A but including 0.5 M NaCl. Filter buffers through 0.2  $\mu$ m filter and degas.

13. SDS-PAGE solutions: Resolving gel buffer (1.5 M Tris-HCl pH 8.8, 0.4% (w/v) SDS); Stacking gel buffer (0.5 M Tris-HCl pH 6.8, 0.4% (w/v) SDS). Running buffer (4×) – 12 g Tris and 57.6 g L-glycine per liter of deionized water. For 1× running buffer, dilute and add SDS to 0.1%. For native-PAGE omit SDS from all solutions. 30% acrylamide (w/v)/0.8% bis-acrylamide stock solution (37.5:1) (National Diagnostics). 10% (w/v) ammonium persulphate solution and TEMED to polymerize.
14. Centriprep/Centricon centrifugal concentrators (10K MWCO; Millipore).

### 2.3. Crystallization

1. Commercial crystallization screens (e.g. Crystal Screen 1&2; Index; PEG/ion (Hampton Research; <http://www.hamptonresearch.com>); MDL Nuclear Receptor Ligand binding domain screen; NR-LBD Extension screen (Molecular Dimensions; <http://www.moleculardimensions.com>) (see **Note 2**).
2. 96-well, sitting drop crystallization plates (see **Note 3**).
3. Optically clear sealing tape (such as Viewseal (Greiner)).
4. Multichannel pipettes (*optional* but greatly speeds up crystallization setup).

### 2.4. Inspection/ Optimization

1. Good quality stereomicroscope (40×) preferably with a cold light source (see **Note 4**).

---

## 3. Methods

Despite the caveats mentioned in the Introduction section, successful structure determination can be greatly enhanced by careful protein preparation. The sample should be of high purity, homogeneous, and monodisperse. A full biophysical characterization of the purified protein is recommended before embarking on crystallization (**Fig. 1**). The sample should typically be at least 90–95% pure as adjudged from a Coomassie stained SDS-polyacrylamide gel. Samples of lower purity may produce crystals but impurities can often affect their diffraction quality. The reader should remember that behind every structure lies good quality crystals and attempts to crystallize a poor quality sample is often destined to failure. It is also vital to keep a history of each batch as it is not uncommon to find that one batch of protein will crystallize whereas the next will not.

The following describes the preparation of human ER $\alpha$ LBD liganded to beta-estradiol as a generic example, although other ER ligands may be substituted. Because of tendency of the apo-form of ER $\alpha$ LBD to aggregate at low/moderate protein

concentrations, it is not possible to prepare unliganded ER $\alpha$ LBD to which ligands could be added prior to crystallization. Consequently, each individual ligand complex should be prepared separately. The purification scheme is unusual in that the exposed free cysteines in the protein are alkylated by iodoacetic acid treatment. This introduces a single negative charge per cysteine and improves solubility and, in our hands, greatly enhances crystallizability of the sample. Most other NR-LBDs will not require such a treatment to obtain crystals.

Hexa-histidine (his<sub>6</sub>)-tagged ER $\alpha$ LBD is initially affinity purified using nickel Sepharose, and the free cysteines are alkylated by treatment with iodoacetic acid (IAA) while still bound to the column. Immobilized, alkylated LBD is then incubated with ligand prior to elution followed by removal of the his-tag by thrombin cleavage. Size-exclusion chromatography allows removal of aggregated species. Finally, ion-exchange chromatography is used as a final polishing step. The purification protocol can be comfortably completed within 4–5 days. The final yield will vary but a conservative estimate is 10–15 mgs purified, liganded ER $\alpha$ LBD per liter of cells.

A generic protocol for obtaining diffraction quality crystals is impossible to provide because of the unique properties of each protein–ligand complex. As the nature of the successful combination of crystallising agents cannot be predicted at the outset, the target LBD/ligand complex is instead screened against a range of preformulated mixtures of chemicals. This approach affords the highest probability of success and should allow the experimenter to identify conditions required for crystal growth. Temperature and protein concentration are important variables, and it is suggested that experiments are carried out in parallel at 4 and 20°C (preferably in incubators). In most structural biology laboratories, the setup and inspection of crystallization experiments is often semiautomated. Nanoliter-sized drops (150–300 nl) comprising protein and reservoir are mixed and equilibrated against the reservoir solution using a liquid handling robot. Small volumes allow many more trials to be carried out from a fixed volume of sample compared with conventional methods. Such volumes cannot be accurately pipetted manually, and the protocol below assumes that the experimenter does not have access to such specialized equipment. The screening strategy outlined below can be equally applied to other NR-LBD complexes.

### 3.1. Expression

1. His<sub>6</sub>-tagged ER $\alpha$ LBD (residues 304–554) can be expressed in soluble form in *Escherichia coli* from a pET15b derived expression plasmid (7). This vector encodes an N-terminal poly-histidine tag that can be cleaved by thrombin (see [Note 5](#)).
2. Dilute (1/50) an overnight culture of *E. coli* strain C41 DE3 (8) transformed with pET15b-ER $\alpha$ LBD (7) into fresh LB supplemented with 100  $\mu$ g/mL ampicillin (see [Note 6](#)).

3. Grow cells at 37°C in a shaker until OD<sub>600nm</sub> is between 0.6–0.8. Induce expression by addition of 1 mM IPTG (1/1,000 IPTG stock) and grow cells overnight at 25°C. Add additional antibiotic (1/1,000 ampicillin stock) at induction to maintain selection.
4. Harvest cells by centrifugation and store pellets at –70°C until required.
5. Samples can be taken preinduction and after overnight incubation for SDS-PAGE analysis according to the method of Laemmli (9) to check the expression level (*see* **Note 7**).

### 3.2. Purification

1. All procedures should be carried at 4°C unless stated. Resuspend frozen cell pellet in SB (25–50 mL SB per liter cells) and sonicate on full power for 10 × 15 s burst (15 s pulse followed by 15 s rest on ice. Repeat ten times).
2. Sonicate is centrifuged at 27,000 × *g* in SS34 rotor for 30 min and supernatant is retained.
3. Supernatant (soluble extract) is filtered through 0.45 μm syringe filter (e.g. Acrodisc/Minisart) to remove large particulates. Add NaCl to a final concentration of 0.3 M. Ensure solution is mixed quickly after NaCl addition to avoid excessive local concentration. Addition of NaCl prior to sonication is not encouraged as this reduces the amount of the hydrophobic LBD recovered from the whole cell extract.

Ni-chelated Sepharose (8–10 mL bed volume) is prepared as manufacturer's instructions and packed into a suitable column (e.g. XK-16 column (*see* **Note 8**)). Resin is equilibrated with NTA-RB1 (10 column volumes (10 CV)), soluble extract is loaded at 3 mL/min and then washed with NTA-RB1 (10 CV or until A280 absorbance baselines). Resin washed with NTA-WB until baseline (9 CV), then with 25 mM Tris pH 8.1 to remove β-ME (5 CV). Resin washed with 2–3 CV IAA-1 buffer. Column is capped, wrapped in foil, and stored overnight.

4. Column washed with buffer (25 mM Tris-HCl pH 8.1) to remove alkylation solution (5 CV).
5. Column washed with E2 ligand solution (4 CV) and then capped and incubated for 30 min (*see* **Note 9**). E2-liganded ERαLBD complex is eluted with NTA-EB in 5 mL fractions. Assess which fractions to pool by SDS-PAGE.
6. Beta-mercaptoethanol (β-ME) is added to pooled fractions to a final concentration of 5 mM and pooled material is dialysed against 2 L of 25 mM Tris pH 8.0/5 mM β-ME in dialysis tubing (12–14 kDa cutoff) for a minimum of 2 h. Buffer is replaced and dialysed for further 1 h. It is not necessary to add additional ligand to the dialysis buffer. Dialysate collected and protein concentration estimated by recording absorbance at 280 m (*see* **Note 10**).

7. The his-tag can be removed with thrombin. NaCl (5 M stock) and CaCl<sub>2</sub> (1 M stock) are added to the dialysate at concentrations of 100 mM and 1.5 mM, respectively. Thrombin stock solution (0.05 units thrombin/mg ER) added and incubated without mixing at 22°C overnight (*see Note 11*).
8. SDS-PAGE analysis can be used to check that thrombin cleavage has proceeded to completion. Thrombin activity is inhibited by addition of AEBSF to a final concentration of 1 mM.
9. Imidazole and NaCl are added to thrombin-treated LBD at final concentrations of 75 and 300 mM, respectively. Addition of imidazole is important as it prevents nonspecific binding of his(-)ERαLBD to Ni-NTA resin while allowing uncleaved material (his(+)-ERαLBD) to be retained. ERαLBD is unusual in that it has a high intrinsic affinity for nickel resin and higher concentrations of imidazole are required to prevent nonspecific binding compared with other proteins.
10. Thrombin-cleaved material is passed down Ni-Sepharose column equilibrated with NTA-RB2 to remove uncleaved material. This is a negative step and column flow-through containing cleaved his(-)ERαLBD should be retained. Check purification progress by SDS-PAGE analysis.
11. Superdex S75 16/60 gel filtration (GF) column is connected to FPLC system and equilibrated with GF-RB overnight.
12. His(-)ERαLBD-E2 complex is transferred to a rinsed 10K Centriprep™ centrifugal concentrator (Millipore) and spun at 4°C to reduce volume to ca. 4 mL. Concentrate is spun at 20,000 × *g* to remove particulates prior to loading onto the GF column via a 5 ml superloop. The column should be run at 1 mL/min. Aggregated material will elute around 42 mL while the majority of the protein elutes around 65 mL (corresponding to ERαLBD dimer). Collect 1–2 mL fractions over the dimer peak. Fractions containing ER are pooled and the concentration estimated.
13. A second alkylation step of the liganded LBD has been found to be necessary for successful crystallization. IAA-2 solution (1×) is added to the pooled fractions and incubated at 22°C for 2–3 h. The reaction is quenched by addition of DTT to a final concentration of 20 mM.
14. The final polishing step uses ion exchange chromatography to partially separate the various charge states introduced by carboxymethylation (*see Note 12*).
15. MonoQ 10/10 column (8 mL bed volume/35–40 mgs capacity) is connected to FPLC system and equilibrated with IEX-A buffer (5 CV). This column can be run at 3–4 mL/min depending on the back pressure.



16. IAA-treated material is diluted 50:50 with 25 mM Tris-HCl pH 8.0 to reduce NaCl concentration to 50 mM. Filter through 0.2  $\mu$ m acrodisc and load onto column in batches from a 10 mL superloop at 3–4 mL/min. Multiple loading will be necessary given volume of diluted material but do not load more than 35–40 mgs. Column is first washed with 5 CV IEX-A then the gradient should be stepped to 30% IEX-B and column washed for a further 5 CV. Bound material is eluted using a gradient from 30–65% IEX-B over a minimum of 10 CV. Finally gradient stepped to 100% IEX-B. Three milliliter fractions are collected. The major peak of ER $\alpha$ LBD should elute between 45 and 55% IEX-B. Fractions should be checked on 15% SDS-PAGE and native 7.5% PAGE before deciding which fractions should be pooled (*see* [Note 12](#)).
17. Most homogeneous fractions are pooled and dialysed thoroughly in 20 mM Tris-HCl 8.0, 150 mM NaCl, 2 mM DTT prior to concentration (*see* [Note 13](#)). his(-)ER $\alpha$ LBD-E2 complex can be concentrated in a Millipore 10K MWCO centrifugal concentrator to 10–12 mg/mL (*see* [Note 14](#)).
18. Concentrated material can be stored in small aliquots (50–100  $\mu$ L) by flash-freezing in liquid nitrogen prior to storage at  $-80^{\circ}\text{C}$ . Thin-walled PCR tubes are recommended for storage. Frozen material should be rapidly thawed by rubbing between the fingers rather than slowly on ice as this will minimize damage. Repeated freeze-thaw cycles should definitely be avoided as this can lead to serious sample heterogeneity. Once thawed, protein should be stored on ice and used up as quickly as possible (i.e., thaw a fresh sample rather than use material that has been thawed and stored for more than 3–4 days).

### 3.3. Crystallization

1. Pipette 40  $\mu$ L of each of the 96 crystallization screen solutions into each reservoir well of the Wilden plate (*see* [Note 15](#)). Repeat for each screen/temperature to be tested using a new plate.
2. Freshly prepared or rapidly-thawed, frozen liganded LBD is centrifuged at  $20,000 \times g$  in a benchtop centrifuge at  $4^{\circ}\text{C}$  to remove particulates.
3. One microliter of concentrated protein–ligand solution is pipetted into subwell A of the crystallization plate ([Fig. 2](#)). An equal volume of the corresponding reservoir solution is pipetted into subwell A on top of the concentrated protein without mixing (*see* [Note 16](#)). If a multisubwell plate is used, additional samples can be set up in other subwells as required (*see* [Note 17](#)).
4. Seal plate with tape (*see* [Note 18](#)).
5. Place at desired temperature (*see* [Note 19](#)).

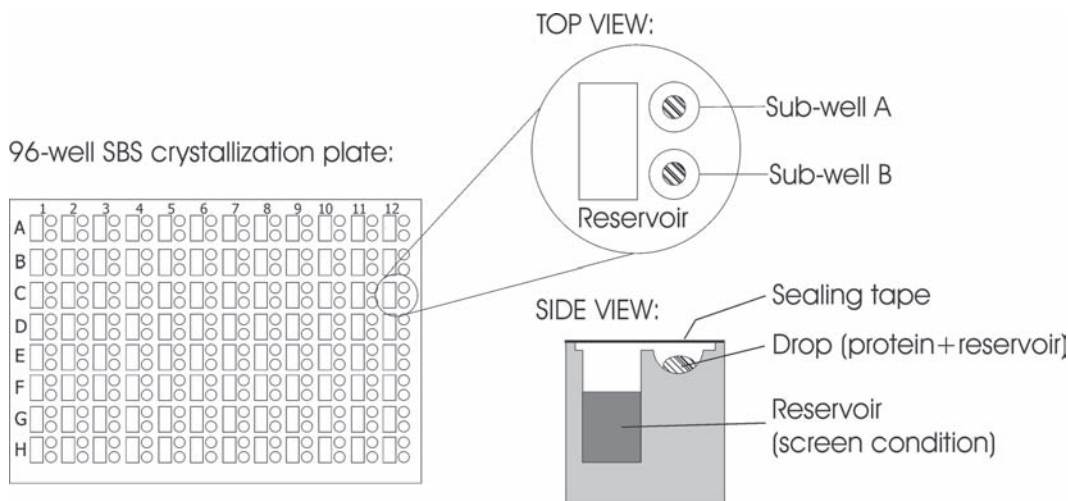


Fig. 2. A 96-well sitting-drop crystallization plate. The layout of one of the 96 individual crystallization chambers is shown in detail on the *right*.

### 3.4. Inspection and Optimization

1. Progress of crystallization experiments should be monitored after 24 h and then on day 2, day 3, day 7 and then at weekly intervals. Inspect each drop under the microscope and record hits (*see Note 20*). Optimize crystallisation conditions as necessary to obtain diffraction quality crystals (*see Note 21*).

---

## 4. Notes

1. The majority of ER ligands are hydrophobic and poorly soluble in water. Ligand stocks should be prepared in 100% dimethylformamide (DMF) or 100% dimethylsulphoxide (DMSO) at appropriate concentrations (5–50 mM). Dilution of the concentrated ligand stock in buffer can result in significant precipitation of ligand and the working solution may appear quite cloudy. Nevertheless, sufficient ligand should remain in solution to saturate the LBD binding sites. Up to 10% DMF can be included in the ligand solution to enhance solubility without affecting Ni-Sepharose column performance. Diluted ligand solutions should be freshly prepared and not reused.
2. A variety of crystallization screens are commercially available. They comprise a set of solutions (referred to as conditions) that can be mixed with the concentrated protein sample and used to induce crystallization. Each solution typically comprises a precipitant (a salt or polyethylene glycol (PEG)) along with

various additive salts at a specific pH. As a whole, each screen has a broad coverage of different precipitants, salts, and pH range (4.5–9.0). Different screens have some unique conditions but there can be considerable overlap between the conditions. The screens listed here have been successfully used in the initial screening of ER–ligand complexes and provide comprehensive set of starting conditions. The Hampton Crystal Screens 1&2 can be combined in a 96-well plate as can the MDL NR-screens. The Hampton Index screen takes up an entire 96-well plate while the PEG/ion screen comprises 48 conditions.

3. A variety of 96-well SBS (Society for Biomolecular Screening) format, sitting-drop crystallization plates are commercially available. 2-drop MRC/Innovaplate SD-2 plates (Wilden/Innovadyne) are recommended as they have large circular wells with excellent optical properties. The advantage of multiple drop plates is that several samples (different ligand complexes) can be setup against the same reservoir solution ([Fig. 2](#)).
4. If possible the microscope should have a large, flat viewing platform with a cold (fiber optic) light source illumination in the base. Protein crystals (and solutions) are highly sensitive to changes in temperature. If a cold light source is unavailable, drop inspection should be carried out in stages allowing the viewing stage/bulb to cool down before resuming.
5. The pET15b expression vector is described here as it consistently (and reproducibly) produces the highest quality protein in our hands. Nevertheless, thrombin cleavage is not particularly efficient/specific/cost-effective and has to be carried out at room temperature to achieve cleavage in a sensible time-frame. Other N-terminally tagged expression vectors may be used (C-terminal tags are best avoided for NR-LBDs due to possible interference with the carboxy-terminal AF2 helix). However, the author has also tested a variety of ER $\alpha$ LBD expression constructs that are not tagged or contain a 3C protease (pET28a based) cleavage site rather than a thrombin site. Despite the inherent advantages of these constructs, expression of soluble LBD is, in all cases, both significantly reduced and much less reproducible.
6. The *E. coli* strain C41 (DE3) (8) was found to give the best percentage of soluble expression under the conditions tested. The expression plasmid is stably retained and transformed C41 cells can be stored at  $-80^{\circ}\text{C}$ .
7. His-tagged (his(+)) ER $\alpha$ LBD has a molecular weight of 31,019 Da (reducing to 29,137 after removal of tag (his(-))). A standard 12 or 15% SDS-PAGE gel can be used to resolve these species.

8. An FPLC system is not required for all steps. A column attached to a simple peristaltic pump will suffice for Ni-NTA affinity chromatography. The column volumes (CV) of each wash step are indicated so that the whole procedure can essentially be carried out “blind”. Although self-packed columns are the most flexible for this step, prepacked 1 or 5 mL Ni-Sepharose HiTRAP columns (GE Healthcare) can also be used. The advantage of the 5 mL columns is that they tolerate high flow rates. Alternatively columns can be left to flow by gravity or the whole procedure can be carried out “in batch” in 50 mL tubes. In cases where working with a precious or limiting quantity of ligand, the amount of resin can be optimized on the basis of the amount of complex being prepared so that the minimum amount of ligand solution is required.
9. It is not necessary to include ligand in all the purification/dialysis buffers after the immobilized LBD has initially been exposed to ligand on the Ni-Sepharose. However, addition of ligand is recommended during the final centrifugal concentration step as it ensures that the LBD is fully saturated with ligand prior to crystallization.
10. Protein concentration can be estimated assuming that a 1 mg/mL solution of his(+)ER $\alpha$ LBD has an absorbance of 0.757 at 280 nm. Use dialysis buffer as a reference and dilute sample to get an accurate measurement (depending on dynamic range of equipment used). After removal of the tag, a 1 mg/mL solution has an absorbance of 0.81. Alternatively, protein concentration can be estimated using standard colorimetric methods such as the Bradford assay.
11. Thrombin cleavage is notoriously inefficient and can be seriously impacted by contaminants. In this case, the tag is specifically cleaved after overnight incubation if the dialysis step is followed prior to addition of enzyme. If SDS analysis suggests incomplete cleavage then additional thrombin solution can be added and incubated further.
12. ER $\alpha$ LBD contains 4 free cysteines of which 3 are accessible to the iodoacetic acid treatment. As ER $\alpha$ LBD dimerizes in the presence of ligand (agonist or antagonist), incomplete alkylation results in a range of charge species. SDS-PAGE analysis will not reveal this heterogeneity, and it is worthwhile to run samples on a native PAGE. For native gel analysis, prepare a 7.5% cross-linked acrylamide/bis-acrylamide gel using resolving/stacking gel buffers that do not contain SDS. Run at 100 V at 4°C in Tris/glycine running buffer (no SDS) and stain with Coomassie.
13. The final material is dialysed against a relatively low concentration of buffer so that the pH can be readily modulated by

the crystallization screen conditions. NaCl can also be added up to 0.5 M to enhance solubility of certain ER–ligand complexes. The amount of NaCl required should be determined on a case-by-case basis.

14. Other ER-LBD ligand complexes, especially those with antagonists may exhibit reduced solubility. It is extremely important that the protein solution is not over-concentrated as this can affect the ability of the sample to crystallize. Concentration should be stopped at the first signs of precipitation – often when thread-like filaments appear in solution or when the rate of ultrafiltration gets very slow (indicative of material precipitating on membrane). The protein solution should also be mixed at regular intervals to avoid over-concentration at the membrane surface of the concentrator. If moderate-to-heavy precipitation occurs it may be reversed by addition of NaCl (up to 0.5 M) but concentration should be halted and any remaining precipitate should be removed by centrifugation. Achieving a “high” protein concentration for all complexes is not necessarily essential as we have successfully crystallized ER complexes as low as 3.5 mg/mL. A precrystallization test (kit available from Hampton Research) can be used to assess whether the protein concentration is suitable for crystallization screening.
15. Each crystallization plate comprises 96 individual compartments. Each compartment comprises a central reservoir for the crystallization solution and a raised platform containing 1–3 wells (subwell) where the protein-reservoir “sitting-drops” are set up (Fig. 2). Once the plate is sealed each set of subwells are able to equilibrate with the parent reservoir. Initially the concentration of components will be halved as the protein and crystallization solution are mixed in a 1:1 ratio. However, the drop will rapidly equilibrate with the reservoir by vapor diffusion (effectively water will be drawn from the drop to the reservoir) so that the drop is slowly dehydrated and the concentration of components will reach or exceed their individual starting concentrations. The minimum amount of reservoir solution (crystallization reagent) required varies depending on plate type (40–100  $\mu$ L).
16. A single channel pipette can be used to dispense protein in columns. A multichannel (8-channel) pipette can then be used to add reservoir solution on a column-by-column basis. Protein solution should always be dispensed first and then reservoir solution added second. Exhaustive mixing is not necessary and solutions can be left to diffuse together. If the protein sample is limited, the drop size may be reduced to 0.5  $\mu$ L protein + 0.5  $\mu$ L reservoir if these volumes can be accurately pipetted.

17. Appropriate coregulator peptides can be added to the protein–ligand complex to stabilize the LBD conformation and increase the chances of success. Alternatively, several initial concentrations of protein–ligand complex can be evaluated (100, 75, 50%). Protein can be diluted with GF-buffer. Coactivator peptides derived from the LxxLL-containing regions will stabilize the agonist-bound state. Antagonist complexes may be stabilized by corepressor peptides or peptides derived from phage-display studies. Peptides should be of high purity (>95%) and cocrystallization will require relatively large amounts (1–5 mg). Peptide stocks (mM) can be prepared in water/buffer and added at two to fivefold molar excess with respect to the LBD concentration followed by brief incubation prior to setting up crystallization drops. Alternatively, peptide can be added to dilute LBD solution to improve solubility and behavior during the final concentration step. Peptide stocks can be stored in aliquots at  $-20^{\circ}\text{C}$ . Additional ligand may also be added prior to crystallization from concentrated stocks to ensure an excess of ligand is present so that all LBDs contain bound ligand. This is particularly important for lower affinity ligands that may have leached out during the purification. Ensure that organic component (DMSO/DMF – see **Note 1**) is around 1–2% (v/v). Higher concentrations may cause precipitation.
18. Drops should not be allowed to dry out/evaporate during setup. This will be an issue if setting up more than one protein–ligand complex per plate. Depending on the relative humidity, it may be necessary to complete a 96-well plate in several stages (e.g., 3 columns at a time), temporarily sealing with clear tape prior to final sealing with optically clear tape.
19. Incubators should be used if available to maintain experiments at a constant temperature. Otherwise plates should be isolated from temperature fluctuations and vibrations, which both have a negative effect on the crystallization process. Plates can be placed in polystyrene boxes, which afford some protection, prior to storage in a fridge/cold room or at room temperature. Temperature fluctuations should also be minimized when inspecting the progress of crystallization experiments and  $4^{\circ}\text{C}$  experiments should ideally be examined in a cold room.
20. The drops will take time to equilibrate and so crystals are unlikely to appear immediately. Because of the wide range of chemical/pH space that the listed crystallization screens cover, it is normal that anywhere from 1/3 to a 1/2 of all drops will produce precipitate. Precipitation is a positive outcome as it suggests that the drop has reached a supersaturated



state – a prerequisite for crystallization. If all the drops are clear then the protein solution is too dilute and should be concentrated further if possible. Conversely, if greater than 75% of drops produce precipitate then consider diluting the sample before repeating the crystallization trials. As mentioned in **Note 17**, it is worthwhile setting up initial experiments at several different protein concentrations if sample is not limiting. Alternatively, a precrystallization test (*see Note 14*) can be performed. In certain cases it may be necessary to further optimize the sample's solubility prior to successful crystallization using buffer and additive screening (*see (6) for protocols detailing these techniques*). If you are lucky some drops will yield crystals of some description. Almost certainly these will not be large or perfectly shaped but rather could be “sea-urchins” of thin needles, stacked plates or showers of tiny crystals so careful observation is necessary. See <http://www.hamptonresearch.com/stuff/Gallery.aspx> for examples of the myriad of protein crystal morphologies.

21. In the majority of cases, initial crystals will be unsuitable for diffraction analysis and will require some degree of improvement/optimization. Because of the sparse-matrix (random) design of the crystallization solutions, a scoring system greatly simplifies the process of identifying conditions (pH, precipitant, additives) that favor crystallization (*see (6) for example*). Briefly, a simple 1–10 scale can be used to score denatured precipitate (will appear brown under the microscope), clear drops, precipitates, and crystals of various sizes. Analysis of the initial screens should provide clues to the pH dependence of the complex's solubility as well as its behavior in the presence of different anions, cations, and metals. Optimization parameters include concentration of both the protein–ligand complex and components of the crystallization solution. The pH of the crystallization solution may also have a large impact on resultant crystals. A strategy for optimization can include a simple dilution screen of the original hit condition that gives crystals (100, 95, 90%, etc, using ultrapure water as diluent) as well as exploring conditions 1.5 pH units either side of condition (using 0.5 pH unit steps). In the case of ER-LBD, the majority of crystals are obtained from polyethylene glycol solutions at pHs greater than 6.5.

Diffraction quality of putative complex crystals should be assessed at the earliest possible stage to avoid optimising salt crystals (common with phosphate containing conditions and when calcium and zinc salts are present). ER-LBD crystals typically diffract X-rays weakly and the author's experience is that the majority of datasets will need to be collected at high brilliance synchrotron sources such as the ESRF (European Synchrotron Radiation Facility; <http://www.esrf.fr>) to obtain sufficiently high resolution data.



Nevertheless, screening crystals on a laboratory rotating anode X-ray source can provide useful information about the quality and diffraction potential of any crystals obtained. In-house diffraction to around 3–4 Å is generally quite encouraging.

Finally, if no crystals are obtained from initial screening then the following approaches could be considered. If sample homogeneity is not a concern (see Biophysical Characterization in [Fig. 1](#)), then more crystallization conditions can be setup at different temperatures. Otherwise try and purify the sample further with additional chromatographic steps such as ion exchange. Different ligands can have widely differing (de-)stabilizing effects on the protein that can impact crystallization, and it is advisable to try as many ligands as possible. Leaving the his-tag intact (i.e., omitting the protease cleavage step) can sometimes result in dramatic changes in crystallization behaviour. Other approaches include protein methylation or partial in-drop proteolysis. Nonetheless, be prepared for some LBD-ligand complexes to resist all attempts at crystallization.

---

## Acknowledgments

The author would like to thank Benita Katzenellenbogen (University of Illinois, USA) for providing the pET15b-ER $\alpha$ LBD expression vector. The described purification protocol evolved over several years and I wish to thank Mats Carlquist (KaroBio, Sweden) and Marek Brzozowski (York) for help, advice, and encouragement. The work was carried out in the York Structural Biology Laboratory at the University of York, UK and supported by a Wellcome Trust Career Development fellowship (Grant number: 064803).

## References

1. Pike, A. C. W. (2006) Lessons learnt from structural studies of the oestrogen receptor. *Best Practice & Research Clinical Endocrinology & Metabolism*. **20**, 1–14.
2. Li, Y., Lambert, M. H., Xu, H. E. (2003) Activation of nuclear receptors: A perspective from structural genomics. *Structure*. **11**, 741–746.
3. Bergfors, T. (1999) Protein Crystallization: Techniques, Strategies, and Tips. A Laboratory Manual. La Jolla, USA: International University Line.
4. McRee, D. E. (1999) Practical Protein Crystallography. 2nd ed. San Diego: Academic Press.
5. Blow, D. (2002) Outline of Crystallography for Biologists. Oxford: Oxford University Press.
6. Benvenuti, M., Mangani, S. (2007) Crystallization of soluble proteins in vapor diffusion for X-ray crystallography. *Nature Protocols*. **2**, 1633–1651.
7. Carlson, K. E., Choi, I., Gee, A., Katzenellenbogen, B. S., Katzenellenbogen, J. A. (1997) Altered ligand binding properties and

enhanced stability of a constitutively active estrogen receptor: Evidence that an open pocket conformation is required for ligand interaction. *Biochemistry*. **36**, 14897–14905.

8. Miroux, B., Walker, J. E. (1996) Over-production of proteins in *Escherichia coli*: Mutant

hosts that allow synthesis of some membrane proteins and globular proteins at high levels. *Journal of Molecular Biology*. **260**, 289–298.

9. Laemmli, U. K. (1970) Cleavage of structural proteins during assembly of head of bacteriophage-T4. *Nature*. **227**, 680–685.

# Chapter 5

## FRAP and FRET Methods to Study Nuclear Receptors in Living Cells

Martin E. van Royen, Christoffel Dinant, Pascal Farla,  
Jan Trapman, and Adriaan B. Houtsmuller

### Abstract

Quantitative imaging techniques of fluorescently-tagged proteins have been instrumental in the study of the behavior of nuclear receptors (NRs) and coregulators in living cells. Ligand-activated NRs exert their function in transcription regulation by binding to specific response elements in promoter and enhancer sequences of genes. Fluorescence recovery after photobleaching (FRAP) has proven to be a powerful tool to study the mobility of fluorescently-labeled molecules in living cells. Since binding to DNA leads to the immobilization of DNA-interacting proteins like NRs, FRAP is especially useful for determining DNA-binding kinetics of these proteins. The coordinated interaction of NRs with promoters/enhancers and subsequent transcription activation is not only regulated by ligand but also by interactions with sets of cofactors and, at least in the case of the androgen receptor (AR), by dimerization and interdomain interactions. In living cells, these interactions can be studied by fluorescence resonance energy transfer (FRET).

Here we provide and discuss detailed protocols for FRAP and FRET procedures to study the behavior of nuclear receptors in living cells. On the basis of our studies of the AR, we provide protocols for two different FRAP methods (strip-FRAP and FLIP-FRAP) to quantitatively investigate DNA-interactions and for two different FRET approaches, ratio imaging, and acceptor photobleaching FRET to study AR domain interactions and interactions with cofactor motifs. Finally, we provide a protocol of a technique where FRAP and acceptor photobleaching FRET are combined to study the dynamics of interacting ARs.

**Key words:** Androgen Receptor, N/C-interaction, Confocal Microscopy, FRET, FRAP.

---

## 1. Introduction

### 1.1. Nuclear Receptors

Nuclear receptors (NRs) are ligand-activated transcription factors amongst which are the steroid receptors including the estrogen- (ER), mineralocorticoid (MR), glucocorticoid- (GR),

progesterone- (PR), and androgen- (AR) receptors (1). The members of the steroid receptor subfamily have roles in regulating cell growth, development, differentiation, and homeostasis.

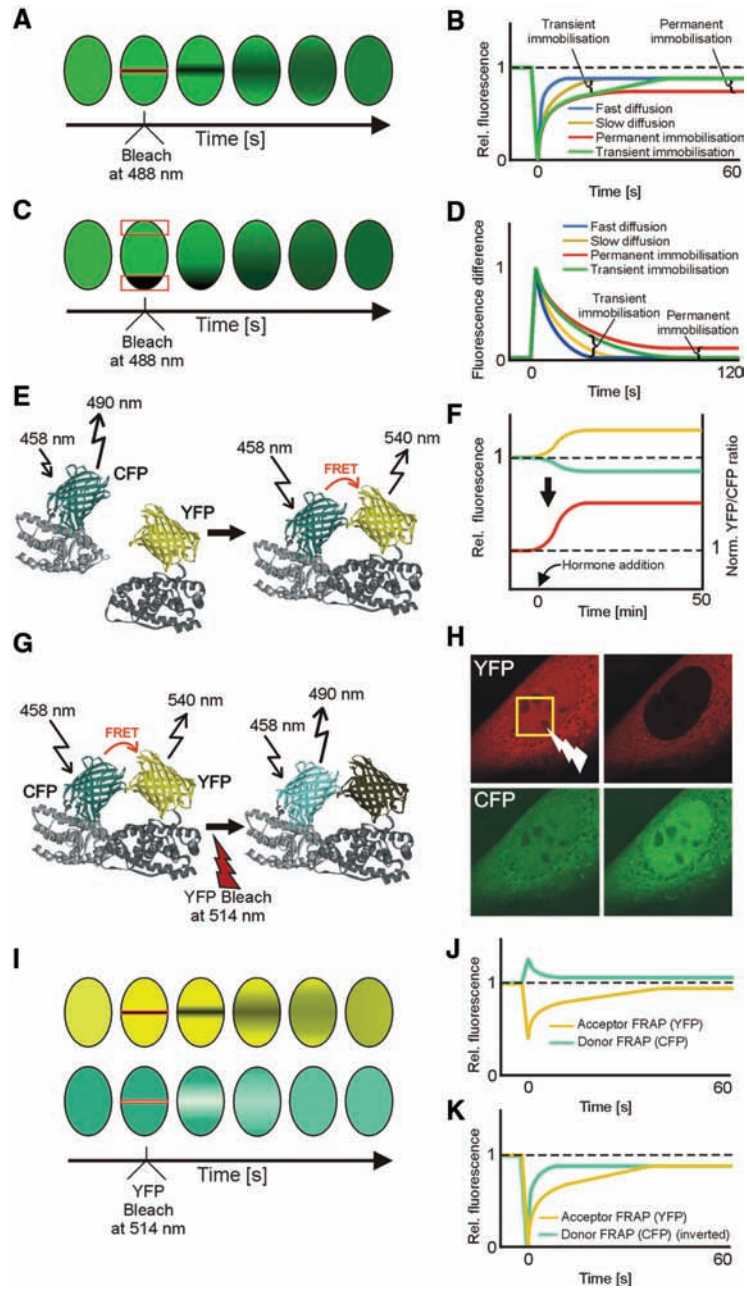
As our research focus is on AR function in living cells, we use this steroid receptor for the examples presented throughout this chapter. The AR is important in the development and maintenance of the male phenotype and also plays a role in the development and progression of prostate cancer (2). Like all nuclear receptors, the AR consists of three functional domains: a highly conserved DNA-binding domain (DBD) flanked by a C-terminal ligand-binding domain (LBD) and a more variable N-terminal domain (NTD) (3). In the absence of ligand, the AR is predominantly, but not exclusively, localized in the cytoplasm in most cell types. Upon binding to ligand, ARs translocate from the cytoplasm to the nucleus, where they exert their function through interaction with coregulators and binding to specific androgen response elements (AREs) in promoter and enhancer sequences of AR-regulated genes (4–7).

## 1.2. FRAP to Study Protein Mobility

For the AR and other nuclear receptors, the live cell dynamics and interactions with chromatin have been investigated extensively. A powerful approach to study proteins mobility in living cells is fluorescence recovery after photobleaching (FRAP) (*see Note 1*) (8–14). In FRAP, fluorescence is recorded in a small volume within a larger volume before and after shortly illuminating the small volume at high laser intensity (**Fig. 1A–D**) (15, 16), and reviewed in 17). During the high intensity laser-pulse,

---

Fig. 1. Strip-FRAP, FLIP-FRAP, abFRET and simultaneous FRAP and FRET experiments: **(A)** In strip-FRAP, the recovery of fluorescence is recorded in time after shortly bleaching a small strip spanning the nucleus. **(B)** FRAP curves of different scenarios normalized to prebleached values and to zero directly after bleaching. Permanent immobilization of GFP tagged proteins (*red curve*) can be identified by an incomplete recovery compared with FRAP curves of freely molecules (*blue curve* with fast diffusion and *yellow curve* with slow diffusion). A transient immobilization results in a delayed fluorescence recovery (*green curve*). **(C)** In FLIP-FRAP experiments, the fluorescence in a bleached region at one pole of the nucleus and in a region at the opposite nuclear pole are recorded in time after photobleaching until steady state is regained. **(D)** The normalized difference in fluorescence between the two opposite poles is plotted in time. Similar to strip-FRAP, a permanent immobilization results in an incomplete redistribution and thus a permanent difference between both signals in the two measured regions (*red curve*) and a transient immobilization results in a delayed fluorescence redistribution (*green curve*). **(E)** Principle of FRET measurement by YFP/CFP ratio imaging. In an inducible system, FRET can readily be measured using YFP/CFP ratio imaging. In absence of interaction, before induction, no FRET occurs. After induction, when YFP and CFP are in each other's vicinity, energy is transferred from CFP to YFP resulting in a decrease in CFP emission and an increase in YFP emission. **(F)** When both CFP and YFP intensities and the YFP/CFP ratio are plotted, FRET is indicated by the decrease of CFP emission (*cyan curve*) and a subsequent increase of YFP emission (*yellow curve*), resulting in a clear YFP/CFP ratio increase (*red curve*). The *curve* indicates the kinetics of the interaction. **(G)** Principle of imaging FRET by acceptor photobleaching. When cyan fluorescent protein (CFP) and yellow fluorescent protein (YFP) are close to each other (<10 nm), that is, if interaction occurs, excitation energy absorbed by CFP is nonirradiatively transferred to YFP resulting in YFP emission (sensitized emission). FRET was evaluated by the increase of donor (CFP) emission intensity after specifically photobleaching of the acceptor (YFP) in the nucleus thereby eliminating its quenching



effect on the donor. **(H)** Images of YFP and CFP in living cells before and after YFP photobleaching in cells transfected with a construct expressing a CFP-YFP fusion protein. The *square* indicates the region of bleaching. Bleaching of YFP results in a clear increase of CFP emission. **(I)** Schematic representation of simultaneous FRAP and FRET measurements. YFP in a small strip spanning the width of the nucleus is bleached shortly and the recovery of YFP (acceptor) fluorescence is monitored at 100 ms intervals. In the presence of FRET, YFP bleaching results in an accompanying increase of CFP (donor) fluorescence. The redistribution of CFP fluorescence, therefore, represents the mobility of interacting molecules only (donor-FRAP). Acceptor emission represents the total pool of YFP-tagged molecules irrespective of interaction (acceptor-FRAP). **(j)** After background subtraction, normalization to prebleach values and inversion of the donor-FRAP signal shows directly the kinetics of both donor and acceptor signals. **(K)** Normalization to values directly after bleaching inverts the donor FRAP curve and the kinetics of both signals can now be compared (*see Color Plates*).

the majority of the fluorescent molecules within the illuminated region irreversibly lose their fluorescent properties, a process termed as photobleaching. After (and during) the pulse, mobile fluorescent and bleached molecules will diffuse in and out of the bleached region eventually leading to their complete redistribution. In contrast, immobilized bleached molecules inside the bleached region will not be exchanged by nonbleached molecules from outside the region, and vice versa. Therefore, the presence of an immobile fraction results in incomplete recovery of the fluorescent signal inside the bleached region relative to the remainder of the nucleus. When molecules are immobilized only transiently (and shorter or not much longer than the period of measurement), as was found for NRs (see below), this will result in a secondary, slower recovery of fluorescence in the bleached region by diffusion of initially immobilized molecules that release from their immobile binding sites (for instance promoters/enhancers of genes) during the measurement period after bleaching (**Fig. 1B**) (9, 11).

To compare FRAP curves from different experiments, and to visually analyze them, it is necessary to normalize the raw fluorescence data. There are several ways to do this, each revealing specific kinetic parameters (*see* also **step 7** in the strip-FRAP protocol) (17, 18). The most straightforward normalization is to express measured intensities relative to the average prebleach intensity ( $I_{\text{prebleach}}$ ) after background subtraction, revealing the fraction of molecules bleached during the bleach pulse, which can be read from the first measurement after bleaching. In addition, if molecules are largely immobile, the recovery of fluorescence in the bleached area will be limited, so a first impression on overall mobility can be obtained from these curves. (Note that in principle, the volume containing the molecules (in our case the nucleus) can also be seen from these curves if freely mobile molecules (for instance GFP) are used and the volume of the bleached region is known). To readily extract more precise information, a second way to normalize the data can be used, where the measured fluorescence is expressed relative to both intensities before as well as directly after bleaching ( $I_0$ ). This way of normalization yields a curve that starts at 1 before bleaching and 0 immediately after bleaching, thereby removing potential differences in the percentage of molecules bleached, and thus allowing comparison between experiments using different laser settings. The final recovery of these curves, when corrected for the fraction of bleached molecules (*see* **Note 2**), reveals the immobilized fraction, if present. A third way of normalization is achieved by expressing fluorescence relative to both the fluorescence directly after bleaching ( $I_0$ ) and after complete recovery ( $I_{\text{postbleach}}$ ). This yields a curve running from 0 immediately after bleaching to 1 at complete recovery, allowing fitting the data to any analytically

derived equation that represents the diffusion process (and transient immobilization) (17). In addition, since this normalization removes the immobile fraction, the apparent diffusion coefficient of the freely mobile fraction can be compared directly between different curves, irrespective of the size of the immobile fraction, if present.

In our investigation of the nuclear dynamics of the AR, we have previously used a combination of FRAP and FLIP (fluorescence loss in photobleaching) assays (see later and **Figs. 1C, D, and 2**) (11, 15, 17). The reason for this dual approach was that in straightforward FRAP experiments often more than one scenario may fit the data, where a scenario of slow diffusion vs. a scenario of fast diffusion and transient immobilization are difficult to distinguish. In the case of the AR, we observed a strongly reduced mobility of liganded ARs compared with nonliganded ARs or liganded mutants that cannot bind DNA. However, although strip-FRAP (see Methods section) analysis favored a model of unaltered diffusion and ligand-induced transient immobilization, the difference with a model of ligand-induced slower mobility (for instance by formation of large transcription holocomplexes) was small. We then verified by computer modeling that two different scenarios (slow mobility vs. high mobility and transient immobilization) often result in two similar curves in a strip-FRAP experiment but very different curves in a complementary FLIP-FRAP experiment or vice versa (17, 18). Therefore, to corroborate the strip-FRAP experiments, we performed another FRAP variant, where we analyzed the recovery of fluorescence in a bleached area (FRAP) at one pole of the nucleus together with the loss of fluorescence at the other pole, distant from the bleached area (fluorescence loss in photobleaching, FLIP) (9, 11). Both procedures are described in detail in the Methods section.

### **1.3. Steroid Receptors are Transiently Immobilized due to DNA-Binding**

The transient immobilization in the nucleus of NRs (and many other DNA-interacting proteins) identified in FRAP measurements most likely reflects the binding of NRs to chromatin. This is corroborated by the absence of an immobile fraction in several AR mutants with mutations in the first zinc finger of the AR DBD (e.g., A573D) that were shown to abolish DNA binding (**Fig. 2A–D**) (11, 19). Surprisingly, FRAP experiments on ARs lacking the AR LBD showed that not only the AR DBD but also the AR LBD is important for stable binding of the AR to DNA but that this stabilization is not essential for transcriptional activity (11). Other studies applying FRAP on NRs also identified a role for chaperones such as Hsp90 and proteasome function in the regulation of NR immobilization at a target sequence (20, 21). In addition, the ligand specificity of several NRs has been studied. For the AR very similar transient immobilizations are found in the presence of the natural agonists testosterone, dehydrotestosterone,



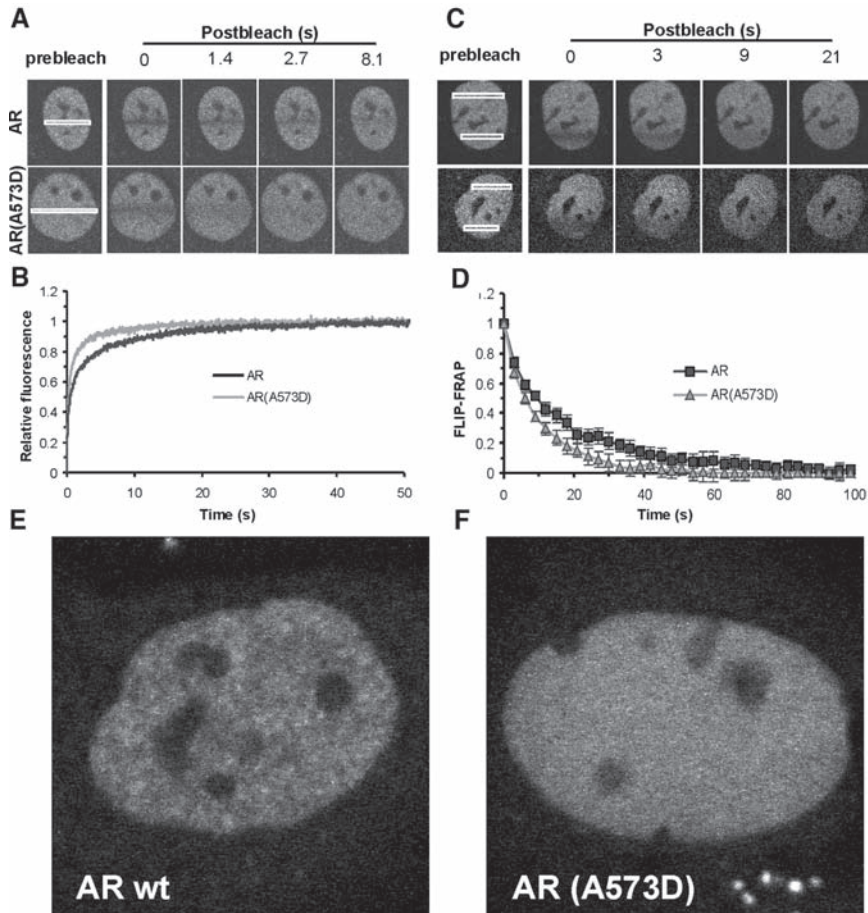


Fig. 2. FRAP on wild type and mutant ARs. **(A and B)** Confocal images **(A)** and the strip-FRAP curve of Hep3B cells stably expressing GFP-AR (wild type) or the non-DNA-binding mutant (GFP-AR (A573D)). The recovery of fluorescence in a small strip spanning the nucleus (*white box* in **A**) is recorded in time after shortly photobleaching the fluorescence. The wild type AR shows a slower total recovery of the fluorescence compared with the non-DNA-binding mutant (AR (A573D)) because of transient immobilization of the wild type AR **(B)**. **(C and D)** Confocal images of Hep3B cells stably expressing the GFP-tagged wild type AR and the non-DNA-binding mutant and their FLIP-FRAP curves **(D)**. The normalized differences in fluorescence intensity in both ROIs (*white boxes* at both poles of the cells) **(C)** is plotted in time **(D)**. In agreement with the strip-FRAP results, a reduced mobility is found for the wild type AR compared with the non-DNA-binding mutant (A573D). **(E and F)** Confocal images of wild type AR and the non-DNA-binding mutant. Immobilization of wild type AR found with FRAP is accompanied with a typical nuclear speckled distribution **(E)**, whereas the non-DNA-binding mutant (AR (A573D)) lacks this pattern **(F)**. Figure adapted from *ref. 9* with permission from The Company of Biologists Limited Ltd.

or the synthetic variant R1881. Antagonist bound ARs (bicalutamide or hydroxyflutamide) are much more mobile, only showing very transient immobilizations in the order of hundreds of milliseconds to seconds (9, 22, 23). However, ChIP data suggested that antagonist bound ARs still bind to their recognition sites (24, 25). Taken together ChIP and FRAP results suggest that anti-androgens prevent stable DNA-binding of the AR (9). These antagonists act as agonists in specific AR mutants such as

T877A and W741C, which were found in patients that developed therapy resistant metastases (26, 27). Interestingly the agonist effect was accompanied by a reduced mobility comparable to R1881, strongly suggesting that we are observing DNA-binding in the FRAP experiments shown (9). The effect of partial antagonists on wild type ARs is less clear, ranging from fast recoveries of ARs in the presence of cyproterone acetate (CPA) to transient immobilizations comparable with agonist of RU486 bound ARs (22). Similar results have been found for other pure and partial antagonist bound NRs (8, 12, 13, 28–31).

An interesting approach to study interaction of NRs with promoters of NR-regulated genes was introduced by Gordon Hager and others. In this approach, cell lines are generated containing a long tandem array of promoters controlling the expression of a reporter gene. The local high concentration of response elements (like the MMTV LTR for GR, PR, and AR studies (8, 14, 21, 22, 31) and prolactin-regulatory element array to study the ER (30)) enables visualization of binding of fluorescently tagged NRs to these specific sequences. FRAP data obtained with the cell line containing the MMTV LTR array cell line are in line with FRAP data obtained using cells that lack these arrays and show residence times in the range from seconds to a minute (8, 12, 21, 28, 31).

Immobilization of NRs is accompanied with a typical nuclear speckled distribution (Fig. 2E), whereas non DNA binding mutants and antagonist bound wild type NRs lack this pattern (Fig. 2F) (9, 28). The correlation between (transient) immobilization and this speckled pattern suggests that these speckles are NRs bound to specific regulatory sequences in gene promoters. This is corroborated by the partial overlap observed in an *in vivo* transcription assay visualizing sites of active transcription using BrUTP incorporation with NR speckles (32). Recently, others and we provided evidence that the speckled pattern observed for many SRs represent transcriptionally active sites, and may be considered the endogenous variant to the MMTV LTR array. Taken together, immobilization of activated NRs most likely reflects DNA binding and leads to a speckled NR distribution in the nucleus.

#### **1.4. FRET to Study Protein–Protein Interactions**

NR activity is not only regulated by hormone binding but also by interactions between their domains (DBD, LBD, and NTD) and interactions with cofactors (33). A powerful method to study protein–protein interactions in living cells is fluorescence resonance energy transfer (FRET) (Fig. 1E–H) (34–38). FRET is the non-radiative transfer of energy from a donor fluorophore in excited state to a nearby acceptor fluorophore, with an excitation spectrum significantly overlapping the emission spectrum of the donor. The critical distance between donor and acceptor fluorophores to

allow energy transfer is within only 10 nm, since FRET efficiency falls off with the sixth power of the distance between the two fluorophores (38, 39). Because these distances are in the range of protein sizes, FRET can be used not only to detect protein–protein interactions but also to study conformational changes proteins tagged with a FRET donor as well as a FRET acceptor (see **Note 3**). The most frequently used fluorophore couples in FRET assays to determine protein–protein interactions currently are GFP variants from the bioluminescent jellyfish *Aequorea Victoria* such as cyan fluorescent protein (CFP) and yellow fluorescent protein (YFP). Site-directed mutagenesis of GFP-like proteins has generated a range of variants with better spectral properties, improved brightness, and solubility (40–43). In particular, optimized CFPs like mCerulean (44), mTFP1 (45), and SCFP3A (46) and optimized YFPs like mCitrine (47, 48), mVenus (49), and SYFP2 (46) are promising candidates for sensitive FRET studies. Furthermore in recent years, a series of improved red shifted fluorophores have been developed, opening up a new range of potential FRET couples (42, 50–52). Spectral unmixing procedures also enable the utilization of spectrally close fluorophores (e.g. a GFP2 or GFP in combination with YFP) (53, 54) (see **Note 4**).

Like in FRAP, in FRET several different approaches have been developed, and the most frequently used being sensitized emission, ratio imaging, acceptor photobleaching FRET (abFRET), and fluorescence lifetime imaging (FLIM) (reviewed in ref. 55). The classical approach in FRET experiments is sensitized emission, where the emission of the acceptor fluorophore is detected while the donor fluorophore is excited (acceptors are sensitized to shorter wavelength excitation by adding donors; hence the term “sensitized emission”). Although sensitized emission is still widely used, cross talk of the donor signal in the acceptor channel and vice versa as well as the direct excitation of the acceptor by the donor excitation wavelength makes the analysis highly dependent on (and sensitive to noise in) control measurements of cells in which only one of the two fluorophore is present (56–58).

An alternative approach to determine FRET is acceptor/donor (e.g., YFP/CFP) ratio imaging where both donor and acceptor emission are detected simultaneously when excited at the excitation wavelength of the donor (**Fig. 1E**). However, the application of ratio imaging is limited to systems where CFP and YFP-tagged proteins are expressed in a constant ratio (e.g., double-tagged ER/AR) or in inducible systems where changes in YFP/CFP ratio can be observed in the same cells after initiating or abolishing the interactions of interest (**Figs. 1E, F and 3**). A procedure more applicable for determining protein–protein interaction in steady state, also when CFP and YFP-tagged proteins are not stoichiometrically expressed, is abFRET where photobleaching of the

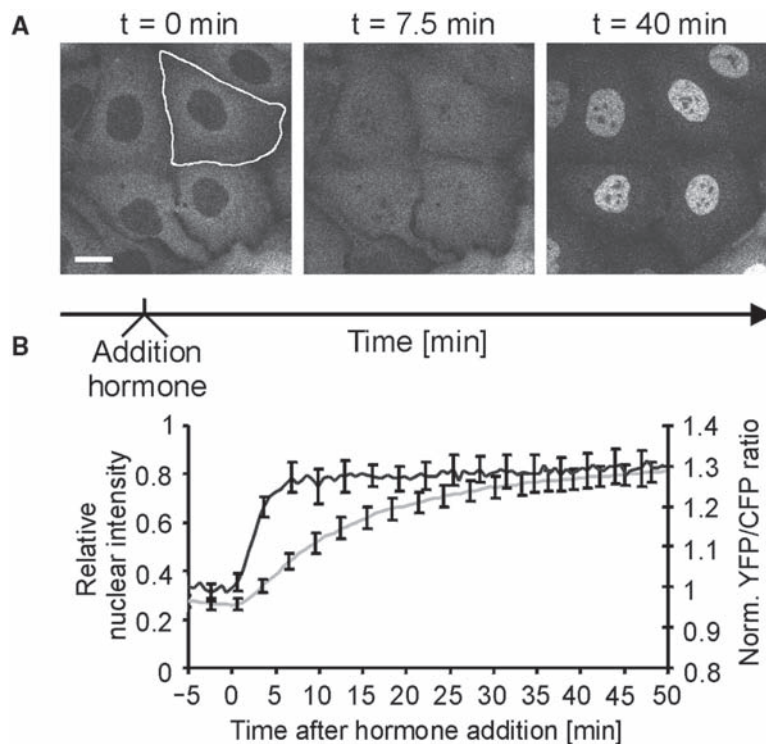


Fig. 3. FRET measurement by YFP/CFP ratio imaging. **(A)** Cells expressing the YFP-AR-CFP double-tagged AR are grown in the absence of hormone, when the AR is predominantly localized in the cytoplasm. Upon induction by hormone, the AR rapidly translocates to the nucleus. To determine FRET, as an indication of the AR N/C interaction, both YFP and CFP signals in the whole cell are detected simultaneously when CFP is excited (458 nm). In addition, the translocation of the AR can be determined by separately measuring the YFP signal (with YFP specific excitation (514 nm)) in the nucleus relatively to the signal in the whole cell. **(B)** Simultaneous detection of YFP and CFP signals (at 458 nm excitation) shows a prompt increase of YFP/CFP ratio after hormone addition at  $t = 0$  minutes (*black curve*;  $n = 10$ ). Translocation of the AR to the nucleus (*gray curve*) is much slower, indicating the N/C interaction (*black curve*) depends on hormone binding rather than cytoplasmic or nuclear localization (83). Error bars represent  $2 \times$  SEM. **Figure 3B** adapted from *ref. 32* with permission from The Rockefeller University Press.

acceptor results in unquenching of the donor and consequently in an increased donor signal (**Figs. 1G, H and 4A**) (38, 59–61). It is required to include the proper positive and negative control samples in the experiments, also to be able to correct for interexperimental variation (61). Moreover, a proper negative control should be used to correct for monitor bleaching effects (*see Note 5*). A fourth method to detect FRET is based on the reduced lifetime of excited donor molecules when they are in the proximity of acceptors (reviewed in *ref. 62, 63*). The fluorescent lifetime, or the average time that a molecule will stay in an excited state before returning to the ground state is a property of the fluorophore. In the occurrence of FRET, donors have an extra way to relax from the excited state by transfer of the energy to the nearby acceptor

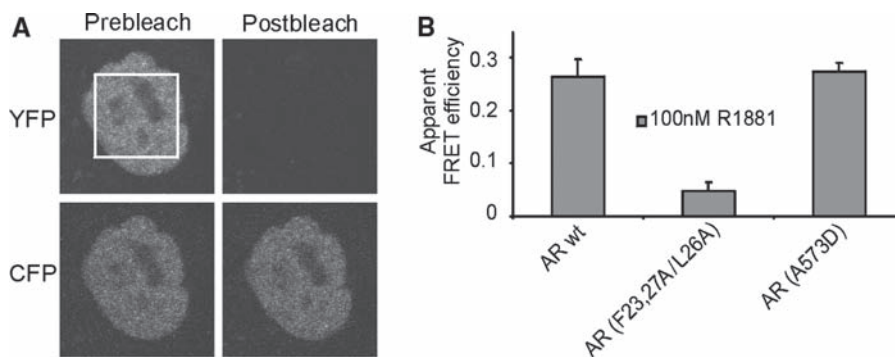


Fig. 4. Acceptor bleaching FRET on cells expressing double-tagged (YFP and CFP) ARs. **(A)** Confocal images of YFP and CFP fluorescence in Hep3B cells expressing YFP-AR-CFP before and after photobleaching YFP in the indicated region. **(B)** The apparent FRET efficiency of wild type YFP-AR-CFP and two mutants deficient in the N/C interaction (AR (F23, 27A/L26A)) or DNA binding (AR(A573D)). The apparent FRET efficiency is calculated as the fraction CFP increase after bleaching of all the YFP fluorescence and presented normalized to the CFP-YFP chimera (= 1) and cotransfected CFP and YFP (= 0). The N/C interaction is disabled when the FQNLF motif is mutated (AR F23,27A/L26A) but not in the non-DNA-binding mutant (AR(A573D)). **Figure 4B** adapted from *ref.* 32 with permission from The Rockefeller University Press.

fluorophore, which will result in a shortened average fluorescent lifetime of the donor fluorophores (64).

### 1.5. Protein Interactions in Steroid Receptor Function

One of the most intensively studied cofactor-binding sites on the NR surface is the hydrophobic cleft in the LBD formed by ligand induced repositioning of helix 12. Several cofactors, including the p160-coregulators SRC1, TIF2 (SRC2), and RAC1 (SRC3) are able to bind to this cleft via LxxLL-like motifs. FRET has been used extensively to study interactions of NRs or NR LBDs with peptides containing cofactor interaction motifs (32, 65–70). To investigate these interactions, several FRET-based ligand activity reporters have been designed in which NR LBDs are fused to cofactor fragments through a flexible linker and tagged with YFP and CFP at either terminus. Interaction of the ligand-activated NR LBD and the cofactor peptide brings the two FRET fluorophores in proximity resulting in an increased FRET signal (71–75). Furthermore, several others have applied FRET in studies on interactions of NRs with full length or fractions of cofactors and other transcription factors (76–78).

Intramolecular domain interactions lead to conformational changes of NRs. For the AR, such a conformational change is explained by the prevalence of the hydrophobic cleft in the AR LBD for FxxLF motifs, one of which is present in the AR NTD initiating the N/C interaction (79–82). To be able to study the AR N/C interaction in living cells by applying FRET technologies, others and we tagged both the N-terminal domain and de C-terminal LBD of the AR with YFP and CFP (22, 32, 83).



FRET-based experiments confirmed the results of previous two hybrid interaction assays indicating that the ligand induced N/C interaction is dependent on the N-terminal FQNLF motif (Fig. 4B). In contrast to intramolecular domain interactions, intermolecular domain interactions (e.g., intermolecular N/C interaction) lead to homo or hetero-dimerization. Several studies used FRET to detect dimerization of NRs including the AR (83–85). Interestingly, intramolecular N/C interactions are already initiated in the cytoplasm before translocation of the AR to the nucleus (Fig. 3B), whereas intermolecular N/C interactions in a dimer configuration are observed only after translocation to the nucleus (32, 83). Similar YFP/CFP ratio imaging experiments were used where it was observed that antiestrogens alter the configurations of ERs (86, 87).

The prevalence of the hydrophobic cleft in the AR LBD for FxxLF motifs initiating the N/C interactions suggest a competition with cofactor binding to this cleft and raises questions on the role of the N/C interaction in orchestrating these cofactor interactions. To extend our data with information on the mobility of specifically the subpopulation of N/C interacting ARs, we developed a new technology where we combined FRAP and abFRET (Fig. 1I–K) (32). As explained earlier, YFP bleaching results in a CFP increase, but only when FRET occurs. By applying FRAP on cells expressing FRETing proteins and simultaneously recording YFP recovery in the strip after photobleaching and the redistribution of the increased (because of YFP photobleaching) CFP signal, it is possible to compare the mobility of the interacting proteins (the CFP redistribution) relative to the mobility of the total pool of proteins (the YFP recovery as in conventional strip FRAP) (Figs. 1I–K and 5). By recording both the recovery of the YFP signal in time and the redistribution in time of the increased CFP signal after YFP photobleaching and comparing the two we were able to conclude that ARs with N/C interaction are not immobilized and therefore not bound to DNA (32).

The procedures of YFP/CFP ratio imaging, abFRET, and simultaneous FRAP and FRET measurements are described here in detail.

---

## 2. Materials

### 2.1. Constructs

1. Standard EGFP, EYFP, and ECFP vectors are used for cloning (Clontech, Palo Alto, CA).
2. pAR0, expressing human full-length wild-type AR (3), and pcDNA-AR0mcs (lacking the AR stop codon) (88) are used to fuse the AR with the fluorescent proteins.

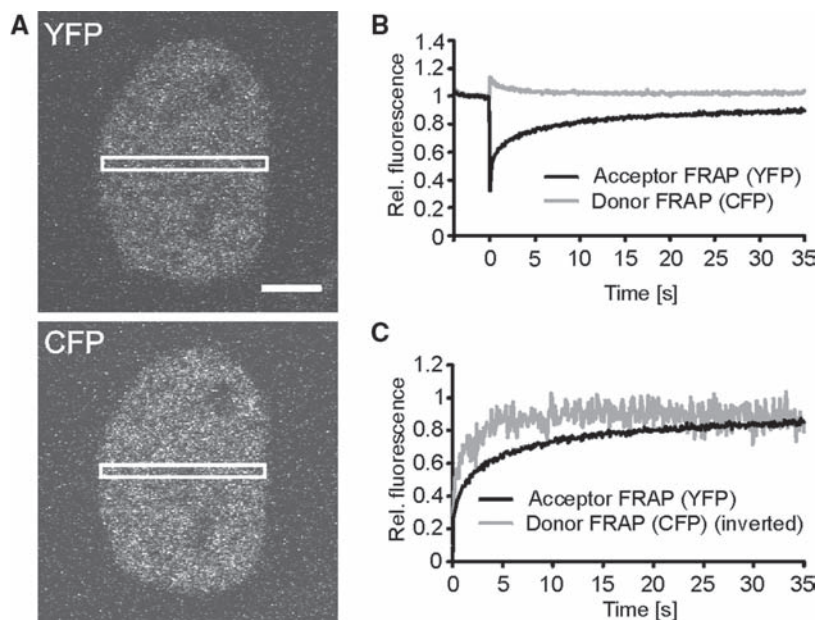


Fig. 5. Simultaneous FRAP and FRET measurements on cells expressing double-tagged ARs (see also Fig. 11–K). (A) Confocal images of Hep3B cells expressing YFP-AR-CFP imaged with the simultaneous FRAP and FRET configuration. The recovery of both YFP and CFP fluorescence in a small strip spanning the nucleus (*white box in A*) is recorded in time after shortly photobleaching YFP fluorescence. Bar represents 5  $\mu\text{m}$ . (B) In the presence of FRET YFP bleaching results in a local increase of CFP fluorescence. Similar to conventional strip-FRAP, the YFP fluorescence recovery represents the redistribution of the complete pool of ARs whereas the redistribution of the CFP fluorescence only represents the mobility of the interacting molecules. (C) When the CFP curve is inverted, and both curves are normalized to prebleach values at 1 and the intensity directly after YFP photobleaching at 0, the mobility of the interacting molecules can be compared with the total pool of ARs. Simultaneous FRAP and FRET on cells expressing YFP-AR-CFP indicates that the N/C interacting ARs have a higher mobility compared with the total pool of ARs. Figure 5C adapted from ref. 32 with permission from The Rockefeller University Press.

## 2.2. Cell Culture and Transfection

1. Hep3B human hepatocellular carcinoma cell line (ATCC) (see Note 6).
2. Alfacinimal essential medium ( $\alpha$ MEM) (Bio-Whittaker/Cambrex, Verviers, Belgium) supplemented with 2 mM L-glutamine (Bio-Whittaker/Cambrex), 100 U/mL Penicillin/100  $\mu\text{g}/\text{mL}$  Streptomycin (Bio-Whittaker/Cambrex) and 5% triple 0.1  $\mu\text{m}$  sterile filtered fetal bovine serum (FBS) (HyClone, South Logan, UT). Store at 2–8°C.
3. HyQ G418 sulfate (HyClone, South Logan, UT), working solution is 100  $\text{mg}/\text{mL}$  active concentration in PBS. Final concentration in culture medium is 0.6  $\text{mg}/\text{mL}$  G418.
4. Methyltrienolone (R1881) (NEN DuPont, Boston, USA). R1881 is dissolved in EtOH to 1 mM stock solution. The stock is stepwise diluted (1:10) in EtOH up to 1 nM R1881 to generate an array of working solutions. For our experiments



we used the 1  $\mu$ M R1881 working solution to obtain a final concentration of 1 nM of hormone in our culture medium. R1881 is light sensitive and store at  $-18^{\circ}\text{C}$ .

5. Trypsin EDTA: 200 mg/L Versene (EDTA), 500 mg/L Trypsin 1:250. Sterile filtered. Store stock at  $-10^{\circ}\text{C}$  and working solution at  $2-8^{\circ}\text{C}$ .
6.  $\varnothing$  24 mm cover slips (thickness: 0.13–0.16 mm) (Menzer-Gläser/Menzel Gerhard GmbH, Braunschweig, Germany) (*see* [Note 7](#)).
7. Polystyrene 6 Wells Cell Culture Cluster (Corning B.V. Life Sciences, Schiphol-Rijk, Netherlands)
8. FuGENE6 transfection medium (Roche Molecular Biochemicals, Indianapolis, IN). Store at  $2-8^{\circ}\text{C}$ .

### 2.3. Confocal Microscopy (FRAP and FRET)

1. All the described techniques are performed on a Zeiss Laser Scanning Microscope LSM510META equipped with a 30 mW Lasos LGK 7812 ML-4 Laser Class 3B Argon laser using the 458, 488, and 514 nm lines, a acousto-optical tunable filter (AOTF) (Carl Zeiss MicroImaging GmbH, Jena, Germany) and appropriate filters for GFP, YFP, and CFP imaging ([Fig. 6](#)).
2. The filter sets we used to specifically image the different fluorophores are shown in [Table 1](#).
3. The LSM 5 software, Version 3.2 controls the microscope, the scanning and laser modules, and the image acquisition process. This software is also used to analyze the images.

---

## 3. Methods

### 3.1. Constructs

1. The GFP-AR coding construct was generated by performing PCR on pAR0 (3) using a sense primer (5'-GCAGAAAGATCTGCAGGTGCTGGAGCAGGTGCTGGAGCAGGTGCTGG-AGAAGTGCAGTTAG-3') to introduce a *Bgl*II restriction site and a (GlyAla)<sub>6</sub> spacer sequence and an antisense primer in the AR cDNA overlapping a *Sma*I site (5'-TTGCTGTTCCCTCATCCAGGA-3'). The PCR product was cloned in pGEM-T-Easy (Promega, Madison, WI) and the sequence was verified. The *Bgl*II-*Sma*I fragment was inserted in the corresponding sites of pEGFP-C1 (Clontech, Palo Alto, CA). Next the *Sma*I fragment from pAR0 was inserted into the *Sma*I site to generate pGFP-(GlyAla)<sub>6</sub>-AR (further referred to as GFP-AR) (*see* [Note 8](#)). The non-DNA-binding mutant was obtained by exchanging the *Asp*718I-*Sca*I fragment from pAR(A573D) in GFP-AR.

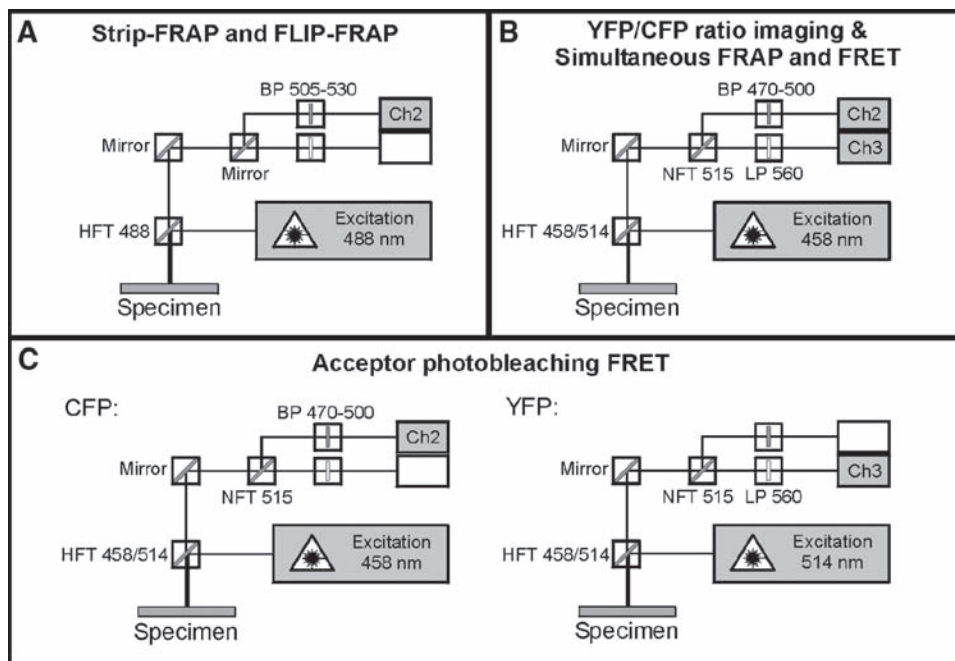


Fig. 6. The configurations to monitor the fluorophores in Strip-FRAP, FLIP-FRAP, abFRET and simultaneous FRAP and FRET experiments. (A) GFP-tagged proteins in strip-FRAP and FLIP-FRAP experiments are monitored using a 488 nm excitation and a specific beam splitter (HFT 488). GFP emission is collected specifically using a 505–530 band-pass filter (BP 505–530). (B) In abFRET, both YFP and CFP are monitored independently by collecting both emissions sequentially, each using their specific beam path. CFP and YFP fluorescence is imaged by applying 458 nm and 514 nm excitations, respectively. Both emissions are collected using a HFT 458/514, NFT 515, and a 470–500 nm band pass filter (BP470–500) for CFP and a 560 nm longpass filter (LP560) for YFP. (C) In simultaneous FRAP and FRET experiments, YFP and CFP are monitored simultaneously using the same filters as for abFRET. Both, CFP and YFP are excited at 458 nm.

2. The construct coding for AR double tagged with YFP and CFP (pEYFP-(GA)<sub>6</sub>-AR-(GA)<sub>6</sub>-ECFP) used for the FRET assays were generated by combining an N-terminally YFP-tagged AR with a C-terminally CFP-tagged AR (pAR-(GA)<sub>6</sub>-ECFP). The N-terminally YFP-tagged AR was generated by replacing EGFP in the EGFP-tagged AR described earlier by an *NheI*/*BglII* EYFP-C1 (Clontech, Palo Alto, CA) fragment. The C-terminally CFP-tagged AR was generated from AR-(GA)<sub>6</sub>-EGFP in which two AR fragments, a *HindIII*/*KpnI* C-terminal AR fragment from pcDNA-AR0mcs (88) lacking the AR stop codon and a N-terminal *HindIII* AR fragment from pAR0 where sequentially inserted in EGFP-N3 (Clontech, Palo Alto, CA) followed by a introduction of a (GlyAla)<sub>6</sub> spacer sequence in the *SacII* site between the AR and ECFP using primers (5'-GGGTGCTGGAGCAGGTGCTGGA GCAGGTGCTGGAGCCGC-3' and 5'-GGCTCCAGCA CCTGCTCCAGCACCTGCTCCAGCACCCGC-3') (see Note 8). After sequence verification EGFP is replaced by an

**Table 1**  
**Filter sets used in FRAP and FRET experiments**

Fluorophore	Excitation (nm)	Main beam splitter	Secondary beam splitter	Emission filter
EGFP	488	HFT 488	Mirror	BP 505–530
ECFP	458	HFT 458/514	NFT 515	BP 470–500
EYFP	514	HFT 458/514	NFT 515	LP 560

ECFP-N3 (Clontech, Palo Alto, CA) *Bam*HI/*Not*I fragment for pAR-(GA)<sub>6</sub>-ECFP. By insertion of the *Nhe*I/*Asp*718I EYFP-(GA)<sub>6</sub>-AR fragment containing the EYFP, the spacer sequence and a part of the AR, in the *Nhe*I/*Asp*718I sites of pAR-(GA)<sub>6</sub>-ECFP, a cDNA construct coding for a EYFP and ECFP-tagged ARs were generated (further referred to as YFP-AR-CFP).

3. pCYFP encoding the ECFP-EYFP chimera was generated by introducing an EYFP PCR fragment in the *Asp*718I site of pECFP-C1. Primers used for PCR: 5'-GCGAAAG-GTACCGATATCACCATGGTGAGCAAGGGC-3' (sense primer) to introduce an *Asp*718I site N-terminal of EYFP and 5'-GCGAAACGTACCGTTAACGGACTTGATCAGCTCGTCCATGC-3' (antisense primer) to introduce a *Bst*WI site at the C-terminus of EYFP that forms is compatible with an *Asp*718I overhang. pCYFP was kindly provided by Dr. Claude Gazin.

### 3.2. Cell Culture and Cell Transfection

1. Hep3B cells are grown in  $\alpha$ MEM supplemented with L-Glutamide, Penicillin, Streptomycin, and 5% FCS at 37°C and 5% CO<sub>2</sub> and passaged when approaching confluence (every 3–4 days) with Trypsin/EDTA to provide experimental cultures.
2. Two days before confocal microscopy Hep3B cells are seeded on a coverslip in a 6-well plate at a concentration of  $\sim 3 \times 10^5$  cells per well in 2 mL  $\alpha$ MEM with 5% FCS. This concentration will provide near confluent cultures at the time of the experiment and enough cells at the time of transfection. The cells are grown overnight at 37°C with 5% CO<sub>2</sub>.
3. Between 24 and 32 h before confocal microscopy the medium is replaced by 1 mL  $\alpha$ MEM supplemented with 5% charcoal striped serum (DCC), L-Glutamide and antibiotics, without washing the cells.
4. After 2 h the transfection mix is prepared for the transfection of 1  $\mu$ g of GFP-AR coding vector. Three microliter FuGENE6 per  $\mu$ g DNA to be transfected is added to 100  $\mu$ l serum free  $\alpha$ MEM. Five minutes later DNA is added. The transfection

mix is gently mixed by pipeting up and down and left at room temperature for at least 30 min.

5. Four hours after medium replacement the transfection mix is gently added to the cells under gentle mixing. The cells further incubated for 4 h at 37°C and 5% CO<sub>2</sub>.
6. Four hours after transfection the medium is replaced again by 2 mL  $\alpha$ MEM supplemented with charcoal striped serum (DCC) with or without 100 nM R1881. The cells are further incubated overnight at 37°C and 5% CO<sub>2</sub> until the experiment.

### 3.3. Confocal Microscopy

#### 3.3.1. Fluorescence Recovery After Photobleaching (FRAP)

##### Strip-FRAP

1. These instructions assume the use of a Zeiss CLSM 510 confocal laser-scanning microscope equipped with an Argon laser (**Fig. 6A**). The Argon laser is adjusted to 6.1 A tube current and allowed to stabilize for at least 15 min.
2. A cover slip with Hep3B cells expressing GFP-tagged AR (EGFP-AR) is placed in a metal holder in which 1.5 mL culture medium is added on top of the coverslip. The holder including the coverslip is placed on a temperature-controlled plate at 37°C. In addition, the objective lens is also kept at 37°C by a temperature-controlled ring, to prevent cooling of cells near the lens, which are exactly the ones being investigated.
3. GFP fluorescence is monitored using 488 nm excitation at the low intensity of 0.5–0.8  $\mu$ W (measured in the focal plane of the 40 $\times$  objective lens used) (*see Note 9*), a main beamsplitter reflecting only light at a wavelength of 488 nm, and a band pass filter BP505–530 (**Fig. 6A**) (*see Table 1*). The pinhole is adjusted to a diameter corresponding to an “optical slice” of approximately 2  $\mu$ m and a high detector gain (900) (*see Notes 10 and 11*). Scanning is performed unidirectional with scan speed of 1.9 ms per line of 512 pixels spaced 70 nm to enable fast recording of the fluorescent signal in the strip. Fluorescent signals are recorded with an 8-bit data depth.
4. A nucleus with a physiologically relevant expression level of GFP-AR is selected at low zoom (*see Note 12*). The scanning area is adjusted using the “center” macro in the macro-directory to put the center of the nucleus in the middle of the scanning area after which the nucleus is aligned vertically using the crop function (*see Note 13*). When the nucleus is oriented correctly sample distance (pixel size) is adjusted to 70 nm.
5. A 10 pixel (= 700 nm) wide region of interest (ROI) spanning the nucleus is selected in the Edit ROI panel, for recording the recovery of the signal. Using the Define Region option the Bleach Control panel, the same ROI is selected to locally bleach GFP (**Fig. 2A**).

6. The fluorescent signal is monitored by scanning the ROI for 4,000 scans (~80s) with a 21 ms time interval (Time Series Control) at low excitation (*see Note 9*) (**Fig. 2A**). After 200 scans the GFP is bleached locally inside the ROI using a scan (1 iteration) of 488 nm laser light at maximum laser intensity. The time-series are initiated using the Mean ROI option in the time-series control (*see Note 14*). After the scan, the data can be copied to for instance a spreadsheet file or can be directly saved as MDB-file for later analysis.
7. Before averaging a sufficient amount of curves the data have to be normalized (*see Note 15*). The most straightforward normalization is to express the data relative to prebleach intensities ( $I_{\text{prebleach}}$ ) after background subtraction:  $I_{\text{norm,t}} = (I_{\text{t,raw}} - I_{\text{background}}) / (I_{\text{prebleach}} - I_{\text{background}})$ . Alternatively, it is also possible to express the raw data relative to both fluorescence before, as well as immediately after bleaching:  $I_{\text{norm,t}} = (I_{\text{t,raw}} - I_0) / (I_{\text{prebleach}} - I_0)$ . This normalization not only removes variations in expression levels but also of the laser intensity used for bleaching, which can lead to differences in bleach depth (*see Note 16*). To allow fitting of the data to simple analytical equations representing the diffusion process, the data can also be expressed relative to the fluorescence intensities immediately after the bleach and after complete recovery, resulting in curves starting at 0 after the bleach and 1 at complete recovery:  $I_{\text{norm,t}} = (I_{\text{t,raw}} - I_0) / (I_{\text{postbleach}} - I_0)$  (**Fig. 2B**) (*see Note 17*) (18).

#### FLIP-FRAP

1. Cells are placed in the Zeiss CLSM 510 confocal laser-scanning microscope and positioned in the focal plane as described in the strip-FRAP section. For FLIP-FRAP, similar settings are used for GFP imaging. A correctly oriented nucleus is imaged using a zoom corresponding to a pixel interval of 70 nm. The pinhole is adjusted to a diameter corresponding to an “optical slice” of approximately 2  $\mu\text{m}$ . Scanning is performed unidirectional with scan speed of 1.9 ms per line of 512 pixels to enable fast recording of the fluorescent signal in the strip. Fluorescent signals are recorded with an 8-bit data depth using a high detector gain (1,000) (*see Notes 10 and 11*).
2. A ROI with a width between approximately 1 and 2  $\mu\text{m}$  (but constant in all experiments to be compared) and spanning the nucleus at one pole is selected in the Edit ROI panel, for recording the recovery of the signal after bleaching. Using the Define Region option the Bleach Control panel, the same ROI is selected to locally bleach GFP. A second ROI of similar width spanning the nucleus at the opposite pole is selected, to measure the decrease of fluorescence due to redistribution of the proteins from the bleached area (FLIP) (**Fig. 2C**).

3. The fluorescent signal is monitored by scanning the two ROIs at a low excitation level with a 3 s time interval for approximately 100 s, dependent on the mobility of the protein under surveillance (Time Series Control) (*see Note 9*). After the first scan GFP is bleached locally inside one of the two ROIs (but always the same in experiments to be compared) using 10 iterations of 488 nm laser light at maximum laser intensity. After the experiment, the data can be copied directly to a spreadsheet file or can be saved as MDB-file for later analysis.
4. The most straight forward analysis is to calculate the fluorescence intensity difference between the FLIP-ROI and the FRAP-ROI and normalize the data ( $I_{\text{FLIP-FRAP}} = (I_{\text{FLIP-ROI}} - I_{\text{FRAP-ROI}})$ ) and normalize to the intensity directly after bleaching (**Fig. 2D**).

### 3.3.2. Fluorescence Resonance Energy Transfer (FRET)

#### Ratio Imaging

1. A coverslip with Hep3B cells expressing double, EYFP and ECFP, tagged AR (EYFP-AR-ECFP) in the absence of hormone is placed in the Zeiss CLSM 510 confocal laser-scanning microscope and cells are positioned in the focal plane as described in the strip-FRAP section.
2. EYFP and ECFP images were collected sequentially using the single-track configuration. Both CFP and YFP are detected using 458 nm excitation at low laser power to avoid photobleaching (*see Note 9*), a 458/514 nm dichroic beam splitter (HFT 458/514) and a 515 nm beam splitter (NFT 515). ECFP and EYFP signals were further separated by a 470–500 nm band pass emission filter (BP470–500) and a 560 nm long pass emission filter (LP560), respectively (**Fig. 6B**). A group of cells with an EYFP-AR-ECFP expression at physiological relevant expression level (*see Note 12*) is selected at a zoom corresponding to a pixel interval of 220 nm. Scanning is performed unidirectional at a scan speed corresponding to 3.84 ms per line of 512 pixels and an average of 2, with the pinhole diameter such that the “optical slice” has an approximate thickness of 3  $\mu\text{m}$ . Detector gain in both the YFP and CFP track is set on 900 (*see Notes 10 and 11*). Sequential images of 512  $\times$  512 pixels are collected with an 8-bit data depth using the timeseries macro or the multitime macro with an interval of 30 s (*see Note 18*) (**Fig. 3A**). At a user-specified moment during the collection of images the AR is induced by adding 100 nM R1881 (synthetic variant of testosterone).
3. EYFP and ECFP image sequences were analyzed using the Zeiss Laser Scanning Microscope LSM510 software selecting ROIs covering each cell (*see Note 19*). After background subtraction FRET is simply calculated as:  $I_{\text{YFP}}/I_{\text{CFP}}$  and plotted in time (**Fig. 3B**) (*see Note 20*).



Acceptor Photobleaching  
FRET (AbFRET)

1. A coverslip with Hep3B cells expressing double, YFP and CFP, tagged androgen receptor (YFP-AR-CFP) is placed in the Zeiss CLSM 510 confocal laser-scanning microscope and cells are positioned in the focal plane as described in the strip-FRAP section.
2. YFP and CFP images of cells with a low EYFP-AR-ECFP expression were collected sequentially using the multitrack option (*see Notes 12 and 21*). For both fluorophores, two specific beam paths are used. Both tracks include a 458/514 nm dichroic beam splitter (HFT 458/514) and a 515 nm beam splitter (NFT 515). ECFP was excited with 10  $\mu$ W (measured at the focus of the 40 $\times$  objective lens with aperture 1.35) 458 nm laser light of an Argon laser and imaged with a 470–500 nm band pass emission filter (BP470–500). EYFP was excited with 5  $\mu$ W 514 nm laser light and imaged with a 560 nm long pass emission filter (LP560) (**Fig. 6C**).
3. In both the tracks, the pinhole diameter is adjusted such that the “optical slice” is 1.2  $\mu$ m. Scanning is preformed unidirectional with scan speed corresponding with 3.07 ms per line of 512 pixels at a pixel interval of 100 nm. Detector gain in the YFP track is set on 800 in the CFP track on 900, the amplifier offset and amplifier gain in both tracks are 0.1 and 1, respectively (*see Notes 10 and 11*). Images of 512  $\times$  512 pixels are generated with an 8-bit data depth.
4. After sequential collection of YFP and CFP images, YFP is bleached by scanning 25 times a nuclear region of  $\sim$ 100  $\mu$ m<sup>2</sup>, covering a large part of the nucleus using the 514 nm argon laser line at high ( $\sim$ 80  $\mu$ W) laser power. After acceptor photobleaching, a second YFP and CFP image pair was collected (*see Note 22*) (**Fig. 4A**).
5. YFP and CFP images were analyzed using the Zeiss Laser Scanning Microscope LSM510 software. After background subtraction, the apparent FRET efficiency was calculated as; Apparent FRET efficiency =  $\frac{((CFP_{\text{after}} - CFP_{\text{before}}) \times YFP_{\text{before}}) \times ((CFP_{\text{after}} \times YFP_{\text{before}}) - (CFP_{\text{before}} \times YFP_{\text{after}}))^{-1}}$ , in which the relative CFP increase due to YFP bleaching is corrected for the fraction of YFP bleached (54). The apparent FRET efficiency was finally expressed relative to control measurements in cells expressing either free CFP and YFP ( $abFRET_0$ ) or the CFP-YFP fusion protein ( $abFRET_{\text{CFP-YFP fusion}}$ ): apparent FRET efficiency =  $\frac{(abFRET - abFRET_0)}{(abFRET_{\text{CFP-YFP fusion}} - abFRET_0)}$  (**Fig. 4B**).

Simultaneous FRAP  
and FRET

1. A coverslip with Hep3B cells expressing YFP and CFP double-tagged androgen receptor (EYFP-AR-ECFP) is placed in the Zeiss CLSM 510 confocal laser-scanning microscope



and are positioned in the focal plane as described in the strip-FRAP section.

2. In contrast to acceptor bleaching FRET, YFP and CFP signals are collected simultaneously using two parallel channels but only one 458 nm excitation at low laser intensity and a 458/514 nm dichroic beam splitter (HFT 458/514) (*see Note 23*). The two specific emission beam paths for both fluorophores are similar to those used for acceptor bleaching FRET. The emission signal is separated using a 515 nm beam splitter (NFT 515). ECFP emission is collected via a 470–500 nm band pass emission filter (BP470–500). EYFP emission is simultaneously collected via a 560 nm long pass emission filter (LP560) (**Fig. 6B**). Scanning is performed unidirectional with scan speed of 1.9 ms per line of 512 pixels spaced 70 nm to enable fast recording of the fluorescent signal in the strip. The pinhole is adjusted to a diameter corresponding to an “optical slice” of approximately 3  $\mu\text{m}$ . Similar as in strip-FRAP experiments a high detector gain (1,000) is used (*see Notes 10 and 11*). Fluorescent signals are recorded with an 8-bit data depth.
3. A nucleus with a low expression of YFP-AR-CFP is selected at low zoom (*see Note 12*). The scanning area is adjusted using the “center” macro in the macro-directory to put the center of the nucleus in the middle of the scanning area. The nucleus is rotated using the crop function to align the nucleus vertically.
4. A 700 nm wide ROI (corresponding to 10 pixels at zoom 6 on a Zeiss LSM 510 meta) spanning the nucleus is selected in the Edit ROI panel, for recording the recovery of the signal. Using the Define Region option the Bleach Control panel, the same ROI is selected to locally bleach YFP (**Fig. 5a**).
5. The fluorescent signal is monitored at low laser intensity (*see Note 9*), by scanning the ROI with interval of 100 ms (Time Series Control) for approximately 80 s, dependent on the mobility of the protein under surveillance. After 400 scans, the YFP is specifically bleached locally inside the ROI using a scan (5 iterations) of 514 nm laser light at maximum laser intensity (*see Note 23*). The time-series are initiated using the Mean ROI option in the time-series control. After the scan, the data can be copied directly to a spreadsheet or can be saved as MDB-file for later analysis.
6. Like in strip-FRAP, it is possible to normalize the donor fluorescence data in different ways. By expressing the raw data relative to prebleach values, one can visualize directly the increase of CFP signal when YFP is bleached ( $I_{\text{norm,t}} = (I_{\text{t,raw}} - I_{\text{background}}) / (I_{\text{prebleach}} - I_{\text{background}})$ ) (**Fig. 5B**), but comparison between the interacting proteins vs. the total pool (i.e., the donor and acceptor fluorescence signals, respectively) requires expressing raw data relative to intensity values immediately

after bleaching and to prebleach intensities ( $I_{\text{norm},t} = (I_{\text{t,raw}} - I_0)/(I_{\text{prebleach}} - I_0)$ ) or after complete redistribution ( $I_{\text{norm},t} = (I_{\text{t,raw}} - I_0)/(I_{\text{postbleach}} - I_0)$ ) where  $I_{\text{prebleach}}$ ,  $I_0$ , and  $I_{\text{postbleach}}$  are the fluorescent intensities before, immediately after the bleach, and after complete recovery, respectively (Fig. 5C) (see Note 24).

---

## 4. Notes

1. Fluorescence *redistribution* after photobleaching may be better description rather than fluorescence *recovery* after photobleaching: in the absence of a permanently immobilized fraction, the fluorescence intensity in the measured region will level off to the average intensity in the nucleus, which will be lower than the initial intensity because of the permanently bleached fraction. The term “recovery” suggests that fluorescence intensity in general returns to the initial levels.
2. In FRAP, a fraction of the fluorescent proteins inside a nucleus will be irreversibly bleached during the bleach pulse, resulting in an incomplete recovery of the fluorescent signal independent of the presence of an immobile fraction. In the case of the AR, this can be corrected by comparing wild type AR with the non-DNA binding mutant (e.g., AR(A573D)), which does not get immobilized due to DNA-binding. Therefore, the incomplete recovery of fluorescence of, for instance, a tagged non-DNA binding AR mutant is only due to irreversibly bleaching of a significant fraction of the molecules during the bleach pulse. In the experimental settings of the strip-FRAP procedure described here, approximately 10% of a nucleus of average size is photobleached.
3. The efficiency of energy transfer does not only depend on the distance between the two fluorophores but also their relative orientation plays a role in FRET efficiency (39). However, in fusion proteins using a flexible linker between the fluorescent protein and the protein of interest, this may be limited because of the rotational freedom of the fluorophores.
4. On the one hand, FRET only occurs when the excitation spectrum of the acceptor fluorophore overlaps significantly with the emission spectrum of the donor fluorophore. On the other hand, the excitation and emission spectra of the FRET couple need sufficient separation to be able to sufficiently separate the two signals. The most widely used FRET couple is the combination between CFP and YFP, but improved fluorophore variants will certainly contribute to the applicability of FRET in protein–protein interaction studies (Discussed in 42).

5. In our experience, monitorbleaching does not fluctuate very much when settings are kept constant and is mostly dependent on excitation power. Therefore, normalization to FRET values measured for cotransfected free YFP and CFP as negative control can be used to correct the apparent FRET efficiency for monitor bleaching when the excitation power is kept constant.
6. Hep3B-cells that lack endogenous nuclear receptors are easy to transfect and they are relatively large, simplifying microscopy. Other type of cells can be used but the presence of endogenous nuclear receptors needs to be taken into account. Endogenous expression of nuclear receptors will dilute FRET values.
7. Coverslips should not be thicker than 0.16 mm, because of the high numerical aperture and short working distance of most lenses used for high-resolution confocal microscopy.
8. It is essential to check the fusion proteins for functionality. For tagged ARs, most often ARE driven luciferase gene reporter assays are used. By using such a luciferase gene reporter assay, we showed that a flexible stretch between the AR and the fluorophores limits the degree to which the activity of the AR is affected by the presence of the large GFP-tag(s). Our data indicated that GFP-AR with a (GlyAla)<sub>6</sub> stretch functions better than with a (Gly)<sub>6</sub> spacer. (11). In addition, the flexible stretch most likely also gives the fluorophores more rotational freedom limiting the influence of fluorophore orientations on FRET efficiencies (see also [Note 3](#)).
9. At this intensity no significant bleaching of GFP, YFP, or CFP should occur during the experiment, which takes between 10 and 80 s. In FRAP experiments, it is important to avoid monitor bleaching by applying excitation at lowest possible laser power. In simultaneous FRAP and FRET experiments, monitor bleaching hampers the analysis because of the opposite effect of monitor bleaching on the redistributions of the YFP and CFP signals. In the acceptor bleaching FRET experiments, monitor bleaching is less problematic because the apparent FRET efficiency can be corrected by normalization to the FRET efficiency of cotransfected CFP and YFP (see also [Note 5](#)).
10. Although a higher detector gain (DG) can be used to obtain higher signals, it does not improve the signal-to-noise ratio. Therefore, a trade-off between settings is necessary to optimize the experimental setup to reduce both noise (e.g., averaging) and monitor bleaching (e.g., lower excitation level and rapid scanning) but still producing a high enough signal in low expressing cells (e.g. wider pinhole; although this is at

the cost of resolution, in many interaction studies the interaction as such is more important than its precise location; however, if it is important, higher laser excitation intensity may be required). These settings might also depend on the level or pattern of expression of the protein of interest.

11. It is important to choose settings that allow selecting low expressing cells in your experiments. This can be achieved by e.g. higher detector gain, wider pinhole, or higher laser excitation intensity, but might be at the cost of signal to noise ratio and resolution (*see* also [Notes 10 and 12](#)).
12. For all the discussed approaches, it is essential to select cells that express the investigated protein at a physiologically relevant level, since overexpression may lead to aggregation and artificial immobilization of the receptors (23) and false positive FRET signals due to high concentration.
13. Not only the size of nucleus but also the shape and the relative position of the bleached region will influence the fluorescence recovery curve. Therefore, it is highly important to keep these parameters similar. We chose to select ellipsoid nuclei and bleach a strip spanning the nucleus at its shortest ellipsoidal axis (*see* for instance [Fig. 2a](#)).
14. In the configuration, the monitordiode (ChM) can be selected to monitor the fluctuations in the laser intensity during scanning.
15. Normalization of FRAP data before averaging is important to remove variation due to differences in absolute amounts of protein. This is justified since fluorescent changes after bleaching are proportional to initial values, and do not depend on fluorophore concentration. Obviously, the investigated cells should have expression levels within physiologically relevant limits. In an average experiment, approximately 10–15 cells are measured.
16. In theory this is only true if the bleach pulse is infinitely short and the first measurement is really immediately after bleaching.
17. Any permanently immobile fraction is removed in this case allowing determination of the (apparent) diffusion coefficient of the mobile fraction.
18. Using the multitime-macro in the LSM510 software enables to image more than one position in parallel. Selecting multiple locations limits the time resolution of the time series.
19. Because of movement of cells it might be necessary to adapt location and/or shape of the ROIs in the analysis of time series.
20. Ratio imaging is only possible in three cases: (1) when signals are compared in the same single cell before and after a

specific treatment, (2) when the FRET pair is tagged to the same molecule, and, (3) when the donor and acceptor are expressed at a constant concentration ratio.

21. To specifically image both fluorescence signals and avoid cross talk in the different channels YFP and CFP are imaged sequentially, exciting YFP and CFP each at their specific wavelength (514 and 458 nm, respectively) and separating their emission signals through specific filtersets (*see* [Table 5.1](#)).
22. Previously we have shown that in the absence of FRET, no CFP signal increase is observed in cells with the low expression level used (32).
23. In principle, the experiment is a standard FRAP experiment on the acceptor, in this case YFP, in which in an additional channel the fluorescence of the donor is being recorded.
24. Subtractions in the donor signal normalization lead to negative numbers, yielding a positive result after division, where the curve starts at 0 and increases until it reaches 1. So the donor loss of fluorescence characteristics is represented by an increasing curve allowing direct comparison with the FRAP-data from the acceptor.

## References

1. Germain, P., Staels, B., Dacquet, C., Spedding, M., and Laudet, V. (2006) Overview of nomenclature of nuclear receptors. *Pharmacol. Rev.* **58**, 685–704.
2. Trapman, J., and Cleutjens, K. B. (1997) Androgen-regulated gene expression in prostate cancer. *Semin. Cancer Biol.* **8**, 29–36.
3. Brinkmann, A. O., Faber, P. W., van Rooij, H. C. J., Kuiper, G. G. J. M., Ris, C., Klaassen, P., van der Korput, J. A. G. M., Voorhorst, M. M., van Laar, J. H., Mulder, E., and Trapman, J. (1989) The human androgen receptor: domain structure, genomic organization and regulation of expression. *J. Steroid Biochem.* **34**, 307–10.
4. Claessens, F., Verrijdt, G., Schoenmakers, E., Haelens, A., Peeters, B., Verhoeven, G., and Rombauts, W. (2001) Selective DNA binding by the androgen receptor as a mechanism for hormone-specific gene regulation. *J. Steroid Biochem. Mol. Biol.* **76**, 23–30.
5. Cleutjens, K. B. J. M., van der Korput, J. A. G. M., van Eekelen, C. C. E. M., van Rooij, H. C. J., Faber, P. W., and Trapman, J. (1997) An androgen response element in a far upstream enhancer region is essential for high, androgen-regulated activity of the prostate-specific antigen promoter. *Mol. Endocrinol.* **11**, 148–61.
6. Tyagi, R. K., Lavrovsky, Y., Ahn, S. C., Song, C. S., Chatterjee, B., and Roy, A. K. (2000) Dynamics of intracellular movement and nucleocytoplasmic recycling of the ligand-activated androgen receptor in living cells. *Mol. Endocrinol.* **14**, 1162–74.
7. Georget, V., Lobaccaro, J. M., Terouanne, B., Mangeat, P., Nicolas, J.C., and Sultan, C. (1997) Trafficking of the androgen receptor in living cells with fused green fluorescent protein-androgen receptor. *Mol. Cell. Endocrinol.* **129**, 17–26.
8. Rayasam, G. V., Elbi, C., Walker, D. A., Wolford, R., Fletcher, T. M., Edwards, D. P., and Hager, G. L. (2005) Ligand-specific dynamics of the progesterone receptor in living cells and during chromatin remodeling in vitro. *Mol. Cell. Biol.* **25**, 2406–18.
9. Farla, P., Hersmus, R., Trapman, J., and Houtsmuller, A. B. (2005) Antiandrogens prevent stable DNA-binding of the androgen receptor. *J. Cell Sci.* **118**, 4187–98.
10. Agresti, A., Scaffidi, P., Riva, A., Caiolfa, V. R., and Bianchi, M. E. (2005) GR and HMGB1 interact only within chromatin and

- influence each other's residence time. *Mol. Cell* **18**, 109–21.
11. Farla, P., Hersmus, R., Geverts, B., Mari, P. O., Nigg, A. L., Dubbink, H. J., Trapman, J., and Houtsmuller, A. B. (2004) The androgen receptor ligand-binding domain stabilizes DNA binding in living cells. *J. Struct. Biol.* **147**, 50–61.
  12. Schaaf, M. J., and Cidlowski, J. A. (2003) Molecular determinants of glucocorticoid receptor mobility in living cells: the importance of ligand affinity. *Mol. Cell. Biol.* **23**, 1922–34.
  13. Stenoien, D. L., Patel, K., Mancini, M. G., Dutertre, M., Smith, C. L., O'Malley, B. W., and Mancini, M. A. (2001) FRAP reveals that mobility of oestrogen receptor- $\alpha$  is ligand- and proteasome-dependent. *Nat. Cell Biol.* **3**, 15–23.
  14. McNally, J. G., Müller, W. G., Walker, D., Wolford, R., and Hager, G. L. (2000) The glucocorticoid receptor: rapid exchange with regulatory sites in living cells. *Science* **287**, 1262–65.
  15. Houtsmuller, A. B., and Vermeulen, W. (2001) Macromolecular dynamics in living cell nuclei revealed by fluorescence redistribution after photobleaching. *Histochem. Cell Biol.* **115**, 13–21.
  16. Houtsmuller, A. B., Rademakers, S., Nigg, A. L., Hoogstraten, D., Hoeijmakers, J. H. J., and Vermeulen, W. (1999) Action of DNA repair endonuclease ERCC1/XPF in living cells. *Science* **284**, 958–61.
  17. Houtsmuller, A. B. (2005) Fluorescence recovery after photobleaching: application to nuclear proteins. in “*Advances in Biochemical Engineering/Biotechnology*” (Rietdorf, J., ed.), Vol. **95**, Springer-Verlag GmbH, Berlin, pp. 177–99.
  18. Van Royen, M. E., Farla, P., Mattern, K. A., Geverts, B., Trapman, J., and Houtsmuller, A. B. (2008) FRAP to study nuclear protein dynamics in living cells. in “*The Nucleus, Volume 2: Physical Properties and Imaging Methods*” (Hancock, R., ed.), Vol. **464**, Humana Press, pp. 363–84.
  19. Bruggenwirth, H. T., Boehmer, A. L. M., Lobaccaro, J. M., Chiche, L., Sultan, C., Trapman, J., and Brinkmann, A. O. (1998) Substitution of Ala564 in the first zinc cluster of the deoxyribonucleic acid (DNA)-binding domain of the androgen receptor by Asp, Asn, or Leu exerts differential effects on DNA binding. *Endocrinology* **139**, 103–10.
  20. Elbi, C., Walker, D. A., Romero, G., Sullivan, W. P., Toft, D. O., Hager, G. L., and DeFranco, D. B. (2004) Molecular chaperones function as steroid receptor nuclear mobility factors. *Proc. Natl. Acad. Sci. USA* **101**, 2876–81.
  21. Stavreva, D. A., Muller, W. G., Hager, G. L., Smith, C. L., and McNally, J. G. (2004) Rapid glucocorticoid receptor exchange at a promoter is coupled to transcription and regulated by chaperones and proteasomes. *Mol. Cell. Biol.* **24**, 2682–97.
  22. Klokk, T. I., Kurys, P., Elbi, C., Nagaich, A. K., Hendarwanto, A., Slagsvold, T., Chang, C.Y., Hager, G. L., and Saaticioglu, F. (2007) Ligand-specific dynamics of the androgen receptor at its response element in living cells. *Mol. Cell. Biol.* **27**, 1823–43.
  23. Marcelli, M., Stenoien, D. L., Szafran, A. T., Simeoni, S., Agoulnik, I. U., Weigel, N. L., Moran, T., Mikic, I., Price, J. H., and Mancini, M. A. (2006) Quantifying effects of ligands on androgen receptor nuclear translocation, intranuclear dynamics, and solubility. *J. Cell. Biochem.* **98**, 770–88.
  24. Masiello, D., Cheng, S., Bublely, G. J., Lu, M. L., and Balk, S. P. (2002) Bicalutamide functions as an androgen receptor antagonist by assembly of a transcriptionally inactive receptor. *J. Biol. Chem.* **277**, 26321–26.
  25. Kang, Z., Pirskanen, A., Janne, O. A., and Palvimo, J. J. (2002) Involvement of proteasome in the dynamic assembly of the androgen receptor transcription complex. *J. Biol. Chem.* **277**, 48366–71.
  26. Veldscholte, J., Ris-Stalpers, C., Kuiper, G. G., Jenster, G., Berrevoets, C., Claassen, E., van Rooij, H. C., Trapman, J., Brinkmann, A. O., and Mulder, E. (1990) A mutation in the ligand binding domain of the androgen receptor of human LNCaP cells affects steroid binding characteristics and response to anti-androgens. *Biochem. Biophys. Res. Commun.* **173**, 534–40.
  27. Hara, T., Miyazaki, J., Araki, H., Yamaoka, M., Kanzaki, N., Kusaka, M., and Miyamoto, M. (2003) Novel mutations of androgen receptor: a possible mechanism of bicalutamide withdrawal syndrome. *Cancer Res.* **63**, 149–53.
  28. Schaaf, M. J. M., Lewis-Tuffin, L. J., and Cidlowski, J. A. (2005) Ligand-selective targeting of the glucocorticoid receptor to nuclear subdomains is associated with decreased receptor mobility. *Mol. Endocrinol.* **19**, 1501–15.
  29. Martinez, E. D., Rayasam, G. V., Dull, A. B., Walker, D. A., and Hager, G. L. (2005) An estrogen receptor chimera senses ligands by nuclear translocation. *J. Steroid Biochem. Mol. Biol.* **97**, 307–21.



30. Sharp, Z. D., Mancini, M. G., Hinojos, C. A., Dai, F., Berno, V., Szafran, A. T., Smith, K. P., Lele, T. T., Ingber, D. E., and Mancini, M. A. (2006) Estrogen-receptor- $\alpha$  exchange and chromatin dynamics are ligand- and domain-dependent. *J. Cell Sci.* **119**, 4101–16.
31. Meijsing, S. H., Elbi, C., Luecke, H. F., Hager, G. L., and Yamamoto, K. R. (2007) The ligand binding domain controls glucocorticoid receptor dynamics independent of ligand release. *Mol. Cell Biol.* **27**, 2442–51.
32. Van Royen, M. E., Cunha, S. M., Brink, M. C., Mattern, K. A., Nigg, A. L., Dubbink, H. J., Verschure, P. J., Trapman, J., and Houtsmuller, A. B. (2007) Compartmentalization of androgen receptor protein-protein interactions in living cells. *J. Cell Biol.* **177**, 63–72.
33. Rosenfeld, M. G., Lunyak, V. V., and Glass, C. K. (2006) Sensors and signals: a coactivator/corepressor/epigenetic code for integrating signal-dependent programs of transcriptional response. *Genes Dev.* **20**, 1405–28.
34. Griekspoor, A., Zwart, W., Neefjes, J., Michalides, R. (2007) Visualizing the action of steroid hormone receptors in living cells. *Nucl. Recept. Signal.* **5**, e003.
35. Sato, M. (2006) Imaging molecular events in single living cells. *Anal. Bioanal. Chem.* **386**, 435–43.
36. Day, R. N., Periasamy, A., and Schaufele, F. (2001) Fluorescence resonance energy transfer microscopy of localized protein interactions in the living cell nucleus. *Methods* **25**, 4–18.
37. Day, R. N., Nordeen, S. K., and Wan, Y. (1999) Visualizing protein-protein interactions in the nucleus of the living cell. *Mol. Endocrinol.* **13**, 517–26.
38. Kenworthy, A. K. (2001) Imaging protein-protein interactions using fluorescence resonance energy transfer microscopy. *Methods* **24**, 289–96.
39. Clegg, R. M. (1995) Fluorescence resonance energy transfer. *Curr. Opin. Biotechnol.* **6**, 103–10.
40. Labas, Y. A., Gurskaya, N. G., Yanushevich, Y. G., Fradkov, A. F., Lukyanov, K. A., Lukyanov, S. A., and Matz, M. V. (2002) Diversity and evolution of the green fluorescent protein family. *Proc. Natl. Acad. Sci. USA* **99**, 4256–61.
41. Zhang, J., Campbell, R. E., Ting, A. Y., and Tsien, R. Y. (2002) Creating new fluorescent probes for cell biology. *Nat. Rev. Mol. Cell Biol.* **3**, 906–18.
42. Shaner, N. C., Steinbach, P. A., and Tsien, R. Y. (2005) A guide to choosing fluorescent proteins. *Nat. Methods* **2**, 905–09.
43. Piston, D. W., and Kremers, G. J. (2007) Fluorescent protein FRET: the good, the bad and the ugly. *Trends Biochem. Sci.* **32**, 407–14.
44. Rizzo M. A., Springer G. H., Granada B, Piston D. W. (2004) An improved cyan fluorescent protein variant useful for FRET. *Nat. Biotechnol.* **22**, 445–9.
45. Ai, H. W., Henderson, J. N., Remington, S. J., and Campbell, R. E. (2006) Directed evolution of a monomeric, bright and photo-stable version of Clavularia cyan fluorescent protein: structural characterization and applications in fluorescence imaging. *Biochem. J.* **400**, 531–40.
46. Kremers, G. J., Goedhart, J., van Munster, E. B., and Gadella, Jr, T. W. J. (2006) Cyan and yellow super fluorescent proteins with improved brightness, protein folding, and FRET Forster radius. *Biochemistry* **45**, 6570–80.
47. Zacharias, D. A., Violin, J. D., Newton, A. C., and Tsien, R. Y. (2002) Partitioning of lipid-modified monomeric GFPs into membrane microdomains of live cells. *Science* **296**, 913–6.
48. Griesbeck, O., Baird, G. S., Campbell, R. E., Zacharias, D. A., and Tsien, R. Y. (2001) Reducing the environmental sensitivity of yellow fluorescent protein. Mechanism and applications. *J. Biol. Chem.* **276**, 29188–94.
49. Nagai, T., Ibata, K., Park, E. S., Kubota, M., Mikoshiba, K., and Miyawaki, A. (2002) A variant of yellow fluorescent protein with fast and efficient maturation for cell-biological applications. *Nat. Biotechnol.* **20**, 87–90.
50. Shaner, N. C., Campbell, R. E., Steinbach, P. A., Giepmans, B. N., Palmer, A. E., and Tsien, R. Y. (2004) Improved monomeric red, orange and yellow fluorescent proteins derived from *Discosoma* sp. red fluorescent protein. *Nat. Biotechnol.* **22**, 1567–72.
51. Karasawa, S., Araki, T., Nagai, T., Mizuno, H., and Miyawaki, A. (2004) Cyan-emitting and orange-emitting fluorescent proteins as a donor/acceptor pair for fluorescence resonance energy transfer. *Biochem J.* **381**, 307–12.
52. Merzlyak, E. M., Goedhart, J., Shcherbo, D., Bulina, M. E., Shcheglov, A. S., Fradkov, A. F., Gaintzeva, A., Lukyanov, K. A., Lukyanov, S., Gadella, Jr, T. W. J., and Chudakov, D. M. (2007) Bright monomeric red fluorescent protein with an extended fluorescence lifetime. *Nat. Methods* **4**, 555–7.
53. Zimmermann, T., Rietdorf, J., Girod, A., Georget, V., and Pepperkok, R. (2002) Spectral imaging and linear un-mixing



- enables improved FRET efficiency with a novel GFP2-YFP FRET pair. *FEBS Lett.* **531**, 245–9.
54. Dinant, C., Van Royen, M. E., Vermeulen, W., and Houtsmuller, A. B. (2008) Fluorescence resonance energy transfer of GFP and YFP by spectral imaging and quantitative acceptor photobleaching. *J. Microsc.* **231**, 97–104.
  55. Jares-Erijman EA, J. T. (2003) FRET imaging. *Nat. Biotechnol.* **21**, 1387–95.
  56. Xia, Z., and Liu, Y. (2001) Reliable and global measurement of fluorescence resonance energy transfer using fluorescence microscopes. *Biophys. J.* **81**, 2395–402.
  57. Gordon, G. W., Berry, G., Liang, X. H., Levine, B., and Herman, B. (1998) Quantitative fluorescence resonance energy transfer measurements using fluorescence microscopy. *Biophys. J.* **74**, 2702–13.
  58. Van Rheenen, J., Langeslag, M., and Jalink, K. (2004) Correcting confocal acquisition to optimize imaging of fluorescence resonance energy transfer by sensitized emission. *Biophys. J.* **86**, 2517–29.
  59. Bastiaens, P. I. H., Majoul, I. V., Verveer, P. J., Söling, H.D., and Jovin, T. M. (1996) Imaging the intracellular trafficking and state of the AB5 quaternary structure of cholera toxin. *EMBO J.* **15**, 4246–53.
  60. Bastiaens, P. I. H., and Jovin, T. M. (1996) Microspectroscopic imaging tracks the intracellular processing of a signal transduction protein: Fluorescent-labeled protein kinase C beta I. *Proc. Natl. Acad. Sci. USA* **93**, 8407–12.
  61. Karpova, T. S., Baumann, C. T., He, L., Wu, X., Grammer, A., Lipsky, P., Hager, G. L., and McNally, J. G. (2003) Fluorescence resonance energy transfer from cyan to yellow fluorescent protein detected by acceptor photobleaching using confocal microscopy and a single laser. *J. Microsc.* **209**, 56–70.
  62. Bastiaens, P. I. H., and Squire, A. (1999) Fluorescence lifetime imaging microscopy: spatial resolution of biochemical processes in the cell. *Trends Cell Biol.* **9**, 48–52.
  63. Wallrabe, H., and Periasamy, A. (2005) Imaging protein molecules using FRET and FLIM microscopy. *Curr. Opin. Biotechnol.* **16**, 19–27.
  64. Van Munster, E. B., and Gadella, Jr, T. W. J. (2005) Fluorescence Lifetime Imaging Microscopy (FLIM) in “*Advances In Biochemical Engineering/Biotechnology*” (Rietdorf, J., ed.), Vol. **95**, Springer-Verlag GmbH, Berlin, pp. 143–75.
  65. Van de Wijngaert, D. J., van Royen, M. E., Hersmus, R., Pike, A. C. W., Houtsmuller, A. B., Jenster, G., Trapman, J., and Dubbink, H. J. (2006) Novel FXXFF and FXXMF motifs in androgen receptor cofactors mediate high affinity and specific interactions with the ligand-binding domain. *J. Biol. Chem.* **281**, 19407–16.
  66. Bai, Y., and Giguere, V. (2003) Isoform-selective interactions between estrogen receptors and steroid receptor coactivators promoted by estradiol and ErbB-2 signaling in living cells. *Mol. Endocrinol.* **17**, 589–99.
  67. Weatherman, R. V., Chang, C.Y., Clegg, N. J., Carroll, D. C., Day, R. N., Baxter, J. D., McDonnell, D. P., Scanlan, T. S., and Schaufele, F. (2002) Ligand-selective interactions of ER detected in living cells by fluorescence resonance energy transfer. *Mol. Endocrinol.* **16**, 487–96.
  68. Llopis, J., Westin, S., Ricote, M., Wang, J., Cho, C. Y., Kurokawa, R., Mullen, T. M., Rose, D. W., Rosenfeld, M. G., Tsien, R. Y., and Glass, C. K. (2000) Ligand-dependent interactions of coactivators steroid receptor coactivator-1 and peroxisome proliferator-activated receptor binding protein with nuclear hormone receptors can be imaged in live cells and are required for transcription. *Proc. Natl. Acad. Sci. USA* **97**, 4363–68.
  69. Mukherjee, R., Sun, S., Santomenna, L., Miao, B., Walton, H., Liao, B., Locke, K., Zhang, J.H., Nguyen, S. H., and Zhang, L. T. (2002) Ligand and coactivator recruitment preferences of peroxisome proliferator activated receptor- $\alpha$ . *J. Steroid Biochem. Mol. Biol.* **81**, 217–25.
  70. Schaufele, F., Chang, C.Y., Liu, W., Baxter, J. D., Nordeen, S. K., Wan, Y., Day, R. N., and McDonnell, D. P. (2000) Temporally distinct and ligand-specific recruitment of nuclear receptor-interacting peptides and cofactors to subnuclear domains containing the estrogen receptor. *Mol. Endocrinol.* **14**, 2024–39.
  71. Awais, M., Sato, M., Umezawa, Y. (2007) Imaging of selective nuclear receptor modulator-induced conformational changes in the nuclear receptor to allow interaction with coactivator and corepressor proteins in living cells. *ChemBioChem.* **8**, 737–43.
  72. Awais, M., Sato, M., Sasaki, K., and Umezawa, Y. (2004) A genetically encoded fluorescent indicator capable of discriminating estrogen agonists from antagonists in living cells. *Anal. Chem.* **76**, 2181–86.
  73. Awais, M., Sato, M., and Umezawa, Y. (2007) Optical probes to identify the glucocorticoid receptor ligands in living cells. *Steroids* **72**, 949–54.

74. Awais, M., Sato, M., and Umezawa, Y. (2007) A fluorescent indicator to visualize ligand-induced receptor/coactivator interactions for screening of peroxisome proliferator-activated receptor- $\gamma$  ligands in living cells. *Biosens. Bioelectron.* **22**, 2564–69.
75. Awais, M., Sato, M., Lee X., Umezawa Y. (2006) A fluorescent indicator to visualize activities of the androgen receptor ligands in single living cells. *Angew. Chem. Int. Ed. Engl.* **45**, 2707–12.
76. Zhou, G., Cummings, R., Li, Y., Mitra, S., Wilkinson, H. A., Elbrecht, A., Hermes, J. D., Schaeffer, J. M., Smith, R. G., and Moller, D. E. (1998) Nuclear receptors have distinct affinities for coactivators: characterization by fluorescence resonance energy transfer. *Mol. Endocrinol.* **12**, 1594–604.
77. Day, R. N. (1998) Visualization of Pit-1 transcription factor interactions in the living cell nucleus by fluorescence resonance energy transfer microscopy. *Mol. Endocrinol.* **12**, 1410–19.
78. Zwart, W., Griekspoor, A., Berno, V., Lakeman, K., Jalink, K., Mancini, M., Neeffjes, J., Michalides, R. (2007) PKA-induced resistance to tamoxifen is associated with an altered orientation of ER $\alpha$  towards co-activator SRC-1. *EMBO J.* **26**, 3534–44.
79. Dubbink, H. J., Hersmus, R., Verma, C. S., van der Korput, J. A. G. M., Berrevoets, C. A., van Tol, J., Ziel-van der Made, A. C. J., Brinkmann, A. O., Pike, A. C. W., and Trapman, J. (2004) Distinct recognition modes of FXXLF and LXXLL motifs by the androgen receptor. *Mol. Endocrinol.* **18**, 2132–50.
80. Hur, E., Pfaff, S. J., Payne, E. S., Gron, H., Buehrer, B. M., and Fletterick, R. J. (2004) Recognition and accommodation at the androgen receptor coactivator binding interface. *PLoS Biol.* **2**, E274.
81. Doesburg, P., Kuil, C. W., Berrevoets, C. A., Steketee, K., Faber, P. W., Mulder, E., Brinkmann, A. O., and Trapman, J. (1997) Functional in vivo interaction between the amino-terminal, transactivation domain and the ligand binding domain of the androgen receptor. *Biochemistry* **36**, 1052–64.
82. He, B., Kemppainen, J. A., and Wilson, E. M. (2000) FXXLF and WXXLF sequences mediate the NH<sub>2</sub>-terminal interaction with the ligand binding domain of the androgen receptor. *J. Biol. Chem.* **275**, 22986–94.
83. Schaufele, F., Carbonell, X., Guerbadot, M., Borngraeber, S., Chapman, M. S., Ma, A. A. K., Miner, J. N., and Diamond, M. I. (2005) The structural basis of androgen receptor activation: Intramolecular and intermolecular amino-carboxy interactions. *Proc. Natl. Acad. Sci. USA* **102**, 9802–07.
84. Nishi, M., Tanaka, M., Matsuda, K., Sunaguchi, M., and Kawata, M. (2004) Visualization of glucocorticoid receptor and mineralocorticoid receptor interactions in living cells with GFP-based fluorescence resonance energy transfer. *J. Neurosci.* **24**, 4918–27.
85. Padron, A., Li, L., Kofoed, E. M., and Schaufele, F. (2007) Ligand-selective interdomain conformations of estrogen receptor- $\alpha$ . *Mol. Endocrinol.* **21**, 49–61.
86. Michalides, R., Griekspoor, A., Balkenende, A., Verwoerd, D., Janssen, L., Jalink, K., Floore, A., Velds, A., van 't Veer, L., and Neeffjes, J. (2004) Tamoxifen resistance by a conformational arrest of the estrogen receptor- $\alpha$  PKA activation in breast cancer. *Cancer Cell* **5**, 597–605.
87. Zwart, W., Griekspoor, A., Rondaij, M., Verwoerd, D., Neeffjes, J., and Michalides, R. (2007) Classification of anti-estrogens according to intramolecular FRET effects on phospho-mutants of estrogen receptor- $\alpha$ . *Mol. Cancer Ther.* **6**, 1526–33.
88. Sui, X., Bramlett, K. S., Jorge, M. C., Swanson, D. A., von Eschenbach, A. C., and Jenster, G. (1999) Specific androgen receptor activation by an artificial coactivator. *J. Biol. Chem.* **274**, 9449–54.

# Chapter 6

## Receptor-DNA Interactions: EMSA and Footprinting

Jason T. Read, Helen Cheng, Stephen C. Hendy, Colleen C. Nelson,  
and Paul S. Rennie

### Abstract

Defining the precise promoter DNA sequence motifs where nuclear receptors and other transcription factors bind is an essential prerequisite for understanding how these proteins modulate the expression of their specific target genes. The purpose of this chapter is to provide the reader with a detailed guide with respect to the materials and the key methods required to perform this type of DNA-binding analysis. Irrespective of whether starting with purified DNA-binding proteins or somewhat crude cellular extracts, the tried-and-true procedures described here will enable one to accurately assess the capacity of specific proteins to bind to DNA as well as to determine the exact sequences and DNA contact nucleotides involved. For illustrative purposes, we primarily have used the interaction of the androgen receptor with the rat probasin proximal promoter as our model system.

**Key words:** Androgen receptor, Probasin promoter, Nuclear extracts, EMSA, DNase I, Methylation interference, Methylation protection.

---

### 1. Introduction

Steroid hormones are heavily involved in many physiological changes associated with growth and development. This class of molecules continues to control and coordinate our physiology through to adulthood and influence the state of our health. Increasingly, aberrant steroid signaling has been shown to be a factor in many disease states including cancer. Although some steroids may provoke short-term physiological changes through signaling cascades, long-term downstream cellular changes by steroids typically involve activation of a cognate steroid receptor

which, in conjunction with other proteins, directly binds to promoters and influences expression levels of target genes (1).

The direct interactions between steroid receptors and their target DNA sequences have been studied using a number of molecular techniques, with electrophoretic mobility shift assay (EMSA) and DNase I footprinting being the two most commonly employed methods for identifying and characterizing steroid receptor binding and response elements within a given DNA promoter sequence. Further refinements of these techniques, such as antibody supershift EMSA and methylation interference/protection footprinting, have helped us to define the precise sites of interaction between steroid receptors and DNA. For illustrative purposes, all our remarks pertain to the androgen receptor (AR) interaction with the probasin proximal promoter (2, 3). Similar to the human PSA promoter, the rat probasin promoter has been extensively studied both from the perspective of a model system for determining the precise DNA motifs that dictate transcriptional enhancement by the androgen receptor (3) and prostate-specific expression (4, 5) as well as for targeting gene expression in the context of developing a gene therapy for prostate cancer (6, 7). The following provides a precise description of the materials and molecular procedures necessary to perform both broad and detailed analyses of protein–DNA promoter interactions.

---

## 2. Materials

### **2.1. Purification of Histidine-Tagged Androgen Receptor DNA-Binding Domain**

1. Lauria-Bertani medium (LB) and bacto-agar plates supplemented with 100  $\mu\text{g}/\text{mL}$  ampicillin.
2. *E. coli* containing plasmid expressing His-AR-DBD under the control of an Isopropyl  $\beta$ -D-1-thiogalactopyranoside (IPTG) inducible promoter.
3. IPTG solution: 1 M in sterile  $\text{dH}_2\text{O}$ .
4. Lysis buffer: 50 mM  $\text{NaH}_2\text{PO}_4$ , pH 8.0, 300 mM NaCl, 10 mM imidazole.
5. Lysozyme solution: 2 mg/mL in lysis buffer.
6. Ni-NTA agarose beads (QIAGEN).
7. Chromatography columns (BioRad Laboratories).
8. Wash buffer 1: 50 mM  $\text{NaH}_2\text{PO}_4$ , pH 8.0, 300 mM NaCl, 20 mM imidazole.
9. Wash Buffer 2: 20 mM HEPES, pH 7.9, 100 mM KCl, 20 mM imidazole, 10% glycerol.
10. Elution buffer: 20 mM HEPES, pH 7.9, 100 mM KCl, 250 mM imidazole, 20% glycerol.

11. SDS-PAGE mini gel apparatus.
12. BCA protein quantification kit (Pierce).

**2.2. Purification of GST-AR1 (AR DNA-Binding and Ligand Binding Domains) and GST-AR2 (AR DNA-Binding Domain) Fusion Proteins**

1. Glutathione-agarose beads (Sigma).
2. Phosphate buffered saline (PBS): 137 mM NaCl, 2.7 mM KCl, 4.3 mM Na<sub>2</sub>HPO<sub>4</sub> and 1.47 mM KH<sub>2</sub>PO<sub>4</sub>, pH 7.4.
3. *E. coli* containing plasmids expressing glutathione-*S*-transferase fused to either the DNA-binding domain (GST-DBD) or ligand and DNA binding domains (GST-LBD) of the AR under the control of an Isopropyl *B*-D-1-thiogalactopyranoside (IPTG) inducible promoter.
4. Lysis Buffer: PBS containing 100 µg/mL of lysozyme, 1× protease inhibitor cocktail and 1 mM PMSF (optional).
5. 10% Triton X-100.
6. 10% Tween 20.
7. GST elution buffer: 10 mM glutathione in Buffer D ([Subheading 2.4, item 17](#)).
8. BioRad protein assay Kit (BioRad Laboratories)

**2.3. Preparation of LNCaP Nuclear Extracts**

1. Dithiothreitol (DTT) (Invitrogen): 100 mM in Buffer D.
2. Buffer A: 10 mM HEPES, pH 7.9, 1.5 mM MgCl<sub>2</sub>, 0.5 mM Dithiothreitol (DTT) added immediately prior to use.
3. Buffer C: 20 mM HEPES, pH 7.9, 25% (v/v) glycerol, 0.42 M NaCl, 1.5 mM MgCl<sub>2</sub>, 0.2 mM disodium ethylenediamine tetraacetate (EDTA), 0.5 mM phenylmethanesulphonyl fluoride (PMSF, optional), 0.5 mM DTT added immediately prior to use.
4. A prechilled, clean glass Dounce homogeniser (Kontes, B type pestle).
5. Teflon cell scraper(s)
6. Tissue culture materials appropriate to the cell line of interest.

**2.4. Generation of Labeled DNA Probe for EMSA, DNase I Footprinting, Methylation Interference and Methylation Protection Experiments**

1. Synthesized dephosphorylated complimentary single-stranded DNA oligomers (typically 18–35 bases) corresponding to the region of interest dissolved in nuclease free TE to a concentration of 20 µg/mL or 3–5 µg of plasmid containing the cloned region of interest.
2. Tris-EDTA buffer (TE): 10 mM Tris base, pH 8.0, 1 mM EDTA.
3. 30% acrylamide: *N,N'*-methylene-bis-acrylamide solution (37.5:1) (BioRad Laboratories).
4. Ammonium persulfate (APS): 10% (w/v) prepared in dH<sub>2</sub>O.

5. *N,N,N,N*-Tetramethyl-ethylenediamine (TEMED) (Invitrogen).
6. 5× Tris–borate buffer (5× TBE): 0.445 M Tris base, pH 8.0, 0.445 M boric acid, 10 mM EDTA.
7. Vertical gel electrophoresis unit of ~30 cm in height with corresponding glass plates, 1.5 mm spacers and combs with 14 wells.
8. Power supply capable of delivering at least 400V/100 mA
9. DNA loading buffer (5×): 50% glycerol (v/v), 0.04% (w/v) Bromophenol Blue, 0.04% (w/v) xylene cyanol in TBE.
10. Deoxynucleotide triphosphates (dNTP's) (dATP, dTTP, dGTP, dCTP) (Invitrogen): diluted to 10 mM with sterile dH<sub>2</sub>O.
11. Klenow enzyme (for plasmid sourced DNA probes) (New England Biolabs) and the necessary restriction enzymes to generate a single-end-labeled DNA on either the upper or lower strand.
12. T4 polynucleotide kinase (PNK) (for oligomer-based DNA probes) (New England Biolabs).
13. [ $\alpha$ -<sup>32</sup>P]dCTP (3,000 Ci/mmol) (Perkin Elmer) (used for Klenow labeling of plasmid sourced DNA probes with 5' overhangs containing guanines).
14. [ $\gamma$ -<sup>32</sup>P]dATP (6,000 Ci/mmol) (Perkin Elmer) (used for T4 PNK labeling of oligomers).
15. PCR cleanup kit (Qiagen).
16. 95 and 70% ethanol.
17. Buffer D: 20 mM HEPES, pH 7.9, 100 mM KCl, 10% glycerol (v/v).
18. Autoradiography films and cassettes, darkroom facilities for film processing.
19. MicroSpin Sephadex G50 spin columns (GE Healthcare).
20. Gel elution buffer: 0.6 M ammonium acetate (NH<sub>4</sub>OAc), 0.1% SDS, 1 mM EDTA.

## **2.5. Protein–DNA Binding Reactions and EMSA**

### **2.5.1. EMSA**

1. Radiolabeled DNA-probe (*see Subheading 2.4*).
2. Poly(dI-dC).(dI-dC) (GE Healthcare) is made up to 2 mg/mL in 100 mM KCl. Heat to 43°C and cool to room temperature to get duplex strands, aliquot, and store at –20°C.
3. 100 mM Dithiothreitol (DTT) in Buffer D.
4. DNA-binding buffer (DBB): Buffer D supplemented with 1 mM DTT.
5. 0.5× TBE: 1/10 dilution of 5× recipe in [Subheading 2.4, item 6](#).



6. 30% acrylamide: *N,N'*-methylene-bis-acrylamide (37.5:1) solution (BioRad Laboratories).
7. Ammonium persulfate (APS) (**Subheading 2.4, item 4**).
8. *N,N,N,N*-Tetramethyl-ethylenediamine (TEMED).
9. Vertical gel electrophoresis unit of ~30 cm in height with corresponding glass plates, 1.5 mm spacers, and combs with 14 wells.
10. 5× DNA loading buffer (**Subheading 2.4, item 9**).
11. Gel drier (heat and vacuum system with vapour trap).
12. Autoradiography films and cassettes, darkroom facilities for film processing or phospho-imager system.

#### 2.5.2. Supershift EMSA

1. Antibodies including test antibodies directed either against the protein of interest or an attached tag molecule and a control nonspecific antibody (e.g., normal IgG or an antibody directed against an unrelated target). Control and test antibodies should be resuspended in similar buffers and at similar concentrations.

#### 2.6. DNase I Footprint Analysis of Receptor-DNA Binding

1. Vacuum concentrator to be used/vented inside the fume hood.
2. Formic acid (Fisher Scientific): Dilute to 2% with sterile dH<sub>2</sub>O. Make fresh each time.
3. Herring sperm DNA (Sigma).
4. Piperidine (Fisher Scientific): Dilute to 10% with sterile dH<sub>2</sub>O. Make fresh each time.
5. Buffer-saturated Phenol/chloroform/isoamyl alcohol (25:24:1) (Invitrogen).
6. Formamide loading buffer: Ultrapure formamide with bromophenol blue and xylene cyanol to 0.01% (w/v).
7. Poly(dI-dC).(dI-dC) (*see Subheading 2.5.1, item 2*).
8. Calcium chloride (CaCl<sub>2</sub>) and magnesium chloride (MgCl<sub>2</sub>) mix: Add 31.2 μL of 1 M CaCl<sub>2</sub> and 50 μL of 1 M MgCl<sub>2</sub> to 418.8 μL of sterile H<sub>2</sub>O.
9. DNase I (GE Healthcare).
10. Proteinase K stop buffer (2×): 500 μg/mL proteinase K (Invitrogen), 0.25% SDS.
11. 300 mM ethylene glycol-bis[β-aminoethyl ether]-*N,N,N'*, *N'*-tetraacetic acid (EGTA).
12. Carrier transfer RNA (t-RNA) (Sigma).
13. Sodium Acetate: 3 M, pH 5.2.
14. Denaturing polyacrylamide gel solution: (7% acrylamide/8.3 M urea): Dissolve 28.8 g of urea in ~20 mL of



H<sub>2</sub>O. Add 10.5 mL of 40% acrylamide/bis (30:1), 12 mL of 5× TBE and H<sub>2</sub>O to a volume of 59.8 mL). Add 240 μL of freshly prepared 10% ammonium persulfate solution and 24 μL of TEMED before casting.

15. Sequencing gel apparatus with 0.4 mm spacers and well-forming combs (Invitrogen).
16. Sigmacote (Sigma) (*see Note 1*).
17. Flat pipette tips for sample loading.
18. Power supply capable of delivering at least 40 W power.
19. Gel drier ([Subheading 2.5.1](#), [item 11](#)).

### **2.7. Methylation Interference Assay**

In addition to the materials listed below, performing the methylation interference assay also requires the materials described in the EMSA protocol ([Subheading 2.5](#))

1. Dimethyl sulfate (DMS) (Sigma) (*see Note 2*).
2. DMS buffer: 50 mM sodium cacodylate, pH 8.0, 10 mM MgCl<sub>2</sub> and 1 mM EDTA.
3. DMS stop buffer: 1.5 M sodium acetate, pH 7.0 and 1 M of 2-mercaptoethanol.
4. Spin filters (BioRad Laboratories).
5. Piperidine ([Subheading 2.6](#), [item 4](#)).
6. Denaturing polyacrylamide gel solution ([Subheading 2.6](#), [item 14](#)).
7. Sequencing gel apparatus ([Subheading 2.6](#), [item 15](#)).
8. Flat pipette tips for sample loading.
9. Formamide loading buffer ([Subheading 2.6](#), [item 6](#)).
10. Power supply capable of delivering at least 40 W power.
11. Phospho-imaging screen and device for quantification of the autoradiograph.

### **2.8. Methylation Protection Assay**

In addition to the materials listed below, performing the methylation interference assay also requires the materials described in the EMSA protocol ([Subheading 2.5](#))

1. Dimethyl sulfate (DMS) ([Subheading 2.7](#), [item 1](#)).
2. Poly(dI-dC).(dI-dC) ([Subheading 2.5.1](#), [item 2](#)).
3. Buffer D ([Subheading 2.4](#), [item 17](#)).
4. Carrier transfer RNA.
5. Piperidine ([Subheading 2.6](#), [item 4](#)).
6. Denaturing polyacrylamide gel solution ([Subheading 2.6](#), [item 14](#)).
7. Flat pipette tips for sample loading.
8. Power supply capable of delivering at least 40 W power.

9. Formamide loading buffer ([Subheading 2.6, item 6](#)).
10. Phospho-imaging screen and device for quantification of the autoradiograph.

---

### 3. Methods

Experiments to characterize the interaction of the AR with the rat probasin proximal promoter target sequences have involved a series of footprinting techniques, which in turn yielded more precise information on the nature and complexity of the protein–DNA interactions (schematically outlined in [Fig. 1](#)). DNase I footprinting experiments ([Figs. 1, 3](#)) using recombinant AR DNA-binding domain (AR-DBD) revealed the cooperative interaction of the AR-DBD mediated by the androgen responsive elements (AREs) ARE-1 and ARE-2 (2, 3). The methylation interference assay ([Figs. 1, 4](#)), in which the guanine N7 (major groove) and, to a lesser extent, adenine N3 (minor groove) within the target sequence are methylated prior to protein binding reactions, identified those guanine residues involved in stabilizing the AR-DBD-DNA complex in the major groove (8). Methylation is carried out such that on average only one residue per DNA molecule is methylated. The methylated DNA is then purified and bound to by the test protein. The bound and free fractions are separated using EMSA, eluted, chemically cleaved, and then analyzed on a denaturing polyacrylamide gel. If a methylated guanine is important for the protein–DNA interaction, it will be enriched in the unbound fraction and under represented in the bound fraction. Methylation protection footprints ([Figs. 1, 5](#)) also identifies protein–DNA interactions at guanine nucleotides. In addition, hypersensitivity to methylation in this assay can indicate DNA structural distortion induced by the protein of interest. In the methylation protection assay, the target DNA is methylated after the protein has bound; such that on average only one guanine residue per DNA molecule is methylated. The bound fraction is then separated from the free fraction by EMSA, eluted and cleaved, and then separated on a denaturing polyacrylamide gel. In our experiments, methylation protection assays revealed two previously undetected guanine-rich AREs located in the probasin proximal promoter (9, 10) as well as binding sites for several unidentified prostate-specific transcription factors (4).

The success of these techniques relies heavily on the quality and activity of the protein preparations used for the DNA-binding reactions. We have included two protocols, one for preparing

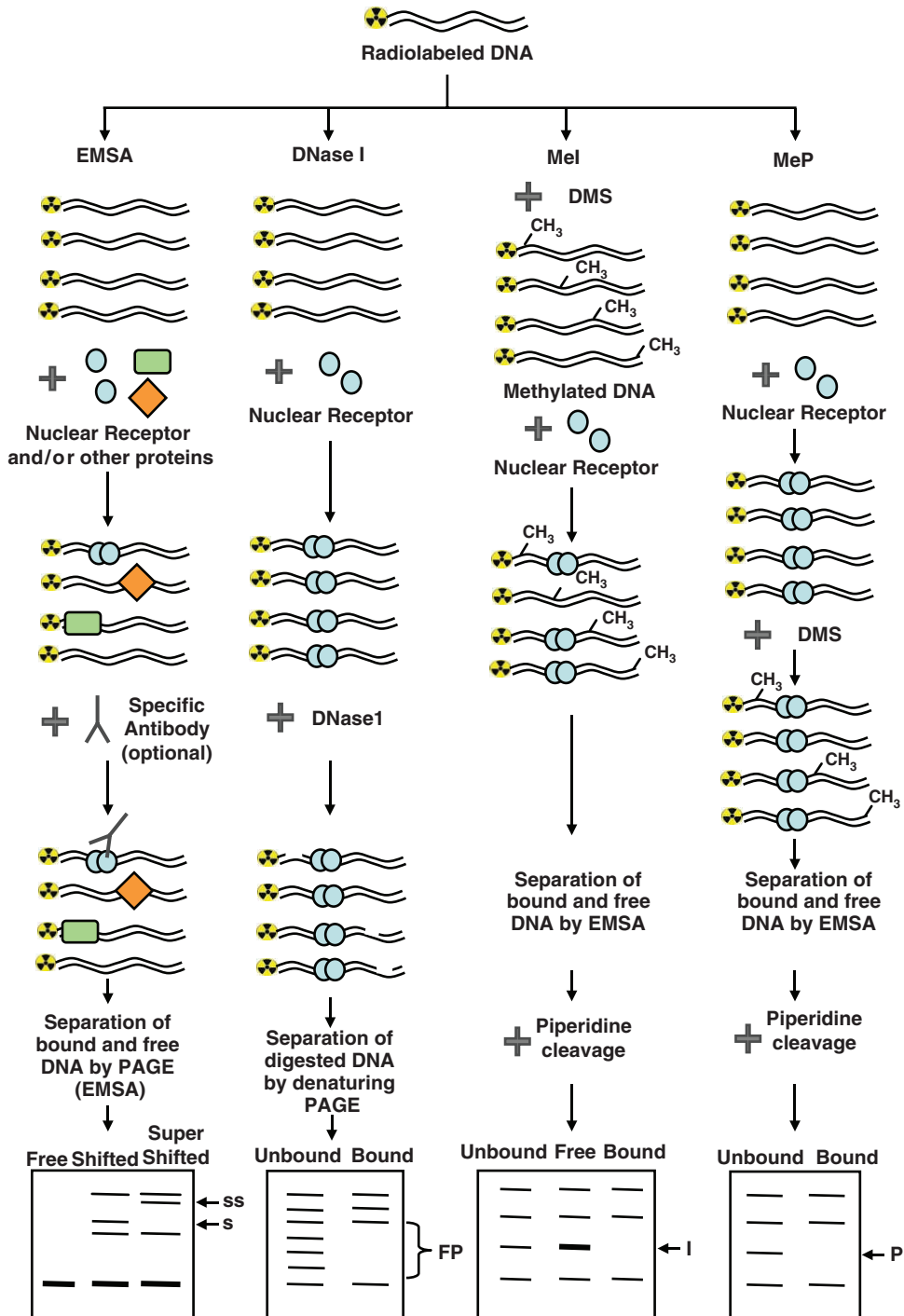


Fig. 1. Schematic outline of the steps involved in EMSA, DNase I footprinting, methylation interference assay, and methylation protection footprinting. EMSA experiments are used to analyze protein–DNA interactions on the basis of differences in migration rates of unbound DNA vs. DNA bound to protein. Radiolabeled DNA is incubated with the protein(s) of interest, then the bound and unbound DNA populations are separated by non-denaturing PAGE. The protein–DNA complex migrates more slowly resulting in a shifted band (S). In a supershift EMSA, an antibody against the protein of interest

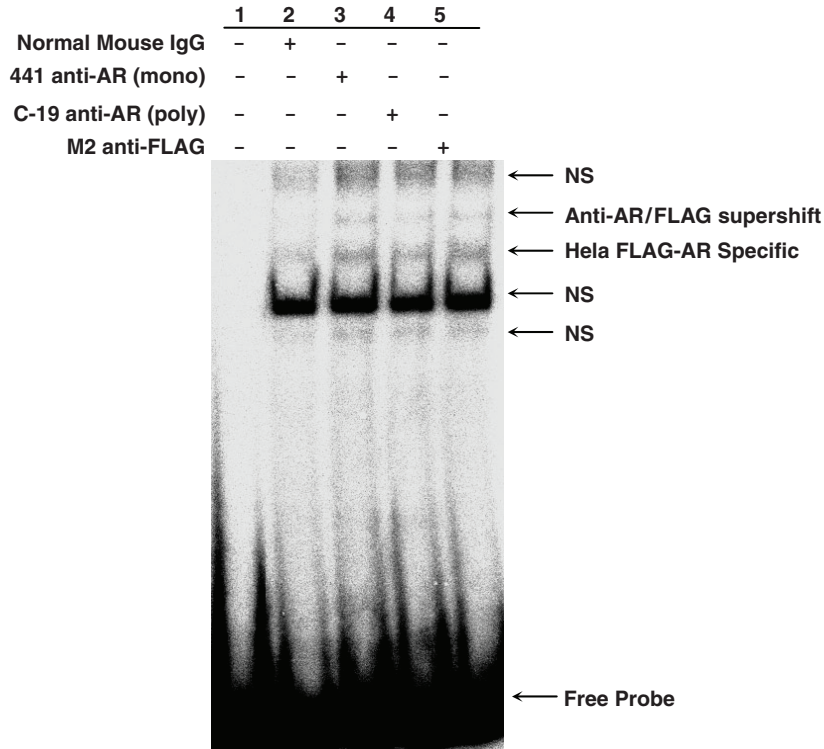


Fig. 2. Electrophoretic mobility assay with the probasin promoter. EMSAs and supershifts were performed in this example using a <sup>32</sup>P-labeled probe corresponding to the versican nuclear receptor response element site 2 (NRE-2) incubated with 20 μg of modified Dignam nuclear extracts from HeLa-FLAG-AR cells engineered to stably overexpress a tagged human androgen receptor. Both cell types were treated with 10 nM R1881 (synthetic androgen) for 24 h prior to harvesting. A number of complexes were formed with the nuclear extract, including several nonspecific (NS) complexes. Lane 1, control free probe; lane 2–5, HeLa-FLAG-AR nuclear extract coincubated with 2 μg of the indicated antibodies (reproduced from ref. 11 with permission from *J Biol Chem*).

←

Fig. 1. (continued) is added to the protein–DNA binding reaction. A further decrease in mobility (supershift, **SS**) of the bound band due to binding of the antibody indicates that the protein of interest is present in the protein–DNA complex. DNase I footprinting identifies the specific regions of promoters that are bound by a protein of interest. DNase I introduces single stranded nicks in DNA molecules, but this activity is blocked by the presence of protein(s) bound to the DNA. A protein–DNA binding reaction is set up followed by addition of DNase I such that on average a DNA molecule receives only one nick. The DNA is then separated by denaturing PAGE. A region of DNA bound by protein produces a footprint (**FP**) relative to the unbound lane due to the inaccessibility of the DNA to enzymatic cleavage. For the methylation interference assay (MeI), radiolabeled DNA is treated with DMS prior to the protein-binding reaction such that only one guanine residue per DNA molecule is methylated. The methylated DNA is then used in an EMSA experiment with the protein of interest, and the bound and unbound bands are each excised, chemically cleaved, and resolved with denaturing PAGE. Guanine residues that are critical for binding are revealed by their disappearance in the bound lane with the corresponding enrichment in the free lane (**I**). In methylation protection footprinting (MeP), the DNA is methylated after the protein is bound, and then EMSA is used to separate the bound DNA from the unbound. The bands are excised, chemically cleaved, and resolved with denaturing PAGE. Guanine residues important for protein binding are detected by fragments under represented in the bound lane relative to the unbound lane (**P**).

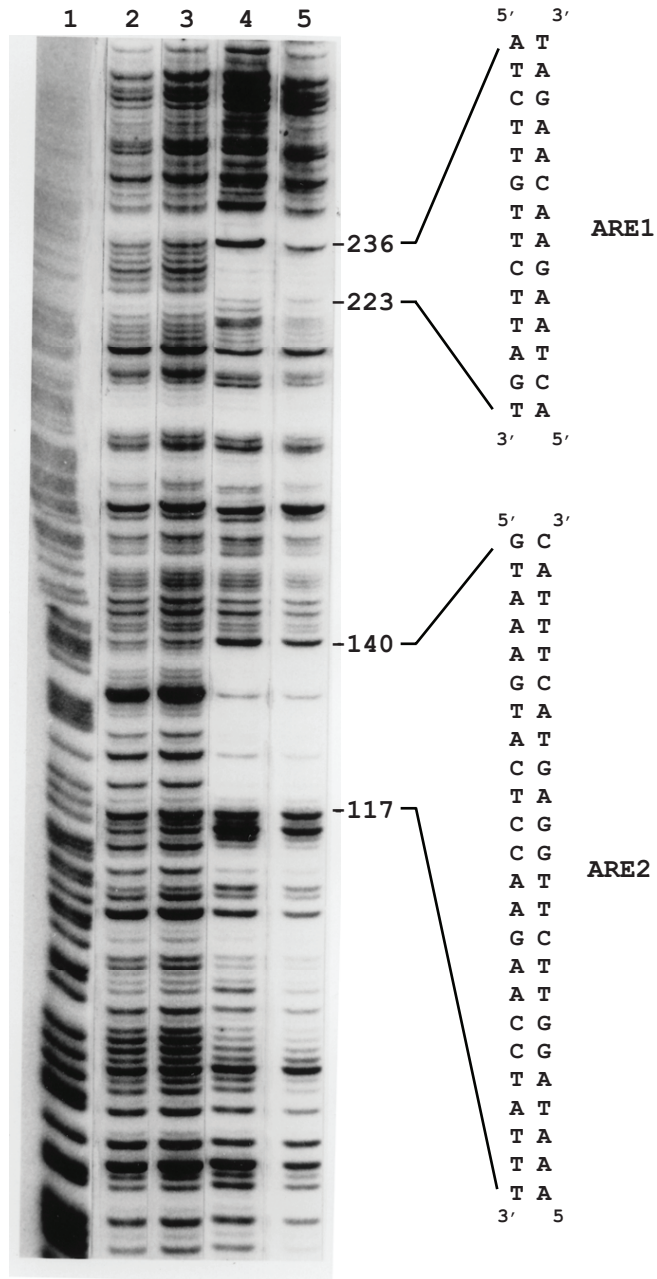


Fig. 3. DNase I footprint of the probasin promoter. DNase I digestion was performed using <sup>32</sup>P-labeled coding strand of the probasin promoter. For these experiments GST fusion recombinant AR-DBD was used. Lane 1, A/G reaction; lane 2, no protein, lane 3, 10 µg of GST protein, lane 4, 20 µg of GST-AR-DBD, lane 5, 10 µg of GST-AR1 (GST fused to the DNA and ligand-binding domains of AR). (Reproduced from ref. 3 with permission from *Molecular Endocrinology*) Copyright 1993 The Endocrine Society.

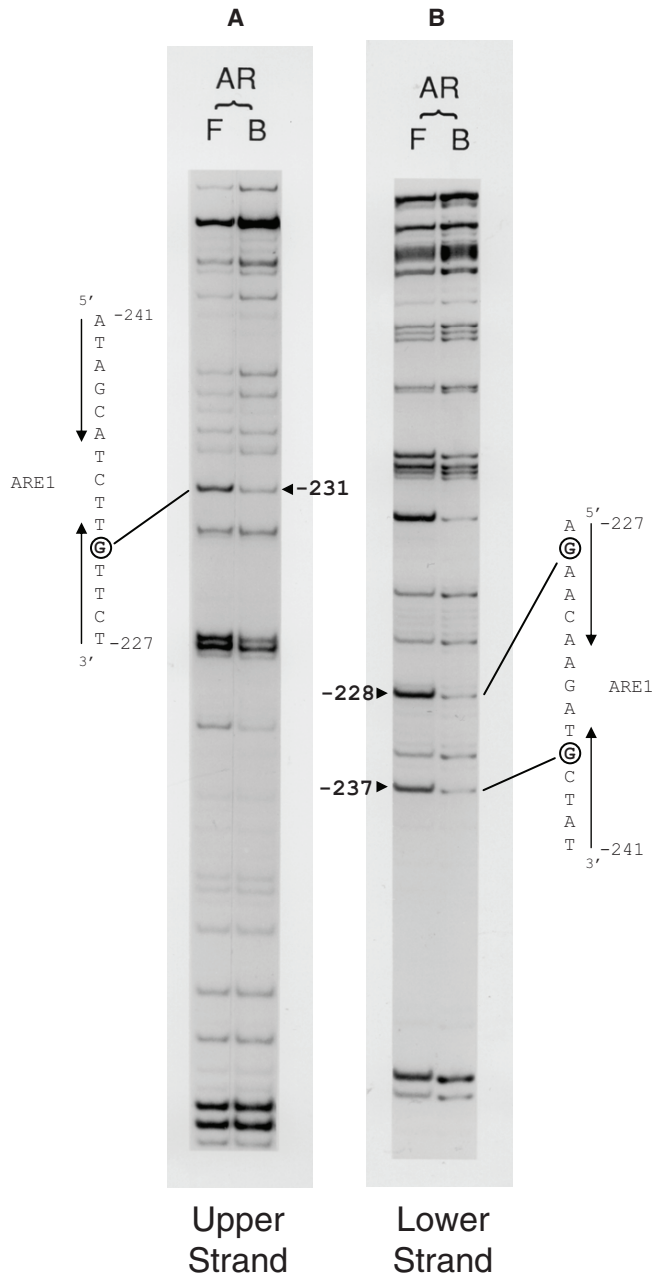


Fig. 4. Methylation interference assay of the probasin promoter. Methylation interference assays were performed using nucleotides -165 to -115 of the probasin proximal promoter and GST-AR-DBD. *Lines* refer to bands that are over-represented in the free (F) fraction compared with the bound (B) and signify guanine contact sites (*circled*). (A) The upper strand of DNA was <sup>32</sup>P-labeled. (B) The lower strand of DNA was radiolabeled. Direction of the *arrows* indicate orientation of the two half sites.



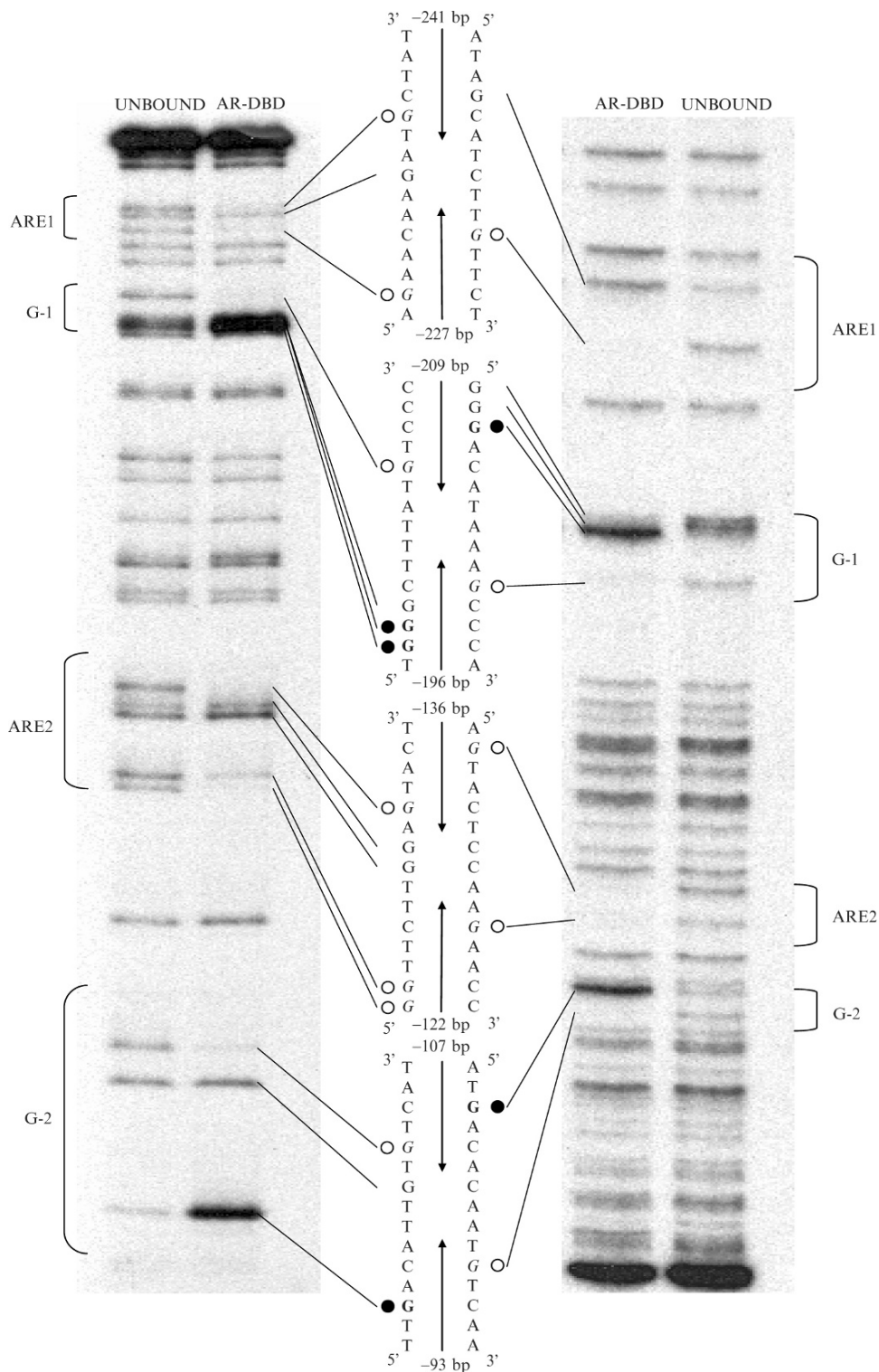


Fig. 5. Methylation protection footprint of the probasin promoter bound by histidine-tagged AR-DBD. Methylation protection footprint of the probasin proximal promoter (-269 to -77) revealed four AR-DBD binding sites as well as the local DNA distortion that results from allosteric interactions between AR-DBD and the DNA. Androgen response elements (ARE1 and ARE2), G-1 and G-2, are illustrated with their sequences. (A) The upper strand of the DNA was radiolabeled. (B) The lower strand of the DNA was <sup>32</sup>P-labeled (the gel image is presented reverse to the direction of electrophoresis)



recombinant histidine and GST-tagged AR-DBD polypeptides and the other for nuclear extracts from cultured mammalian cells, including LNCaP human prostate cancer cells, which we have found to yield consistently good results in the EMSA and footprinting procedures. Success will likely require initial protein titrations to determine the optimal concentrations to resolve regions of protein–DNA interactions.

**3.1. Purification  
of Recombinant  
Histidine-Tagged AR  
DNA-Binding Domain  
(AR-DBD)**

1. Streak the bacterial stock onto a fresh agar plate containing the appropriate antibiotic and incubate overnight at 37°C.
2. Pick a single colony into 5 mL of LB supplemented with the same antibiotic and incubate at 37°C with vigorous shaking overnight.
3. Inoculate 250 mL of LB supplemented with the same antibiotic with 2–5 ml of the starter culture and return to the shaking incubator. Monitor the culture at 600 nm and remove to room temperature when the OD reaches 0.6.
4. Remove a 50 µL sample of this culture and save it as a preinduction control.
5. Add 250 µL of the 1 M IPTG solution to the 250 mL bacterial culture to give a final IPTG concentration of 1 mM. Continue to shake the culture at room temperature.
6. At the 60, 120, and 180 min time points collect further 50 µL samples.
7. After 3 h, harvest the bacteria by centrifugation in preweighed tubes and dispose the supernatant. Freeze the pellets (overnight at –20°C or longer term at –80°C).
8. Resuspend the bacterial pellet in 4 mL of lysis buffer per gram of pellet by pipetting up and down.
9. Add 1 mL of the prepared 2 mg/mL lysozyme in lysis buffer solution to the bacterial suspension and incubate on ice for 30 min.
10. Sonicate on ice (typically 6 × 10 s pulses with 10 s cooling intervals).
11. Transfer the bacterial lysate to labeled 1.5 mL tubes and centrifuge at 18,000 × *g* at 4°C for 30 min.
12. Carefully pool the supernatant into a fresh 15 mL tube. Remove a 10 µL sample for SDS-PAGE analysis.

←

Fig. 5. (continued) to facilitate correlating a protected guanine to the DNA sequence). *Arrows* indicate AR half site location and orientation. *Open circles* represent guanine residues protected from DMS methylation due to protein contacts. *Solid circles* represent guanine residues hypersensitive to DMS methylation due to local DNA distortion resulting from DNA–protein allosteric interactions (reproduced from *ref. 10* with permission from *J Biol Chem*).

13. Add 1 mL of a 50% Ni-NTA bead slurry to the lysate supernatant.
14. Incubate the supernatant with the beads at 4°C with rotation for 60 min.
15. Load the supernatant/bead slurry into a chromatography column and let the liquid drain by gravity flow. Collect a 10  $\mu$ L aliquot of the flow through for SDS-PAGE analysis.
16. Wash the column by applying 2  $\times$  4 mL of wash buffer 1, followed by 2  $\times$  4 mL of wash buffer 2.
17. Elute the column 4 $\times$  with 0.5 mL of elution buffer. Collect a 10  $\mu$ L aliquot of each elution for SDS-PAGE analysis.
18. Analyze the collected samples (bacterial induction time points, lysate, flow through and elutions) by running a 12% SDS-PAGE and staining for total protein (Coomassie Brilliant Blue or similar). Typically, the highest concentration of His-tagged AR-DBD is found in the second elution fraction, at about 3–5  $\mu$ g/ $\mu$ L determined by the BCA protein assay. Aliquot elution fractions containing significant amounts of AR-DBD and store at –80°C.

**3.2. Purification of GST-AR1 (AR DNA-Binding and Ligand Binding Domains) and GST-AR2 (AR DNA-Binding Domain) Fusion Proteins**

*3.2.1. Preparation of Glutathione-Agarose Beads*

*3.2.2. Purification of GST-Fusion Proteins*

1. At the start of the experiment, weigh out 0.078 g of beads in a 15 mL screw-capped conical tube and add 13 mL of cold phosphate buffered saline (PBS).
  2. Let the beads swell on ice until needed.
  3. Centrifuge for 25 s at 800  $\times g$  in a table top centrifuge and remove the PBS. Wash once with PBS and the beads are ready to use.
1. Transfer an aliquot of frozen stock of JM109 bacteria containing GST alone, GST-AR1, or GST-AR2 in pGEX into 10 mL of Luria-Bertani Medium (LB) containing 100  $\mu$ g/mL of ampicillin.
  2. On the following day, transfer the whole amount into 400 mL of LB and allow to grow for 2 h at 37°C with shaking, until OD<sub>600</sub> reaches 0.5–0.8. For the GST alone control, half of the overnight volume is used.
  3. At the end of the 2 h period, remove 1 mL of the culture to set aside as the noninduced sample. Add 40  $\mu$ L of 1 M IPTG (final concentration of 0.1 mM) to the remaining culture and continue shaking for 2 h at room temperature.
  4. Remove 1 mL of the culture as the induced sample.
  5. Centrifuge at 3200  $\times g$  for 10 min to harvest the bacteria.
  6. Discard the supernatant and resuspend the pellet in 4 mL (0.5 mL of buffer for 50 mL culture) of cold lysis buffer and pipet up and down with a 10 mL pipet to obtain a homogeneous suspension.

7. Incubate on ice for 30 min.
8. Sonicate sample on ice (typically  $6 \times 10$  s pulse with 30 s cooling).
9. Add  $560 \mu\text{L}$  each of 10% Triton X-100 and 10% Tween 20 to the lysate followed by vortexing.
10. Transfer the lysate to three 1.5 mL microcentrifuge tubes and centrifuge at  $18,000 \times g$  for 30 min at  $4^\circ\text{C}$ .
11. Combine the supernatants and add to preswelled glutathione-agarose beads (*see Subheading 3.2.1*). Incubate at room temperature for 30 min on a horizontal rotator.
12. Transfer beads to 50 mL screw cap conical tubes and centrifuge at  $800 \times g$  for 25 sec in a table top centrifuge.
13. Remove the supernatant (nonbound fraction) and put aside 1 mL for PAGE.
14. Wash beads with cold PBS and centrifuge at  $800 \times g$  for 30 s. Repeat for a total of four washes.
15. Elute the GST proteins by adding 1 mL of GST elution buffer to the beads and incubate with rotation for 15 min at room temperature.
16. Pellet the beads by centrifugation at  $800 \times g$  for 25 s and transfer the eluate to a 1.5 mL microcentrifuge tube. Repeat the elution  $2\times$  and collect in separate tubes.
17. Remove  $100 \mu\text{L}$  of each fraction for determination of protein concentration and  $50 \mu\text{L}$  for SDS-PAGE analyses. For GST alone control, only  $50 \mu\text{L}$  is required.
18. Aliquot the eluates in  $500 \mu\text{L}$  volumes and snap freeze in liquid  $\text{N}_2$  and store at  $-80^\circ\text{C}$ .
19. Analyze the collected samples (pre and postinduction, non-bound, eluates) on a SDS-PAGE and stain for total proteins using Coomassie Blue and determine protein concentration using the BioRad protein assay. The highest concentration of GST-tagged proteins is found in the first elution and, typically, the yield is between 100 and  $300 \mu\text{g}/\text{mL}$ .

### **3.3. Preparation of Nuclear Extracts**

We use the following protocol for preparing nuclear extracts for DNA-binding studies using LNCaP, HeLa, and Flag-tagged AR HeLa cells. The reagent volumes suggested are for a single 15 cm tissue culture plate, approximately 75% confluent ( $\sim 2 \times 10^7$  cells).

1. Wash cells twice with ice cold PBS to remove media (care should be taken not to dislodge LNCaP cells).
2. Scrape cells into 10 mL of ice cold PBS, collect in a 15 mL conical tube.
3. Pellet cells by centrifuging at  $800 \times g$  for 10 min at  $4^\circ\text{C}$ .

4. Remove supernatant and resuspend cells (gentle vortexing) in 5 mL ice cold PBS, centrifuge as before.
5. Remove supernatant and resuspend cells (by gentle vortexing) in 5 mL ice cold Buffer A and incubate on ice for 10 min.
6. Centrifuge at  $800 \times g$  for 10 min at  $4^{\circ}\text{C}$ , remove supernatant, and resuspend in 1.5 mL ice cold Buffer A. Incubate on ice for 10 min.
7. Disrupt cells with 10 strokes of a prechilled, clean glass Dounce homogeniser (Kontes, B type pestle).
8. Place cell lysate into a chilled 1.5 mL microcentrifuge tube and centrifuge at  $18,000 \times g$  at  $4^{\circ}\text{C}$  for 1 min.
9. Remove supernatant (cytoplasmic fraction) and discard. Repeat centrifugation and remove any remaining residue.
10. Resuspend nuclei in 200  $\mu\text{L}$  chilled Buffer C. Incubate at  $4^{\circ}\text{C}$  for 30 min with mixing (gentle vortexing is best).
11. Centrifuge at maximum speed (microcentrifuge) for 20 min at  $4^{\circ}\text{C}$ . Recover and aliquot supernatant (25  $\mu\text{L}$  volumes work well) (*see* [Note 3](#)).

### **3.4. Labeling of DNA Probe for EMSA**

#### *3.4.1. Using Cloned Plasmid DNA*

Appropriate safety measures and adherence to local and national rules should be followed when working with ionizing radiation sources and discarding waste materials.

1. Digest 5  $\mu\text{g}$  of plasmid DNA in a 50  $\mu\text{L}$  reaction with enzymes, which liberate the cloned DNA fragment of interest leaving 5' overhangs.
2. Label the DNA fragments using a Klenow reaction assembled as follows for filling in the 5' overhangs (*see* [Note 4](#)).  
2.5  $\mu\text{g}$  digested DNA in restriction buffer.  
5  $\mu\text{L}$  10 $\times$  Klenow Reaction buffer (supplied by manufacturer).  
2  $\mu\text{L}$  each of 10 mM dNTP solution minus dCTP.  
1  $\mu\text{L}$  5 U/ $\mu\text{L}$  Klenow enzyme.  
2.5  $\mu\text{L}$  [ $\alpha$ - $^{32}\text{P}$ ]dCTP (25 uCi).  
sterile  $\text{dH}_2\text{O}$  to 50  $\mu\text{L}$ .
3. Incubate the reaction at room temperature for 25 min.
4. Remove the unincorporated nucleotides by passing through a G25 spin column according to the manufacturer's instructions.
5. Gel purify the labeled DNA probe as described in [Subheading 3.4.4](#).

#### *3.4.2. Using Synthetic Complimentary Oligomers*

1. Radiolabel 100 ng of one complimentary oligomer using T4 polynucleotide kinase and [ $\gamma$ - $^{32}\text{P}$ ]dATP in the following reaction:

100 ng oligomer  
 5  $\mu$ L 10 $\times$  T4 kinase buffer (supplied with the enzyme by the manufacturer).  
 10 U T4 polynucleotide kinase.  
 2.5  $\mu$ L [ $\gamma$ - $^{32}$ P]dATP (25 uCi).  
 sterile dH<sub>2</sub>O to 50  $\mu$ L.

2. Incubate at 37°C for 1 h.
3. Remove the unincorporated nucleotides as in **Subheading 3.4.1, step 4**.
4. Anneal the radiolabeled oligomer to its complimentary molecule by adding an equimolar amount of the second oligomer to the labeled oligomer and heating to 95°C for 5 min followed by slowly cooling to room temperature.
5. Gel purify the DNA probe as described in **Subheading 3.4.4**.

**3.4.3. Labeling of DNA Probe for DNase I Footprinting, Methylation Interference, and Methylation Protection Assays**

1. Digest 5  $\mu$ g of probasin promoter (-426 to + 28) in pUC119 with the first restriction enzyme (*Hinf*I) to generate a 5' overhang in the upper strand for filling in a single [ $\alpha$ - $^{32}$ P]dCTP (See **Note 5**).
2. Cleanup the DNA using a PCR cleanup kit as per the manufacturer's instructions.
3. Radiolabel 2.5  $\mu$ g of digested DNA as in **Subheading 3.4.1, step 2**.
4. Mix the reaction gently, centrifuge briefly, and incubate for 25 min at room temperature.
5. At the end of the incubation period, add 2  $\mu$ L of 10 mM dCTP for 10 minutes as a cold chase to ensure that all the labeled fragments have the same number of base pairs. Add 1  $\mu$ L of 0.5 M EDTA to stop the reaction.
6. Remove unincorporated nucleotides using Sephadex G50 spin columns as in **Subheading 3.4.1, step 4**. Remove 1  $\mu$ L of sample and count in a scintillation counter to assess the efficiency of incorporation. Typically,  $\sim 1 \times 10^5$  dpm is expected.
7. Digest the labeled DNA with the second enzyme (*Hind*III) to generate a restriction fragment labeled on only one strand.
8. Gel purify the DNA probe as described in **Subheading 3.4.4**.

**3.4.4. Gel Purification of Labeled DNA Probes**

1. Assemble a 1 mm vertical nondenaturing 5% acrylamide in 0.5 $\times$  TBE gel, using the appropriate spacers and comb (see **Note 6**).
2. Prerun the acrylamide gel at 400V for 3 min in 0.5 $\times$  TBE.

3. Add 1/5 volume of 5× DNA loading dye to the labeled DNA reaction (described in [Subheading 3.4.1](#), [3.4.2](#) or [3.4.3](#)) and load it into one well of the gel.
4. Run the gel at 400 V until the bromophenol blue (dark blue) dye-front has migrated approximately 2/3 of the way down the gel.
5. Stop the reaction and disassemble the gel running apparatus. Lay the gel flat and remove the top glass plate, leaving the gel adhered to the bottom plate.
6. Wrap the gel and glass plate in plastic wrap and place it into an X-ray film cassette. Use a method of registering the film to the gel during exposure such that the registration can be reproduced on the bench after the film is exposed. We typically use phosphorescent stickers on the plastic wrap to leave registration exposures on the film following developing.
7. In the dark room, expose wet gel to film for 1 min and develop film.
8. Reorientate the film on top of the plastic wrapped-gel. Using a razor blade or scalpel cut out the section of the gel containing the DNA of interest and transfer it to a 1.5 mL microcentrifuge tube. For the labeled probe in [Subheading 3.4.3](#), the film should show 2 bands corresponding to the plasmid backbone (toward the top of the gel) and the DNA fragment to be analysed (toward the bottom of the gel) (*see* [Note 7](#)).
9. Elute the DNA fragment in 500 μL gel elution buffer by rotating overnight (*see* [Note 8](#)).
10. Carefully transfer the elution buffer containing the DNA probe to a new tube (do not transfer any fragments of the acrylamide) and add 1 mL of 95% ethanol and mix thoroughly by inverting the tube (*see* [Note 9](#)).
11. Precipitate the DNA probe by incubating on ice for 30 min and centrifuge at maximum rpm in a microcentrifuge, at 4°C for 30 min.
12. Remove the supernatant and wash twice with 500 μL 70% ethanol, centrifuge at maximum rpm for 5 min and again, aspirate the supernatant. The location of the probe DNA through these manipulations can be followed by Geiger counter to ensure the pellet is not lost.
13. Air dry the pelleted DNA and resuspend in 20 μL of buffer D
14. Count 1 μL of the radiolabeled DNA using a scintillation counter and dilute the DNA probe to 10,000 dpm/μL in buffer D.

### 3.5. Protein–DNA Binding Reactions and EMSA

#### 3.5.1. EMSA

Assemble a 1.5 mm vertical 0.5×TBE nondenaturing 5% acrylamide gel using the appropriate spacers and combs.

1. Thaw either nuclear extracts or recombinant protein and 2 μg/μL poly(dI-dC).(dI-dC) aliquots on ice (*see Note 10*).
2. Prepare a master mix containing 7 μL of DNA-binding buffer and 1 μL of 2 μg/μL poly(dI-dC).(dI-dC) for each reaction (include one extra tube for free probe control).
3. Aliquot 8 μL of the master mix for each reaction and add 2 μL of nuclear extract or recombinant protein. Gently mix by pipetting up and down and avoid introducing air bubbles.
4. For the free probe control, add 2 μL of buffer D.
5. Incubate the EMSA reaction tubes at room temperature for 15 min (*see Note 11*).
6. Add 2 μL of radiolabeled DNA probe at 10,000 dpm/μL to each tube, again gently mixing by pipetting up and down and avoiding air bubbles.
7. Incubate for a further 15 min.
8. Prerun the gel at 300 V for 10 min in 0.5× TBE.
9. Stop the gel and load 1× DNA loading buffer into an outside well. Load the free probe control and all other reactions into the appropriate wells without DNA loading buffer.
10. Run the gel for approximately 1.5 h at 300 V.
11. Dry the gel on filter paper in a vacuum gel drier and expose to a phospho-imaging screen or autoradiography film overnight (*see Fig. 2*).

#### 3.5.2. Antibody Supershift EMSA

1. Assemble the EMSA reactions as described in **Subheading 3.5.1, steps 1–4**.
2. To one supershift EMSA reaction, add 0.5–1 μL (usually 1–2 μg) specific antibody to supershift reaction and nonspecific antibody to the control reaction (*see Note 12*).
3. Incubate at room temperature for 15 min, then add 2 μL of radiolabeled DNA probe at 10,000 dpm/μL to each tube and incubate for a further 15 min.
4. Load and electrophorese the reactions on a vertical 0.5× TBE nondenaturing 5% acrylamide gel as described for EMSA in **Subheading 3.5.1, steps 8–11** (*see Notes 13 and 14*).

### 3.6. DNase I Footprint Analysis of Receptor-DNA Binding

#### 3.6.1. Generation of an A/G Purine Ladder Using the Maxam-Gilbert Method

1. Aliquot 20,000 dpm of labeled DNA from **Subheading 3.4.4** into a microcentrifuge tube, freeze in a dry ice/ethanol bath, and lyophilize in a vacuum concentrator.
2. Add 2.5 μL of 2% formic acid and 1 μg of herring sperm DNA to the dried DNA fragment. Incubate at 37°C for 10 min.
3. Stop the reaction by snap freezing in a dry ice/ethanol bath.



4. Remove the formic acid by lyophilisation in a vacuum concentrator. This usually requires about 1 h.
5. In the fume hood, resuspend the dried DNA samples in 100  $\mu$ L 10% piperidine and incubate at 90°C for 30 min.
6. Stop the reaction by placing the tube in dry ice/ethanol bath.
7. Remove the piperidine using vacuum concentrator. This usually requires about 90 min.
8. Wash thrice with 100  $\mu$ L of sterile dH<sub>2</sub>O, and dry by lyophilization between each wash.
9. Resuspend the cleaved DNA in 5  $\mu$ L of formamide loading buffer and run the sample alongside the DNase I treated samples from [Subheading 3.6.2](#); methylation interference samples from [Subheading 3.7](#); or methylation protection samples from [Subheading 3.8](#).

### 3.6.2. DNase I Footprinting

1. Prepare an A + G Maxam-Gilbert purine ladder as described in [Subheading 3.6.1](#).
2. Preincubate 5–20  $\mu$ g of recombinant AR-DBD (*see* [Note 15](#)), or the equivalent amount of bovine serum albumin (BSA), with 1  $\mu$ g of poly(dI-dC).(dI-dC) in a total volume of 99  $\mu$ L of DNA-binding buffer for 10 min on ice.
3. Add 20,000 dpm of the single-end-labeled DNA and incubate for 15 min at room temperature. The amount of recombinant AR-DBD used should be determined empirically.
4. Add 4  $\mu$ L of the CaCl<sub>2</sub> and MgCl<sub>2</sub> mix to a final concentration of 2.5 and 4 mM, respectively.
5. Add 1–2 U of DNase I (*see* [Note 16](#)) to the sample and incubate for exactly 2 min at room temperature.
6. Stop the digest by adding 100  $\mu$ L of 2 $\times$  proteinase K stop buffer and incubate the samples at 37°C for 1 h to inactivate the DNase I.
7. Add 200  $\mu$ L of TE buffer containing 85  $\mu$ g/mL of carrier t-RNA.
8. Add equal volume of phenol/chloroform/isoamyl alcohol (25:24:1) mixture to the samples. Mix vigorously for 15 s and centrifuge at 18,000  $\times g$  for 15 min or until the aqueous phase and the organic phase are separated.
9. Remove the aqueous phase to a fresh tube and precipitate the DNA with 0.3 M sodium acetate, and 2.5 volumes of 95% ethanol, for 30 min in a dry ice/ethanol bath.
10. Centrifuge at 18,000  $\times g$  in a microcentrifuge at 4°C for 30 min.

11. Remove the supernatant and wash the precipitate twice with 70% ethanol, air dry the pellet and resuspend in 5  $\mu$ L of formamide loading buffer.
12. Heat the samples at 90°C for 10 min and rapidly cool on ice.
13. Load the samples onto a prerun 7% polyacrylamide/urea sequencing gel (*see* **Note 17**) and run the gel in 1 $\times$  TBE buffer at 40W until the bromophenol-blue dye is 1/2 inch (1.25 cm) from the bottom. Include the A + G Maxam-Gilbert purine ladder alongside the samples.
14. After electrophoresis, remove the top plate from the gel and layer a piece of 3 MM chromatography paper on top of the gel. Gently rub the paper so that the gel will adhere to the paper.
15. Dry the gel under vacuum in a gel dryer.
16. Autoradiograph the dried gel with autoradiography film in a cassette without an intensifying screen and left at room temperature until the bands are discernible (from 3 days to 1 week) (*see* **Fig. 3** and **Note 18**).

**3.7. Methylation Interference Assay to Identify Guanine Contact Sites Required for Protein Binding.**

1. To  $\sim 10^6$  dpm of single-end-labeled DNA (–286 to –166 of the probasin promoter) in 5–10  $\mu$ L of TE, add 200  $\mu$ L of dimethyl sulfate (DMS) buffer.
2. Add 1  $\mu$ L of DMS and incubate for exactly 5 min at room temperature.
3. Stop the reaction with 40  $\mu$ L of DMS stop buffer.
4. Add 1  $\mu$ L of 10 mg/mL of t-RNA, 600  $\mu$ L of 95% ethanol, mix and incubate in a dry ice/ethanol bath for 30 min, and centrifuge at 18,000  $\times g$  for 30 min.
5. Remove the supernatant carefully with a pipet tip and dispose in a DMS waste container.
6. Resuspend the pellet in 250  $\mu$ L of 0.3 M sodium acetate/1 mM EDTA. Add 750  $\mu$ L of ice cold 95% ethanol, mix and incubate in a dry ice/ethanol bath for 30 min. Centrifuge at 18,000  $\times g$  for 30 min.
7. Repeat the precipitation step.
8. Wash the pellet twice with 70% ethanol and air dry the pellet.
9. Initially, resuspend the pellet in 40  $\mu$ L TE. Count 1  $\mu$ L in a scintillation counter and dilute to 20,000 dpm/ $\mu$ L.
10. Prepare an EMSA binding reaction as in **Subheading 3.5.1, steps 1–7** (*see* **Note 19**) except scale up the reaction volumes 5 $\times$ .
11. Divide the sample into three lanes and electrophorese the gel for approximately 1.5 h at 300 V.

12. After removing the top glass plate, wrap the gel in plastic wrap and expose to autoradiography film for approximately 2–4 h. Mark the film for registration as described in **Subheading 3.4.4, step 6**.
13. Excise, elute the bands that correspond to the free probe and the DNA–protein complex and precipitate the eluted DNA as described in **Subheading 3.4.4, steps 8–14**. Remove any residual acrylamide pieces using spin filters.
14. Resuspend and cleave the eluted DNA in 10% piperidine as described in **Subheading 3.6.1, steps 5–8**).
15. After the final lyophilization, dissolve the samples in 11  $\mu\text{L}$  of formamide loading buffer. Determine the radioactivity of the samples by counting 1  $\mu\text{L}$  of each sample in a scintillation counter.
16. Heat denature equal counts of free and bound probes (2,000–4,000 dpm) at 90°C for 10 min, cool on ice and load onto a preheated 10% polyacrylamide/urea gel.
17. Dry and autoradiograph the gel as in **Subheading 3.6.2, steps 14–16**, or expose the gel to a phospho-imaging screen for quantification (*see Fig. 4*).

**3.8. Methylation Protection Assay to Identify Receptor Contact Sites on the DNA and Local DNA Distortion.**

1. Prepare single-end-labeled DNA probe as described in **Subheadings 3.4.3 and 3.4.4**.
2. Prepare an A + G Maxam-Gilbert purine ladder as described in **Subheading 3.6.1**.
3. Assemble a 1.5 mm vertical 0.5 $\times$  TBE nondenaturing 5% polyacrylamide gel using the appropriate spacers and combs.
4. Prepare an EMSA binding reaction by preincubating 5  $\mu\text{g}$  recombinant AR-DBD (*See Note 20*) with 2  $\mu\text{g}$  of poly(dI-dC)(dI-dC) and Buffer D (final volume 25  $\mu\text{L}$ ) for 15 min at room temperature. Also prepare one reaction without recombinant protein as a control.
5. Pre-run the EMSA gel at 300 V.
6. Add 350,000 dpm (26.5 fmoles) of single-end-labeled DNA probe (probasin promoter: from –276 to –76) in 5  $\mu\text{L}$  Buffer D and incubate a further 10 min at room temperature.
7. Add 3  $\mu\text{L}$  of 2% DMS and incubate for exactly 2 min.
8. Load the reaction into a well of the EMSA gel while the current is running (*See Note 21*) at 300 V.
9. Electrophorese the gel for approximately 45 min to 1 h.
10. Disassemble the EMSA apparatus. After removing the top glass plate, wrap the gel in plastic wrap and expose to autoradiography film for approximately 2–4 h. Mark the film for registration as described in **Subheading 3.4.4, step 6**.

11. Excise, elute, and precipitate the isolated free and bound DNA fraction as described in **Subheading 3.4.4**, steps 9–14.
12. Continue with the piperidine cleavage denaturing PAGE analysis as described in the methylation interference protocol, **Subheading 3.7**, step 14–17 (*see Fig. 5*).

---

## 4. Notes

1. To facilitate separation of the sequencing gel plates after electrophoresis, the top glass plate may be silanized. Add 3 mLs of Sigmacote to the plate in a fume hood. Use tissue paper to evenly spread the solution onto the plate. Let dry in the fume hood.
2. DMS is an extremely hazardous compound, both in liquid and vapor form. Be sure to consult the DMS MSDS and be familiar with the appropriate storage, handling, and waste requirements for your area.
3. It is important not to disturb the pellet; it is preferable to sacrifice yield to ensure the pellet is not disturbed and contaminates the extract.
4. The use of labeled dCTP assumes the presence of guanine bases in the restriction overhangs, adjust as necessary. We do not use dTTP for fill-in labeling because the incorporation is inefficient.
5. A 5' overhang on the upper strand will give a labeled lower strand whereas a 5' overhang on the lower strand will give a labeled upper strand. Protected areas on both strands can thus be obtained. The length of the probe can be from 100–300 base pairs, preferably with the area of interest located in the middle of the DNA.
6. Using narrower gel spacers improves elution efficiency; however, if the gel is too thin, it is difficult to work with and can easily tear.
7. Bands can be curved because of the relatively high salt content of the labeling reaction. If no column clean up was performed, there may also be a “cloud” at the bottom of the gel due to the presence of unincorporated radionucleotides. Cut out the portion of the gel corresponding to the DNA fragment of interest. To maximize the recovery of DNA, macerate the gel fragment (we use a pipet tip) prior to the elution step. This procedure is particularly useful when recovering relatively small amounts of DNA from methylation interference and protection assays.

8. The duration of the elution can be shortened by gently heating the elution mixture with rotation for 3 h at 45°C. If available, a hybridization oven is suitable.
9. If the gel fragment was macerated after being excised, filter the elution mixture through a spin filter (800 × g for 2 min) to remove any fine acrylamide fragments prior to adding ethanol. Samples contaminated with acrylamide will give inaccurate estimation of the amount of radioactivity and will also affect the electrophoresis.
10. The overall salt concentration in the EMSA reaction should be in the range of 100–120 mM (including all buffer salts, NaCl, KCl, etc.). The optimal salt concentration for a given protein must be determined empirically, however concentrations outside this range are nonphysiological.
11. Incubation temperature may influence the binding reaction, particularly for supershift reactions. Performing the incubations on ice may stabilize the bound antibody–protein complex.
12. Care should be taken to ensure that the added antibody does not significantly alter the overall salt concentration of the reaction.
13. Antibody/protein reactions in supershift experiments may cause interference rather than a shifted band; if antibody binding sterically interferes with DNA–protein interactions, a shifted band normally seen in the absence of antibody may be attenuated or absent.
14. Shifts using nuclear extracts, in particular, may generate a number of different bands representing a variety of DNA/protein species. Binding reaction specificity can be determined by using a cold DNA competition; 10 to 100-fold excess unlabeled DNA probe is added to the binding reaction prior to addition of the labeled DNA probe. Bands that persist under these conditions are likely the result of nonspecific DNA/protein interactions.
15. The amount of protein used should be titrated. Ideally, it will be best to have saturation binding of the labeled DNA probe. If this cannot be achieved, then an EMSA should be set up after DNase I treatment with the bound complex cut out and eluted as in [Subheading 3.4.4, step 5–13](#) and [Subheading 3.7, step 11–16](#).
16. The amount of DNase I used should be determined empirically. Typically, 1–2 units are used for each reaction.
17. The sequencing gel is preheated to ~50°C. (A gel temperature indicator can be placed onto the gel plate to monitor the temperature). Rinse the wells thoroughly to remove any residual acrylamide or urea that has leached out of the gel before sample loading. The acrylamide concentration and the

- length of the run will depend on the size of the DNA fragment. For long fragments, double loading may be required.
18. Exposing the gel to the film without an intensifying screen will give sharper bands.
  19. The amount of protein used should be titrated to give equal proportion (50%) of free and bound probe. The disappearance of a band (corresponding to the methylated guanine site) from the DNA-protein complex can only be seen when compared with the free.
  20. The first step of the methylation protection assay proceeds as an EMSA reaction, but requires precise ratios of protein, target DNA, and DMS for successful results. The DNA and DMS concentrations described have consistently given good results for us, thus we recommend optimizing the sensitivity of the protection assay by first performing titrations of the protein of interest in the DNA-binding reaction.
  21. Loading the gel while it is running ensures that each sample receives equal methylation treatment. As DMS is a neutral molecule, the negatively charged DNA will migrate from the DMS thus terminating the methylation reaction. Additionally, the EMSA step allows separation of bound DNA from free DNA, relieving the requirement to achieve saturation binding of the DNA by the protein of interest, which can be challenging in some cases. Obviously, caution should be exercised to avoid electrocution while loading the gel. If uncertain how to proceed seek advice for your particular apparatus from the manufacturer.

---

## Acknowledgments

The authors acknowledge the work of Kimberly J. Reid, Lillian H. Yeung, and Pernille Sorenson in the development of these techniques in our lab.

This work was supported by grants from the Terry Fox Foundation and the National Cancer Institute of Canada.

## References

1. Lonard, D. M., Lanz, R. B., and O'Malley, B. W. (2007) Nuclear receptor coregulators and human disease. *Endocr Rev* **28**, 575–587.
2. Kasper, S., Rennie, P. S., Bruchovsky, N., Sheppard, P. C., Cheng, H., Lin, L., Shiu, R. P., Snoek, R., and Matusik, R. J. (1994) Cooperative binding of androgen receptors to two DNA sequences is required for androgen induction of the probasin gene. *J Biol Chem* **269**, 31763–31769.
3. Rennie, P. S., Bruchovsky, N., Leco, K. J., Sheppard, P. C., McQueen, S. A., Cheng, H., Snoek, R., Hamel, A., Bock, M. E., and MacDonald, B. S., et al. (1993) Characterization

- of two cis-acting DNA elements involved in the androgen regulation of the probasin gene. *Mol Endocrinol* **7**, 23–36.
4. Yeung, L. H., Read, J. T., Sorenson, P., Nelson, C. C., Jia, W., and Rennie, P. S. (2003) Identification and characterization of a prostate-specific androgen-independent protein-binding site in the probasin promoter. *Biochem J* **371**, 843–855.
  5. Gao, N., Zhang, J., Rao, M. A., Case, T. C., Mirosevich, J., Wang, Y., Jin, R., Gupta, A., Rennie, P. S., and Matusik, R. J. (2003) The role of hepatocyte nuclear factor-3 alpha (Forkhead Box A1) and androgen receptor in transcriptional regulation of prostatic genes. *Mol Endocrinol* **17**, 1484–1507.
  6. Zhang, J., Thomas, T. Z., Kasper, S., and Matusik, R. J. (2000) A small composite probasin promoter confers high levels of prostate-specific gene expression through regulation by androgens and glucocorticoids in vitro and in vivo. *Endocrinology* **141**, 4698–4710.
  7. Yu, D., Scott, C., Jia, W. W., De Benedetti, A., Williams, B. J., Fazli, L., Wen, Y., Gleave, M., Nelson, C., and Rennie, P. S. (2006) Targeting and killing of prostate cancer cells using lentiviral constructs containing a sequence recognized by translation factor eIF4E and a prostate-specific promoter. *Cancer Gene Ther* **13**, 32–43.
  8. Rennie, P.S., and Cheng H. unpublished data.
  9. Reid, K. J., and Nelson, C. C. (2001) Improved methylation protection-based DNA footprinting to reveal structural distortion of DNA upon transcription factor binding. *Bio-techniques* **30**, 20–22.
  10. Reid, K. J., Hendy, S. C., Saito, J., Sorensen, P., and Nelson, C. C. (2001) Two classes of androgen receptor elements mediate cooperativity through allosteric interactions. *J Biol Chem* **276**, 2943–52.
  11. Read, J. T., Rahmani, M., Boroomand, S., Allahverdian, S., McManus, B. M., and Rennie, P. S. (2007) Androgen receptor regulation of the versican gene through an androgen response element in the proximal promoter. *J Biol Chem* **282**, 31954–31963.



# Chapter 7

## Chromatin Immunoprecipitation (ChIP) Methodology and Readouts

Charles E. Massie and Ian G. Mills

### Abstract

The identification of direct nuclear hormone receptor gene targets provides clues to their contribution to both development and cancer progression. Until recently, the identification of such direct target genes has relied on a combination of expression analysis and *in silico* searches for consensus binding motifs in gene promoters. Consensus binding motifs for transcription factors are often defined using *in vitro* DNA binding strategies. Such *in vitro* strategies fail to account for the many factors that contribute significantly to target selection by transcription factors in cells beyond the recognition of these short consensus DNA sequences. These factors include DNA methylation, chromatin structure, posttranslational modifications of transcription factors, and the cooperative recruitment of transcription factor complexes. Chromatin immunoprecipitation (ChIP) provides a means of isolating transcription factor complexes in the context of endogenous chromatin, allowing the identification of direct transcription factor targets. ChIP can be combined with site-specific PCR for candidate binding sites or alternatively with cloning, genomic microarrays or more recently direct high throughput sequencing to identify novel genomic targets. The application of ChIP-based approaches has redefined consensus binding motifs for transcription factors and provided important insights into transcription factor biology.

**Key words:** Nuclear hormone receptor, Androgen receptor, Estrogen receptor, Chromatin immunoprecipitation, ChIP, High throughput sequencing, Array, Transcription, Hormone, Cancer.

---

### 1. Introduction

Chromatin immunoprecipitation has revolutionised our understanding of transcriptional biology by providing insights into chromatin dynamics and transcription factor recruitment. For example, the oestrogen receptor (ER) has been shown to cycle on and off chromatin using ChIP and quantitative PCR, demonstrating the transient association of transcription factors with

their target genes (1). By combining ChIP with whole genome arrays, the ER has been shown to bind genomic regions > 100 kb from the nearest transcriptional start site and also to require other transcription factors (e.g., FOXA1) for recruitment to a subset of its target genes (2, 3). Data from ChIP studies of the androgen receptor (AR) and glucocorticoid receptor (GR) have reported similar dynamics, distal-binding sites, and cooperative recruitment with other transcription factors, suggesting similar mechanisms of transcriptional control by these nuclear hormone receptors (NHR)s (4–6). Although the computational prediction of binding sites and *in vitro* DNA-binding assays are powerful tools, it would not have been possible to uncover these findings by using these techniques alone, highlighting the utility of ChIP-based protocols in the study of transcriptional biology.

As stated above transcription factors such as the NHRs interact with their cognate DNA-binding sites transiently. RNA polymerase and other members of the core transcriptional machinery track along the genome. Histone modifications are also turned-over, and the protein complexes that elicit these modifications also cycle on and off chromatin. Therefore, the use of cross-linking reagents which “fix” these transient protein–DNA interactions is highly advantageous when trying to determine the genomic locations of proteins. In most ChIP studies, this first step is achieved by cross-linking in a 1% formaldehyde solution. The resolution of ChIP data is determined by the size of the chromatin fragments, since ChIP for a given factor will pull-down all continuous DNA to which that factor is bound. For this reason, the second major step in the ChIP protocol is chromatin fragmentation, most often achieved by sonication. The subsequent immunoprecipitation of DNA that is bound by a protein relies on antibodies with high specificity and affinity. Incubation of a specific antibody with the sonicated chromatin results in antibody–protein–DNA complexes, which are collected on Protein-A/G beads, washed thoroughly to reduce nonspecific background, and then eluted. Protein–DNA cross-links are then reversed and enriched DNA fragments are purified (Fig. 1 for overview of the ChIP procedure).

---

## 2. Materials

### 2.1. Cell Culture and Cross-Linking

1. RPMI (Invitrogen) supplemented with 10% foetal bovine serum (FBS, HyClone).
2. Phenol red free RPMI (Invitrogen) supplemented with 10% charcoal dextran stripped FBS (HyClone).

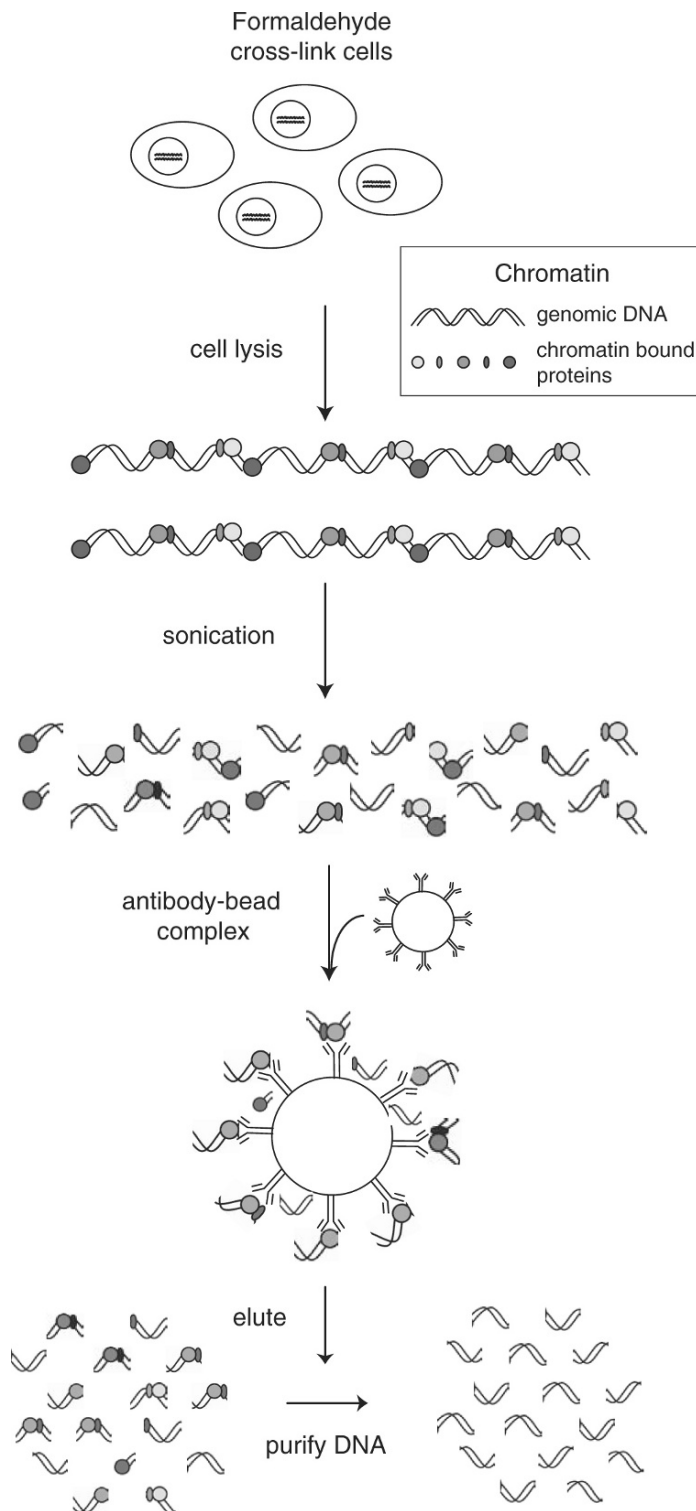


Fig. 1. Overview of ChIP methodology. Schematic showing the steps involved in ChIP from cross-linking live cells, cell lysis, fragmentation of chromatin (e.g., by sonication), immunoprecipitation using antibodies to a specific chromatin bound factor, elution, and purification of enriched genomic regions.

3. Nuclear hormone receptor ligands (e.g., synthetic androgen R1881).
4. 1% Formaldehyde in culture media or 1× PBS (*see Note 1*).
5. Glycine solution (2.5 M).

### **2.2. Harvesting Cells and Sonication**

1. Cell scrapers (Corning).
2. Phosphate buffered saline (PBS) supplemented with Complete protease inhibitors (Roche).
3. ChIP lysis buffer: 1% SDS, 10 mM EDTA, 50 mM Tris-HCl pH 8, 1× Complete protease inhibitors (Roche).
4. Sonicating water bath or probe sonicator.
5. Agarose, TBE, and electrophoresis equipment.

### **2.3. Immunoprecipitation**

1. ChIP dilution buffer: 25 mM Tris-HCl pH 8, 140 mM NaCl, 1% Triton X-100, 0.1% SDS, 3 mM EDTA, Complete protease inhibitors (Roche).
2. Protein A/G sepharose beads (GE Healthcare) (*see Note 2*).
3. Antibodies to target proteins (e.g., rabbit anti-AR N20, Santa Cruz) (*see Note 3* for resources for identifying validated ChIP grade antibodies).
4. Bovine serum albumin (BSA, New England Biolabs).
5. TSE-I wash buffer: 0.1% SDS, 1% Triton X-100, 2 mM EDTA, 20 mM Tris-HCl pH 8, 150 mM NaCl (stable for up to 1 year at 4°C).
6. TSE-II wash buffer: 0.1% SDS, 1% Triton X-100, 2 mM EDTA, 20 mM Tris-HCl pH 8, 200 mM NaCl (stable for up to 1 year at 4°C).
7. Wash buffer-III: 0.25 M LiCl, 1% Np40, 1% sodium deoxycholate, 1 mM EDTA, 10 mM Tris-HCl pH 8 (make fresh as required).
8. TE pH 8.0: 10 mM Tris-HCl pH8, 1 mM EDTA.
9. Elution buffer: 1% SDS, 0.1 M NaHCO<sub>3</sub>.

### **2.4. DNA Isolation**

1. Sodium chloride: 5 M NaCl.
2. Proteinase-K reagent stock solution: 0.5 M EDTA, 1 M Tris-HCl pH 6.7 and 20 mg/mL Proteinase-K.
3. Glycogen (Roche) or suitable carrier for precipitation.
4. Phenol/chloroform/isoamyl alcohol (25:24:1).
5. Isopropanol.
6. Ethanol, 75%.

## 2.5. Analysis of Enrichment

### 2.5.1. Realtime PCR

1. Realtime PCR instrument (e.g., ABI 7900).
2. Oligonucleotide primers to genomic regions of interest.
3. Sybr Green PCR master mix (Applied Biosystems).
4. Optical PCR plates and adhesive covers compatible with the Realtime PCR instrument.

### 2.5.2. Chip-Chip

1. Nanodrop spectrophotometer.
2. Microarray hybridisation station or slide incubator.
3. Microarray scanner and image analysis software.
4. Linker oligonucleotides (P1: GCGGTGACCCGGGA-GATCTGAATTC, P2: GAATTCAGATC).
5. T4 DNA polymerase.
6. T4 DNA ligase.
7. Taq polymerase.
8. dNTP mix.
9. BioPrime array CGH labelling kit (Invitrogen).
10. Cy3-dUTP and Cy5-dUTP.
11. Sephadex G-50 columns.
12. Microarray hybridisation apparatus (e.g., Nimblegen Hybridisation System and Nimblegen Hybridisation Kit).
13. Microarray scanner (e.g., GenePix 4,000).
14. Image analysis software (e.g., NimbleScan).
15. Bioinformatics support for detailed analysis of ChIP-chip data.

---

## 3. Methods

The method outlined below is a detailed protocol that has been used for the identification of AR genomic binding sites in the LNCaP prostate cancer cell line. However, this protocol is also applicable to other transcription factors, DNA associated proteins, and histone modifications. ChIP may be performed for any epitope on chromatin, provided that there are antibodies available, which have high specificity and avidity (*see Subheading 2.3, item 3*). In general, it is necessary to have a control ChIP reaction against which the fold enrichment and specificity of the test ChIP reaction is measured. In the protocol given below, a treatment contrast (i.e., androgen stimulation vs. vehicle alone) is used to provide a control experiment; however, there are many options for ChIP control experiments (*see Note 4*).

### 3.1. Cell Culture and Cross-Linking

1. Maintained LNCaP cells in RPMI supplemented with 10% FBS in 5% CO<sub>2</sub> at 37°C and passaged at a dilution of 1:3 when approaching confluence with Trypsin/EDTA.
2. Aspirate media from culture flasks and wash cells with 1× PBS, before replacing media with phenol red free RPMI supplemented with 10% charcoal dextran stripped FBS (*see Note 5*).
3. After 48 h replace culture media with media containing the synthetic androgen R1881 (90 pM) or an equal volume of ethanol (vehicle) and return cells to incubators for 1 h.
4. Remove culture media and replace with media containing 1% formaldehyde to cross-link protein–DNA interactions. Incubate flasks at 37°C for 10 min (*see Note 1*).
5. Stop the cross-linking reaction by adding glycine to culture media to give a final concentration of 125 mM and incubate for 5 min at 37°C.

### 3.2. Harvesting Cells and Sonication

1. Transfer flasks to ice, remove media, and wash cells twice with ice-cold 1× PBS supplemented with protease inhibitors.
2. Aspirate PBS from cells and harvest cells using a cell scraper. Transfer cells to a 1.5 mL tube using a wide-bore pipette tip and centrifuge cells at 800 × *g* for 3 min at 4°C.
3. Aspirate residual PBS and add 1 mL of ChIP lysis solution per 10<sup>7</sup> cells (1 × T150 cm<sup>2</sup> flask). Allow cells to lyse on ice for 10 min.
4. Fragment chromatin to an average size of 500 bp. This can be accomplished for 300 μL aliquots of LNCaP cells using a prechilled Biorupter (Diagenode) sonicating waterbath at high output setting (200 W) for 15 min with 30 s pulses and 30 s rests. However, the conditions required may vary depending on the cell type used and may require specific optimisation (*see Note 6*).
5. Remove insoluble debris by centrifugation at 13,000 × *g* for 15 min. Transfer supernatant to a fresh tube.
6. Assess the extent of sonication by taking 50 μL of sonicated lysates, reversing cross-links, and isolating DNA (*see below*). Running a 1% agarose gel. A smear should be visible between 250 bp and 1 kb (*see Fig. 2A*).

### 3.3. Immunoprecipitation

1. Add 500 μL of ChIP dilution buffer per 1 mL of ChIP lysis solution.
2. Preclear chromatin by adding 80 μL of a 50% slurry of Protein-A/G sepharose beads and incubation at 4°C for 1 h with gentle mixing (*see Note 2*). Centrifuge samples at 300 × *g* for 3 min to pellet beads and transfer the precleared supernatant to a fresh tube.

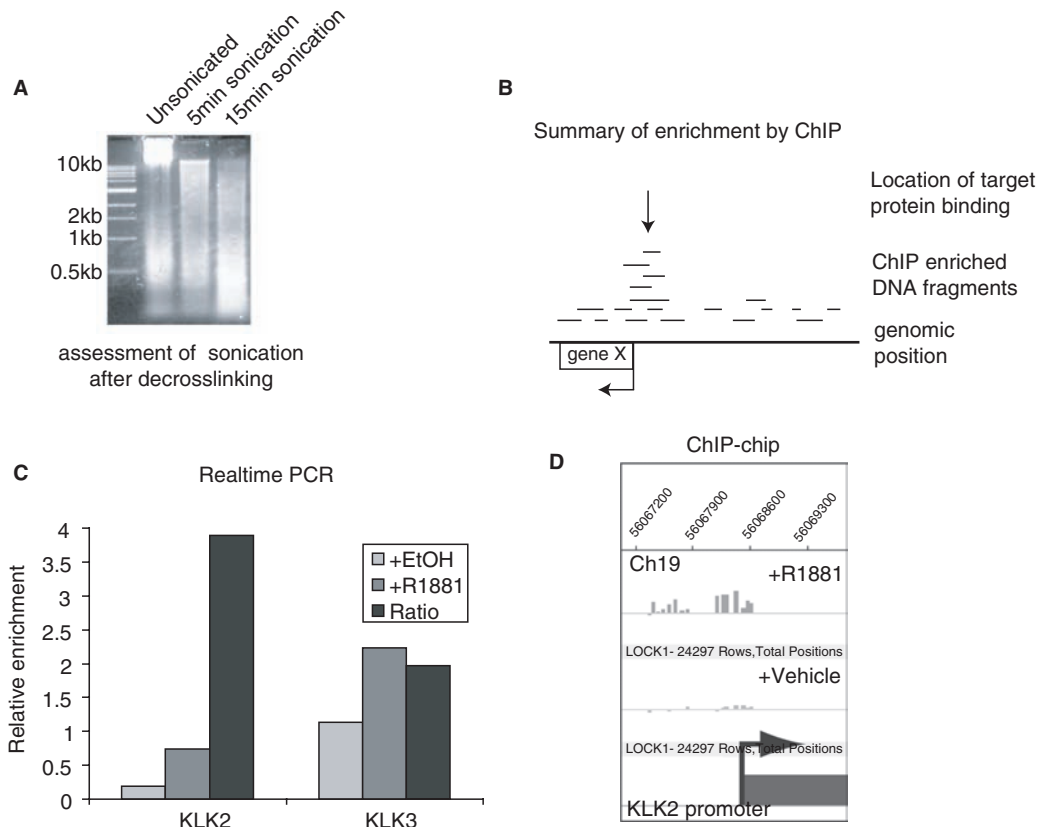


Fig. 2. Summary of read-outs from ChIP experiments. **(A)** Example of gel electrophoresis analysis of chromatin before and after sonication. **(B)** Summary of DNA fragment enrichment by ChIP, showing the large number of low abundance nonspecific DNA fragments and high abundance specific ChIP-enriched DNA fragments. **(C)** Analysis of AR ChIP enrichment by Realtime quantitative PCR for the KLK2 and KLK3 promoters. Values shown are relative to input material and beta-actin control PCR. **(D)** Example of AR ChIP-chip data showing enrichment of the KLK2 promoter region in the androgen (+R1881) vs. control (+Vehicle) treated conditions. Genomic positions are shown above ChIP-chip data “tracks” from androgen (+R1881) and control (+Vehicle) conditions. The level of enrichment is shown by the height of vertical bars. Below the position of the *KLK2* gene is indicated by a *rectangle* and the *arrow* indicates the direction of transcription.

3. Add 5  $\mu\text{g}$  of ChIP antibody (e.g., AR N20, Santa Cruz), 100  $\mu\text{g}/\text{mL}$  BSA, and incubate for 16h at 4°C with gentle mixing.
4. Centrifuge samples at 300  $\times g$  for 3 min to pellet beads, discard supernatant, and repeat this following 5 min washes in each of the following buffers: TSE-I wash buffer, TSE-II wash buffer, wash buffer-III, TE pH 8.
5. Centrifuge samples at 300  $\times g$  for 3 min to pellet beads, discard supernatant. Elute ChIP material by adding 250  $\mu\text{L}$  of ChIP elution buffer and incubating at room temperature for 15 min with vigorous mixing. Centrifuge samples at 300  $\times g$



for 3 min to pellet beads and transfer the supernatant to a fresh tube. Repeat the elution and combine eluates.

### 3.4. DNA Isolation

1. Reverse protein–DNA cross-links by adding NaCl to a final concentration of 200 mM and incubate at 65°C for 5 h.
2. Digest proteins by adding EDTA (10 mM final concentration), Tris-HCl pH 6.7 (20 mM final concentration) and Proteinase K (80 µg/mL final concentration). Incubate at 45°C for 1 h.
3. Recover DNA by adding an equal volume of phenol/chloroform/isoamyl alcohol, vortex vigorously, and centrifuge at 13,000 × *g* for 15 min. Carefully transfer the aqueous phase to a fresh tube, add 20 µg Glycogen, and an equal volume of isopropanol. Vortex vigorously and centrifuge at 13,000 × *g* for 15 min. Discard supernatant and add 1 volume of 70% ethanol per volume of isopropanol used. Centrifuge at 7,000 × *g* for 7.5 min, discard supernatant, and air-dry pellet. Dissolve pellet in 50 µL of UP water.

### 3.5. Analysis of Enrichment

There are several options for the analysis of ChIP-enriched DNA; however, it is important for all of these analysis methods to be aware that although the specifically enriched protein-bound DNA fragments isolated by ChIP will be present in many copies, these fragments will likely represent only a small fraction of the total ChIP DNA. Therefore, the majority of DNA isolated from a ChIP reaction is likely to comprise low abundance nonspecific DNA fragments (i.e., fragments not bound by the protein of interest), purely because these DNA fragments constitute such a large proportion of the genome. Therefore, it is important to take these facts into consideration when designing and analysing the read-outs from ChIP enrichment. ChIP for candidate genomic targets of transcription factor binding can be assessed by Realtime quantitative PCR. Unbiased assessment of ChIP-enriched DNA can be achieved by cloning and sequencing, microarray hybridisation or utilising next generation high throughput sequencing technologies ([Fig. 2](#)).

#### 3.5.1. Realtime PCR

While analysing ChIP enrichment using Realtime PCR, it is necessary to compare the test ChIP with a control ChIP (*see* [Note 4](#)) to assess specific enrichment over background ([Fig. 2C](#)). It is also necessary to compare the candidate genomic region (i.e., the region believed to be bound by the protein of interest) with a control genomic region which is not bound by the protein. The control genomic region allows an assessment of the nonspecific DNA from each ChIP and can be used to normalise between the test and control ChIPs. Finally, to avoid bias caused by differences in PCR efficiency between test and control PCR reactions,

it is advisable to use a serial dilution of input material as a standard curve for each PCR (e.g., 1× to 1/128).

1. Into an optical PCR plate aliquot 1–2 μL of ChIP DNA and standard curve samples in triplicate for each genomic region to be analysed by Realtime PCR (usually a minimum of two PCR reactions, for the candidate region and the control region).
2. Mix 10 pmol of each primer with water and SybrGreen Master mix to a 1× final concentration in a final volume of 10–20 μL.
3. Aliquot PCR mix onto ChIP DNA, seal plates with adhesive covers, mix and centrifuge briefly.
4. Use the PCR conditions suggested for use with the SybrGreen mix used (e.g., hot-start: 50°C 2 min, 95°C 10 min, [95°C 15 s, 60°C 1 min] repeat 40 times). The addition of a dissociation curve at the end of the PCR reaction allows an assessment of the specificity of the PCR.
5. Specific enrichment by ChIP is assessed using the equation:

$$\text{Relative Enrichment} = \frac{\text{ControlEff}^{(\text{control sample Ct} - \text{test sample Ct})}}{\text{TestEff}^{(\text{control sample Ct} - \text{test sample Ct})}}$$

where “ControlEff” is the efficiency of the control PCR and “TestEff” is the efficiency of the test PCR, both calculated using the formula:  $10^{(1/\text{slope of standard curve})}$ . “Control sample Ct” and “test sample Ct” are the cycle thresholds (Ct) at which the PCR reactions for control or test samples becomes exponential.

### 3.5.2. Array Detection

Microarray detection of ChIP DNA has been widely used to allow an unbiased assessment of the regions enriched by ChIP (2, 4, 6–8). This approach allows the identification of novel binding sites for transcription factors, as well as the locations of other chromatin marks without prior knowledge of specific bound genomic regions. The use of tiling microarrays to detect ChIP DNA has been referred to as ChIP-chip, ChIP-on-chip, or genome-wide location analysis (Fig. 2D). ChIP-chip has provided many insights into NHR and transcriptional biology, including redefinition of the preferred *in vivo* binding sequences, identification of cooperative transcription factor complexes and, not least, the lists of direct transcriptional targets, which may represent the key initiating signals of a given transcription factor (2–4, 6–8). However, this technology does have several limitations. The use of microarrays means that these experiments are subject to the same problems that affect all array experiments (e.g., labeling bias, hybridisation effects, scanning artefacts, significant analysis issues). Further, ChIP yields small amounts of enriched DNA (typically in the ng range), meaning that either multiple replicate ChIP reactions must be pooled or that amplification is required

to yield sufficient material for array hybridisation. This may be problematic since amplification may introduce bias into the data if certain genomic fragments are amplified preferentially, resulting in changes in the proportions of DNA fragments in the ChIP samples. Many ChIP-chip studies have utilised the linker mediated PCR (LMP) amplification outlined below, although certain proprietary amplification kits (e.g., Sigma WGA) may introduce less bias during amplification.

A key consideration in ChIP-chip experiments is the array platform, since this will set the genome coverage and resolution of the data. Most arrays used for ChIP-chip, studies are genomic tiling, arrays comprising PCR products or, for most commercial arrays, oligo probes. There are high resolution whole genome tiling arrays available for higher mammals with larger genomes, but these are printed on multiple arrays (e.g., Affy human genome tiling is printed as a 14 array set), which means that if multiple conditions and/or multiple factors are to be compared together with replicates, the numbers of arrays required and the cost can quickly spiral. Because of the difficulties of designing unique probes in repeat regions these “whole-genome” array sets do not offer full coverage of the genome and therefore do not allow a completely unbiased assessment of ChIP enriched regions. The alternatives to whole-genome arrays are to make use of single or double slide promoter arrays or custom arrays for well-annotated genomic regions or candidate regions. Although useful data and biological insights may be generated from these limited coverage arrays, it is certain that binding sites will be missed, especially for the NHR superfamily given data from ER and AR ChIP-chip studies showing that many binding sites reside > 100 kb from the nearest gene (2, 6). It is therefore important to carefully consider the question being addressed when selecting an array platform for ChIP-chip experiments.

1. Blunt ends of 15  $\mu$ L ChIP DNA with T4 DNA polymerase (0.6 U) in 1 $\times$  T4 DNA polymerase reaction buffer supplemented with 45 ng/ $\mu$ L BSA and 90  $\mu$ M dNTP mix. Incubate at 12°C for 20 min. Purify blunted ChIP DNA by adding 0.1 volume of 3 M NaOAc and 10  $\mu$ g glycogen. Mix and then add 1 volume of Phenol/chloroform/isoamyl alcohol (25:24:1), vortex and centrifuge for 15 min at 13,000  $\times g$ . Transfer aqueous phase to a fresh tube and add 2.5 volumes of 100% ethanol, vortex and centrifuge for 15 min at 13,000  $\times g$ . Discard supernatant and wash pellet with 2.5 volumes 70% ethanol. Centrifuge 7.5 min at 13,000  $\times g$ . Discard supernatant, air-dry pellet, and resuspend in 25  $\mu$ L UP water
2. Anneal unidirectional linkers (P1: GCGGTGACCCGGGAGATCTGAATTC, P2: GAATTCAGATC) by mixing 15  $\mu$ mol of each primer in 250 mM Tris-HCl pH 8, heating to 95°C for 5 min then cooling slowly (<1°C/min). Ligate 6.7  $\mu$ L

annealed linkers to 25  $\mu$ L blunt ended ChIP DNA with 5 U T4 DNA ligase in 1 $\times$  T4 DNA ligase buffer for 16 h at 16°C. Precipitate linker-ligated ChIP DNA by adding 0.1 volume 3 M NaOAc and 2.5 volumes 100% ethanol. Vortex and centrifuge for 15 min at 13,000  $\times g$ . Discard supernatant and wash pellet with 2.5 volumes of 70% ethanol. Air dry pellet and resuspend in 25  $\mu$ L UP water.

3. Amplify 5  $\mu$ L linker-ligated-ChIP DNA and 1  $\mu$ L of total input DNA for each planned array in 1 $\times$  PCR buffer supplemented with 2 mM MgCl<sub>2</sub>, 0.5 mM dNTP mix, 1  $\mu$ M linker primer P1 and 5 U Taq polymerase. Using the PCR program: 5°C 2 min, 72°C 5 min, 95°C 2 min, [95°C 30 s, 55°C 30 s, 72°C 1 min] repeat 28–35 times (*see Note 7*) and 72°C 2 min. Visualise amplification by loading 0.1 volume of the PCR reaction on a 1.5% gel. Successful amplification results in a smear from 200–600 bp (i.e., slightly shorter fragments than the smear before amplification).
4. Label amplified ChIP DNA with Cy5-dUTP and amplified total input DNA with Cy3-dUTP using the BioPrime array CGH labeling kit, according to the manufacturers instructions (*see Note 8*). Purify labeled samples using Sephadex G-50 columns and measure Cy dye incorporation using a Nanodrop spectrophotometer.
5. Hybridise Cy5-labeled ChIP DNA together with Cy3-labeled total input DNA. Hybridisation and array washing conditions vary with the type of array used, the array manufacturer, and the hybridisation apparatus used. Refer to the microarray or hybridisation platform manufacturers guidelines for detailed protocols. For example, hybridisation to Nimblegen oligo arrays on a Nimblegen Hybridisation System with NimbleChip Hybridisation Mixers at 42°C for 16–20 h in Nimblegen Hybridisation Buffer. Wash Nimblegen arrays at room temperature with vigorous agitation in Nimblegen Wash Buffer I supplemented with 100  $\mu$ M DTT for 2 min, transfer slides to Nimblegen Wash Buffer II supplemented with 100  $\mu$ M DTT for 1 min and finally Nimblegen Wash Buffer III supplemented with 100  $\mu$ M DTT for 15 s. Dry Nimblegen arrays in a Microarray High-Speed Centrifuge.
6. Scan arrays using a microarray scanner (e.g., GenePix 4,000 scanner) and extract numeric data from scanned images using image analysis software (e.g., NimbleScan). It is possible to perform preliminary data analysis using image analysis software; however, detailed downstream analysis of ChIP-chip data represents a significant bioinformatics challenge. Several analysis methodologies for ChIP-chip data have been suggested (9–12).

### 3.5.3. Direct Sequencing

The combination of sequencing-based approaches with ChIP circumvents many of the problems associated with ChIP-chip (e.g., probe design, probe specificity, genome coverage, and bias introduced by amplification). High throughput approaches to sequencing ChIP-enriched DNA have utilised sequence tag generation methodologies, including SAGE (serial analysis of gene expression) and PET (paired-end diTag)-based methods (13, 14). ChIP-PET has been used successfully to map ER binding sites. Data from ER ChIP-PET had a 50% overlap with data from a whole-genome ER ChIP-chip study, with the suggestion that many of the nonoverlapping sites were associated with repeat sequences not represented on the arrays due to probe design limitations (14). However, it is the combination of ChIP with next generation sequencing technologies that appears to be the most promising technique for mapping genomic locations of transcription factors and other chromatin-associated proteins (15, 16). The Solexa next generation sequencing platform can generate ~20 million sequence reads of ~30 bp, which gives deep coverage of ChIP-enriched DNA fragments. The combination of ChIP with Solexa sequencing has been termed ChIP-seq and unlike the tag generation-based methodologies involves a single step linker ligation and limited cycle PCR amplification, before solid-state sequence cluster generation and “sequencing by synthesis” (15, 16). Comparison of ChIP-seq and ChIP-chip for the STAT1 transcription factor revealed a 64–71% overlap between the binding sites identified by both techniques, although ChIP-seq found 3.8-fold more binding sites in total suggesting that it is the more sensitive method (15).

---

## 4. Notes

1. Crosslinking of protein–DNA interactions is commonly used when studying transcription factor binding. Formaldehyde is most widely used for this purpose and will produce covalent crosslinks between amino or imino groups, which are within 2 Å from each other. It is also possible to use other crosslinking agents such as imidoesters or NHD-esters (e.g., DMP [Dimethyl pimelimidate] or DSG [disuccinimidyl glutarate]) in combination with formaldehyde to increase the efficiency of crosslinking, which may be most applicable to low abundance DNA-binding proteins (17). The use of imidoesters or NHD-esters as crosslinkers also provides an opportunity to alter the resolution from 2–20 Å, depending on the spacer length of the ester used (17). It is possible to perform ChIP without crosslinking (i.e., native ChIP); however, this is only

suitable for proteins that bind stably to DNA and is mainly used in ChIP assays for histones (18).

2. Protein-A/G Sepharose beads should be washed 3–5 times in 2-volumes of PBS or ChIP dilution buffer prior to use, to remove preservatives such as ethanol and to remove any free protein-A/G and small beads that do not pellet efficiently. It is also possible to use magnetic protein-A/G beads (e.g., Dynabeads, Invitrogen), which bind less non-specific DNA, which lowers the overall yield of ChIP DNA but increases specific enrichment.
3. A number of research groups and companies are now offering searchable databases and compendia of validated ChIP grade antibodies. A particularly helpful Website covering a wide range of suppliers and target proteins is <http://www.chipon-chip.org/Antibody/chip.html>.
4. There are many control ChIP experiments that can be used as a reference to assess specific enrichment in the test ChIP. The choice of which control to use will depend on the system under investigation and the question to be addressed. Many studies use an IgG ChIP control to assess nonspecific enrichment caused by protein–DNA complexes binding to beads or IgG. However, this control does not account for any “off-target” binding of the specific antibody used for ChIP. To assess the specific enrichment by a ChIP antibody, it is necessary to compare isogenic cells in which the protein of interest is not bound to DNA or alternatively lacks the target protein completely. In the case of many NHRs, it is possible to compare hormone-deprived cells to cells treated with the specific NHR ligand, which causes activation, nuclear translocation, and DNA binding (e.g., androgen treatment to activate the AR). Where possible the best controls for ChIP may be isogenic cells, which are null for the target protein (e.g., have targeted deletions of the gene encoding the target protein) or alternatively RNAi “knock-down” of the target protein.
5. Cells are grown in culture media supplemented with charcoal dextran stripped serum, which is depleted for growth-factors including ligands for NHR. After 24–72 h in this media, NHR (e.g., AR and ER) activity is diminished. The addition of a single hormone (e.g., androgen/dihydrotestosterone) stimulates a single nuclear hormone receptor (e.g., the AR), which is then recruited to its’ cognate genomic targets and controls the transcription of associated genes. This method is widely used in the study of many NHRs; however, it should be noted that depleting all growth factors has profound effects on cell signalling and synchronises the cells in G1/G0 which may have undesired effects on transcription.



6. It is essential to optimize sonication conditions for each cell type and sonicator, since this step defines the resolution of ChIP. It is advisable to test a range of conditions including length of pulse, number of pulses, and amplitude of sonication. The efficiency of sonication should be assessed by resolving a sample of total chromatin after sonication and decrosslinking on an agarose gel (*see Fig. 2a*).
7. When using LMP to amplify ChIP material fewer rounds of amplification should introduce less bias, therefore it is recommended that a range of PCR cycles (e.g., 28–35 cycles) are tested. The lowest cycle number to yield the required amount of DNA should be used for downstream applications. Although it is possible to perform multiple rounds of LMP on the same sample, it should be noted that this may introduce more bias into the ChIP enriched DNA.
8. Several methods can be employed to label ChIP material for hybridisation on microarrays. These include direct incorporation as described above (e.g., Bioprime kit), indirect labelling by aa-dUTP incorporation during LMP amplification, and subsequent coupling with monoreactive ester Cy dyes or finally by using Cy dye labeled random 7/9mer oligonucleotide primers.

---

## Acknowledgments

C.E.M. is a postdoctoral researcher funded by a Cancer Research UK Programme Grant and I.G.M is a CRUK core-funded Associate Scientist.

## References

1. Reid, G. et al. Cyclic, proteasome-mediated turnover of unliganded and liganded ERalpha on responsive promoters is an integral feature of estrogen signaling. *Mol Cell* 11, 695–707 (2003).
2. Carroll, J.S. et al. Genome-wide analysis of estrogen receptor binding sites. *Nat Genet* 38, 1289–97 (2006).
3. Laganier, J. et al. From the cover: Location analysis of estrogen receptor alpha target promoters reveals that FOXA1 defines a domain of the estrogen response. *Proc Natl Acad Sci USA* 102, 11651–6 (2005).
4. Massie, C.E. et al. New androgen receptor genomic targets show an interaction with the ETS1 transcription factor. *EMBO Rep* 8, 871–8 (2007).
5. So, A.Y., Chaivorapol, C., Bolton, E.C., Li, H. & Yamamoto, K.R. Determinants of cell- and gene-specific transcriptional regulation by the glucocorticoid receptor. *PLoS Genet* 3, e94 (2007).
6. Wang, Q. et al. A hierarchical network of transcription factors governs androgen receptor-dependent prostate cancer growth. *Mol Cell* 27, 380–92 (2007).
7. Bolton, E.C. et al. Cell- and gene-specific regulation of primary target genes by the androgen receptor. *Genes Dev* 21, 2005–17 (2007).



8. Takayama, K. et al. Identification of novel androgen response genes in prostate cancer cells by coupling chromatin immunoprecipitation and genomic microarray analysis. *Oncogene* 26, 4453–63 (2007).
9. Ji, X., Li, W., Song, J., Wei, L. & Liu, X.S. CEAS: cis-regulatory element annotation system. *Nucleic Acids Res* 34, W551–4 (2006).
10. Peng, S., Alekseyenko, A.A., Larschan, E., Kuroda, M.I. & Park, P.J. Normalization and experimental design for ChIP-chip data. *BMC Bioinformatics* 8, 219 (2007).
11. Scacheri, P.C., Crawford, G.E. & Davis, S. Statistics for ChIP-chip and DNase hypersensitivity experiments on NimbleGen arrays. *Methods Enzymol* 411, 270–82 (2006).
12. Toedling, J., Sklyar, O. & Huber, W. Ringo—an R/Bioconductor package for analyzing ChIP-chip readouts. *BMC Bioinformatics* 8, 221 (2007).
13. Roh, T.Y., Ngau, W.C., Cui, K., Landsman, D. & Zhao, K. High-resolution genome-wide mapping of histone modifications. *Nat Biotechnol* 22, 1013–6 (2004).
14. Lin, C.Y. et al. Whole-genome cartography of estrogen receptor alpha binding sites. *PLoS Genet* 3, e87 (2007).
15. Robertson, G. et al. Genome-wide profiles of STAT1 DNA association using chromatin immunoprecipitation and massively parallel sequencing. *Nat Methods* 4, 651–7 (2007).
16. Barski, A. et al. High-resolution profiling of histone methylations in the human genome. *Cell* 129, 823–37 (2007).
17. Nowak, D.E., Tian, B. & Brasier, A.R. Two-step cross-linking method for identification of NF-kappaB gene network by chromatin immunoprecipitation. *Biotechniques* 39, 715–25 (2005).
18. West, A.G., Huang, S., Gaszner, M., Litt, M.D. & Felsenfeld, G. Recruitment of histone modifications by USF proteins at a vertebrate barrier element. *Mol Cell* 16, 453–63 (2004).

# Chapter 8

## Yeast-Based Reporter Assays for the Functional Characterization of Cochaperone Interactions with Steroid Hormone Receptors

Heather A. Balsiger and Marc B. Cox

### Abstract

Steroid hormone receptor-mediated reporter assays in the budding yeast *Saccharomyces cerevisiae* have been an invaluable tool for the identification and functional characterization of steroid hormone receptor-associated chaperones and cochaperones. This chapter describes a hormone-inducible androgen receptor-mediated  $\beta$ -galactosidase reporter assay in yeast. In addition, the immunophilin FKBP52 is used as a specific example of a receptor-associated cochaperone that acts as a positive regulator of receptor function. With the right combination of receptor and cochaperone expression plasmids, reporter plasmid, and ligand, the assay protocol described here could be used to functionally characterize a wide variety of nuclear receptor-cochaperone interactions. In addition to the functional characterization of receptor regulatory proteins, a modified version of this assay is currently being used to screen compound libraries for selective FKBP52 inhibitors that represent attractive therapeutic candidates for the treatment of steroid hormone receptor-associated diseases.

**Key words:** Yeast, Reporter,  $\beta$ -galactosidase, Cochaperone, FKBP52, Androgen receptor, Steroid hormone receptor, Hsp90.

---

### 1. Introduction

The steroid hormone receptors serve as model substrates for heat shock protein 90 (Hsp90) largely because there is a wealth of receptor functional assays available, including coimmunoprecipitations to assess Hsp90 binding, *in vitro* receptor-Hsp90 complex assembly assays, hormone-binding assays, and receptor-mediated reporter assays in both yeast and mammalian cells. Apart from

simply assessing receptor function, these assays can also serve as the basis for identifying and characterizing steroid hormone receptor modulators. The yeast-based assays have provided much of the evidence regarding the importance of chaperones and cochaperones in steroid hormone receptor signaling pathways. Although *Saccharomyces cerevisiae* lacks steroid hormone receptors, most of the chaperone components known to function in steroid hormone receptor complexes are highly conserved in yeast (1). Thus, vertebrate receptors exogenously expressed in yeast can fold to a hormone-binding conformation and, in the presence of hormone, activate a hormone-inducible reporter gene (2). This, combined with the fact that yeast is a genetically tractable organism, makes yeast genetics a highly attractive model system for the identification and characterization of steroid hormone receptor modulators. In fact, some of the first evidence of a role for Hsp90 (3–6), Hsp40 (7, 8), Hsp organizing protein (Hop) (9), and the p23 cochaperone (10, 11) in steroid hormone receptor signaling pathways was obtained in yeast model systems.

Although yeast genetics represents a powerful tool for the identification and characterization of steroid hormone receptor modulators, the yeast model system must be viewed as an exploratory system. Any data obtained from the yeast assays should lead to the development of hypothesis and the design of additional experiments in higher vertebrate model systems to establish physiological relevance. However, we are confident that observations in yeast are physiologically relevant as a large majority of the data gleaned from yeast has ultimately been corroborated in higher vertebrate model systems. For example, David Smith and colleagues demonstrated that the large FK506-binding protein 52 (FKBP52), but not the closely related protein FKBP51, potentiates receptor-mediated expression of a reporter gene in yeast (12). These results have not only been corroborated in similar mammalian cell assays, but also in mouse gene knockout models (13, 14). Thus, we have a high level of confidence in the data that we glean from the yeast-based assays. This chapter specifically describes the yeast-based androgen receptor (AR)-mediated  $\beta$ -galactosidase reporter assay used to show that FKBP52 is a positive regulator of AR function, which serves as the basis for comparing FKBP point mutants, truncation mutants, and chimeric proteins. The assay described here only compares the effects of wild type FKBP51 and FKBP52 on receptor function. However, by simply including rationally designed FKBP and/or AR mutants, this assay can be used to characterize functional domains important for FKBP52 potentiation. In addition, by simply changing the receptor, cochaperone expression plasmids, reporter plasmid, or ligand, this assay can be used to functionally characterize any potential nuclear receptor regulatory protein.

This assay has been used extensively to identify and characterize regions of functional importance on FKBP52 (12, 15, 16). We are currently using this assay in conjunction with AR random mutagenesis to identify the FKBP52-binding site on AR. In addition, a variation of this assay using the *HIS3* selectable marker as an AR-mediated reporter was used in conjunction with random mutagenesis to show that a proline-rich loop overhanging the PPIase catalytic pocket in the FKBP52 FK1 domain is not only critical for FKBP52 potentiation of receptor function, but also contributes to the functional divergence between FKBP51 and FKBP52 (17). Finally, we are currently using a variation of this assay adapted to a 96-well plate format to screen compound libraries for selective FKBP52 inhibitors.

---

## 2. Materials

### 2.1. Yeast Cell Culture

1. Difco Yeast Nitrogen Base without amino acids (Beckton Dickinson; Sparks, MD).
2. Anhydrous Dextrose (Fisher Scientific).
3. Synthetic Complete amino acid dropout mix minus histidine, leucine, tryptophan, and uracil (MP Biomedicals, Solon, OH).
4. Amino acids omitted from dropout mix. L-Histidine, 98% (Acros Organics; Geel, Belgium) stock is made by dissolving in distilled water at 1.0 g/100 mL, stored in the refrigerator, and added at 2 mL for each liter of medium. L-Tryptophan, 99% (Acros Organics; Geel, Belgium) stock is made by dissolving in distilled water at 1.0 g/100 mL, stored in the refrigerator, and added at 2 mL for each liter of medium. L-Leucine (Fisher Bioreagents) stock is made by dissolving in distilled water at 1 g/100 mL, stored in the refrigerator, and added at 10 mL for each liter of medium. Uracil, greater than 99% (Acros Organics; Geel, Belgium) stock is made by dissolving in distilled water at 0.2 g/100 mL, stored at room temperature, and added at 10 mL for each liter of medium. All stock solutions are filter sterilized and may be stored for extended periods.
5. Agar (Fisher Scientific) added at 2% to medium, autoclaved on liquid cycle, and poured into Petri dishes for plate preparation.
6. Polystyrene Petri dishes, sterile and stackable 100 × 15 mm (VWR).

7. For one liter of synthetic complete (SC) dropout media combine 6.7 g Yeast Nitrogen Base without amino acids, 20 g dextrose, 2 g dropout mix, the appropriate volume of additional amino acids (of the five omitted) and distilled water up to 250 mL (*see Note 1*). Allow to mix thoroughly. Filter sterilize this portion and set aside. Autoclave 750 mL of distilled water (for liquid medium) or 20 g agar plus distilled water up to 750 mL (for plate medium preparation) (*see Note 2*). Combine these two portions and store liquid medium at room temperature. For plates, combine the two portions and pour into Petri dishes while still liquid. Allow plates to cool and harden, and then store at 4°C.

### 2.2. Yeast Transformation

1. Salmon sperm DNA (10 mg/mL) (Invitrogen; Carlsbad, CA) stored at -20°C and denatured for 5 min at 95°C just before use.
2. TE/LiAc (1×): 10 mM Tris-HCl (pH 8.0), 1 mM EDTA, and 0.1 M lithium acetate made up in distilled water. Sterilize by autoclaving on liquid cycle.
3. 50% polyethylene glycol (PEG): Prepare 50% (w/v) PEG (Sigma Aldrich; St. Louis, MO; ave. mol wt 3,350) in distilled water and autoclave on liquid cycle (*see Note 3*).
4. LiAc (10×): Prepare in distilled water using 1 M lithium acetate (pH 7.5). Sterilize by autoclaving on liquid cycle.
5. TE (10×): 100 mM Tris (pH 7.5) and 10 mM EDTA. Sterilize by autoclaving on liquid cycle.
6. TE/LiAc/PEG solution, prepared using 320 μL of 50% PEG and 40 μL of both 10× LiAc and 10× TE per transformation.

### 2.3. Yeast AR-Mediated $\beta$ -Galactosidase Reporter Assay

1. The AR-mediated  $\beta$ -galactosidase reporter plasmid pUC $\Delta$ s-26x is a high-copy-number *URA3* marked *lacZ* reporter plasmid containing three hormone response elements (a kind gift from Brian Freeman, University of Illinois) (*see Note 4*).
2. Yeast expression vectors for human AR (p425GPD-hAR containing a *LEU2* marker), human FKBP51 (p424GPD-h51 containing a *TRP1* marker), and human FKBP52 (p424GPD-h52 containing a *TRP1* marker) were constructed previously and are available from our laboratory (*see Note 5*).
3. The haploid parent yeast strain w303 (MATa *leu2-112 ura3-1 trp1-1 his3-11,15 ade2-1 can1-100 GAL SUC2*) (*see Note 6*).
4. Dihydrotestosterone (DHT) stored as a 10 mM stock solution in ethanol at -20°C (*see Note 7*).

5. Tropix Gal Screen (Applied Biosystems; Bedford, MA). Store buffer and substrate at 4°C (Buffer B is used with yeast cells).
6. Disposable plastic cuvettes (Fisher Scientific).
7. 96-well white polystyrene flat bottom opaque plates (Whatman).
8. New Brunswick I-24 incubated orbital shaking water bath.
9. ThermoSpectronic Genesys 20 visible light spectrophotometer.
10. Luminoskan Ascent microplate luminometer (Labsystems).

#### **2.4. Yeast Protein Extract Preparation and Western Immunoblots**

1. 0.5 mm glass beads (Biospec Products, Bartlesville, OK).
2. Yeast lysis buffer: Composed of 20 mM Tris-HCl, pH 7.5, 100 mM NaCl, 5% glycerol, 2 mM  $\beta$ -mercaptoethanol, and protease inhibitors (Protease Inhibitor Cocktail Tablets; Roche Diagnostics; Penzberg, Germany).
3. Standard vortex mixer.
4. Coomassie Plus Protein Assay Reagent (Pierce; Rockford, IL). Store at 4°C.
5. AR antibody (AB561, Millipore) (*see Note 8*).
6. L3 antibody, a kind gift from Jonathan Warner, Albert Einstein College of Medicine (*see Note 9*).
7. HI52D and HI51B mouse monoclonal antibodies: both developed in the laboratory of Dr. David Smith and available from our laboratory (*see Note 10*).
8. Goat anti-mouse IgG(H + L)-AP, human adsorbed secondary antibody (Southern Biotech).
9. Standard equipment and reagents for polyacrylamide gel electrophoresis (SDS-PAGE) and Western blotting.

---

### **3. Methods**

Traditional receptor-mediated reporter assays in yeast were performed 12–24 h after hormone addition, used colorimetric substrates, and required high, nonphysiological concentrations of hormone. With the advent of new chemiluminescent substrates, a hormone-induced signal can be detected within 30 min using high picomolar to low nanomolar concentrations of hormone. The assay described in this chapter is based on methods described by Riggs et al. (12) and utilizes a chemiluminescent  $\beta$ -galactosidase substrate to measure AR-mediated reporter gene expression over a 2-h period after hormone addition. As mentioned above,

FKBP52, but not the closely related protein FKBP51, potentiates receptor-mediated reporter gene expression up to 20-fold in some cases using this assay. Yeast lack homologues of the large FK506-binding protein immunophilins, so there is no need to delete an endogenous gene (*see Note 11*). Thus, the immunophilins are expressed in the yeast in the presence of the receptor and reporter plasmids, and hormone-induced  $\beta$ -galactosidase expression serves as a measure of receptor function. Prior to assaying a potential receptor regulatory protein, it is important to perform a dose-response curve to determine the optimum hormone concentration to use in the assays. The specific assay described in this chapter measures AR function at a single hormone concentration, which was chosen based on preliminary dose-response curves. The hormone concentration used (5 nM) is at the bottom of the AR dose-response curve in the absence of FKBP52 and was chosen because the FKBP52-mediated enhancement of receptor function is maximized at this dose.

### **3.1. Transformation of Yeast Cells in Preparation for Reporter Assays**

1. Streak the parent strain (W303a) onto an agar plate containing synthetic complete (SC) medium and allow to grow for at least 2 days at 30°C. After several days of growth, this plate can be stored at 4°C for up to 1 month to be used as a stock. Glycerol freezer stocks can also be made if desired by placing the cells in 15% glycerol and storing at -80°C indefinitely.
2. The yeast transformation method described here is based on methods described previously (18). Inoculate W303a into 5 mL of SC medium in a 50 mL conical tube and incubate overnight at 30°C. Unless otherwise stated all liquid yeast cultures are grown in a shaking water bath at 30°C.
3. Prior to harvesting the cells place the salmon sperm DNA at 95–100°C to denature, and prepare the appropriate volume of PEG/TE/LiAc solution as detailed in the **Subheading 2.2**.
4. The next morning harvest the saturated yeast culture at 1000  $\times g$  for 5 min, resuspend the cells in 1 mL 1 $\times$  TE/LiAc, and transfer to a 1.5 mL microcentrifuge tube (*see Note 12*).
5. Harvest the cell suspension in a microcentrifuge for 10s at maximum speed and resuspend in 1 mL fresh 1 $\times$  TE/LiAc.
6. For transformation of the reporter plasmid mix 50  $\mu$ L of cell suspension, 5  $\mu$ L denatured salmon sperm DNA (50  $\mu$ g), 3  $\mu$ L of the pUCAs-26x miniprep plasmid, and 300  $\mu$ L PEG/TE/LiAc in a 1.5 mL microcentrifuge tube. Mix gently and do not vortex.
7. Incubate at 30°C for 30 min followed directly by 12 min incubation in a water bath at 42°C.
8. Harvest the cells in a microcentrifuge for 12s at maximum speed and resuspend in 100  $\mu$ L sterile deionized, distilled water (ddH<sub>2</sub>O).



9. Spread the entire 100  $\mu$ L cell suspension on an agar plate containing SC medium lacking uracil (SC-U) and incubate at 30°C for 2–3 days until colonies appear.
10. Pick a single colony and inoculate into 5 mL of SC-U medium and incubate overnight at 30°C.
11. Repeat steps 3–9 for each plasmid to be transformed (*see Note 13*). After transformation of the AR expression vector (p425GPD-hAR), the transformants will be grown in SC medium lacking leucine and uracil (SC-LU). Finally after transformation of the expression vectors for FKBP51 and FKBP52 (p424GPD-h51 or p424GPD-h52), the transformants will be grown in SC medium lacking leucine, uracil, and tryptophan (SC-LUW). Be sure to also perform a transformation with empty vector (p424GPD) to be used as a control in the reporter assays.
12. The final result of these transformations will be three separate strains all containing the reporter plasmid and AR expression vector, but differing in the particular immunophilin expression vector that they contain (empty vector, FKBP51, or FKBP52).

### **3.2. AR-Mediated $\beta$ -Galactosidase Reporter Assays**

1. Using a sterile toothpick or swab pick three separate colonies from each transformation plate and inoculate each into 5 mL SC-LUW in a 50 mL conical tube and incubate overnight at 30°C with shaking. These colonies represent three independent isolates each of cells containing empty vector, FKBP51, or FKBP52 (*see Note 14*).
2. The next morning determine the optical density at 600 nm ( $OD_{600}$ ) of each culture and dilute each back to an  $OD_{600}$  of 0.08 in 5 mL of fresh SC-LUW in a new 50 mL conical tube. Place the diluted cultures in the water bath at 30°C and incubate with shaking. The  $OD_{600}$  of the cultures can be monitored during this time. Typically after 2 h the cultures have exited lag phase and begun to grow.
3. Once the cultures reach an  $OD_{600}$  of approximately 0.1 add 5  $\mu$ L of 5  $\mu$ M DHT so that the final DHT concentration in the 5 mL cultures is 5 nM (*see Note 15*). Also record the  $OD_{600}$  of each culture as this will be taken as the OD reading at time 0.
4. Allow the cultures to grow with shaking for another 80 min before taking any more readings. Having the spectrophotometer setup directly adjacent to the shaking water bath is best as you will need to take five  $OD_{600}$  measurements including the 0 time point and five 100  $\mu$ L samples for the luminometer measurements over a 2 h period. This can become quite cumbersome when assaying many samples (*see Note 16*).

5. Several minutes before taking any more measurements prepare the Tropix Gal Screen reagent and place on ice. This is prepared by diluting the substrate 1:25 in Buffer B. You will need 100  $\mu$ L per sample taken. In this assay, five 100  $\mu$ L samples will be taken from each of nine cultures. Thus, 4.5 mL of Tropix Gal Screen reagent will need to be prepared. Be sure to make a little extra. Also, it is necessary to have an opaque 96-well plate ready for the assay.
6. Starting at 80 min after hormone addition four more OD<sub>600</sub> measurements will need to be taken and five 100  $\mu$ L samples transferred to the 96-well plate for each of the nine cultures over the assay time period. The times at which the OD<sub>600</sub> is measured and samples taken can be spaced out over the 2 h period. We have standardized this process and always take the OD<sub>600</sub> measures at 0, 80, 110, 125, and 150 min after hormone addition. Sterility is not an issue as the assay time is short so the cultures that are poured into the cuvette can be poured back into the 50 mL conical tube after each reading.
7. Transfer a 100  $\mu$ L sample of each culture to one well of a 96-well plate at 85, 115, 130, and 155 min after hormone addition and add 100  $\mu$ L Tropix Gal Screen reagent. Mix by pipetting up and down.
8. Once all samples have been taken cover the wells with tape or film to prevent evaporation and incubate the plate at room temperature for 2 h.
9. After the 2 h incubation read the plate in the microplate luminometer using a gain of 1.0 and a voltage between 750 and 1,100. The voltage used depends upon the strength of the signal. We typically take a first reading at 900 V, which is sufficient in most cases. If the signal is weak the voltage can then be increased to increase the sensitivity.

### **3.3. Data Analysis**

1. Although we use GraphPad Prism software, any graphing and data analysis software package will be sufficient. The first step is to plot the yeast growth curves to determine the OD<sub>600</sub> of the cultures at the times the 100  $\mu$ L samples were taken for the luminometer readings. On GraphPad Prism plot the OD<sub>600</sub> vs. time in minutes on an X/Y plot for each assay culture. On the data table in the X values column also include the times at which the samples for the luminometer were taken without entering Y values. Using the analysis option Log transform the Y values ( $Y = \text{Log}Y$ ) and then perform a linear regression. When log transforming the Y values check the box telling the software to interpolate unknowns from standard curve. This will give you the OD<sub>600</sub> values (Y values) at the times the samples were taken for the luminometer. Finally, transform the Y values back to standard values ( $Y = 10^Y$ ). In the assay

described here, there are a total of three lines for each variable (vector alone, FKBP51, or FKBP52). An example is shown in Fig. 1A.

- Using the  $OD_{600}$  values determined from linear extrapolation on the yeast growth curves in step 1, plot the values obtained on the luminometer (relative light units or RLU) vs.  $OD_{600}$  on an X/Y plot for each assay culture and perform a linear regression. Note

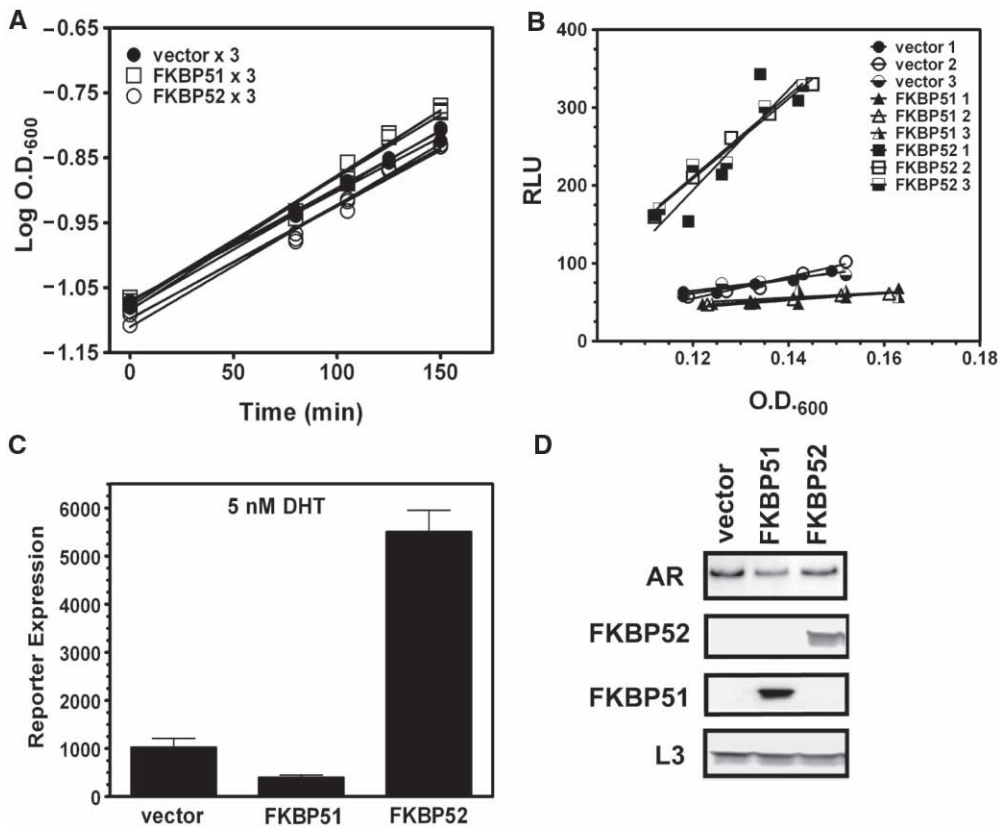


Fig. 1. An AR-mediated  $\beta$ -galactosidase reporter assay to assess FKBP52 potentiation of receptor function. The yeast AR reporter strain was cotransformed with an empty plasmid vector or plasmid expressing FKBP51 or FKBP52 and assayed for AR-mediated  $\beta$ -galactosidase reporter gene expression over a 2 h period. (A) The yeast growth curves were plotted and linear extrapolation was used to determine the  $OD_{600}$  values corresponding to the times at which samples were taken for measurements on the luminometer. (B) The  $OD_{600}$  values that were extrapolated from the graph in (A) were plotted against the luminometer readings (RLU), a linear regression was performed, and the slope of each line was taken to represent AR-mediated reporter expression normalized to differences in yeast growth. (C) The slope values for each sample determined in (B) were averaged and plotted on a column graph. (D) To control for general effects on transcription, translation, and/or protein stability Western immunoblots of representative yeast isolates containing vector alone, FKBP51, or FKBP52 expression plasmids were probed with antibodies directed against AR, FKBP52, FKBP51, or the yeast ribosomal protein L3 as a loading control. Note the enhancement of AR function in the presence of FKBP52, which serves as the basis for comparing FKBP52 and/or AR point mutants, truncation mutants, and chimeric proteins. The results presented are meant to serve as a specific example and do not represent novel findings. Similar results demonstrating a positive role for FKBP52 in AR signaling were reported previously (13).

the slope value for each line as this is the value that is taken to represent receptor-mediated reporter expression and is normalized for differences in growth between the yeast cultures. An example is shown in [Fig. 1B](#).

3. For the final data figure, average the slopes of the three replicates for the vector alone, FKBP51 and FKBP52 containing strains and determine the standard deviation. Plot this data on a standard column graph as demonstrated in [Fig. 1C](#). Note the potentiation of receptor function in the presence of FKBP52.

#### **3.4. Yeast Protein Extract Preparation and Western Immunoblots**

1. Using a sterile toothpick or swab inoculate each isolate into 5 mL SC-LUW in a 50 mL conical tube and incubate overnight at 30°C with shaking (*see Note 17*).
2. The next morning measure the OD<sub>600</sub> of each culture. Dilute each culture back to an OD<sub>600</sub> of 0.5 in 10 mL of fresh SC-LUW and incubate at 30°C with shaking until the culture reaches an OD<sub>600</sub> of 0.8–1.0. It is important to ensure that the cultures are in exponential phase growth at the time of lysate preparation.
3. Before harvesting the cells prepare the yeast lysis buffer containing protease inhibitors as described in the Materials section and place on ice (*see Note 18*). In addition, for each culture prepare a 1.5 mL microcentrifuge tube and fill each tube to the 500 µL mark with 0.5 mm glass beads. A second empty microcentrifuge tube will also be needed for lysate collection at a later step.
4. Harvest the cells at 1,000 × *g* for 2 min, resuspend in 500 µL lysis buffer, transfer to the microcentrifuge tube with glass beads, and place on ice. At this point, the samples should not be removed from the ice for periods longer than 1 min.
5. Vigorously vortex each sample five to seven times for 1 min. Place samples on ice between vortexing (*see Note 19*).
6. Use a syringe needle to punch a hole in the bottom of each tube and insert them into the empty microcentrifuge tubes. Finally, punch a hole in the lid to allow the lysates to flow into the empty tubes.
7. Spin the assemblies very briefly at 900–1,000 × *g* in a microcentrifuge to separate the lysate from the glass beads. Depending on the microcentrifuge, the internal lid may need to be removed to accommodate the assemblies. **Be cautious and do not override any safety features.**
8. Place the lysates back on ice. The glass beads can be saved and acid washed for reuse. Soak beads with 5.8 M HCl, allow to incubate at room temperature for 1 h, then rinse thoroughly with distilled water.

9. Clarify the lysates at maximum speed in a microcentrifuge for 20 min.
10. Use the Coomassie Plus Protein Assay Reagent to determine the total protein concentration of each sample according to the manufacturer's instructions.
11. Perform denaturing polyacrylamide gel electrophoresis (SDS-PAGE) and Western blotting according to standard procedures. An example is shown in [Fig. 1D](#). Loading 20 µg of total cellular protein per lane should be sufficient for the immunophilin and the L3 loading control Westerns. Additionally, using the primary and secondary antibodies at a 1:5,000 dilution in blocking buffer will be sufficient. Western immunoblotting for the steroid hormone receptors in yeast is more difficult. It is best if the protein is loaded onto a gel immediately as opposed to storing the lysates in the freezer and running the gel later as we have found that the receptors can precipitate after the freeze-thaw cycle. If possible, load 30–50 µg of total cellular protein per lane for the AR Western blot. Finally, use the AR antibody at 1 µg/mL in blocking buffer.

---

#### 4. Notes

1. The additional amino acids and/or nucleosides added will depend upon the genotype of the strain used and the plasmids present in the strain. For example, if the strain is carrying a plasmid with a *URA3* selectable marker, it will be grown in media lacking uracil to select for maintenance of the plasmid. The plasmid will be lost from the cells over time if the cells are grown in media containing uracil.
2. We prefer to filter sterilize the media and autoclave the water and agar separately to prevent caramelizing of the glucose. Additionally, autoclaving the agar in the presence of the glucose and yeast nitrogen base can result in “mushy” plates using some autoclaves.
3. The PEG will not go into solution completely until it is autoclaved.
4. Various reporter plasmids are available through many different laboratories but we prefer pUCΔs-26x as it displays very little leaky expression and provides for a high level of hormone-dependent expression. In addition, this reporter can be activated by AR, GR, PR, and MR. Thus, by simply changing the receptor expression plasmid and the hormone, this reporter plasmid can serve as the basis for assaying the function of four different steroid hormone receptors.

5. We use a set of yeast expression vectors (19) that allows for flexibility in regards to the level of expression (different promoters) and selectable markers (*HIS3*, *LEU2*, *TRP1*, or *URA3*). In addition, each plasmid is available as either a low-copy or high-copy-number plasmid. The entire set of plasmids is available from the American Type Culture Collection (ATCC). In general, we typically use the high-copy-number plasmids containing the glyceraldehyde-3-phosphate dehydrogenase (GPD) promoter, which provides for the highest level of expression. Yeast expression vectors for the steroid hormone receptors, immunophilins, and all of the known steroid hormone receptor-associated cochaperones are widely available either in our laboratory or in other laboratories.
6. Although we typically use the w303 genetic background, many other strains will also be sufficient. If you do not have access to w303, we recommend purchasing one of the deletion strains used in the *Saccharomyces* Genome Deletion Project (e.g. BY4742; [http://www-sequence.stanford.edu/group/yeast\\_deletion\\_project/deletions3.html](http://www-sequence.stanford.edu/group/yeast_deletion_project/deletions3.html)). These strains are available from Invitrogen (Carlsbad, CA) or ATCC. We also recommend that you purchase the *pdr5* deletion strain as Pdr5p is a membrane bound transporter that can transport some hormones out of the cell (e.g., dexamethasone). By starting with the *pdr5* deletion strain you can avoid these problems later when expanding to different receptors and ligands. Pdr5p is not a problem for testosterone and dihydrotestosterone.
7. The purchase of testosterone and derivatives in the United States requires a license from the U.S. Drug Enforcement Administration. Check with the Environmental Health and Safety Office at your institution for application procedures.
8. All of the commercial antibodies directed against AR that we have tried work well in yeast Westerns.
9. Although we typically use an antibody directed against a yeast ribosomal protein (L3) as a loading control, commercially available antibodies directed against yeast  $\beta$ -actin are also sufficient.
10. A series of monoclonal FKBP51 and FKBP52 antibodies that recognize a range of epitopes across the entire length of the proteins were developed by the Smith lab (HI51A-D and HI52A-D) (20). All of these antibodies work well in Westerns and many are also good for coimmunoprecipitation. In addition to the FKBP51 and FKBP52 antibodies, our laboratory has antibodies directed against other known receptor-associated cochaperones including HSP interacting protein (Hip) and Hsp organizing protein (Hop).

11. In many cases, a traditional deletion/complementation experiment may be needed in which the endogenous yeast gene of a potential receptor regulatory protein is deleted and assessed for effects on the receptor. If effects on the receptor are evident, it is then important to replace the gene exogenously on a plasmid to demonstrate the specificity of the effect. If this type of experiment is desired, the yeast gene deletion strains can be purchased from Invitrogen (Carlsbad, CA) or ATCC. A set of plasmids is also available from the European *Saccharomyces cerevisiae* Archive for Functional Analysis (EUROSCARF, Frankfurt, Germany, <http://www.uni-frankfurt.de/fb15/mikro/euroscarf/>) that can be used to delete endogenous genes in yeast (21). Information regarding the viability of a particular yeast gene deletion strain can be found on the *Saccharomyces* Genome Database (<http://www.yeastgenome.org/>).
12. In most cases transforming a saturated culture with 3  $\mu$ L of a typical miniprep plasmid will yield more than enough transformants. If increased transformation efficiency is desired, the yeast culture should be diluted to an OD<sub>600</sub> of 0.5 and allowed to grow at 30°C for 2–4 h to ensure that the cells are in exponential phase growth before harvesting. In this instance we typically harvest the cells at an OD<sub>600</sub> of 0.8–0.9.
13. Multiple plasmids can be transformed at the same time but the efficiency of transformation is poor. Also, it is best if the final transformants used in the assays are derived from a clonal population of yeast containing the reporter plasmid and AR expression vector. Thus, we prefer to do the plasmid transformations sequentially. It is also important to point out that only three plasmids can be maintained stably in yeast at any given time. If expression of more than three constructs is needed consider integrating one or more of the constructs into the yeast genome (22) and/or using yeast expression vectors with bidirectional promoters (23).
14. At this stage it is not a good idea to perform three replicate assays on a single isolate. First, both the low and high-copy-number plasmids can be present at different copy numbers between isolates resulting in different levels of reporter expression. Transforming a clonal population of cells containing the receptor and reporter as discussed in Note 13 will help minimize this problem. Second, intercellular genetic differences can result in variable effects. It is also not good practice to assay a range of isolates and select the isolate that produces the desired effect as this introduces bias. Selecting a single isolate for continuous use is acceptable only when the observed effects are highly consistent across many isolates.



15. Yeast can tolerate up to 1% ethanol without any toxic effects. Thus, always set up the hormone stock concentrations so that ethanol is added at a final volume of no more than 1%. In instances where dimethylsulfoxide (DMSO) is used as a solvent the yeast can also tolerate up to 1% DMSO.
16. Because of the nature of this assay, no more than 20 samples can typically be assayed at one time. We take multiple readings and use the slope as discussed in the Data Analysis section as this makes the assay more sensitive. However, when assaying many samples or doing large dose-response curves, a single-time-point assay at 2 h after hormone addition may be more practical. In this instance, one would simply divide the luminometer readings by the  $OD_{600}$  of the cultures at 2 h to normalize for differences in cell growth. When modified to a 96-well plate format, a single-time-point assay at 2 h after hormone addition is also performed. In this instance, the yeast cultures are grown in tubes until they reach log phase growth and are then aliquoted into the 96-well plate followed by hormone treatment. When using a single strain for screening compound libraries and/or environmental samples, normalizing to differences in cell growth is not necessary. When comparing the multiple-time-point vs. the single-time-point assays, any differences observed between samples are correlative, but the overall level of reporter expression is smaller in the single-time-point assay.
17. In yeast reporter assays, it is important to show that any enhancements or reductions in reporter expression observed are not due to general effects on transcription, translation, and/or protein stability. Western immunoblots must be performed to control for this possibility. Using one representative isolate for the immunoblots will be sufficient if the data are consistent across many isolates. However, if the data are variable, it is good practice to include all isolates in the immunoblots. The example shown here includes one representative isolate for each variable.
18. It is important to use protease inhibitors in all yeast lysates as yeast cells are notorious for having high protease activity.
19. You can use a bead beater if available. However, vortexing is more than sufficient to produce a yeast lysate.

---

## Acknowledgments

The authors thank Dan Riggs for developing the yeast assays described. The authors are also grateful to David Smith for his

continued support and encouragement and to Manuel Miranda-Arango for critically reading the manuscript. Work in the authors' laboratory is supported in part by the Grant Number 5G12RR008124 (to the Border Biomedical Research Center (BBRC)/University of Texas at El Paso) from the National Center for Research Resources (NCR), a component of the National Institutes of Health (NIH). The contents of this chapter are solely the responsibility of the authors and do not necessarily represent the official views of NCR or NIH. We thank the Biomolecule Analysis Core Facility (BACF) for the use of the instruments. The BACF is supported by the NIH/NCR Grant Number 5G12RR008124.

## References

1. Chang, H., and Lindquist, S. (1994) Conservation of Hsp90 macromolecular complexes in *Saccharomyces cerevisiae*. *J Biol Chem* **269**, 24983–88.
2. Schena, M., and Yamamoto, K. R. (1988) Mammalian glucocorticoid receptor derivatives enhance transcription in yeast. *Science* **241**, 965–7.
3. Borkovich, K. A., Farrelly, F. W., Finkelstein, D. B., Taulien, J., and Lindquist, S. (1989) hsp82 is an essential protein that is required in higher concentrations for growth of cells at higher temperatures. *Mol Cell Biol* **9**, 3919–30.
4. Picard, D., Khursheed, B., Garabedian, M. J., Fortin, M. G., Lindquist, S., and Yamamoto, K. R. (1990) Reduced levels of hsp90 compromise steroid receptor action in vivo. *Nature* **348**, 166–8.
5. Bohen, S. P., and Yamamoto, K. R. (1993) Isolation of Hsp90 mutants by screening for decreased steroid receptor function. *Proc Natl Acad Sci USA* **90**, 11424–8.
6. Nathan, D. F., and Lindquist, S. (1995) Mutational analysis of Hsp90 function: interactions with a steroid receptor and a protein kinase. *Mol Cell Biol* **15**, 3917–25.
7. Caplan, A. J., Langley, E., Wilson, E. M., and Vidal, J. (1995) Hormone-dependent transactivation by the human androgen receptor is regulated by a dnaJ protein. *J Biol Chem* **270**, 5251–7.
8. Kimura, Y., Yahara, I., and Lindquist, S. (1995) Role of the protein chaperone YDJ1 in establishing Hsp90-mediated signal transduction pathways. *Science* **268**, 1362–5.
9. Chang, H. C., Nathan, D. F., and Lindquist, S. (1997) In vivo analysis of the Hsp90 cochaperone Sti1 (p60). *Mol Cell Biol* **17**, 318–25.
10. Bohen, S. P. (1998) Genetic and biochemical analysis of p23 and ansamycin antibiotics in the function of Hsp90-dependent signaling proteins. *Mol Cell Biol* **18**, 3330–9.
11. Freeman, B. C., Felts, S. J., Toft, D. O., and Yamamoto, K. R. (2000) The p23 molecular chaperones act at a late step in intracellular receptor action to differentially affect ligand efficacies. *Genes Dev* **14**, 422–34.
12. Riggs, D. L., Roberts, P. J., Chirillo, S. C., Cheung-Flynn, J., Prapapanich, V., Ratajczak, T., Gaber, R., Picard, D., and Smith, D. F. (2003) The Hsp90-binding peptidylprolyl isomerase FKBP52 potentiates glucocorticoid signaling in vivo. *EMBO J* **22**, 1158–67.
13. Cheung-Flynn, J., Prapapanich, V., Cox, M. B., Riggs, D. L., Suarez-Quian, C., and Smith, D. F. (2005) Physiological role for the cochaperone FKBP52 in androgen receptor signaling. *Mol Endocrinol* **19**, 1654–66.
14. Tranguch, S., Cheung-Flynn, J., Daikoku, T., Prapapanich, V., Cox, M. B., Xie, H., Wang, H., Das, S. K., Smith, D. F., and Dey, S. K. (2005) Cochaperone immunophilin FKBP52 is critical to uterine receptivity for embryo implantation. *Proc Natl Acad Sci USA*. **102**, 14326–31.
15. Cox, M. B., Riggs, D. L., Hessling, M., Schumacher, F., Buchner, J., and Smith, D. F. (2007) FK506-binding protein 52 phosphorylation: A potential mechanism for regulating steroid hormone receptor activity. *Mol Endocrinol* **21**, 2956–67.
16. Cheung-Flynn, J., Roberts, P. J., Riggs, D. L., and Smith, D. F. (2003) C-terminal sequences outside the tetratricopeptide repeat domain of FKBP51 and FKBP52 cause differential binding to Hsp90. *J Biol Chem* **278**, 17388–94.

17. Riggs, D. L., Cox, M. B., Tardif, H. L., Hessling, M., Buchner, J., and Smith, D. F. (2007) Noncatalytic role of the FKBP52 peptidyl-prolyl isomerase domain in the regulation of steroid hormone signaling. *Mol Cell Bio.* **27**, 8658–69.
18. Gietz, D., St Jean, A., Woods, R. A., and Schiestl, R. H. (1992) Improved method for high efficiency transformation of intact yeast cells. *Nucleic Acids Res* **20**, 1425.
19. Mumberg, D., Muller, R., and Funk, M. (1995) Yeast vectors for the controlled expression of heterologous proteins in different genetic backgrounds. *Gene* **156**, 119–22.
20. Nair, S. C., Rimerman, R. A., Toran, E. J., Chen, S., Prapapanich, V., Butts, R. N., and Smith, D. F. (1997) Molecular cloning of human FKBP51 and comparisons of immunophilin interactions with Hsp90 and progesterone receptor. *Mol Cell Biol* **17**, 594–603.
21. Gueldener, U., Heinisch, J., Koehler, G. J., Voss, D., and Hegemann, J. H. (2002) A second set of loxP marker cassettes for Cre-mediated multiple gene knockouts in budding yeast. *Nucleic Acids Res* **30**, e23.
22. Rothstein, R. (1991) Targeting, disruption, replacement, and allele rescue: integrative DNA transformation in yeast. *Methods Enzymol* **194**, 281–301.
23. Miller, C. A., III, Martinat, M. A., and Hyman, L. E. (1998) Assessment of aryl hydrocarbon receptor complex interactions using pBEVY plasmids: Expressionvectors with bi-directional promoters for use in *Saccharomyces cerevisiae*. *Nucleic Acids Res.* **26**, 3577–83.

# Chapter 9

## High Throughput Analysis of Nuclear Receptor–Cofactor Interactions

Michael L. Goodson, Behnom Farboud, and Martin L. Privalsky

### Abstract

Various assays have been employed to study the nuclear receptor/cofactor interactions. Coimmunoprecipitation protocols, both yeast and mammalian two-hybrid systems, and electrophoretic mobility shift/supershift assays are all commonly used. One of the most useful assays for studying direct protein–protein interactions is the glutathione-*S*-transferase “pull-down” assay. We have developed a high-throughput version of this assay that utilizes a filter microplate to allow parallel processing of many samples, significantly reducing the time and reagents required for the assay and increasing the sensitivity of the assay for weaker protein–protein interactions.

**Key words:** GST-pulldown, Glutathione agarose, Protein binding assay, Immobilized protein, Nuclear receptor interaction assay.

---

### 1. Introduction

Nuclear receptors are hormone-regulated transcription factors that play central roles in metazoan development and homeostasis. As understanding of nuclear receptors has evolved, a remarkably vast and complex network of intermolecular interactions has been discovered to underlay many aspects of nuclear receptor function. Most nuclear receptors bind to DNA as protein dimers; consequently not only DNA–protein, but also protein–protein interactions contribute to their DNA recognition and target gene specificity (1–2). Once bound to DNA, nuclear receptor dimers recruit additional auxiliary proteins, denoted as corepressors and

coactivators, that mediate the specific molecular events required for target gene repression or activation (3–9). Corepressors and coactivators in turn form larger multiprotein complexes and exert many of their functions by mediating still additional interactions with chromatin proteins and with the general transcriptional machinery. The actions of both the nuclear receptors and their auxiliary factors is further fine-tuned, controlled, and adapted through transient interactions with a wide assortment of kinases, ligases, and other enzymes that introduce or remove covalent modifications (e.g. (10–12)).

The “GST pulldown” assay has been used extensively to study many of these protein–protein interactions. In this assay, a “bait” protein is expressed as a fusion with glutathione-*S*-transferase (GST) and is immobilized on glutathione agarose. The extent to which a second “prey” protein, typically expressed and radiolabeled using *in vitro* translation, can bind to and be retained by the immobilized bait protein through repeated washings has proven to be a useful and relatively accurate measure of the ability of the two proteins to interact directly.

The GST-pulldown assay traditionally has been done in individual microfuge tubes, a laborious and time consuming process that involves multiple liquid handling and transfer steps. As the number of proteins (and the number of conditions) to be tested has increased, it has become necessary to develop a more high-throughput assay method (13). We describe here a modification of the pulldown assay that permits the use of filter microplates. By adapting the conventional GST pulldown assay to a filter microplate, the liquid handling steps can be performed in parallel using a multichannel pipette, which reduces the time involved in performing multiple assays. This reduction in effort substantially simplifies the generation of apparent affinity curves and the determination of the effects of modifiers and reagent conditions (Fig. 1). The filter microplate also requires significantly less glutathione resin and allows for smaller reaction volumes. This reduction in time and reaction volume also increases the sensitivity of the assay for weaker protein–protein interactions compared with the individual tube assay (Fig. 2).

---

## 2. Materials

### 2.1. GST-Fusion Protein Expression and Lysis

1. Luria-Bertani Medium: 10% (W/V) Bacto Tryptone, 5% (W/V) Bacto Yeast Extract, 5% (W/V) NaCl. Use as liquid broth or add 1.5% (W/V) Bacto Agar for pouring Petri plates. Autoclave immediately after preparation. If plates or broth are to be used to select for bacterial transformants bearing specific

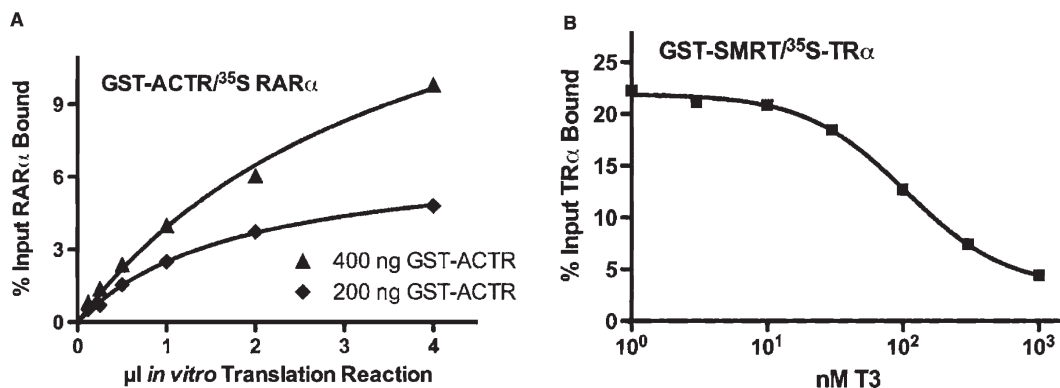


Fig. 1. Example of the use of the GST-pulldown assay for receptor and hormone titrations. (A) GST-ACTR (amino acids 621–821), either 400 ng (*triangles*) or 200 ng (*diamonds*), was bound to glutathione agarose and was incubated with increasing amounts of in vitro translated <sup>35</sup>S-methionine radiolabeled RAR $\alpha$  in the presence of 1  $\mu$ M all-*trans* retinoic acid (*atRA*, an RAR-agonist). The resulting immobilized GST-ACTR/RAR $\alpha$  complexes were washed, eluted with glutathione, and resolved by electrophoresis in a SDS-10% PAGE system. The gel was fixed, stained, dried, and scanned with a Molecular Dynamics Storm 840 Phosphorimager. Data were fit to a single-site hyperbolic binding curve using GraphPad Prism v. 4.0. (B) GST-SMRT $\tau$  (amino acids 2077–2471) bound to glutathione agarose was incubated with in vitro translated <sup>35</sup>S-methionine radiolabeled TR $\alpha$ 1 protein in the presence of increasing amounts of thyroid hormone agonist (T3). Samples were analyzed using the filter plate method as in (A). Data were fit to a sigmoidal dose response curve with variable slope using GraphPad Prism v. 4.0.

plasmids, an appropriate antibiotic (filter sterilized) can be added to the autoclaved media once it has cooled below 50°C. Typically, 100  $\mu$ g/mL ampicillin is used for the pGEX series of GST expression vectors. Store medium at room temperature (or 4°C if an antibiotic is added).

2. Isopropyl- $\beta$ -D-thiogalactopyranoside (IPTG): 1 M stock in water, sterilized by syringe filtration. Store aliquots at –20°C.
3. Branson S-250A Sonifier (Branson Ultrasonics, Danbury, CT) with 1/2 inch tapped disruptor horn (or equivalent).
4. Tris-Buffered Saline (TBS): 25 mM Tris-HCl, pH 7.5, 150 mM NaCl. Prepared as a 10 $\times$  stock solution. Autoclaved solutions can be stored at room temperature indefinitely.
5. COMPLETE Protease Inhibitor Cocktail (Roche, Indianapolis, IN), or equivalent.
6. Lysis Buffer: TBS containing 1 mM dithiothreitol (DTT), 0.5% Triton X-100, 1 $\times$  COMPLETE protease inhibitor. Make fresh immediately before use. Triton X-100 can be made up as a 10% (w/v) solution in water, filter sterilized, and stored at room temperature.

## 2.2. In Vitro Transcription and Translation of Prey Proteins

1. TNT™ T7 Quick Coupled in vitro transcription/translation kit (Promega, Madison, WI).

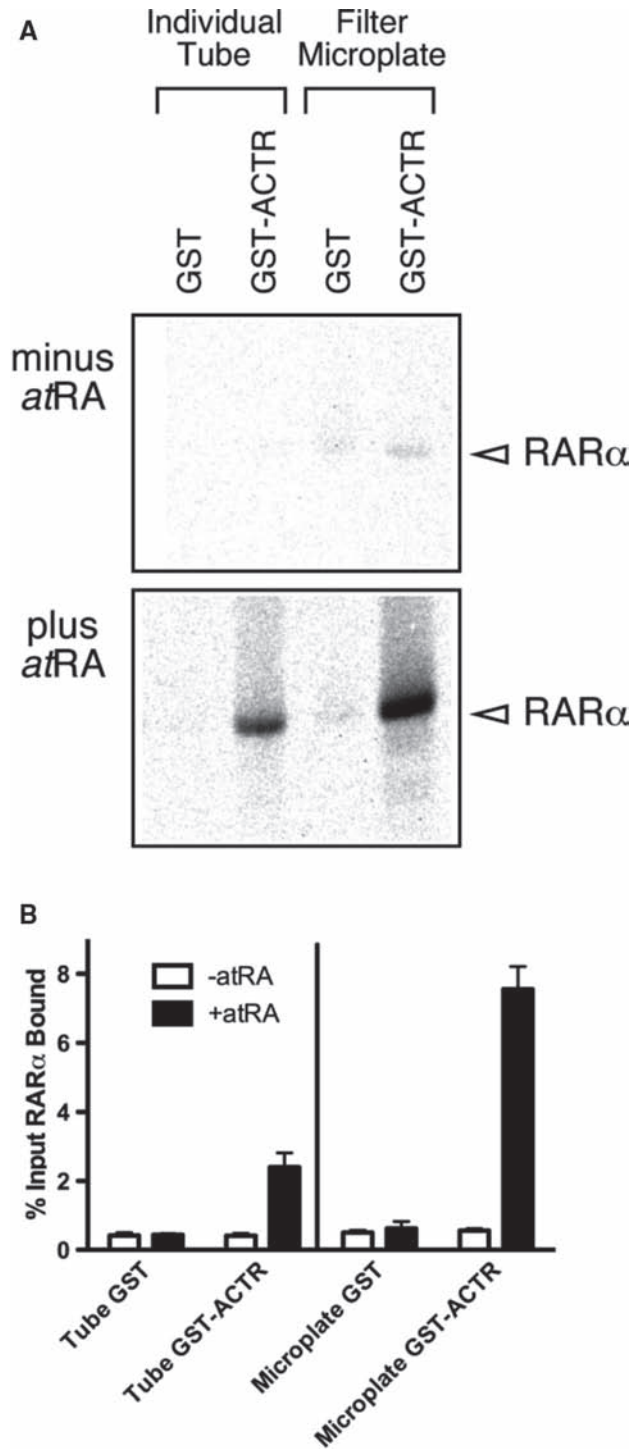


Fig. 2. Comparison of GST-pulldown methodologies: microfuge tube vs. filter-plate protocols. (A) Recombinant GST or GST-ACTR (amino acids 621–821) were bound to glutathione agarose and were incubated with *in vitro* translated <sup>35</sup>S-methionine radiolabeled RAR $\alpha$  protein in either the absence or presence of 1  $\mu$ M *atRA* using the



2. L-<sup>35</sup>S-Methionine (1000 Ci/mmol; Perkin Elmer, Waltham, MA). Use appropriate radioactive handling and disposal procedures, as this material contains the radioactive isotope <sup>35</sup>S. Of particular note: certain formulations of this radiolabel can leach volatile forms of the <sup>35</sup>S isotope; manipulations of the source vial should be performed in appropriate fume hoods and/or in containment devices that use activated charcoal to adsorb these volatiles.
3. A prey protein expression plasmid that contains a viral RNA polymerase promoter (e.g. T7 or SP6). The pSG5 and pcDNA3.1 series of mammalian expression vectors are particularly useful in this regard. For the purpose of this manuscript, we will assume that the prey protein is in a mammalian expression plasmid with a T7 promoter. If a bacterial expression plasmid (such as the pET vectors) is employed, an in vitro transcription/translation system that uses bacterial lysates instead of reticulocyte lysates can be used.

### **2.3. GST-Fusion Protein Immobilization and Prey Protein Interaction Analysis**

1. Millipore (Billerica, MA) MultiScreen-HV96 well filter microplate plate.
2. Millipore MultiScreen alignment frames for securing the filter plate to the collection plate.
3. Buffer A Binding Buffer: 25 mM HEPES pH 7.8, 50 mM KCl, 5 mM EDTA, 5 mM MgCl<sub>2</sub>, 0.5% Triton X-100, 6% glycerol, 1 mM dithiothreitol (DTT), 5 mg/mL bovine serum albumin (BSA), 1× COMPLETE protease inhibitor cocktail. Buffer A containing the first six ingredients can be made up in advance, filter sterilized, and stored at 4°C for an extended time period; BSA, protease inhibitor, and DTT can then be added and the reconstituted buffer stored at 4°C for up to a week.
4. Glutathione agarose (Sigma, St. Louis, MO), prepared as a 50% slurry in sterile TBS by swelling the resin (provided as a lyophilized solid) in ten volumes of TBS, discarding the supernatant and washing four additional times with ten volumes of TBS before resuspending the swollen resin in an equal volume of TBS. The glutathione agarose slurry can be stored at 4°C for up to a month. Do not freeze the resin slurry (the lyophilized resin can be stored indefinitely at -20°C).

←  
 Fig. 2. (continued) conventional individual tube assay ("Individual Tube"), or the modified filter microplate assay ("Filter Microplate"). After repeated washes, the bound RAR $\alpha$  was eluted with glutathione and was resolved by electrophoresis in a SDS-10% PAGE system. The gel was fixed, stained, dried, and scanned with a Molecular Dynamics Storm 840 Phosphorimager. (B) Quantification of the binding reactions in Fig. 2A. *Open bars* represent binding reaction performed in absence of *atRA*; *solid bars* represent binding reaction performed in the presence of 1  $\mu$ M *atRA*.

5. Wash Buffer: TBS containing 0.5% Triton X-100, 1 mM DTT. Prepare fresh.
6. Polystyrene V-bottom 96-well microplate (Corning).
7. Template adhesive sealing film (USA Scientific, Ocala, FL) for sealing microplates, or equivalent.
8. Impulse heat sealer (American International Electric model AIE-300) and 4 mil polyethylene bags (Fisher Scientific).
9. Roto-Shake Genie (Scientific Industries, Bohemia, NY) rotating/rocking platform.
10. IEC Centra MP4 tabeltop centrifuge with microplate rotor.
11. Glutathione Elution Buffer: 20 mM reduced L-Glutathione (Sigma, St. Louis, MO), 100 mM Tris-Cl, pH 8.0. Store aliquots of the elution buffer at  $-20^{\circ}\text{C}$ . (*see* [Note 1](#)).
12. 4× SDS-PAGE Sample Buffer: 125 mM Tris-HCl pH 6.8, 20% Glycerol, 4% (W/V) sodium dodecyl sulfate (SDS), 10%  $\beta$ -Mercaptoethanol, 0.5 mg/mL bromophenol blue dye. Store at room temperature for up to a month. Store at  $-20^{\circ}\text{C}$  indefinitely.

#### **2.4. SDS-PAGE and Phosphorimager Analysis**

1. Novex NuPAGE™ 9 or 17 well Bis-Tris Gels and MOPS Buffer systems (Invitrogen, Carlsbad, CA) or other SDS-PAGE Gel System.
2. BenchMark™ Protein Ladder (Invitrogen, Carlsbad, CA) or other SDS-PAGE molecular weight standards.
3. Fairbanks Coomassie Staining Solution: 0.1% (W/V) Coomassie Brilliant Blue R-250, 25% isopropyl alcohol, 10% acetic acid. Dissolve the Coomassie dye in the isopropyl alcohol and water and then add the acetic acid. Store at room temperature tightly capped.
4. Ten percent acetic acid destaining solution.
5. Molecular Dynamics Storm Phosphorimager (or equivalent).
6. Fuji BAS-MS 3543 Imaging plate (or equivalent) and exposure cassette.

---

### **3. Methods**

The GST pulldown assay can be divided into two basic steps: (1) expression of both bait and prey proteins and (2) analysis of the interaction between bait and prey proteins. In theory the interaction will work with either protein being the bait or the prey in this assay. Although this is often true in practice, we generally favor using the cofactor as the GST fusion protein bait

and using the nuclear receptor as the *in vitro* translated prey, as this methodology permits the receptor to be assayed in its native state. Alternatively, practical considerations, such as which protein concentration is to be varied to generate a quantitative binding curve, may dictate the bait vs. prey decision. Although this chapter assumes that the bait protein is expressed as a GST fusion in *E. coli*, it is also possible to use other affinity-tagged fusions (e.g., six histidines or maltose binding protein) or to express the protein in other systems, such as in insect cells or mammalian cells. This protocol assumes that the prey protein is radiolabeled by *in vitro* translation. It is also possible to incorporate biotin and detect the prey protein with streptavidin or with antibodies specific to the prey protein, though this may prove more difficult to quantify than using radioactive tracer. Finally, detection of the prey protein involves separation of the eluates on an SDS-PAGE gel (14) and visualization with a Phosphorimager. Although the SDS-PAGE method has the advantage of being able to visualize the quantity and quality of both the GST bait protein and the prey protein, it is sometimes adequate to simply quantify the prey protein eluted from the bait-glutathione-agarose by liquid scintillation counting; this works best for particularly robust, clean, and well-characterized protein-protein interactions.

### **3.1. GST-Fusion Protein Expression and Lysis**

1. Transform GST-fusion expression plasmid into a suitable strain of *E. coli* (e.g., the BL21 strain). Plate on LB-agar plates containing selective antibiotic (e.g., ampicillin for pGEX plasmids) and grow over night at 37°C.
2. Use a freshly transformed bacterial colony to inoculate 2 mL of LB broth containing the selective antibiotic. Grow overnight at 37°C with 300 rpm agitation to aerate the culture.
3. Inoculate 50 mL of LB containing selective antibiotics with 500 µL of the overnight culture. Grow at 37°C with 300 rpm agitation until the culture reaches an OD<sub>600</sub> of 0.6–0.8. Induce expression of the GST fusion protein by adding IPTG to a final concentration of 1 mM. Continue growing the culture for three additional hours to allow for protein expression. (see **Note 2**).
4. Harvest the culture by centrifuging at 4,000 × *g* for 10 min at 4°C. Discard the supernatant medium and wash the pellet by resuspension with 20 mL of TBS and recentrifugation.
5. Resuspend the bacterial pellet in 5 mL Lysis Buffer. This steps and all subsequent steps should be performed on ice or at 4°C unless otherwise noted.
6. Ultrasonically disrupt the cells using four 15 s pulses (100% duty cycle) at 80% maximal output (Setting 8). Keep the sample on ice during the sonication and take care to avoid foaming (see **Note 3**). Incubate the samples on ice for 2 min between pulses to allow cooling.

7. Clear the lysate by centrifuging at  $30,000 \times g$  for 20 min. Collect the supernatant.
8. Lysates can be rapidly frozen in liquid nitrogen and stored at  $-80^{\circ}\text{C}$  as aliquots until needed.

### **3.2. In Vitro Transcription and Translation of Prey Proteins**

1. Thaw the TNT mix (in vitro transcription/translation reticulocyte lysate mix) on ice immediately before use.
2. Mix  $40\ \mu\text{L}$  of TNT mix,  $1\ \mu\text{g}$  of plasmid DNA for the prey protein,  $5\ \mu\text{L}$  of L- $^{35}\text{S}$ -Methionine, and sufficient nuclease-free water for a total reaction volume of  $50\ \mu\text{L}$ . Appropriate safety measures and adherence to local and national rules should be followed when working with ionizing radiation sources and when discarding waste materials.
3. Incubate the reaction at  $30^{\circ}\text{C}$  for 90 min. Ideally, reactions should be used immediately or can be briefly stored on ice until use. If necessary, however, reaction can be rapidly frozen in liquid nitrogen and stored at  $-80^{\circ}\text{C}$  until needed.

### **3.3. GST-Fusion Protein Immobilization and Prey Protein Interaction Analysis**

#### *3.3.1. Binding of the GST-Protein Fusions to Glutathione-Agarose*

1. The first step is to determine the amount of each GST-protein fusion to use in subsequent assays. Mix 1, 5, 20 or  $50\ \mu\text{L}$  of each GST-protein lysate to be analyzed with  $10\ \mu\text{L}$  of 50% glutathione agarose slurry and sufficient Buffer A Binding Buffer for a  $100\ \mu\text{L}$  total volume binding reaction. Add to corresponding wells of the filter microplate. Unless otherwise indicated, maintain the samples on ice or at  $4^{\circ}\text{C}$ .
2. Seal the top of the filter plate with sealing film.
3. Place the filter plate over a V-bottom 96 well collection microplate using the alignment frame.
4. Seal the two plate stack in a polyethylene bag using the impulse heat sealer (setting 2).
5. Attach the filter plate assembly to the platform of a Roto-Shake Genie using magnetic strips.
6. Incubate the binding reactions with constant inversion mixing (rotating mode at approximately 5 rpm) for 30 min at  $4^{\circ}\text{C}$ .
7. Remove the plate assembly from the polyethylene bag and centrifuge the assembly briefly (10 s) at room temperature to collect the resin in the bottom of the wells, away from the sealing tape.
8. Remove the sealing tape and centrifuge the plate assembly again for 40 s at  $1,000 \times g$  (removal of the sealing tape and the longer centrifugation helps ensure a more complete elution of the binding buffer from the resin). Discard the flow-through (containing buffer and the nonrecombinant *E. coli* proteins) from the V-bottom microplate. The collection V-bottom microplate will be reused for each of the subsequent wash steps; replace it under the filter microplate.

9. Wash the glutathione-agarose, now containing the immobilized GST protein fusions, three times with 200  $\mu$ L each of wash buffer, centrifuging and discarding the flow-through that collects in the V-bottom microplate each time as above. (*see Note 4*).
10. Place a fresh V-bottom microplate under the filter microplate. Add 50  $\mu$ L of Glutathione Elution Buffer to each well. Seal the assembly with adhesive film and a polyethylene bag as steps 2–4.
11. Attach the plate assembly to the Roto-Shake Genie platform and incubate the reactions with constant inversion mixing for 30 min.
12. Remove the plate assembly from the polyethylene bag and centrifuge the assembly briefly (10s) at room temperature to collect the resin in the bottom of the wells, away from the sealing tape.
13. Remove the sealing tape and centrifuge the plate assembly again for 40s at 1,000  $\times g$  (removal of the sealing tape and the longer centrifugation helps ensure a more complete elution of the samples from the resin).
14. Discard the filter plate (containing the exhausted resin). Add 20  $\mu$ L 4 $\times$  SDS-PAGE Sample Buffer to each well of the V-bottom plate (containing the eluted proteins). The eluted proteins can be analyzed immediately. Alternatively, the V-bottom plates containing the protein eluates in SDS Sample Buffer can be sealed with adhesive sealing film and stored at  $-20^{\circ}\text{C}$  prior to analysis.
15. Analyze 20  $\mu$ L of each eluate by SDS-PAGE as described in **Subheading 3.4**. Compare the intensities of the Coomassie stained bands to determine the appropriate amount of each GST-protein fusion to use in the subsequent analyses. (*see Note 5*).

### 3.3.2. Analysis of Protein–Protein Interaction

Note: All steps in this portion of the procedure involve radioactive material.

1. Mix an appropriate amount of each of the GST fusion protein lysates (as determined in the previous section), 5  $\mu$ L of in vitro translation mix, 10  $\mu$ L of 50% glutathione agarose slurry, and sufficient Buffer A Binding Buffer for a 100  $\mu$ L total volume binding reaction. Add each sample to a corresponding well of the filter microplate. (*see Note 6*).
2. Seal the filter plate with sealing film.
3. Place the filter plate over a V-bottom 96-well collection microplate using the alignment frame.
4. Seal the two plate stack in a polyethylene bag using the impulse heat sealer (setting 2).

5. Attach the filter plate assembly to the platform of the Roto-Shake Genie using magnetic strips.
6. Incubate the binding reactions with constant inversion mixing (rotating mode at approximately 5 rpm) for 30 min at 4°C.
7. Remove the plate assembly from the polyethylene bag and centrifuge briefly to collect the resin in the bottom of the wells (away from the sealing tape).
8. Remove the sealing tape and centrifuge the plate assembly again for 40 s at  $1,000 \times g$ . Discard the flow-through from the V-bottom microplate (containing unbound proteins, buffer, and unincorporated radiolabel) and replace the V-bottom microplate under the filter microplate.
9. Wash the glutathione agarose, now containing the immobilized GST protein bait and any prey proteins bound to it, three times with 200  $\mu$ L each of wash buffer, centrifuging and discarding the flow through collecting in the V-bottom microplate each time as above.
10. Place a fresh V-bottom microplate under the filter microplate. Add 50  $\mu$ L of Glutathione Elution Buffer to each well. Seal the assembly with adhesive film and a polyethylene bag as **steps 2–4**.
11. Attach the plate assembly to the Roto-Shake Genie platform and incubate the reactions with constant inversion mixing for 30 min.
12. Remove the plate assembly from the polyethylene bag. Place the V-bottom plate back under the filter microplate and centrifuge briefly to collect the resin in the bottom of the wells.
13. Remove the sealing tape and centrifuge again for 40 s at  $1,000 \times g$  to completely drive the eluate into the V-bottom microplate. Discard the filter plate (containing the exhausted resin) as radioactive waste. Add 20  $\mu$ L 4 $\times$  SDS-PAGE Sample Buffer to each well of the V-bottom plate (containing the eluted proteins). Seal the V-bottom plates containing the eluates/SDS-PAGE buffer with an adhesive sealing film and mix gently. Eluates can be heated and analyzed immediately (as below) or stored at  $-20^{\circ}\text{C}$  prior to analysis.
14. Analyze 20  $\mu$ L of each eluate by SDS-PAGE as described below.

### **3.4. SDS-PAGE and Phosphorimager Analysis**

1. These instructions assume the use of the Novex XCell Sure-Lock™ Mini-Cell and the Novex NuPAGE Gel 9 or 17 well Bis-Tris Gel system with NuPAGE MOPS buffers (Invitrogen, Carlsbad, CA). The 9 and 17 well gel systems are compatible with multichannel pipettes. However, any SDS-PAGE gel system will work for this analysis. It may be necessary to run multiple gels to accommodate the number of samples analyzed.

2. Assemble the gel apparatus and running buffers according to the manufacturers instructions.
3. Heat the 96-well V-bottom plate on top of a heating block at 95°C for 5 min to assist in SDS-denaturation of the samples. Centrifuge the sealed microplate at  $1,000 \times g$  for 20 s prior to unsealing.
4. Unseal the microplate and load 20  $\mu$ L of each eluate on the SDS-PAGE gel. Also load 5  $\mu$ L of the Benchmark Protein Ladder on each gel.
5. Electrophorese the samples at 150 V for 50 min (or until the bromophenol blue dye is near the bottom of the gel).
6. Disassemble the gel from the apparatus and from the plates.
7. Place the gel in 50 mL of Fairbanks Coomassie Gel solution. Microwave the stain solution on medium power until the solution boils. Gently agitate the stain solution every 30 s to prevent uneven heating and potential damage to the gel (*see Note 7*).
8. Incubate the gel in the stain solution for 15 min with gentle (60 rpm) shaking.
9. Remove the stain solution. Add 50 mL 10% acetic acid. Microwave the destain solution on medium power until the solution boils. Gently agitate the stain solution every 30 s to prevent uneven heating and potential damage to the gel (*see Note 8*).
10. Incubate the gel in the destain solution for 5 min with gentle (60 rpm) shaking.
11. Repeat steps 9 and 10 until the gel is sufficiently destained to allow adequate visualization of protein bands.
12. Place the gel on a piece of cellulose filter paper (any cellulose filter paper will work; Whatman #1 or 3 MM are typically used). Dry the gel at 80°C for 1 h on a vacuum gel dryer.
13. Place the dried gel in the exposure cassette with the Phosphorimager screen. Expose the gel over night (typically sufficient for most experiments).
14. Visualize and quantify the cofractionated protein bands using a Phosphorimager.

---

#### 4. Notes

1. Unbuffered glutathione is acidic and requires the buffering capacity of the 100 mM Tris-Cl, pH 8.0 to maintain the pH of the elution buffer in the neutral range.



2. The bacterial host, GST-fusion plasmid, and protein expression conditions may vary considerably depending on the specific protein being expressed. We use the conditions described above for coactivators, such as ACTR and for GST. For corepressors (such as SMRT), a 1 L culture (inoculated at 1:100) is used. Once the culture reaches the desired optical density (0.6–0.8), the culture is moved to 16°C and expression is induced for 16 h with 1 mM IPTG before proceeding as above. Also, strains of *E. coli* that express rare tRNAs (e.g., BL21 CodonPlus, Stratagene, La Jolla, CA) can help in some problematic cases.
3. The heat and the foaming produced by sonication can cause protein denaturation, which will reduce the protein yield and may adversely affect the subsequent analysis. Small scintillation vials or sawed off 50 mL disposable centrifuge tubes work well as containers for sonication. It can be helpful to start sonicating at a lower power setting and increase the power to avoid foaming. If foaming occurs, stop the sonication immediately, allow the sample to settle for several minutes and then cautiously continue sonicating with the tip further immersed in the sample.
4. The washes in this manuscript are performed using a centrifuge and collection plate. It is possible to further streamline this method by using a microplate vacuum manifold under the filter plate to pull through the various wash solutions. However, extra care should be taken as the given wash solutions, vacuum manifold, and tubing will contain radioactivity.
5. The purpose of this step is to determine the amount of GST protein fusion expressed in each lysate and to normalize the amount of GST fusion protein added to each binding reaction when comparing different lysates. The amount of GST fusion protein can also be determined by including known amounts of a reference protein, such as ovalbumin, on the SDS-PAGE gel in adjacent lanes. The amounts of protein can be estimated visually or determined more accurately by using a scanner and image analysis software (such as NIH ImageJ or other commercial software), or a gel documentation system. Typically, 50–1,000 ng of GST fusion protein per binding are used.
6. The amount of in vitro translated protein can be varied over a range of concentrations to define a binding curve suitable for estimating an apparent affinity constant for the protein–protein interaction. Typically, 10,000–1,000,000 counts/min of incorporated <sup>35</sup>S-methionine per reaction are used. For analyzing an interaction between receptors and coactivators that requires hormone or other agonist, the agonist should be added both to the binding reaction and to the wash buffers. It is not necessary to add agonist to the elution buffer.

7. This method of staining and destaining is based on the method of Wong et al. (15) Microwaving the solutions dramatically decreases the time required stain and destain SDS-PAGE gels. However, this hot stain/destain method releases significant amounts of acetic acid fumes that represent both respiratory and burn hazards. These steps should be performed in a chemical fume hood and extra precautions against skin exposure or burns should be followed. Alternatively, any accepted method for staining SDS-PAGE gels will suffice.
8. Staining and destaining not only fixes the proteins in the gel, but also allows visualization of the GST fusion proteins to insure equivalent amounts were used in the pulldown assay. The quick (hot) stain/destain method described here is adequate for most purposes, but for extra accuracy in quantification, we recommend an alternative, but slower process: stain the gels at room temperature for 2 h. in Fairbanks Coomassie Staining Solution, then destain the gels for 1 h. in the same solution lacking Coomassie blue and for at least 4 h in several changes of 10% (v/v) acetic acid prior to drying.

## References

1. Glass, C. K. (1996). Some new twists in the regulation of gene expression by thyroid hormone and retinoic acid receptors. *J Endocrinol* **150**, 349–57.
2. Mangelsdorf, D. J. & Evans, R. M. (1995). The RXR heterodimers and orphan receptors. *Cell* **83**, 841–50.
3. Glass, C. K. & Rosenfeld, M. G. (2000). The coregulator exchange in transcriptional functions of nuclear receptors. *Genes Dev* **14**, 121–41.
4. Lazar, M. A. (2003). Nuclear receptor corepressors. *Nucl Recept Signal* **1**, e001.
5. Lee, J. W., Lee, Y. C., Na, S. Y., Jung, D. J. & Lee, S. K. (2001). Transcriptional coregulators of the nuclear receptor superfamily: coactivators and corepressors. *Cell Mol Life Sci* **58**, 289–97.
6. Leo, C. & Chen, J. D. (2000). The SRC family of nuclear receptor coactivators. *Gene* **245**, 1–11.
7. McKenna, N. J. & O'Malley, B. W. (2002). Minireview: nuclear receptor coactivators—an update. *Endocrinology* **143**, 2461–5.
8. Ordentlich, P., Downes, M. & Evans, R. M. (2001). Corepressors and nuclear hormone receptor function. *Curr Top Microbiol Immunol* **254**, 101–16.
9. Xu, J. & Li, Q. (2003). Review of the in vivo functions of the p160 steroid receptor coactivator family. *Mol Endocrinol* **17**, 1681–92.
10. Rochette-Egly, C. (2003). Nuclear receptors: integration of multiple signalling pathways through phosphorylation. *Cell Signal* **15**, 355–66.
11. Stallcup, M. R., Kim, J. H., Teyssier, C., Lee, Y. H., Ma, H. & Chen, D. (2003). The roles of protein-protein interactions and protein methylation in transcriptional activation by nuclear receptors and their coactivators. *J Steroid Biochem Mol Biol* **85**, 139–45.
12. Weigel, N. L. (1996). Steroid hormone receptors and their regulation by phosphorylation. *Biochem J* **319** (Pt 3), 657–67.
13. Goodson, M. L., Farboud, B. & Privalsky, M. L. (2007). An improved high throughput protein-protein interaction assay for nuclear hormone receptors. *Nucl Recept Signal* **5**, e002.
14. Laemmli, U. K. (1970). Cleavage of structural proteins during the assembly of the head of bacteriophage T4. *Nature* **227**, 680–5.
15. Wong, C., Sridhara, S., Bardwell, J. C. & Jakob, U. (2000). Heating greatly speeds Coomassie blue staining and destaining. *Bio-techniques* **28**, 426–8, 430, 432.

# Chapter 10

## Binding Affinity and Kinetic Analysis of Nuclear Receptor/Co-Regulator Interactions Using Surface Plasmon Resonance

Derek N. Lavery

### Abstract

Knowledge of the kinetics of protein–protein interactions has become important in defining nuclear receptor function. Such knowledge allows characterization of interactions that occur with high affinity and/or selectivity. Surface plasmon resonance is a useful and sensitive tool for studying protein–protein interactions. This technique involves immobilization of a “ligand” to the surface of a sensor chip and subsequently passing over multiple concentrations of “analyte” to generate binding curves. Interaction between the receptor and target protein is monitored by the density at the sensor chip surface and allows calculation of the association and dissociation stages (and therefore affinity) of interactions to be assessed in real-time. Using software packages, these kinetic parameters can be quantified. Importantly, the levels of recombinant protein required are much less than that needed for other affinity techniques such as isothermal titration calorimetry and anisotropy fluorescence spectroscopy.

**Key words:** Surface plasmon resonance, Protein–protein interactions, Kinetics, Affinity, association, Dissociation.

---

### 1. Introduction

Nuclear receptors (NRs) regulate a multitude of genes in response to an increase in cellular ligand levels. During the process of gene regulation, NRs interact and communicate with a variety of coactivators (CBP/p300, SRC/p160), corepressors (NCoR, SMRT), and members of the basal transcription machinery (TFIIF, TFIID) (reviewed in **ref. 1**). These interactions have been mapped predominantly to the activation function-1 (AF1) and AF2 domains

in the NR N- and C-termini, respectively (reviewed in **ref. 1**). In some cases, the importance of individual coactivators has been investigated further using a variety of gene knock-out/disruption or siRNA approaches (reviewed in **ref. 2**). In the absence of such technically challenging approaches, it can be difficult separating important protein coregulators from nonselective or promiscuous partners. Surface plasmon resonance (SPR) is an experimental tool that can be used to assess and quantify the kinetic parameters of protein–ligand, protein–DNA and protein–protein interactions and therefore separate selective and nonselective interactions. The methodology of SPR is simple and is outlined in **Fig. 1**. A ligand of interest is immobilized to the surface of a sensor chip and different concentrations of an analyte protein are subsequently passed over. An increase in surface density occurs if two proteins interact and changes the refractive angle ( $\delta\theta$ ) generating binding curves. Recently, SPR has been used to characterize the interactions of TRAP220 and TIF2 binding to thyroid receptor-AF2 (3). Using a combination of SPR and GST-pull down techniques, the authors were able to show competition between the two transcriptional coregulators and suggested that TRAP220 could act as a “bridging” factor between receptor and basal transcription machinery (3). Furthermore, TRAP220 was also found to interact with both estrogen receptor (ER) $\alpha$  and ER $\beta$  with affinities occurring in the submicromolar range ( $\sim$ 150–160 nM) and the affinities of these interactions were increased when receptors were bound to estradiol ( $\sim$ 60–70 nM) (4). Differences were also noted between binding of agonists and antagonists to ER $\alpha$  using SPR. It was observed that formation of an antagonist/ER $\alpha$  complex occurred more slowly and with lower affinity than agonist/ER $\alpha$  complexes (5).

ER $\alpha$  and ER $\beta$  interactions with TBP have also been characterized using SPR (6). The ER $\alpha$ -AF1/TBP interaction was calculated to occur within the micromolar range. Interestingly, no interaction was detected when this experiment was repeated with the AF1 domain of ER $\beta$  suggesting a different mechanism of transcription initiation for ER isoforms (6). In addition, the affinity of AR-NTD (amino acids 360–548) and cochaperone BAG-1L have been calculated (0.6  $\mu$ M) (7). We have recently investigated the interactions of AR-AF1 with domains of RAP74, the large subunit of TFIIF (9). We observed differential affinities of AR-AF1 interactions with RAP74 termini and hypothesize that this may have a role in AR-dependent gene regulation *in vivo* (9).

Despite the above studies, there generally remains a large gap in knowledge regarding specific interaction kinetics of coregulators and NRs. Analysis of a variety of protein–protein interactions by SPR will enable the comparison of both different coactivators

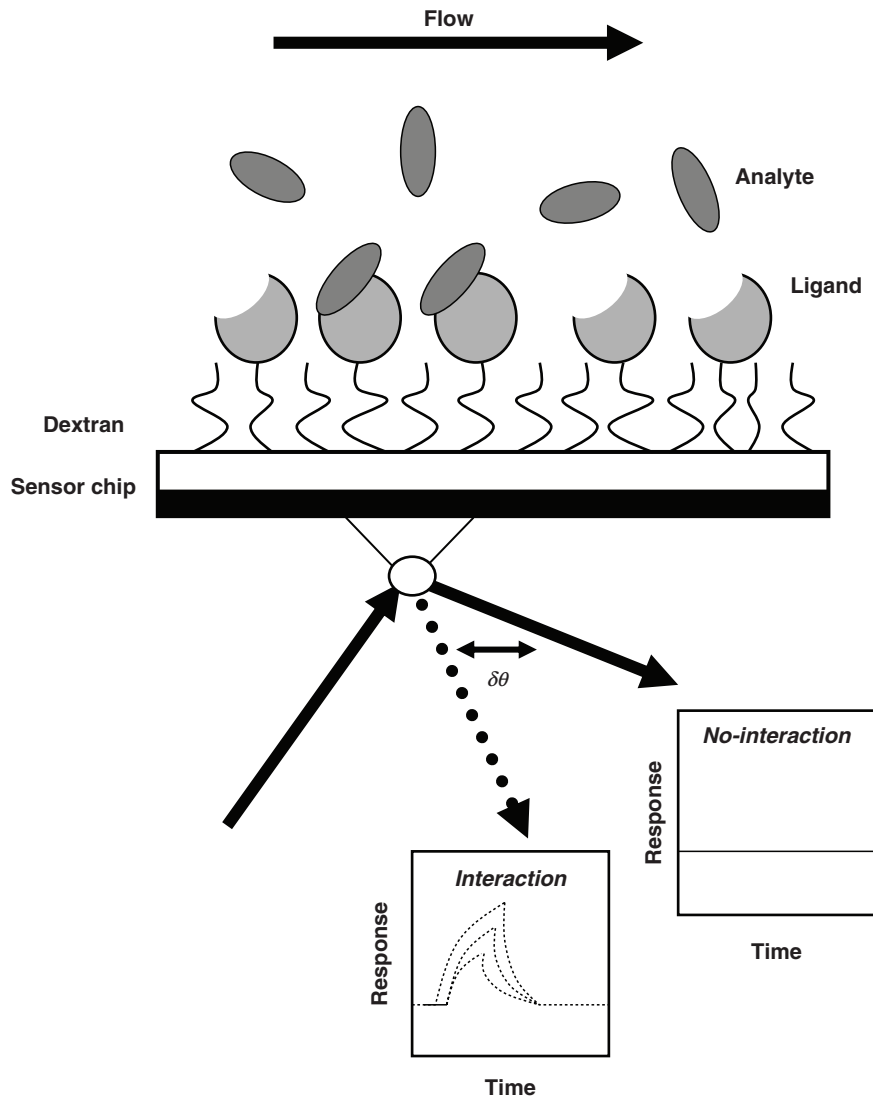


Fig. 1. Surface Plasmon resonance. Portions of purified “ligand” protein are immobilized on to the dextran-coated sensor chip surface by chemical coupling. Portions of “analyte” protein are then passed over the sensor chip surface in a controlled fashion (e.g., a flow rate of 10–20  $\mu\text{L}/\text{min}$ ). Protein–protein interactions increase the density at the sensor chip surface and change the angle of refracted light ( $\delta\theta$ ) generating real-time binding profiles.

and nuclear receptors and will aid discrimination of selective and nonselective interactions. The relatively small amounts of protein needed, assay speed, and ease of data analysis enables the technique to be applied to a variety of interactions in combination with other protein–protein assay approaches.

## 2. Materials

### 2.1. Recombinant Protein Expression and Purification

1. SOC medium: 2% (w/v) tryptone, 0.5% (w/v) yeast extract, 0.5% (w/v) NaCl, 5 mM MgSO<sub>4</sub>, 10 mM MgCl<sub>2</sub>, 0.4% (w/v) glucose.
2. Luria-Bertani (LB) broth: 1% (w/v) tryptone, 1% (w/v) yeast extract, 1% (w/v) NaCl or equivalent.
3. BLR (DE3) *Escherichia coli* expression cells (Novagen).
4. Ampicillin (Sigma) dissolved in dH<sub>2</sub>O at a stock concentration of 50 mg/mL, filter sterilized. Working concentration of 200–400 µg/mL.
5. Isopropyl β-D-thiogalactoside (IPTG, Roche) dissolved in dH<sub>2</sub>O at a stock concentration of 1 M, filter sterilized. Working concentration between 0.1 and 1 mM.
6. Complete mini protease inhibitors (Roche).
7. Dithiothreitol (DTT, Sigma) dissolved in dH<sub>2</sub>O at a stock concentration of 1 M, filter sterilized. Working concentration of 1 mM.
8. Phenylmethylsulphonyl fluoride (PMSF, Roche) dissolved in 100% (v/v) ethanol at a stock concentration of 0.2 M, filter sterilized. Working concentration of 0.2 mM.
9. RNase A (Roche) dissolved in dH<sub>2</sub>O at a stock concentration of 10 mg/mL, filter sterilized. Working concentration of 100 µg/mL.
10. DNase I (Roche) dissolved in dH<sub>2</sub>O at a stock concentration of 1 mg/mL, filter sterilized. Working concentration of 10 µg/mL.
11. Ni-NTA Agarose (Qiagen).
12. Purification columns (Qiagen).
13. Resuspension buffer: 20 mM Tris-HCl (pH 7.9), 50 mM NaCl, 1 mM EDTA, 0.2 mM PMSF, 1 mM DTT.
14. Charge buffer: 50 mM NiSO<sub>4</sub>.
15. Binding buffer: 5 mM imidazole, 500 mM NaCl, 20 mM Tris-HCl, pH 7.9.
16. Wash buffer: 60 mM, 500 mM NaCl, 20 mM Tris-HCl, pH 7.9.
17. Elution buffer: 200 mM imidazole, 500 mM NaCl, 20 mM Tris-HCl, pH 7.9, 5% glycerol, 0.2 mM PMSF, 1 mM DTT.
18. Dialysis tubing (Sigma).
19. 30% (v/v) acrylamide:bisacrylamide stock solution (37.5:1, Sigma).
20. Tris-HCl (1 M) (pH 8.8).

21. Tris-HCl (1 M) (pH 6.8).
22. Ammonium persulfate (10% (w/v)) (APS, Sigma) dissolved in dH<sub>2</sub>O and stored in 50  $\mu$ L aliquots at  $-20^{\circ}\text{C}$ .
23. Sodium dodecyl sulfate (10% (w/v)) (SDS, Sigma) dissolved in dH<sub>2</sub>O.
24. *N,N,N',N'*-tetramethyl-ethane-1,2-diamine (TEMED, Sigma).
25. SDS-PAGE running buffer (5 $\times$ ): 125 mM Tris, 960 mM glycine, 0.5% (w/v) SDS diluted to a working concentration of 1 $\times$  with dH<sub>2</sub>O.
26. SDS-PAGE Sample buffer (2 $\times$ ): 100 mM Tris-HCl (pH 6.8), 4% SDS, 0.2% bromophenol blue (w/v), 20% glycerol (v/v), 20 mM DTT.
27. Coomassie stain buffer: 0.5% (w/v) coomassie stain "R", 50% (v/v) methanol, 10% (v/v) glacial acetic acid.
28. Destain buffer: 30% (v/v) methanol, 10% (v/v) glacial acetic acid.
29. Dialysis buffer: 25 mM HEPES, 100 mM sodium acetate, 5% (v/v) glycerol, 1 mM DTT pH 7.9) or HBS (see below).

## **2.2. Surface Plasmon Resonance**

1. Highly pure ligand and analyte proteins,  $>0.2$  mg/mL,  $>500$   $\mu$ L (see [Subheadings 2.1 and 3.1](#)).
2. HBS running buffer: 10 mM HEPES, 150 mM NaCl, pH 7.4 (Biacore).
3. CM5 sensor chip (Biacore).
4. Vials (Biacore).
5. Sodium acetate (10 mM) (at a range of pH).
6. Regeneration buffer: NaOH at a range of concentrations.
7. Amine coupling kit (0.4 M 1-ethyl-3-(3-dimethylpropyl)-carboïimide, EDC), 0.1 M *N*-hydroxysuccinimide, NHS, 1 M ethanolamine-HCl, pH 8.5, ethanolamine), available from Biacore.

## **2.3. Analysis of Kinetic Data**

1. Computer work station.
2. Biaevaluation 3.0 software or equivalent.

---

## **3. Methods**

For SPR experiments, a critical requirement is highly pure recombinant protein that is stable at temperatures ranging from  $4^{\circ}\text{C}$  to room temperature. This can be achieved by optimizing the expression levels and purification protocols for recombinant proteins, SDS-PAGE analysis, and test incubations at a variety of



temperatures (*see* **Note 1**). During the kinetic analyses of protein–protein interactions, sequestering the ligand protein to the sensor chip surface, duration of each kinetic run and regeneration of sensor chip surface must also be optimized to obtain reliable data. Finally, data analysis can be performed in a variety of ways depending on the type of interaction (e.g., 1:1 binding, conformational change) and type of information required (e.g., rates of association, dissociation and/or affinity).

### **3.1. Expression and Purification of Recombinant Protein**

The following expression/purification method is performed using Novagen BLR (DE3) competent cells and the Qiagen Ni-NTA system but is adaptable to other expression/purification systems (*see* **Note 2**).

1. Transform Novagen BLR (DE3) *Escherichia coli* expression cells with the expression plasmid and select by antibiotic resistance by incubating 1–2  $\mu\text{L}$  of plasmid DNA with 50  $\mu\text{L}$  competent cells for 30 min on ice.
2. Heat-shock the reaction for 45 s at 42°C and return to ice for 2 min.
3. Add 500–1,000  $\mu\text{L}$  SOC to the competent cells and incubate in a shaking incubator at 37°C for 1 h.
4. Plate 100–200  $\mu\text{L}$  of reaction mix on antibiotic selective plates and incubate overnight at 37°C.
5. Inoculate a small vessel containing 10 mL LB with ampicillin to a final concentration of 400  $\mu\text{g}/\text{mL}$  with 2–3 individual colonies and grow overnight (12–16 h) in a shaking incubator at 37°C (*see* **Note 3**).
6. The following day inoculate a large flask containing 200 mL of LB and ampicillin with the overnight culture (a 1/20 dilution) and grow in a shaking incubator for 1–2 h until an  $\text{OD}_{600} = 0.4\text{--}0.6$  is reached (*see* **Note 4**).
7. To induce recombinant protein expression IPTG is spiked directly into the culture medium to a final concentration of 1 mM and cultures are placed back in the shaking incubator for 2 h at 37°C (*see* **Note 5**).
8. After this incubation, the culture medium should be centrifuged at  $5000 \times g$ , for 20 min at 4°C to pellet the *E. coli*.
9. During this centrifugation step, reagents used in the resuspension of the cell slurry should be made ready and chilled on ice (*see* **Note 6**).
10. Remove the spin supernatant and resuspend the cell pellet completely in resuspension buffer containing 1 $\times$  protease inhibitors, 1 mM DTT, and 0.2 mM PMSF and replace on ice.

11. Place the cell slurry in the  $-70^{\circ}\text{C}$  or  $-80^{\circ}\text{C}$  freezer and leave overnight (*see Note 7*).
12. The next day prepare a 0.75 mm thickness SDS-polyacrylamide gel. The following instructions assume the use of a Bio-Rad mini-gel Protean II system but are adaptable to a variety of other formats. Make a 12.5% resolving gel by mixing 3.13 mL 30% acrylamide/bisacrylamide stock solution (37.5:1), 0.94 mL 3 M Tris-HCl, pH 8.8, 75  $\mu\text{L}$  10% SDS, 7.7 mL  $\text{dH}_2\text{O}$  and finally 75  $\mu\text{L}$  of 10% APS and 5  $\mu\text{L}$  of TEMED just before loading. Pour the gel leaving enough space for the stacking gel and comb and layer on top 70% ethanol to keep gel level. The gel should take 20–40 min to polymerize depending on room temperature. After this time remove the ethanol by pouring and prepare the stacking gel by mixing 800  $\mu\text{L}$  30% acrylamide/bisacrylamide stock solution (37.5:1), 0.63 mL 1 M Tris-HCl, pH 6.8, 50  $\mu\text{L}$  10% SDS, 3.5 mL  $\text{dH}_2\text{O}$  and finally 50  $\mu\text{L}$  of 10% APS and 5  $\mu\text{L}$  of TEMED just before loading. Apply the stacking gel and slide in the well combs. The gel should take 10–20 min to polymerize depending on room temperature (*see Note 8*).
13. Thaw the cell slurry quickly on ice and add lysozyme to a final concentration of 500  $\mu\text{g}/\text{mL}$  and place the tube on a roller at  $4^{\circ}\text{C}$  for 15 min.
14. Subsequently, add DNase I and RNase A to final concentrations of 10 and 100  $\mu\text{g}/\text{mL}$  and place the slurry back on the roller for a further 15 min.
15. At this point, cell lysis (*see Note 9*) should be complete and the slurry should become more viscous. Spike in NaCl to a final concentration of 500 mM to decrease nonspecific interactions and inhibit aggregation.  
The cell slurry should be centrifuged at high speed (14000  $\times g$ ) for 30 min at  $4^{\circ}\text{C}$ .
16. During this centrifugation step, reagents and materials can be assembled for protein purification. All subsequent steps should be performed at  $4^{\circ}\text{C}$  and on ice. Assemble the purification column (Bio-Rad) and place in a suitable holder (e.g. 50 mL tube or measuring cylinder). Remove the  $\text{Ni}^{2+}$ -agarose from storage, mix completely and apply 2 mL to the purification column to give a final bed volume of 1 mL. Allow the storage buffer to flow through and wash the agarose with 20 mL  $\text{dH}_2\text{O}$ , 20 mL charge buffer and 20 mL binding buffer.
17. Collect a 20  $\mu\text{L}$  sample and then apply the remaining spin supernatant (total soluble cellular protein) to the column and allow to flow-through by gravity. Collect flow-through and take a 20  $\mu\text{L}$  sample for SDS-PAGE analysis, store at  $-20^{\circ}\text{C}$ .

18. Wash the column containing the bound recombinant protein with 10 mL binding buffer and 10 mL wash buffer allowing buffers to pass fully through the column. Collect flow-through and take a 20  $\mu$ L sample for SDS-PAGE analysis, store at  $-20^{\circ}\text{C}$ .
19. Move the column to a 1.5 mL microcentrifuge tube (the tip of the column will sit firmly inside). Add 1 mL Elution buffer and allow to flow completely through the column. Collect and store the microcentrifuge tube on ice after taking a 20  $\mu$ L sample for SDS-PAGE analysis. Repeat this step a further 2–3 times (*see Note 10*).
20. Apply 20  $\mu$ L of 2 $\times$  sample buffer to all aliquots that will be analyzed by SDS-PAGE and heat to  $75^{\circ}\text{C}$  on a hot-block for 5–10 min to denature. Allow samples to cool to room temperature and centrifuge briefly to collect condensation.
21. Prepare the SDS-PAGE gels and tank. Apply 1 $\times$  SDS-PAGE running buffer to both chambers of the gel tank. Mix samples and apply 10–15  $\mu$ L to each well, include a suitable molecular weight marker in a separate well.
22. Resolve the proteins by applying a voltage of 160–200V for 45–60 min or until the dye front reaches the bottom of the gel.
23. Remove the gel from the glass plates and place in a suitable dish and rinse off excess running buffer in 100 mL  $\text{dH}_2\text{O}$ . Remove the  $\text{dH}_2\text{O}$  and apply 50–100 mL coomassie stain to the gel and incubate at room temperature for 30–60 min. Remove the coomassie stain and wash briefly in  $\text{dH}_2\text{O}$ . Apply destain solution and leave for 1–2 h (*see Note 11*).
24. After the gel has detained to preference the gel can either be analyzed and imaged or dried under vacuum using a Bio-Rad gel dryer for 1–2 h at  $80^{\circ}\text{C}$ . To do this wet a 20  $\times$  20 cm piece of Whatman filter paper with  $\text{dH}_2\text{O}$  and carefully apply the gel. Remove all bubbles gently with a wet finger and cover with a large piece of Saran wrap. Place the gel on the slab dryer and heat to  $80^{\circ}\text{C}$  for 1–2 h (*see Note 12*).
25. Analyze the gel for protein expression and elution of specific protein from the beads. A representative SDS-PAGE gel for the expression/purification of amino acids 142–485 of the AR N-terminal domain is shown in **Fig. 2**.
26. At this stage, recombinant protein fractions can be either pooled and dialyzed or dialyzed individually for several hours or overnight as follows. Take a 40-cm length of dialysis tubing (Sigma) and prewet in prechilled ( $4^{\circ}\text{C}$ ) dialysis buffer. Tie one end and position a crocodile clip or equivalent on the end to ensure no loss of recombinant protein. Apply the recombinant protein elutions and tie the remaining

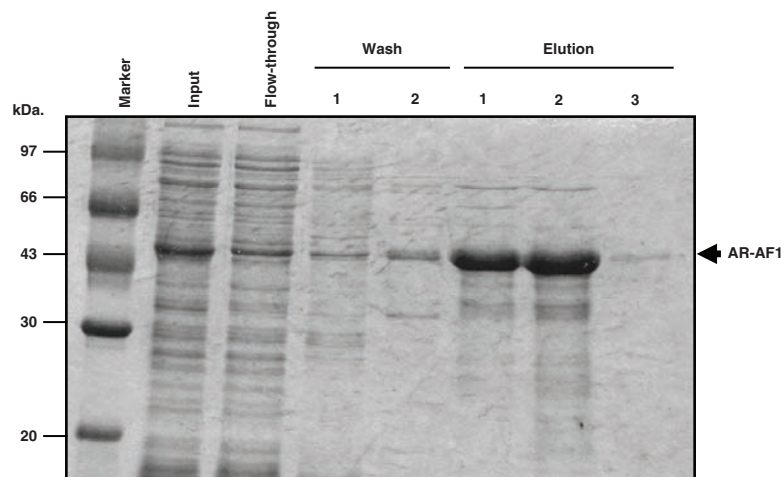


Fig. 2. Expression and purification analysis of recombinant AR-AF1 used in SPR studies. (A) Coomassie stained SDS-PAGE gel of purified amino acids 142–485 of the AR N-terminal domain. BLR (DE3) *E. coli* cells carrying an AR-AF1 expression plasmid were induced with 1 mM IPTG for 2 h at 37°C. Samples of 5  $\mu$ L were taken at each purification step and analysed to assess expression levels and AR-AF1 purity. *see Subheading 3.1* for details.

end in a similar way. Place the tubing in a beaker containing 300–500 mL dialysis buffer and dialyze the solution for 3–5 h (or overnight) changing the dialysis buffer occasionally (*see Note 13*).

27. After dialysis, remove the tubing, clean any remaining drips and carefully cut the upper end of the tubing and decant into a suitable container (e.g., universal or bijou) on ice. Analyze the solution for signs of precipitation. This may occur with proteins that are misfolded or domains that are highly charged or hydrophobic. If precipitation is observed centrifuge the protein mixture at  $18,000 \times g$  for 10 min at 4°C and remove the supernatant. Mix carefully and aliquot into 0.8 mL microcentrifuge tubes and snap-freeze in liquid  $N_2$ . Take 20  $\mu$ L and quantify protein concentration by the method of Bradford (8) or equivalent. A typical yield of recombinant protein using this protocol is 1–2 mg/mL.
28. Store protein aliquots at  $-70$  or  $-80^\circ C$ .

### 3.2. Sequestering Ligand to the Sensor Chip Surface

The following method is based on sequestering purified AR-AF1 (Fig. 2) using the Biacore 2000 instrument and covalent attachment/immobilization to the CM5 sensor chip (*see Note 14*). The CM5 sensor chip is coated with negatively-charged dextran matrix therefore the immobilization of purified proteins to the surface relies on the protonation of amino acid groups. In light

of this a series of buffers with pH values less than the isoelectric point (pI) of the protein of interest should be assessed (*see Note 15*). Optimal binding of the protein to the CM5 sensor chip surface should be assessed as follows.

1. Dilute recombinant ligand protein in a variety of 10 mM sodium acetate buffers to a final concentration of 10  $\mu\text{g}/\text{mL}$  (aim for a pH range of 1–3 units below the pI of ligand protein).
2. Open up the Biacore 2000 software package and select “*new application wizard*” from the file menu. Select “*surface preparation*” from the list and then select “*immobilization pH scouting*”.
3. Choose the immobilization buffers (e.g. 10 mM sodium acetate, pH 4–6), contact time, flow rate, and flow cell.
4. Choose the regeneration buffer (e.g. 5 mM NaOH) and injection characteristics as above.
5. Arrange vials (supplied by Biacore) containing protein, immobilization and regeneration buffers as directed by the software and run the wizard template.
6. Analyze the results and choose the buffer that gives the greatest response and therefore the highest binding of the protonated protein to the negatively-charged dextran.
7. For immobilization proper, use the Biacore amine coupling kit, which contains EDC, NHS, and ethanolamine solutions (available from Biacore). In the wizard “*surface preparation*” file, choose the “*immobilization*” procedure and configure the flow cell type (e.g., CM5) and coupling chemistry (e.g., amine). Select the amount of protein required to be immobilized on the chip. Routinely, 500 response units (RU) will result in good kinetic data by minimizing mass transport effects. Arrange the vials of EDC, NHS, ethanolamine, and protein as prompted by the wizard template.
8. Run the method and examine the results. The wizard will indicate the target and actual levels of protein immobilization. The ligand protein is now immobilized on the sensor chip surface and kinetic runs can be performed (*see Note 16*).

### **3.3. Regeneration of the Sensor Flow Cell Surface**

Before full kinetic runs can be performed, optimization of both individual response (observed upon protein–protein interactions) and regeneration of the sensor chip surface should be assessed. The selected regeneration buffer(s) should remove all bound analyte protein without affecting the amount of immobilized ligand protein and the sensogram should return to baseline (*see Note 17*).

1. Prepare a set of analyte protein dilutions (e.g. 1–20  $\mu\text{g}/\text{mL}$ ) and a regeneration buffer at various concentrations (e.g. 1–10 mM NaOH).

2. Select the “*regeneration scouting*” wizard and input the desired analyte contact time, flow rate, and flow cell.
3. Input various regeneration buffers, contact time, and flow rate (*see Note 18*).
4. Run the wizard and analyze the results. Inserting report points may aid analysis of individual buffers.
5. Repeat the analysis for a range of analyte protein concentrations (*see Note 19*).

### 3.4. Kinetic Analysis

To generate binding curves, multiple concentrations of analyte protein must be passed over the immobilized ligand protein at a low flow rate with responses falling within a specific range.

1. Select the “*binding analysis*” program in the software menu.
2. Insert data relating to concentrations of analyte (e.g., 10–100  $\mu\text{g}/\text{mL}$ ), flow rate (10–20  $\mu\text{L}/\text{min}$ ), association/dissociation time for the analyte/ligand complex (e.g., 160s association and 200s dissociation or as determined empirically), Regeneration buffer volume/contact time and flow cell that you aim to flow the analyte over (*see Note 19*).
3. Prepare the samples and regeneration buffer(s) and run the program (*see Note 20*).
4. The following day, or after the completion of the run, analyze each individual cycle looking for normal association/dissociation and accurate regeneration (*see Note 21*).
5. Make any additional changes that could range from addition/removal of analyte concentrations or manipulation of the regeneration buffer.
6. Repeat the run if desired.
7. Complete binding runs for AR-AF1 with several concentrations of a Target protein are shown in **Fig. 3**.

### 3.5. Data Analysis

The following protocol for data analysis is based on the software program Biaevaluation 3.0 (Biacore); however, there are other programs (such as CLAMP) that can be utilized to evaluate protein–protein interaction data.

1. Open the Biaevaluation software package and select the kinetic runs you wish to analyze and these are likely to be a range of 10–15 different concentrations of analyte (*see Note 22*).
2. Highlight the kinetic runs you wish to analyze and plot them using the “*plot overlay*” control.
3. Using the “*X-transform*” and “*Y-transform*” functions normalize each run for time and response.
4. Using the “*Y-transform*” function subtract the control cells from each kinetic run and select “*replace original*”. It should

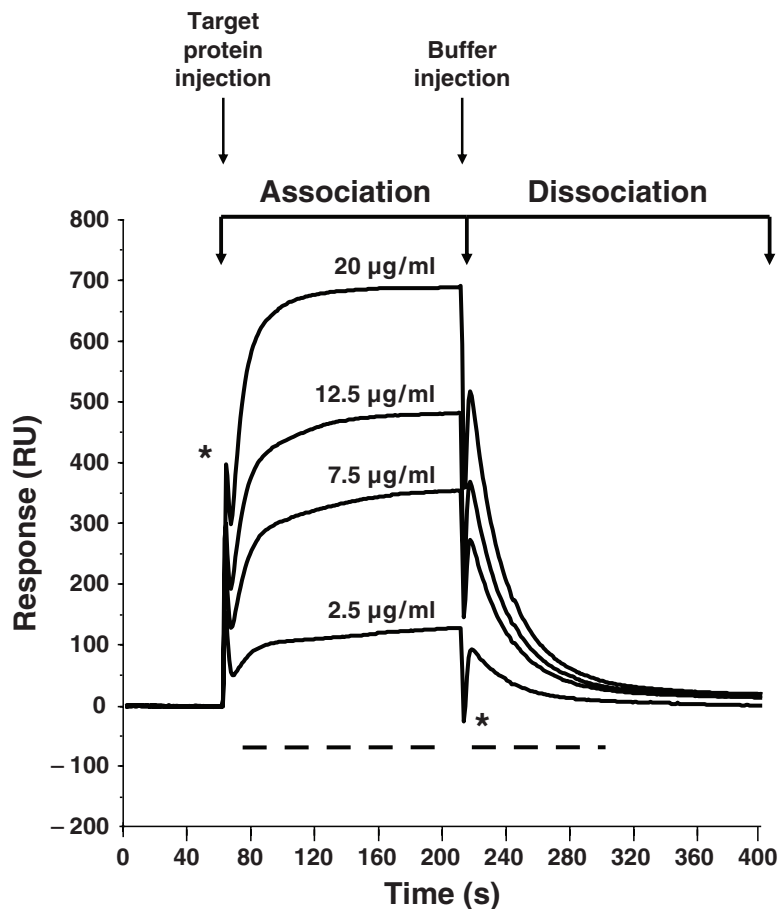


Fig. 3. Binding kinetics of RAP74-CTD and AR-AF1. Concentrations of recombinant RAP74-CTD (2.5, 7.5, 12.5, and 20  $\mu\text{g}/\text{mL}$ ) were passed over immobilised AR-AF1. Arrows indicate points of RAP74-CTD (association) and buffer (dissociation) injection, buffer spikes are indicated by an asterisk, and regions used for kinetic analyses are indicated by a dashed line (see Note 25).

be obvious if you have carried out this subtraction correctly as the control run will be flat throughout (see Note 23).

5. Choose the binding model (e.g., 1:1 Langmuir binding), and select “fit kinetics, simultaneous  $k_a/k_d$ ” and highlight the regions of selected curves you wish to analyze (see Note 24 and 25).
6. At this point enter the concentration of analyte in each run and fit data. The subsequent screen will show your fitted curves with optimal fitting lines (in black).
7. At this stage you should determine whether your data fits the model. If it does not then changing the binding model (e.g.,



from 1:1 Langmuir to conformational change) may increase the accuracy of the data.

8. Each analyte concentration should present roughly the same kinetic data. It is useful then, to include standard deviation when presenting data.

---

## 4. Notes

1. It may be beneficial to incubate your proteins of choice at a range of temperatures for a range of times to estimate stability. Protein precipitation is easily observed after centrifugation at  $18,000 \times g$  for 10 min and assessing any “pellet” formation. Protein stability can also be visualized by SDS-PAGE analysis and the presence of high molecular weight aggregates or low molecular weight degradation fragments.
2. Purification systems are available for a wide range of tagged proteins (including histidine, glutathione-*S*-transferase, chitin-binding domain, or FLAG tags) and a range of commercial chromatography set-ups. The choice of system should be determined for each recombinant protein by the researcher, taking in to consideration solubility, expression levels, and yield.
3. Retaining several hundred microliters of culture until the end of the experiment is a clever strategy for preserving a highly expressing colony. Glycerol stocks can then be produced and stored at  $-80^{\circ}\text{C}$  and subsequent expression experiments can be initiated from this culture.
4. Retain 1 mL of media before inoculation for use as a blank.
5. The user should test a variety of IPTG concentrations and culture incubation temperatures to achieve optimum expression levels.
6. Complete protease inhibitors, DTT and PMSF should be added to the Resuspension buffer just prior to use. Crystals may form during freeze/thawing of PMSF aliquots. It is important to completely resuspend PMSF before addition to buffers.
7. The freezing and subsequent thawing of resuspended cultures increases cellular lysis. By leaving the tube on its side, the culture will freeze in a thin layer and thus reduce the time needed to thaw the culture the following morning.
8. Preparing SDS-PAGE gels before protein purification enables a quicker analysis and reduces the time that the purified protein remains on ice. Routinely, it becomes easier to prepare gels and store them at  $4^{\circ}\text{C}$  in a moistened paper towel wrapped in Saran wrap.

9. Bacterial cell lysis can be achieved by several methods in addition to chemical lysis (Lysozyme) including disruption by sonication and increased pressure (i.e., French Press). Optimum lysis conditions may have to be assessed empirically by the user.
10. We have found that three elutions in total should be sufficient to remove all bound recombinant protein, with most protein eluting in fractions 1 and 2 (**Fig. 2**). These elutions can be stored on ice in the 4°C cold-room overnight enabling more time to analyze subsequent SDS-PAGE gels.
11. Coomassie stain and Destain solutions can be reused multiple times, commonly for 1–2 months and the only consequences are longer incubation times to stain/destain each gel. Quicker destaining can be achieved by rapid change of Destain solutions.
12. Several problems can be encountered during gel drying. The most common is the cracking of gels due to trapped air bubbles or the presence of small tears. Also, gels will inevitably crack if they are wrapped too tightly in Saran wrap and so this should be avoided. Routinely, it was found that over drying gels can result in dehydration and cracking. For mini-gels, ~1 h drying time is sufficient.
13. There are a variety of dialysis buffers that can be used and should relate to the end point experiments that will be conducted and the properties of the proteins being studied. For SPR, it is useful to dialyze proteins directly into HBS buffer (Biacore, 10 mM HEPES, 150 mM NaCl, pH 7.4). This will result in smoother buffer exchange during SPR runs and reduce “buffer spikes” that are observed when different buffers are used.
14. A variety of commercial systems are available for SPR experiments. Furthermore, Biacore have a range of instruments (e.g. Biacore 2000, 3000, X) and different immobilization procedures/sensor chips can be followed/used that are out with the scope of this chapter (*see also* **Note 16**).
15. Many bioinformatic programs are available that can assess the pI of proteins (including ProtParam available at <http://www.expasy.org>).
16. A variety of immobilization methods are available depending on experimental set-up or nature of recombinant protein. For example, affinity tags (GST or Histidine) can be captured by direct antibody coupling to the sensor chip.
17. Regeneration steps may be arduous but successful selection of Regeneration buffers ensures a sensor chip surface with intact ligand protein protein/nobuild up of bound analyte protein that can be used multiple times.

18. Initial regeneration steps should be performed with mild Regeneration buffers for minimal contact times to ensure that over-stripping of ligand protein does not occur. The stringency of buffers can be increased easily during the procedure.
19. Different Regeneration buffers or injection protocols of the same Regeneration buffer may be needed to remove different bound analyte proteins and should be determined by the user.
20. Note that it is important to include a control flow cell that will be used as a blank and therefore subtracted from each analyte concentration. This may be a blank flow cell (activated and deactivated) or protein of similar molecular weight to ligand but of unrelated function.
21. Runs can be saved after completion. Depending on the sample number and each “cycle” time complete runs may take several hours, and it may be easier to perform experiments overnight.
22. It is beneficial to analyze/compare the first and the last run checking the baseline level. A rise or fall in this level indicates an accumulation of analyte protein or excessive removal of ligand and protein, respectively. This will affect your data analysis.
23. At this stage, it is smart to edit the file names to correspond exactly to each individual run. This will benefit the user during kinetic analyses of multiple analyte/ligand interactions.
24. The user may observe “spikes” due to differences in buffer composition (if analyte proteins have not been dialyzed into HBS).
25. Using “*split view*” may aid selection of the appropriate region of binding curves. For example, the “*ln[abs(dy/dx0)]*” tool enables observation of binding curves (that appear linear) exhibiting single-binding kinetics (6).

## References

1. Lavery, D.N. and McEwan, I.J. (2005) Structure and function of steroid receptor AF1 transactivation domains: induction of active conformations. *Biochem.J.*, **391**, 449–464.
2. Xu, J. and Li, Q. (2003) Review of the in vivo functions of the p160 steroid receptor coactivator family. *Mol.Endocrinol.*, **17**, 1681–1692.
3. Treuter, E., Johansson, L., Thomsen, J.S., Warnmark, A., Leers, J., Pelto-Huikko, M., Sjoberg, M., Wright, A.P., Spyrou, G. and Gustafsson, J.A. (1999) Competition between thyroid hormone receptor-associated protein (TRAP) 220 and transcriptional intermediary factor (TIF) 2 for binding to nuclear receptors. Implications for the recruitment of TRAP and p160 coactivator complexes. *J.Biol.Chem.*, **274**, 6667–6677.
4. Burakov, D., Wong, C.W., Rachez, C., Cheskis, B.J. and Freedman, L.P. (2000) Functional interactions between the estrogen receptor and DRIP205, a subunit of the heteromeric DRIP coactivator complex. *J.Biol.Chem.*, **275**, 20928–20934.
5. Rich, R.L., Hoth, L.R., Geoghegan, K.F., Brown, T.A., LeMotte, P.K., Simons, S.P., Hensley, P. and Myszka, D.G. (2002) Kinetic analysis of estrogen receptor/ligand interactions. *Proc. Natl.Acad.Sci.USA.*, **99**, 8562–8567.
6. Warnmark, A., Wikstrom, A., Wright, A.P., Gustafsson, J.A. and Hard, T. (2001) The

- N-terminal regions of estrogen receptor alpha and beta are unstructured in vitro and show different TBP binding properties. *J.Biol.Chem.*, **276**, 45939–45944.
7. Shatkina, L., Mink, S., Rogatsch, H., Klocker, H., Langer, G., Nestl, A. and Cato, A.C. (2003) The cochaperone Bag-1L enhances androgen receptor action via interaction with the NH2-terminal region of the receptor. *Mol.Cell.Biol.*, **23**, 7189–7197.
  8. Bradford, M.M. (1976) A rapid and sensitive method for the quantitation of microgram quantities of protein utilizing the principle of protein-dye binding. *Anal.Biochem.*, **72**, 248–254.
  9. Lavery, D.N. and McEwan, I.J. (2008) Functional characterization of the native NH2-terminal transactivation domain of the human androgen receptor: binding kinetics for interactions with TFIIIF and SRC-1a. *Biochemistry*, **47**, 3352–3359.

# Chapter 11

## Using RNA Interference to Study Protein Function

Carol D. Curtis and Ann M. Nardulli

### Abstract

RNA interference can be extremely useful in determining the function of an endogenously-expressed protein in its normal cellular environment. In this chapter, we describe a method that uses small interfering RNA (siRNA) to knock down mRNA and protein expression in cultured cells so that the effect of a putative regulatory protein on gene expression can be delineated. Methods of assessing the effectiveness of the siRNA procedure using real time quantitative PCR and Western analysis are also included.

**Key words:** RNA interference, siRNA, Transcription regulation, Gene silencing.

---

### 1. Introduction

Regulating gene expression in eukaryotic cells requires a complex array of proximal sequence-specific recognition sites and distal enhancer elements as well as the association of various populations of transcription factors and coregulatory proteins with these DNA regions. Together, these protein–DNA complexes modulate gene expression in response to various extracellular signals and changing cellular environments. The capacity of transcription factors and coregulatory proteins to influence gene expression has historically been defined by testing the effect of overexpressed proteins on expression of transiently-transfected heterologous promoters. In recent years, it has been possible to define the effects of endogenously-expressed proteins involved in regulating native gene expression by employing RNA interference (RNAi, **refs. 1, 2**). Using this method, an RNA transcript can be targeted for destruction by small interfering RNAs (siRNAs, **refs. 3–5**). An siRNA consists of 21 nucleotide coding and noncoding RNA

strands with 3' overhangs (6–8) and has a sequence identical to a small portion of a target cellular RNA (9). When transfected into cells, the siRNA is recognized by RNA-induced silencing complex (RISC), which initiates transcript-specific destruction resulting in the subsequent decrease of the corresponding protein (6, 7, 10). Thus, RNAi can allow one to determine the effect of a protein in a cell where the RNA and protein are normally expressed and involved in cellular function. We have found that knocking down the expression of a single protein involved in influencing transcription oftentimes differentially alters expression of endogenous target genes (11–15). Importantly, these studies have shown that transient transfections using heterologous promoters are unable to fully recapitulate the gene-specific effects of regulatory proteins on native gene expression and that siRNA experiments provide more biologically-relevant evidence of a protein's role in regulating gene expression than previous methods.

---

## 2. Materials

### 2.1. Preparation of Cultured Cells

1. Phenol red containing minimal essential medium, MEM (Gibco/Invitrogen, Carlsbad, CA): Supplement with 100  $\mu$ M nonessential amino acids (NEAA), 10 mM HEPES, 2 mM L-glutamine, 100 U/mL Penicillin, 100  $\mu$ g/mL Streptomycin, 25  $\mu$ g/mL Gentamicin, and 5% calf serum (Atlanta Biologicals, Lawrenceville, GA).
2. Hanks buffered salt solution, HBSS (Cellgro, Herndon, VA).
3. Trypsin/EDTA: Dilute a 10 $\times$  solution of 0.5% Trypsin and 7 mM EDTA (Gibco/Invitrogen, Carlsbad, CA) 1:10 in 1 $\times$  HBSS.
4. Phenol red-free MEM (Cellgro, Herndon, VA) with antibiotics and serum (PRF): Supplement with 100  $\mu$ M NEAA, 10 mM HEPES, 2 mM L-glutamine, 100 U/mL Penicillin, 100  $\mu$ g/mL Streptomycin, 25  $\mu$ g/mL Gentamicin and 5% charcoal dextran-treated calf serum. Calf serum (Atlanta Biologicals, Lawrenceville, GA) is treated with charcoal dextran to remove endogenous steroid hormones and growth factors.
5. Phenol red-free MEM without antibiotics (PRF-A): Supplement with 100  $\mu$ M NEAA, 10 mM HEPES, 2 mM L-glutamine (*see Note 1*) and 5% charcoal dextran-treated calf serum. Calf serum (Atlanta Biologicals, Lawrenceville, GA) is treated with charcoal dextran to remove endogenous steroid hormones and growth factors.

6. Phenol red-free MEM without antibiotics or serum (PRF-AS): Supplement with 100  $\mu$ M NEAA, 10 mM HEPES and 2 mM L-glutamine.

## **2.2. siRNA Transfection**

1. Control (*see Note 2*) and experimental (*see Note 3*) siRNA can be procured from a number of commercial vendors.
2. SiLentFect Lipid (BioRad, Hercules, CA), which we have found to be effective in transfecting siRNA into mammalian cell lines, is used in the protocol described. However, other transfection reagents can be utilized.

## **2.3. Preparation of Cell Lysate**

1. TNE: 40 mM Tris-HCl pH 7.5, 140 mM NaCl, 1.5 mM EDTA. Store at 25°C.
2. Lysis Buffer: 20 mM Tris-HCl pH 8.0, 200 mM NaCl, 1 mM EDTA, 0.2% (v/v) NP40. Make fresh from stock solutions.

## **2.4. Protein Assay**

1. 5 $\times$  Protein Assay Solution (BioRad, Hercules, CA): Dilute 1:5 in dH<sub>2</sub>O and run through a Whatman filter (Fisher Scientific, Pittsburgh, PA). Store the 5 $\times$  solution at 4°C. Make 1 $\times$  solution fresh as needed.
2. Bovine Serum Albumin, BSA (BioRad, Hercules, CA): Dissolve to a concentration of 12.5  $\mu$ g/mL in deionized water (dH<sub>2</sub>O) and store at 4°C. Standards are prepared by diluting the 12.5  $\mu$ g/mL BSA to 10, 7.5, 5, and 2.5  $\mu$ g/mL in dH<sub>2</sub>O.

## **2.5. SDS-Polyacrylamide Gel Electrophoresis (SDS-PAGE)**

1. Mini-PROTEAN 3 gel system (BioRad, Hercules, CA).
2. Separating Gel Mix: 10% acrylamide prepared from a 40% 37.5:1 acrylamide/bisacrylamide, 750 mM Tris base pH 8.8, 0.1% SDS. Store at 4°C. Acrylamide is a neurotoxin when unpolymerized and should be handled with care.
3. Stacking Gel Mix: 4% acrylamide prepared from a 40% 37.5:1 acrylamide/bisacrylamide, 125 mM Tris base pH 6.8, 0.1% SDS. Store at 4°C. Acrylamide is a neurotoxin when unpolymerized and should be handled with care.
4. Ammonium persulfate (APS) (30% (w/v)): Prepare in dH<sub>2</sub>O.
5. N,N,N,N'-tetramethyl-ethylenediamine (TEMED).
6. SDS Running Buffer: 25 mM Tris base, 192 mM glycine, 3.5 mM SDS. Store at 25°C.
7. SDS Sample Buffer (4 $\times$ ): 250 mM Tris-HCl pH 6.8, 300 mM SDS, 40% glycerin (v/v), 2% (v/v)  $\beta$ -mercaptoethanol, 0.02% (w/v) bromophenol blue. Store 1 mL aliquots at -20°C.
8. Prestained molecular weight markers, for example Kaleidoscope (BioRad, Hercules, CA).



**2.6. Western Blot**

1. Mini-Trans Blot Cell (BioRad, Hercules, CA).
2. Whatman paper, > 6  $\mu\text{m}$  retention.
3. GE Nitrocellulose Hybridization and Transfer Membrane, 0.45  $\mu\text{m}$  (Fisher Scientific, Pittsburgh, PA).
4. Transfer Buffer: 25 mM Tris base, 192 mM glycine, 3.5 mM SDS, 20% (v/v) methanol. Store at 4°C.
5. 5% Milk Solution: 50 mM Tris-HCl pH 7.5, 150 mM NaCl, 0.5 mM thimerosal, 0.5% (v/v) Tween-20, 5% (w/v) instant dry milk.
6. Wash Buffer: 50 mM Tris-HCl pH 7.5, 150 mM NaCl, 0.5 mM thimerosal, 0.5% (v/v) Tween-20.
7. Supersignal West Femto Maximum Sensitivity Substrate (Pierce, Rockford, IL).
8. Kodak BioMax XAR film (Fisher Scientific, Pittsburgh, PA).

**2.7. Stripping and Reprobing Blots**

1. Restore Western Blot Stripping Buffer (Pierce, Rockford, IL).
2. Wash Buffer: 50 mM Tris-HCl pH 7.5, 150 mM NaCl, 0.5 mM thimerosal, 0.5% (v/v) Tween-20.
3. 5% Milk Solution: 50 mM Tris-HCl pH 7.5, 150 mM NaCl, 0.5 mM thimerosal, 0.5% (v/v) Tween-20, 5% (w/v) instant dry milk.

**2.8. RNA Harvest and Isolation**

1. Trizol (Invitrogen, Carlsbad, CA). Trizol is toxic and should be used in a ventilation hood. Store at 4°C.
2. Chloroform. Chloroform is toxic and should be used in a ventilation hood. Store at 25°C.
3. Isopropanol: Store at 25°C.
4. Ethanol (75%): Prepare by mixing 37.5 mL ethanol and 12.5 mL dH<sub>2</sub>O (see [Note 4](#)). Store at 25°C.
5. RQ1 RNase-Free DNase (Promega, Madison, WI). Store at -20°C.
6. Phenol/Chloroform: Prepare phenol/chloroform/isoamyl alcohol at 25:24:1. Store at 4°C.
7. Ammonium acetate (NH<sub>4</sub>OAc): Prepare a 5 M stock in dH<sub>2</sub>O and store at 25°C.

**2.9. cDNA Preparation**

1. Reverse Transcription System (Promega, Madison, WI). Store at -20°C.

**2.10. Quantitative Real Time PCR**

1. iQ SYBR Green Supermix (BioRad, Hercules, CA).
2. iCycler Thermal Cycler (BioRad, Hercules, CA).

### 3. Methods

Performing RNA interference (RNAi) experiments in mammalian cells requires (1) a double-stranded siRNA that specifically targets the RNA transcript of interest, (2) an effective siRNA delivery system, (3) controls to ensure the specificity of the siRNA treatment, and (4) a biological assay to detect the effect of knocking down the target RNA. The amount of siRNA needed and the length of time required for destruction of the target RNA must be determined empirically and may vary with different cell lines and the confluency of the cells. A protein's turnover rate will also affect the length of time required to decrease its expression. We have found that knocking down expression of estrogen receptor  $\alpha$  (ER $\alpha$ ) associated proteins in MCF-7 breast cancer cells, which endogenously express ER $\alpha$  and the coregulatory proteins needed for estrogen-responsive gene expression, generally requires ~24 h but sometimes can take as long as 96 h (11–16).

The effectiveness of target siRNA in knocking down a specific mRNA transcript can be determined using quantitative real-time PCR (qRT-PCR). This is a straight-forward method in which cellular RNA is isolated and reverse transcribed to produce complementary DNA (cDNA). Amplification of the cDNA with gene-specific primers is then used to detect the levels of cDNA present. In addition to monitoring target mRNA levels, the target protein levels should also be examined to ensure that the biological moiety responsible for mediating a cellular response has been knocked down. Western blot analysis is useful for this purpose. Protein expression should be monitored in cells that have been exposed to target siRNA and to control siRNA.

Once the conditions needed to knock down a protein's expression have been determined, the biological consequence of reducing the target mRNA and protein can be defined. One common endpoint is monitoring gene expression, but protein activity can also be assessed. We typically monitor the expression of a number of estrogen-responsive genes in MCF-7 breast cancer cells that have been exposed to control or target siRNA in the absence or in the presence of 17 $\beta$ -estradiol (E<sub>2</sub>, refs. 11–16). In this manner, we can determine the effect of ER $\alpha$ -associated proteins on gene expression in a biologically-relevant cellular environment.

#### 3.1. Preparation of Cultured Cells

1. MCF-7 breast cancer cells are maintained in MEM in 75 cm<sup>2</sup> flasks and are passaged at confluency with 1 $\times$  trypsin/EDTA.
2. Two days before transfection, the cells are washed twice with HBSS and media is replaced with PRF.
3. The day before transfection, cells are washed twice with HBSS, trypsinized, resuspended in PRF, and seeded into a 12-well

plate at  $5 \times 10^5$  cells per well. The number of wells seeded will depend on the conditions being tested.

### 3.2. siRNA Transfection

1. Prepare a 5 mL polystyrene tube for the target siRNA and another for control siRNA. For each well to be transfected, mix 50 pmol siRNA (*see Note 5*) in 50  $\mu$ L PRF-AS (*see Note 1*). Prepare enough reagent for all of the target siRNA wells in one tube and all of the control siRNA wells in another tube in order to minimize well-to-well variation. For example, to transfect 6 wells of a 12-well plate with target siRNA, add 300 pmol target siRNA to 300  $\mu$ L PRF-AS. In another tube, add 300 pmol control siRNA to 300  $\mu$ L PRF-AS to transfect the other half of the 12-well plate.
2. In another polystyrene tube, combine 1.5  $\mu$ L SiLentFect Lipid with 52.5  $\mu$ L PRF-AS for each well to be transfected (*see Note 1*) and swirl gently. In order to limit well-to-well variation, prepare enough reagent for the target wells and the control wells in one tube. For example, to prepare enough reagent for one 12-well plate, combine 18  $\mu$ L SiLentFect Lipid and 630  $\mu$ L PRF-AS.
3. Add half of the diluted SiLentFect to the target siRNA tube and add the other half of the diluted SiLentFect to the control siRNA tube. Mix by swirling gently. *DO NOT VORTEX!* Incubate the mixture for 20 min at 25°C. The solutions will become turbid during this time.
4. During the incubation, carefully aspirate the media from the wells, wash the cells once with PRF-A and add 500  $\mu$ L fresh PRF-A to each well (*see Note 1*).
5. After the 20 min incubation, dispense 100  $\mu$ L of the siRNA/SiLentFect mixture dropwise into each well. The small amount of reagent remaining can be discarded.
6. Gently rock the plate back and forth to mix and place in a 37°C CO<sub>2</sub> incubator for the length of time needed to knock down target mRNA and protein levels (*see Note 6*). For example, although nonmetastatic protein 23 homolog 1 (NM23-H1) protein levels decrease slightly 24 h after siRNA transfection, 96 h is required to achieve an appreciable decrease in NM-3-H1 expression (**Fig. 1**).

### 3.3. Preparation of Cell Lysate

1. Remove the media from each well. Add 500  $\mu$ L TNE to each well. Pipet up and down 4–5 times to displace the cells. Transfer the cells to a 1.5 mL microcentrifuge tube.
2. Centrifuge at  $900 \times g$  for 5 min. Discard the supernatant and resuspend the cells in 30  $\mu$ L Lysis Buffer.
3. Place the resuspended cells on dry ice for 5 min or until frozen. Then incubate the cells at 25°C for 5 min or until thawed.

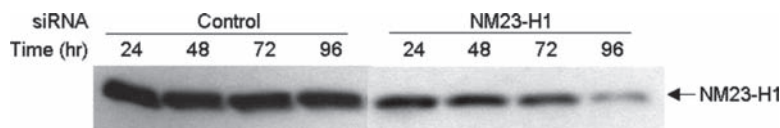


Fig. 1. Decreasing endogenous NM23-H1 protein levels. MCF-7 breast cancer cells were transfected with control siRNA, which targets renilla luciferase mRNA (which is not expressed in these cells) or with NM23-H1 siRNA, that targets NM23-H1 mRNA for destruction. After 24–96 h, cells were lysed and subjected to Western blot analysis with an NM23-H1 specific antibody.

Repeat the freeze/thaw step and spin down the cell debris by centrifugation at  $20,000 \times g$  for 10 min.

4. Transfer the cell lysate to a new tube and discard the pellet.

### 3.4. Protein Assay

1. Set up 11 disposable test tubes and add 1 mL of  $1\times$  protein assay solution to each tube. One tube is reserved for a blank.  $10\mu\text{L}$  of the 5 diluted BSA standards (12.5, 10, 7.5, 5, or  $2.5\mu\text{g}$ ) are dispensed in duplicate. Vortex.
2. Incubate at  $25^\circ\text{C}$  for 5 min.
3. Determine the absorbance of each protein standard at 595 nm using a spectrophotometer. Plot the standards on a curve with protein concentration on the  $x$ -axis and absorbance at 595 nm on the  $y$ -axis.
4. Bring  $1\text{--}2\mu\text{L}$  cell lysate to a total volume of  $10\mu\text{L}$  with  $\text{dH}_2\text{O}$  and combine with 1 mL  $1\times$  protein assay solution. Prepare in duplicate and vortex.
5. Incubate at  $25^\circ\text{C}$  for 5 min.
6. Measure the absorbance of each sample at 595 nm and use the standard curve to determine the protein concentration of each cell lysate.

### 3.5. SDS-Polyacrylamide Gel Electrophoresis (SDS-PAGE)

1. These instructions assume the use of a Mini-PROTEAN 3 gel system, but can be adapted to other systems. Before use, wash the glass plates with detergent, rinse extensively with deionized water, and allow the plates to dry completely.
2. Slide the dry glass plates into the casting frame with the short plate in front. Ensure that both plates are flush at the bottom and lock into place.
3. Prepare a 1.0-mm thick, 10% acrylamide gel by mixing 5 mL Separating Gel Mix with  $15\mu\text{L}$  of 30% APS and  $5\mu\text{L}$  of TEMED. Immediately pour the separating gel, leaving space for the stacking gel, and carefully overlay with  $\text{dH}_2\text{O}$ . Allow the gel to polymerize.

4. Once the gel has polymerized, pour off the dH<sub>2</sub>O.
5. Prepare the stacking gel by mixing 2 mL Stacking Gel Mix with 5  $\mu$ L of 30% APS and 2  $\mu$ L of TEMED. Immediately pour the Stacking Gel Mix on top of the polymerized separating gel and insert the comb. Allow the gel to polymerize.
6. Once the stacking gel has polymerized, remove the gel from the casting frame and pull out the comb. Gently rinse the wells with dH<sub>2</sub>O. Snap the gel into the electrode assembly with the short plate facing inward. Slide the gel and the electrode assembly into the clamping frame and lock into place.
7. Lower the assembly into the mini tank and fill the inner chamber with ~125 mL SDS Running Buffer. Add ~200 mL SDS Running Buffer to the lower buffer chamber of the mini tank. Using a syringe, rinse the wells with SDS Running Buffer.
8. Bring 20  $\mu$ g cell lysate to 15  $\mu$ L with 1 $\times$  Lysis Buffer. Add 5  $\mu$ L of 4 $\times$  SDS Sample Buffer. Heat samples at 95°C for 3 min.
9. Load the prestained molecular weight markers into the first well and 20  $\mu$ L of each sample into subsequent wells.
10. Place the lid on the mini tank and connect it to a power supply. Run the gel at 200 V for 45 min or until the dye front reaches the bottom of the gel.

### **3.6. Western Blot**

1. Several hours before beginning the transfer process, fill the plastic cooling unit with dH<sub>2</sub>O and store at -20°C until frozen. The filled cooling unit can also be stored at -20°C between runs.
2. Prepare to transfer the proteins from the gel to a nitrocellulose membrane. These instructions assume the use of the Mini-Trans Blot cell system. However, they can easily be adapted to other systems.
3. Place 2 Scotchgard pieces and 4 pieces of Whatman paper (cut to the size of the cassette) in cold Transfer Buffer.
4. Turn off the electrophoresis power supply and disconnect the gel system. Pour off the buffer and disassemble the apparatus. Remove the gel from the plate and discard the stacking gel.
5. Cut a piece of nitrocellulose to the size of the gel and carefully slide the nitrocellulose into the cold Transfer Buffer starting with one edge. Be sure to use clean gloves when handling the nitrocellulose.
6. Assemble the transfer sandwich. Place the black side of the gel holder cassette down. Place one piece of Scotchgard on the black side of the gel holder cassette, then place two pieces of Whatman paper on the Scotchgard. Lay the gel on

the Whatman paper and position the nitrocellulose on the gel. Place two pieces of Whatman paper on the nitrocellulose and complete the sandwich by positioning the last piece of Scotchgard on the Whatman paper. Remove any bubbles from the layers by rolling a Pasteur pipette back and forth over the sandwich. Close the cassette firmly and place the cassette in the module (*see Note 7*).

7. Remove the cooling unit from the freezer and place it in the tank. Position the module in the tank and add a small stir bar to the bottom. Fill the tank completely with cold Transfer Buffer.
8. Place the Mini-Trans Blot cell system on a magnetic stirrer. Set the magnetic stirrer on medium high to keep the ion distribution and temperature even in the tank. Place the lid on the tank and plug the cables into a power supply. Transfer for 1 h at 100 V at 4°C.
9. Disconnect the system from the power supply and disassemble the apparatus. Remove the nitrocellulose. The gel can be discarded or stained to verify that the proteins have transferred. Transfer of the prestained markers to the nitrocellulose membrane is also a good indicator that the proteins have been effectively transferred.
10. Place the blot in a 5% Milk Solution for ~30 min at 25°C with vigorous shaking. This process will block nonspecific binding of antibody to the membrane.
11. Prepare the primary antibody to detect the protein of interest by diluting the antibody in 5% Milk Solution (*see Note 8*). Incubate at 25°C for 1 h to overnight with vigorous shaking.
12. Discard the primary antibody and quickly rinse the blot with Wash Buffer (pour, swirl, and discard). Add 5 mL of Wash Buffer and place the blot on the shaker for 5 min at 25°C. Repeat the wash two times.
13. Dilute the secondary antibody in 5% Milk Solution (*see Note 8*). Incubate with the blot at 25°C for 1 h with vigorous shaking.
14. Discard the secondary antibody, rinse and wash as described in **Subheading 3.6, step 12**.
15. During the final wash, prepare the chemiluminescent substrate. We have found Supersignal West Femto Substrate (Pierce, Rockford, IL) to be extremely sensitive in detecting low abundance proteins (*see Note 9*).
16. Add the substrate to the blot and incubate at 25°C for 5 min.
17. Carefully remove the substrate mix with a pipette and wick away any remaining substrate with an absorbent tissue. Wrap the blot with one layer of plastic wrap. Tape the blot in the corner of an X-ray film cassette.

18. In a dark room, expose the blot to film for ~2–10 min depending on the intensity of the signal and develop the film. If possible, it is useful to demonstrate that the siRNA knocks down the target, but not a related protein. As seen in **Fig. 2**, NM23-H1 siRNA effectively reduces the level of NM23-H1 protein, but does not affect the expression of the related homolog NM23-H2.

### 3.7. Stripping and Reprobing Blots

1. The blot can be stripped and reprobed to determine the effect of siRNA knockdown on the expression of other proteins. It is necessary to verify that the target siRNA does not affect the expression of other proteins and that equal amounts of cell lysate have been added (*see Note 10*). As seen in **Fig. 2**, neither the NM23-H1 siRNA nor the E<sub>2</sub> alters expression of the housekeeping gene glyceraldehyde-3-phosphate dehydrogenase (GAPDH). Furthermore, the similarity in GAPDH levels in each of the lanes confirms that the lysates were evenly loaded.
2. Wash the blot with Wash Buffer for 10 min to fully rehydrate and remove any residual chemiluminescent substrate.
3. Transfer the blot to a small glass container with a tight seal. Add 5–10 mL of Stripping Buffer. Incubate with rotation at 37°C for 10 min.
4. Discard the Stripping Buffer and quickly rinse twice with Wash Buffer. Extensively wash the blot with Wash Buffer while vigorously shaking for 10 min at 25°C. Repeat twice.
5. Block the membrane in 5% Milk Solution for 30 min at 25°C. The membrane is then ready to be reprobed with another antibody as described in **Subheading 3.6**, steps 11–17.

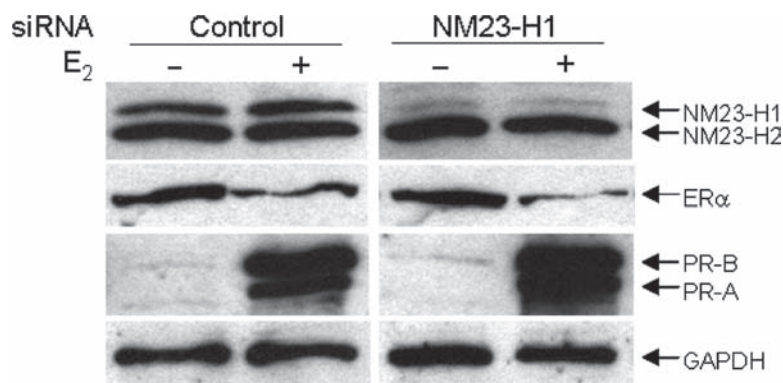


**Fig. 2.** Effect of knocking down NM23-H1 on protein levels. MCF-7 cells were transfected with control or NM23-H1 siRNA for 96 h. Cells were then treated with ethanol vehicle or 17 $\beta$ -estradiol (E<sub>2</sub>) for 24 h, lysed, and subjected to Western blot analysis with an antibody that recognizes NM23-H1 and NM23-H2, ER $\alpha$ , the progesterone receptors PR-A and PR-B, or GAPDH.



6. Monitor the expression of proteins of interest when cells have been exposed to control and target siRNA. As shown in [Fig. 2](#), the levels of ER $\alpha$  are decreased in the presence of E<sub>2</sub>, but are unaffected by the NM23-H1 siRNA. In contrast, expression of the estrogen-responsive progesterone receptors A and B (PR-A and PR-B) are increased when NM23-H1 is knocked down. The relative expression of a protein can be determined by using phosphorimager or infrared imaging analysis.

### 3.8. RNA Harvest and Isolation

1. Aspirate the media from the 12-well plate and replace with 500  $\mu$ L Trizol per well. Incubate for 5 min and collect the cells by pipetting up and down 4–5 times. Transfer the cell lysate to a 1.5 mL microcentrifuge tube (*see* [Note 11](#)).
2. Add 100  $\mu$ L chloroform and vortex at high speed for 30 s. Centrifuge at 20,000  $\times g$  for 15 min at 4°C.
3. Following centrifugation, transfer the colorless upper aqueous phase to a fresh tube being careful to leave the interface undisturbed.
4. Precipitate the RNA by adding an equal volume of isopropanol. Vortex at high speed for 30 s and incubate for 10 min at 25°C. Centrifuge at 20,000  $\times g$  for 10 min at 4°C. The RNA precipitate forms a gel-like pellet at the bottom of the tube.
5. Remove the supernatant and wash the pellet with 500  $\mu$ L of 75% ethanol. Vortex and centrifuge at 7000  $\times g$  for 5 min at 4°C.
6. Remove the supernatant and air dry the pellet for ~10 min at 25°C. DO NOT VACUUM DRY! Drying the RNA pellet completely will decrease its solubility.
7. Add 56.5  $\mu$ L dH<sub>2</sub>O to dissolve the RNA pellet (*see* [Note 12](#)). Place on ice.
8. Digest any residual DNA by adding 6.5  $\mu$ L of 10 $\times$  DNase buffer and 2  $\mu$ L RQ RNase-free DNase I enzyme to each tube. Incubate at 37°C for 30 min.
9. Add 35  $\mu$ L dH<sub>2</sub>O to bring to a final volume of 100  $\mu$ L. Add an equal volume of phenol/chloroform. Vortex at high speed for 30 s. Centrifuge at 20,000  $\times g$  for 2 min at 4°C. Transfer the upper phase to a new 1.5 mL microcentrifuge tube and discard the lower phase in a chemical waste container.
10. Add 15  $\mu$ L of 5 M NH<sub>4</sub>OAc and 287.5  $\mu$ L ethanol and precipitate the RNA at –20°C overnight.
11. Centrifuge at 20,000  $\times g$  for 30 min at 4°C. Discard the supernatant.
12. Wash the pellet with 700  $\mu$ L of 75% ethanol. Centrifuge at 20,000  $\times g$  for 10 min at 4°C. Air dry the pellet for 10–15 min at 25°C.
13. Resuspend the pellet in 24  $\mu$ L dH<sub>2</sub>O (*see* [Note 12](#)). Store at –20°C.

### 3.9. cDNA Preparation

1. The isolated RNA is used for cDNA synthesis. Determine the absorbance of each RNA sample at 260 nm using a spectrophotometer (*see Note 13*).
2. To prepare the RNA samples for cDNA synthesis, aliquot 0.5  $\mu$ g RNA from each sample into a 0.5 mL microcentrifuge tube, and add dH<sub>2</sub>O to a final volume of 10.5  $\mu$ L. If hormone or another treatment is used, a total of 4 tubes will be needed for the control siRNA in the absence and in the presence of hormone and target siRNA in the absence and in the presence of hormone.
3. Prepare a cDNA sample, which will be used to derive a standard curve for each primer set during qRT-PCR. Aliquot 2.0  $\mu$ g RNA from a control siRNA sample into another 0.5 mL microcentrifuge tube and add dH<sub>2</sub>O to a final volume of 10.5  $\mu$ L.
4. Vortex, spin briefly in a microcentrifuge and then place all samples on ice.
5. To limit variability, make a master mix with enough reagent for all of the samples. Each sample will include 4  $\mu$ L of 25 mM MgCl<sub>2</sub>, 2  $\mu$ L of 10 $\times$  Reverse Transcription buffer, 1  $\mu$ L of 10 mM dNTP, 0.5  $\mu$ L of RNasin Ribonuclease Inhibitor, 15 U of AMV Reverse Transcriptase, 0.5  $\mu$ L of Random Primers and dH<sub>2</sub>O to 9.5  $\mu$ L. The reagents should be combined in the order given in a single 0.5 mL microcentrifuge tube.
6. Aliquot 9.5  $\mu$ L of the master mix into each RNA-containing tube.
7. Incubate the reaction mixture at 42°C for 1 h and then at 95°C for 5 min (*see Note 14*). Chill on ice and then store at -20°C.

### 3.10. Quantitative Real Time PCR

1. These instructions assume the use of iQ SYBR Green Supermix and the iCycler Thermal Cycler, but can be adapted to other systems.
2. Design primers for the mRNA of interest (*see Note 15*) and dissolve in dH<sub>2</sub>O to a concentration of 10  $\mu$ M. Primers should be designed for the target mRNA to confirm that the siRNA has knocked down the transcript. As seen in **Fig. 3**, NM23-H1 mRNA levels are significantly decreased in the presence of the target siRNA containing NM23-H1 mRNA sequence, but not in the presence of control siRNA containing renilla mRNA sequence.
3. Primers should also be designed to assess the mRNA levels of genes of interest (*see Note 16*). As seen in **Fig. 3**, the estrogen-responsive *PR* gene is significantly enhanced when NM-3-H1 expression is decreased, which is consistent with the Western analysis shown in **Fig. 2**. In contrast, neither pS2 nor ER $\alpha$  mRNA levels are significantly altered by the NM23-H1 siRNA.

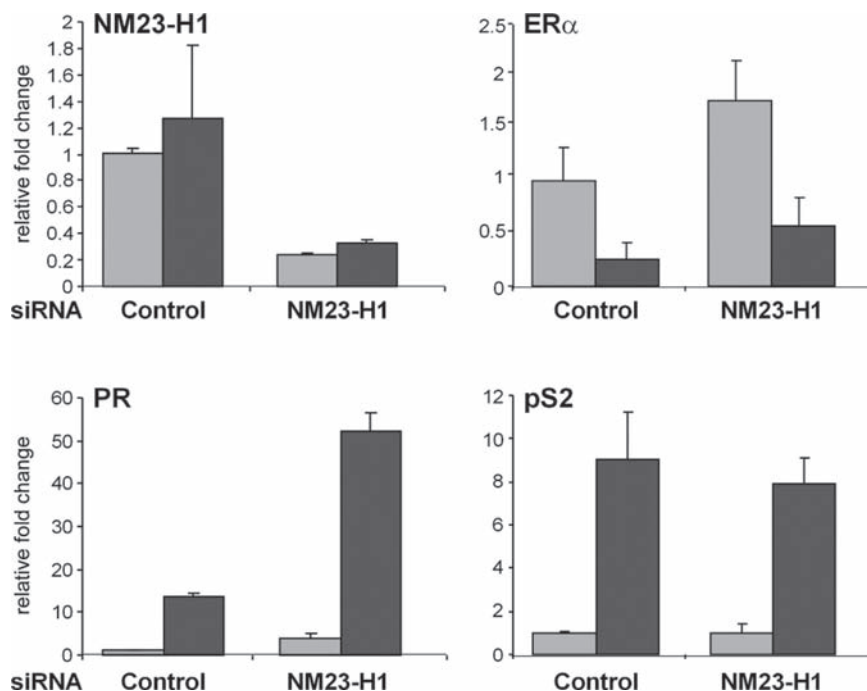


Fig. 3. Effect of decreased NM23-H1 on cellular mRNA levels. MCF-7 cells were transfected with control or NM23-H1 siRNA for 96 h, treated with ethanol vehicle (*light gray bars*) or E<sub>2</sub> (*dark gray bars*) for 24 h, and lysed. RNA was isolated, cDNA was synthesized, and qRT-PCR was carried out with gene-specific primers. Relative fold change was determined using the comparative Ct method and the housekeeping gene, 36B4, as the internal control. Data from one experiment, which had been done in triplicate, is presented as the mean  $\pm$  SD.

4. Dilute the cDNA samples prepared in Subheading 11.3.9, step 2 (0.5  $\mu$ g) 1:5 in dH<sub>2</sub>O (*see Note 17*).
5. Dilute the cDNA prepared in **Subheading 3.9, step 3** (2.0  $\mu$ g) 1:5 in dH<sub>2</sub>O. Next, make three 1:10 serial dilutions in dH<sub>2</sub>O (*see Note 18*).
6. Make a master mix with enough reagents for all of the qRT-PCR standards and samples, which are run in triplicate. Each reaction consists of 12.5  $\mu$ L of 2 $\times$  iQ SYBR Green Supermix, 9.5  $\mu$ L dH<sub>2</sub>O, 1  $\mu$ L of 10  $\mu$ M Forward primer and 1  $\mu$ L of 10  $\mu$ M Reverse primer.
7. Prepare a 96-well plate for qRT-PCR. Aliquot 24  $\mu$ L of the master mix per well and add 1  $\mu$ L cDNA into each well. Make sure to keep track of the placement of each sample.
8. Place the plate into the iCycler and start the program.
  - Cycle 1, 3 min 95°C
  - Cycle 2, 40 times
    - 10<sup>s</sup> 95°C Denaturation
    - 30 s 56°C Annealing (*see Note 19*)
    - 10 s 72°C Extension

Cycle 3, 1 min 95°C

Cycle 4, 1 min 50°C

Cycle 5, 45 times Melt Curve 1°C/10 s 50°C

9. Analyze the data using the standard curve to ensure that the efficiency of the primers is sufficient (*see* **Note 19**). The melting curve of each amplicon should be examined to help ensure that a single product has been produced. Southern blot analysis can also be used to verify that the correct target sequence has been amplified.
10. The comparative Ct method (*see* **Note 20**) is useful in analyzing qRT-PCR data because it takes into consideration an internal housekeeping gene (*see* **Note 16**). Each of the samples shown in **Fig. 3** has been normalized for 36B4 expression using the comparative Ct method.

---

## 4. Notes

1. Antibiotic free media (PRF-A and PRF-AS) should be used just prior to the time of siRNA addition until the time of harvest.
2. The control siRNA should not be present in any endogenous cellular transcript and is used to demonstrate that neither the transfection reagent nor the procedure alters gene expression. A number of pretested control siRNAs such as renilla luciferase (Ambion, Austin, TX), which is used in **Figs. 1–3**, are available commercially. A scrambled siRNA sequence can also be used as a negative control, but care must be taken to ensure that the scrambled sequence will not recognize any endogenously-expressed mRNA sequence. BLAST searches (<http://www.ncbi.nlm.nih.gov/blast/Blast.cgi>) should be used to determine whether other mRNA or genomic sequences might be targeted. If overlap does exist, the sequence of the target siRNA and the mRNA transcript should have at least 2–3 mismatches.
3. Guidelines for designing target siRNA duplexes have been described in detail by the Tuschl laboratory (<http://www.rockefeller.edu/labheads/tuschl/sirna.html>) and on various company Websites. While it was previously necessary to design and order target siRNAs for each gene of interest, there are now several commercial suppliers that offer validated siRNAs, which have been tested for effectiveness in reducing target mRNA levels, and predesigned siRNAs, which have not been tested experimentally. All of the validated

siRNAs we have used to date have been effective in knocking down mRNA and protein expression. If nonvalidated, pre-designed siRNAs are used, two different target siRNAs should be tested.

4. Solutions used for RNA and cDNA procedures should be prepared with deionized (resistivity of 18.2 M $\Omega$ -cm and total organic content < 10 ppb) and autoclaved water, which is referred to as “dH<sub>2</sub>O” in this text. All solutions, reagents, and supplies used for RNA work should be RNase free.
5. Fifty picomole per well (100 nM) of a 21mer is generally a good starting point, but may need to be increased to effectively knock down the protein of interest or decreased so that it does not have unintended effects on the expression of other mRNA species.
6. The length of time needed to knock down the target mRNA and protein levels must be determined empirically and may range from 24 to 96 h. Although qRT-PCR can determine whether the target mRNA level has been reduced, it is important to ensure that the target protein is effectively knocked down as well. If used, hormone is added to the media after the protein has been effectively knocked down, and the plate is incubated for the length of time required for the biological endpoint being examined. Although siRNAs are effective in reducing target protein expression for ~3–5 days, it may be necessary to knock down expression of a protein for a week or more. In this case, short hairpin RNA (shRNA) expression vectors with antibiotic resistance can be utilized (17–19). Interpretation of these experiments may be difficult; however, since a change in the biological endpoint may not necessarily be attributed to the absence of the target protein, but may reflect a change in expression of another cellular protein whose presence or activity is affected by the target protein.
7. Make certain that the nitrocellulose membrane is placed between the gel and the anode. If the sandwich is not appropriately oriented or is inserted into the apparatus backward, the proteins will be eluted into the buffer rather than being transferred to the nitrocellulose membrane.
8. Primary and secondary antibody dilutions and incubation conditions must be determined individually. We typically start with primary antibody dilutions of 1:2,000–40,000 and secondary antibody dilutions of 1:5,000–100,000.
9. The Pierce chemiluminescent substrate is prepared at a 1:1 ratio of solutions 1 and 2. Approximately 25  $\mu$ L of this chemiluminescent substrate mix is needed for each cm<sup>2</sup> of nitrocellulose membrane. For example, a 5  $\times$  7 cm blot = 35 cm<sup>2</sup>  $\times$  25  $\mu$ L/cm<sup>2</sup> = 875  $\mu$ L. Thus, use 437.5  $\mu$ L each of Solution 1 and 2.

10. A protein (such as GAPDH or  $\beta$ -actin) that is unaffected by siRNA knockdown of the protein of interest should be used to verify that samples have been equally loaded. This loading control also helps to ensure that the target siRNA is specific.
11. Cell lysate may be stored in Trizol at  $-80^{\circ}\text{C}$  for up to 1 month.
12. Pass the RNA pellet through a  $200\ \mu\text{L}$  pipette tip 8–10 times to dissolve. If the pellet is difficult to resuspend, incubate at  $55\text{--}60^{\circ}\text{C}$  for 10 min, and draw through a pipette 8–10 times.
13. An  $A_{260}/A_{280}$  ratio of 2.0 indicates that the RNA is pure. However, an  $A_{260}/A_{280}$  ratio of 1.8–2.0 is acceptable for use in cDNA synthesis. To determine RNA concentration, use the following equation:
 
$$\text{RNA concentration } (\mu\text{g}/\mu\text{L}) = [(Abs_{260})(43\ \mu\text{g}/\text{mL}) \text{ (dilution factor)}]/1,000$$
14. A thermocycler can be programmed to carry out the reverse transcription reaction.
15. It is very important to use the mRNA or cDNA sequence when designing primers and not the DNA sequence which may contain an intronic sequence that is not transcribed. Amplicons of  $\sim 100$  bp in length are efficiently produced. Longer length amplicons are acceptable, but generally should not exceed 250 bp.
16. Gene-specific primers are used to monitor endogenous gene expression after cells have been exposed to the target or control siRNA. It is also essential to monitor the expression of a gene that is unaffected by the siRNA treatment to ensure that the effects of the target siRNA are specific. When choosing a control gene, it is important to keep in mind that the gene should not be affected by any treatment used. Commonly used housekeeping genes might include GAPDH,  $\beta$ -actin or 36B4, which was used in the experiments shown in [Fig. 3](#).
17. cDNA concentration =  $0.5\ \mu\text{g}/20\ \mu\text{L}$ . After 1:5 dilution, cDNA concentration =  $0.5\ \mu\text{g}/100\ \mu\text{L}$  or  $5\ \text{ng}/\mu\text{L}$ .
18. For the standard curve: cDNA concentration =  $2.0\ \mu\text{g}/20\ \mu\text{L}$ . After 1:5 dilution, cDNA concentration =  $2.0\ \mu\text{g}/100\ \mu\text{L}$  or  $20\ \text{ng}/\mu\text{L}$ . Three 1:10 serial dilutions will produce standards of 2, 0.2 and  $0.02\ \text{ng}/\mu\text{L}$ . By running standards in parallel, it is possible to determine the initial number of RNA transcripts present in the experimental wells.
19. The annealing temperature of individual primer sets will vary, but optimal annealing temperatures are generally provided

by primer design software. The ideal primer set will have a standard curve  $r$ -value  $> 0.980$  and an efficiency of 90–110%. An efficiency value significantly larger than 100% indicates the formation of primer dimers.

20. In qRT-PCR, the threshold cycle (Ct) refers to the point where the fluorescence generated within a reaction reaches threshold, indicating that the number of copies has accumulated significantly. Each well is assigned a Ct value and it can be used to compare copy number between samples. Thus,  $\Delta\Delta Ct = \Delta Ct_{t, \text{sample}} - \Delta Ct_{t, \text{reference}}$ , where  $\Delta Ct_{t, \text{sample}}$  is the Ct value for any sample normalized to the housekeeping gene and  $\Delta Ct_{t, \text{reference}}$  is the Ct value for the control siRNA vehicle treated sample also normalized to the housekeeping gene. Relative fold change is  $2^{-\Delta\Delta Ct}$ .

---

## Acknowledgments

We are grateful to J. Bonéy Montoya, A. Rao, D. Thorngren, and Y. Ziegler for assistance in the preparation of this manuscript. This work was supported by NIH grant R01 DK 53884 (to AMN).

## References

1. Harborth, J., Elbashir, S. M., Beichert, K., Tuschl, T., and Weber, K. (2001) Identification of essential genes in cultured mammalian cells using small interfering RNAs. *J Cell Sci* **114**, 4557–65.
2. Harborth, J., Elbashir, S. M., Vandenburg, K., Manninga, H., Scaringe, S. A., Weber, K., and Tuschl, T. (2003) Sequence, chemical, and structural variation of small interfering RNAs and short hairpin RNAs and the effect on mammalian gene silencing. *Antisense Nucleic Acid Drug Dev* **13**, 83–105.
3. Fire, A., Xu, S., Montgomery, M. K., Kostas, S. A., Driver, S. E., and Mello, C. C. (1998) Potent and specific genetic interference by double-stranded RNA in *Caenorhabditis elegans*. *Nature* **391**, 806–11.
4. Montgomery, M. K., and Fire, A. (1998) Double-stranded RNA as a mediator in sequence-specific genetic silencing and co-suppression. *Trends Genet* **14**, 255–8.
5. Tuschl, T., Zamore, P. D., Lehmann, R., Bartel, D. P., and Sharp, P. A. (1999) Targeted mRNA degradation by double-stranded RNA in vitro. *Genes Dev* **13**, 3191–7.
6. Bernstein, E., Caudy, A. A., Hammond, S. M., and Hannon, G. J. (2001) Role for a bidentate ribonuclease in the initiation step of RNA interference. *Nature* **409**, 363–6.
7. Elbashir, S. M., Harborth, J., Lendeckel, W., Yalcin, A., Weber, K., and Tuschl, T. (2001) Duplexes of 21-nucleotide RNAs mediate RNA interference in cultured mammalian cells. *Nature* **411**, 494–8.
8. Elbashir, S. M., Lendeckel, W., and Tuschl, T. (2001) RNA interference is mediated by 21- and 22-nucleotide RNAs. *Genes Dev* **15**, 188–200.
9. Jackson, A. L., Bartz, S. R., Schelter, J., Kobayashi, S. V., Burchard, J., Mao, M., Li, B., Cavet, G., and Linsley, P. S. (2003) Expression profiling reveals off-target gene regulation by RNAi. *Nat Biotechnol* **21**, 635–7.
10. Schwarz, D. S., Tomari, Y., and Zamore, P. D. (2004) The RNA-induced silencing complex is a Mg<sup>2+</sup>-dependent endonuclease. *Curr Biol* **14**, 787–91.



11. Curtis, C. D., Likhite, V. S., McLeod, I. X., Yates, J. R., and Nardulli, A. M. (2007) Interaction of nonmetastatic protein 23 homolog H1 and estrogen receptor alpha alters estrogen-responsive gene expression and DNA nicking. *Cancer Res* **67**, 10600–7.
12. Marzouk, S., Schultz-Norton, J., McLeod, I., Yates, J., and Nardulli, A. (2007) Rho GDP dissociation inhibitor alpha interacts with estrogen receptor alpha and influences estrogen responsiveness. *J Mol Endocrinol* **39**, 249–59.
13. Rao, A. K., Ziegler, Y. S., McLeod, I. S., Yates, J. R., and Nardulli, A. M. (2008) Effects of Cu/Zn Superoxide Dismutase (SOD1) on estrogen responsiveness and oxidative stress in human breast cancer cells. *Mol Endocrinol* **22**, 1113–1124.
14. Schultz-Norton, J. R., McDonald, W. H., Yates, J. R., and Nardulli, A. M. (2006) Protein disulfide isomerase serves as a molecular chaperone to maintain estrogen receptor  $\alpha$  structure and function. *Mol Endocrinol* **20**, 1982–95.
15. Schultz-Norton, J. R., Walt, K. A., Ziegler, Y. S., McLeod, I. X., Yates, J. R., Raetzman, L. T., and Nardulli, A. M. (2007) The DNA repair protein flap endonuclease-1 (FEN-1) modulates estrogen-responsive gene expression. *Mol Endocrinol* **21**, 1569–80.
16. Schultz-Norton, J. R., Gabisi, V. A., Ziegler, Y. S., McLeod, I. X., Yates, J. R., and Nardulli, A. M. (2007) Estrogen receptor alpha interaction with the DNA repair protein proliferating cell nuclear antigen (PCNA). *Nucleic Acids Res* **35**, 5028–38.
17. Brummelkamp, T. R., Bernards, R., and Agami, R. (2002) Stable suppression of tumorigenicity by virus-mediated RNA interference. *Cancer Cell* **2**, 243–7.
18. Brummelkamp, T. R., Bernards, R., and Agami, R. (2002) A system for stable expression of short interfering RNAs in mammalian cells. *Science* **296**, 550–3.
19. Paddison, P. J., Caudy, A. A., Bernstein, E., Hannon, G. J., and Conklin, D. S. (2002) Short hairpin RNAs (shRNAs) induce sequence-specific silencing in mammalian cells. *Genes Dev* **16**, 948–58.

# Chapter 12

## Using Intrinsic Fluorescence Emission Spectroscopy to Study Steroid Receptor and Coactivator Protein Conformation Dynamics

Kate Watt and Iain J. McEwan

### Abstract

X-ray crystallography and nuclear magnetic resonance (NMR) spectroscopy have proved powerful methods for studying the structure of the isolated ligand and DNA-binding domains of nuclear receptors. However, the N-terminal domain (NTD), which in some members of the superfamily is important for transcriptional regulation, and the full-length receptor proteins have proved more challenging. The NTD of different nuclear receptors show little sequence homology and can vary dramatically in length from a few to several hundred amino acids. Low resolution structural analysis using circular dichroism, NMR, steady-state fluorescence spectroscopy, and Fourier transformed infrared spectroscopy has provided valuable information on the conformation and folding of the structurally plastic NTD. In this chapter, we discuss protocols for measuring the intrinsic fluorescence emission spectrum for tryptophan residues under different experimental conditions of protein folding and unfolding.

**Key words:** Steroid hormones, Androgen receptor, Activation function 1, Steroid receptor coactivator 1, Acrylamide quenching, Basic-helix-loop-helix PAS domains.

---

### 1. Introduction

Understanding the structure and conformational properties of nuclear receptors (NR) is an important aspect of determining their molecular mechanism of action. High resolution structures determined by X-ray crystallography or nuclear magnetic resonance (NMR) spectroscopy are available for the isolated ligand-binding (LBD) and DNA-binding (DBD) domains (*see refs. 1, 2 and references therein*). However, to date, these methods

have been unsuccessful at providing three-dimensional structural information for the N-terminal domain (NTD), any two-domain receptor molecule or indeed an intact receptor protein. A number of reasons may explain this lack of progress, including structural plasticity, difficulties in purifying large quantities of homogenous protein sample and in the case of NMR, restrictions on the size of polypeptides that can be easily analysed.

**Table 1**  
**Analysis of secondary and tertiary structure of nuclear receptors using spectroscopy techniques**

Receptor	Domain(s)	Method <sup>a</sup>	Structural information	Refs.
AR	NTD/AF1	Far UV CD	Secondary structure	(15)
		Fluorescence	Local tertiary structure; folding/unfolding	
		FTIR	Secondary structure	(17)
	NTD-DBD	Fluorescence	Local tertiary structure	(18)
ER $\alpha/\beta$	NTD/ AF1 Full-length	Far UV CD	Secondary structure	(19–21)
		Fluorescence	Tertiary structure; folding	
GR	AF1 NTD-DBD	Far UV CD	Secondary structure	(22)
		Near UV CD	Tertiary structure	(14)
		FTIR	Secondary structure	(23)
		Fluorescence	Tertiary structure; folding/unfolding	(14)
		NMR	Secondary structure; folding/unfolding	(22, 23)
PR	NTD NTD-DBD	Far UV CD	Secondary structure	(24)
PPAR $\alpha$	NTD/AF1	Far UV CD	Secondary structure	(25)

<sup>a</sup>CD circular dichroism, FTIR Fourier transformed infrared spectroscopy, NMR nuclear magnetic spectroscopy

To get round these difficulties a range of spectroscopy methods have been employed successfully by a number of laboratories to probe the conformational dynamics of intact receptor proteins or the isolated NTD/AF1 domain and to provide low resolution structural information (**Table 1**). The data obtained from these analyses has proved very valuable in building up models for the folding of the NTD or a two-domain polypeptide consisting of the NTD and DBD of a number of steroid receptors (reviewed in **refs. 3–5**).

NR function primarily as transcription factors to positively or negatively regulate patterns of gene expression in target cells. Once bound to specific DNA response elements, the receptor makes multiple direct and indirect interactions through coregulatory proteins with the transcription machinery. Protein targets serving as coactivators for the receptor can act to modify chromatin structure through specific enzyme activities (i.e., acetylation) or function as bridging factors to help recruit or stabilize the formation of a preinitiation complex involving general transcription factors and the RNA polymerase II enzyme (**6, 7**). The available structural information for coregulatory proteins alone (e.g. **ref. 8**) or interacting with each other (e.g. **ref. 9**) or binding to the surface of the nuclear receptor LBD (e.g. **refs. 10–12**) has relied on the use of small peptides or polypeptide fragments. Again in order to gain a better understanding of the mechanism of action of this diverse group of proteins, it will be necessary to determine structural properties in the absence or presence of a NR-binding partner. In this chapter, we describe the use of intrinsic fluorescence emission spectroscopy to study the structural dynamics of receptor (**Fig. 1**) and coactivator (**Fig. 2**) folding (*see Note 1*).

---

## 2. Materials

### **2.1. Expression and Purification of Recombinant Proteins**

1. Suitable bacterial expression plasmids (*see Note 2*).
2. BLR(DE3) expression cells (Novagen).
3. Lauria Bertani (LB) medium: 1% (w/v) Bacto-tryptone, 1% (w/v) yeast extract, 1% (w/v) NaCl. Sterilize by autoclaving.
4. SOC Medium: 2% (w/v) tryptone, 0.5% (w/v) yeast extract, 0.5% (w/v) NaCl, 5 mM MgSO<sub>4</sub>, 10 mM MgCl<sub>2</sub>, 0.4% (w/v) glucose. Sterilize by autoclaving.
5. Isopropyl- $\beta$ -D-thiogalactopyranoside (IPTG) (Melford Laboratories Ltd).
6. Phenylmethanesulfonyl fluoride (PMSF) (Sigma-Aldrich Company Ltd).
7. Dithiothreitol (DTT) (Melford Laboratories Ltd).

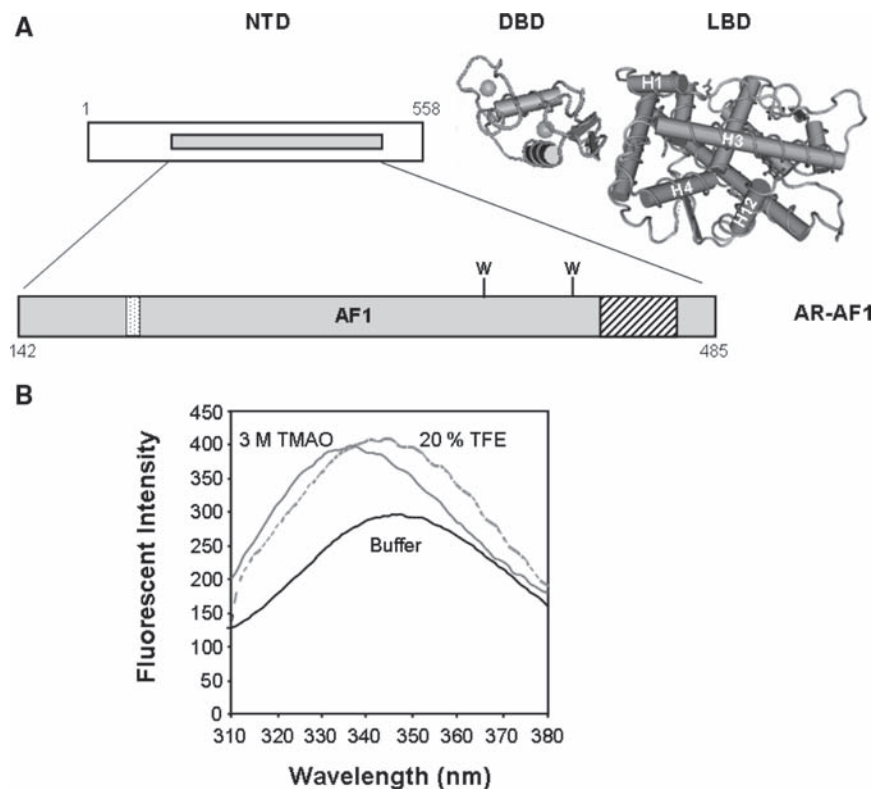


Fig. 1. Steady-state fluorescence analysis of the androgen receptor AF-1 domain. **A** Schematic representation of the human androgen receptor (AR), showing the stably folded ligand-binding (LBD) and DNA-binding domains and the structurally plastic N-terminal domain (NTD). The activation function (AF) 1 is shown in detail, with the two tryptophans at positions 396 and 432 and a short poly-glutamine repeat (*stippled box*) and poly-glycine repeat (*hatched box*) illustrated. **B** Steady-state tryptophan emission spectra for 30  $\mu\text{g}/\text{mL}$  AR-AF1 in buffer ( $\lambda_{\text{ex}}$  295 nm), 3 M TMAO ( $\lambda_{\text{ex}}$  287 nm), and 20% (v/v) TFE ( $\lambda_{\text{ex}}$  295 nm). The  $\lambda_{\text{max}}$  for tryptophan blue shifts from 346 nm (buffer) to 339 nm (TMAO) and 341 nm (TFE), indicating the tryptophan become less solvent exposed in the presence of the structure stabilizing agents. There is also a significant increase in the fluorescence intensity.

8. Resuspension Buffer: 20 mM Tris-HCl pH 8.0, 50 mM NaCl, 1 mM EDTA. Immediately prior to use add PMSF (final concentration 2 mM) and DTT (final concentration 1 mM).
9. Ni-NTA Agarose (Qiagen).
10. DNaseI (Roche Molecular Biochemicals).
11. RNaseA (Roche Molecular Biochemicals).
12. Ni-NTA Binding buffer: 20 mM Tris-HCl, pH 7.9, 500 mM NaCl, 5% (v/v) glycerol, 5 mM Imidazole.
13. Ni-NTA Wash buffer: 20 mM Tris-HCl, pH 7.9, 500 mM NaCl, 5% (v/v) glycerol, 60 mM Imidazole.

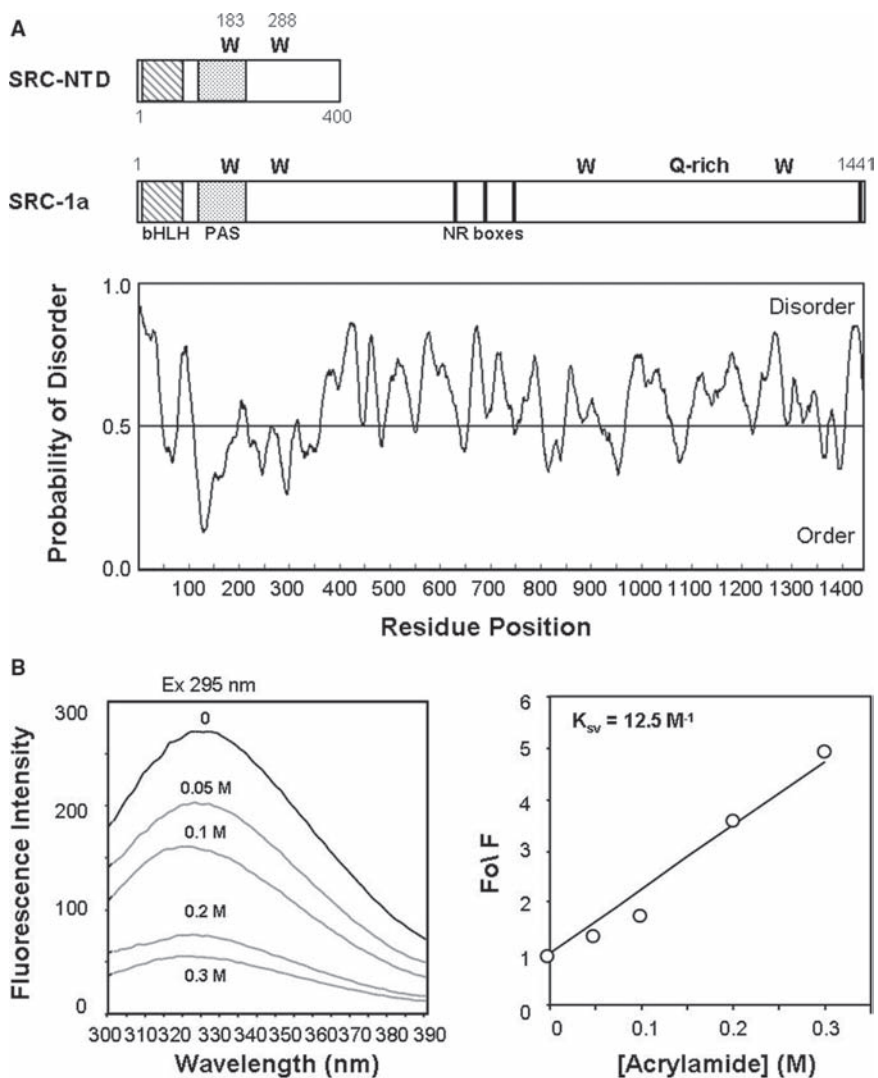


Fig. 2. Steady-state fluorescence analysis of the coactivator protein SRC-1a. **A** Schematic representation of the p160 protein SRC-1a showing the basic-helix-loop-helix (bHLH) and Per-ARNT-Sim (PAS) domains in the NTD. The location of four tryptophan residues are indicated together with the location of four LxxLL nuclear receptor binding motifs (*Black box*). The SRC-NTD, amino acids 1–400 and tryptophans 183 and 288 is shown in detail above. The *bottom panel* shows a PONDR plot for the prediction of natural disordered structure (values above 0.5 threshold). This indicates that the SRC-1-NTD is predicted to be relatively structured, but the remainder of the protein has significant levels of natural disordered structure. **B** Steady-state tryptophan emission spectra for 10  $\mu\text{g/mL}$  SRC-NTD after  $\lambda_{\text{ex}}$  295 nm in the absence (0) or presence of increasing amounts of acrylamide. A linear plot of  $F_0/F$  against  $[Q]$  and the calculated Stern-Volmer constant ( $K_{sv}$ ) of  $12.5/\text{M}^{-1}$  (see [Note 11](#)).

14. Ni-NTA Elution buffer: 20 mM Tris-HCl, pH 7.9, 500 mM NaCl, 5% (v/v) glycerol, 200 mM Imidazole.
15. BSA Fraction V (Sigma-Aldrich Company Ltd).
16. Bradford Protein Assay Reagent (Bio-Rad Laboratories).

### 2.2. Steady State Tryptophan Emission Spectra

1. Trimethylamine *N*-oxide (TMAO) (Sigma-Aldrich Company Ltd) (*see* [Note 3](#)).
2. 2,2-Trifluoroethanol (TFE) (Sigma-Aldrich Company Ltd).
3. Urea.
4. PBS tablets. (Sigma-Aldrich Company Ltd): 0.01 M phosphate buffer, pH 7.4, 0.0027 M KCl, 0.137 M NaCl.
5. UV Quartz cuvettes (Fisher Scientific UK).
6. Hellma ultra micro fluorescent cell (Fisher Scientific UK).
7. Spectrofluorometer: Shimadzu RF-1501.

### 2.3. Acrylamide Quenching

1. Acrylamide (*see* [Note 4](#)).

---

## 3. Methods

### 3.1. Expression and Purification of Recombinant Proteins

#### 3.1.1. Transformation of Plasmid into Expression Plasmid

1. Gently mix 1  $\mu$ L of the NR expression plasmid (i.e. pET-AR-AF1; [Fig. 1A](#)) or coactivator expression plasmid (i.e. pET-SRC-1a-NTD; [Fig. 2A](#)) with 40  $\mu$ L BLR(DE3) *Escherichia coli* expression cells and incubate on ice for 30 min.
2. Transform by heat shocking the reaction at 42°C for 45 s and return to ice for 2 min.
3. Add 1 mL of room temperature SOC to the cells and incubate in a shaking incubator for 60 min at 37°C.
4. Plate out 200  $\mu$ L of the mix on antibiotic selective LB plates and incubate overnight (16 h) at 37°C.

#### 3.1.2. Large-Scale Induction of *E. Coli* Cells

1. Take 200  $\mu$ L of an initial overnight culture from colonies that are found to be expressing the desired protein and use to inoculate a 25 mL LB plus antibiotic plus 0.5% (w/v) glucose overnight culture (*see* [Note 5](#)).
2. Dilute this culture 1:20 into 200 mL LB plus antibiotic plus 0.5% (w/v) glucose and grow at 37°C with shaking until an optical density  $A_{600\text{nm}}$  between 0.4 and 0.6 is reached.
3. Induce with 1 mM IPTG (final concentration) for 90 min at 37°C with shaking (*see* [Note 6](#)).
4. Harvest cells at 6000  $\times g$  for 15 min and resuspend the pellet in 5 mL of resuspension buffer and freeze at -80°C overnight.

#### 3.1.3. Purification of His-Tagged Proteins by Nickel-Agarose Affinity Chromatography

1. Thaw frozen cells on ice and treat with lysozyme at a concentration of 0.5 mg/mL at 4°C for 15 min followed by 100  $\mu$ g DNase I, 10  $\mu$ g RNase A, MnCl<sub>2</sub> to 10 mM, and MgCl<sub>2</sub> to 10 mM for a further 15 min at 4°C.



2. Centrifuge at  $4000 \times g$  for 20 min at  $4^{\circ}\text{C}$ .
3. Apply the supernatant containing recombinant proteins to a column containing 1 mL packed volume of Ni-NTA agarose at  $4^{\circ}\text{C}$  (a small sample of the flow through may be kept for analysis by SDS-PAGE).
4. Wash the column with  $10\times$  bed volumes of Ni-NTA binding buffer (a small sample of the binding flow through may be kept for analysis by SDS-PAGE).
5. Wash the column with  $5\times$  bed volumes of wash buffer (a small sample of the wash flow through may be kept for analysis by SDS-PAGE).
6. Elute the proteins from the column with  $3 \times 1$  mL of elution buffer and store on ice. Add protease inhibitors immediately to each eluted sample (*see Note 7*).
7. Take samples of the eluates, and saved fractions from **Steps 3** to 5, and analyze by SDS-PAGE.
8. The eluted fraction(s) containing the highest purity and/or yield of recombinant protein is(are) dialysed against an excess of PBS at  $4^{\circ}\text{C}$  (*see Note 8*). Proteins can then be stored at  $-20^{\circ}\text{C}$  or snap frozen and stored at  $-80^{\circ}\text{C}$ .
9. The concentration of the dialysed protein is estimated by the Bradford assay using BSA standards (**Subheading 3.1.4**). The Bradford colorimetric assay is a very fast, fairly accurate method of protein determination which uses a small amount of protein. The purity of the recombinant proteins can be confirmed by SDS-PAGE and staining with Coomassie blue and the dried gels scanned and the relative amounts of each protein quantified using ImageJ software (or equivalent).

#### 3.1.4. Bradford Assay

1. Dilute the Bradford reagent 1:5 with distilled water prior to use.
2. Prepare a series of BSA standards ( $0.5\text{--}10\mu\text{g}$ ) in the same buffer as the samples to be assayed.
3. To  $5\mu\text{L}$  sample/standard add 1 mL diluted reagent and mix gently.
4. Record the absorbance at 595 nm. If the sample absorbance is out with the absorbance for the standards, dilute the samples and re-assay.
5. Prepare a standard curve of absorbance vs.  $\mu\text{g}$  BSA.
6. Determine concentrations of purified proteins from standard curve.

#### 3.2. Steady-State Tryptophan Emission Spectra

The intrinsic fluorescence of tyrosines and tryptophan residues within proteins can be measured using an excitation wavelength of 278 nm. Tryptophan residues alone can be measured at an

excitation wavelength of 295 nm. In both cases, an emission spectrum is obtained by scanning over a range of wavelengths from 300 to 450 nm using a spectrofluorometer. The emission spectrum of tryptophan is very sensitive to exposure to solvent and therefore can provide information on the local structure surrounding the aromatic residue. In stably folded proteins, tyrosine emission is not usually observed as the fluorescence emission is sensitive to distance-dependent energy transfer to tryptophan residues.

### 3.2.1. Spectrofluorometer Settings

1. Set excitation and emission slit widths to 1.0 cm.
2. All measurements must be done in duplicate with a 1 cm path length cuvette.
3. All measurements must be made using UV quartz cuvettes. 1 mL samples can be accurately measured in semimicro cuvettes; however, the volume of purified protein required can be dramatically reduced by using a Hellma ultra micro fluorescent cell.
4. The volumes stated here are those required when using semi-micro cuvettes (1 mL) and all samples should be measured in duplicate or triplicate.

### 3.2.2. Steady State Fluorescence

1. Dilute 10–50  $\mu\text{g}$  protein in 1 mL of room-temperature PBS.
2. Measure the emission spectra of PBS (without protein) by scanning from 300 to 450 nm after excitation at both 278 and 295 nm.
3. Repeat this with the protein sample diluted in PBS.
4. ASCII translate the spectrum. This will allow you to work with the data in Microsoft Excel.
5. The spectra obtained for the PBS (or buffer of choice *see* [Note 8](#)) must be subtracted from the spectra obtained for the protein sample thus correcting for the influence, if any, of the PBS/buffer used.

### 3.2.3. The Effect of Trimethylamine N-Oxide (TMAO) and TFE

Protein folding can be induced or stabilized by the addition of the naturally occurring osmolyte trimethylamine N-oxide (TMAO) or the hydrophobic solvent trifluoroethanol (TFE). TMAO has been found to induce native folded structure on polypeptides that have significant regions of natural disordered structure (13–15). TFE stabilizes helical conformation. To investigate the effect of TMAO or TFE on the conformation of the protein, the steady-state spectrum is compared with changes in the spectrum following the addition of increasing concentrations of TMAO or TFE.

1. Prepare a 6 M fresh stock solution of TMAO in PBS.

2. Dilute TMAO with PBS to give final concentrations of 1 M, 2 M, and 3 M TMAO.
3. Prepare protein samples as follows:
  - a. Dilute 10–50 µg protein in 1 mL of room-temperature PBS.
  - b. Dilute 10–50 µg protein in 1 mL of room-temperature PBS containing 1, 2 and 3 M TMAO.
4. Measure the emission spectra of PBS (without protein) by scanning from 300 to 450 nm with excitation at both 278 and 295 nm (*see Note 9*).
5. Repeat this with each concentration of TMAO diluted in PBS.
6. Measure the emission spectra of the protein samples in each concentration of TMAO in PBS.
7. The values obtained from the spectra for the protein samples at each concentration of TMAO is then corrected for the contribution of the buffer and respective TMAO concentrations.
8. To measure the steady-state spectra in the presence of TFE prepare 10, 25, 50% (v/v) TFE in PBS in the absence or presence of protein (*see Step 3*). The spectra are then measured as for **Steps 4–7**. **Figure 1** shows typical steady-state emission spectra for AR-AF1 in the absence or presence of the structure stabilising agents TMAO and TFE (*see Note 10*).

#### 3.2.4. Protein Unfolding: The Effect of Urea

Urea is a common chemical known to denature proteins and disrupt their structure. The presence of structure can be confirmed by the addition of urea and the unfolding profile of a polypeptide can be measured by comparing the steady-state fluorescence emission as a function of urea concentration.

1. Prepare a solution of 8 M urea in PBS, pH 7.0.
2. Prepare protein samples as follows:
  - a. Dilute 10–50 µg protein in 1 mL of room-temperature PBS.
  - b. Dilute 10–50 µg protein in 1 mL of room-temperature PBS containing increasing amounts of urea i.e. 0.2, 0.5, 1, 3, 5, and 6 M.
3. Measure the emission spectra of PBS (without protein) in the absence or presence of urea by scanning from 300 to 450 nm after excitation at both 278 and 295 nm.
4. Measure the emission spectra of diluted protein in the absence or presence of urea by scanning from 300 to 450 nm after excitation at both 278 nm and 295 nm.

5. The values obtained from the spectra for the samples at each concentration of urea is then corrected for the contribution of the buffer and respective urea concentrations.

### 3.3. Acrylamide Quenching

The surface exposure of tryptophan residues to solvent can also be probed by using quenching agents such as molecular oxygen or the ionic quencher  $I^-$ . The nonpolar quencher acrylamide is known to act as a dynamic quencher of tryptophan fluorescence and can be used to investigate the accessibility of this aromatic residue (16). A tryptophan on the surface of a protein will be more readily quenched than one which is buried in the protein core and the intensity of tryptophan fluorescence will be progressively reduced by the addition of the quencher (Fig. 2) (see Note 11). The ability of acrylamide to quench the tryptophan fluorescence emission can be analysed under different experimental conditions i.e., the presence of a binding partner or the natural osmolyte TMAO (see ref. 15).

#### 3.3.1. Acrylamide Quenching in Buffer

1. Prepare protein samples as follows:
  - a. Prepare a solution of 1 M acrylamide.
  - b. Dilute 1–10  $\mu\text{g}$  protein in 1 mL PBS at room temperature.
  - c. Dilute 1–10  $\mu\text{g}$  protein in 1 mL PBS at room temperature containing increasing amounts of acrylamide i.e. 0.05, 0.1, 0.2 and 0.3 M.
2. Measure the emission spectra of PBS (without protein) in the absence and presence of different concentrations of acrylamide by scanning from 300 to 450 nm with excitation at 295 nm.
3. Measure the emission spectra of diluted protein in the absence and presence of different concentrations of acrylamide by scanning from 300 to 450 nm with excitation at 295 nm.
4. The values obtained from the spectra for the samples at each concentration of acrylamide are then corrected for the contribution of the buffer and the respective acrylamide concentrations.

#### 3.3.2. Acrylamide Quenching After Folding

1. Prepare a 6 M solution of TMAO.
2. Repeat 1–4 as above including 500  $\mu\text{L}$  of 6 M TMAO (final concentration of 3 M).
3. The values obtained from the spectra for the samples at each concentration of TMAO, with or without acrylamide, is then corrected for the contribution of the buffer alone and the respective TMAO/acrylamide concentrations. This analysis allows the environment of the tryptophan residue(s) to be probed before and after induced folding.

---

## 4. Notes

1. In the absence of aromatic amino acids, there are a number of extrinsic fluorescent probes that can be covalently coupled to proteins via free amino groups. Two of the most common are dansyl chloride (DNS-Cl; 5-dimethylamino-1-naphthalene-sulphonyl chloride) and fluoresceine isothiocyanate (FITC), which will emit in blue and green wavelengths, respectively.
2. We routinely work with his-tagged polypeptides for biophysical analysis, using the pET series (Novagen) of expression plasmids. However, other types of tags may be used, for example glutathione-*S*-transferase (pGEX plasmids; GE Healthcare Life Sciences), although the fusion partner will need to be cleaved (removed) prior to analysis if tryptophan residues are present.
3. TMAO should be stored desiccated at room temperature. Solutions should be made fresh immediately prior to use. TMAO and TFE are both irritants and the appropriate precautions taken.
4. Acrylamide is hazardous in the case of skin contact (permeator), eye contact (irritant), ingestion, and inhalation. Severe over-exposure can result in death. Personal protection i.e. Lab coat, goggles, and gloves must be worn. An approved/certified dust respirator or equivalent should be used when handling this chemical.
5. Prior to scaling up expression, single colonies are selected and small cultures (2 mL) are grown and whole cell extracts prepared in SDS-sample buffer after IPTG induction to screen for colonies giving best expression. We typical grow multiples of 200 mL cultures when we scale up the expression of recombinant proteins.
6. We have found that incubation with 1 mM IPTG for 2 h at 37°C are suitable conditions for expressing a wide range of his-tagged recombinant polypeptides. However, the optimum conditions will need to be determined empirically. If problems are experienced with expressing soluble protein or yield it is possible to reduce the concentration of IPTG and/or incubate at a lower temperature e.g., 25 or 30°C.
7. Ni-NTA used columns can be regenerated by stripping and recharging with nickel sulphate as follows:
  - a. Wash the column with 3× bed volumes of strip buffer: 20 mM Tris-HCl, pH 7.9, 100 mM EDTA, 500 mM NaCl.
  - b. Wash the column with 3× bed volumes of sterile H<sub>2</sub>O.
  - c. Recharge the column with 5× bed volumes of 50 mM NiSO<sub>4</sub>.

- d. Then equilibrate the column with 10× bed volumes of Ni-NTA Binding buffer.
8. We have used other buffers to measure fluorescence emission spectra i.e., 20 mM HEPES pH 7.9, 100 mM sodium acetate, 5% glycerol, 1 mM DTT. The buffer used should be run alone under identical conditions to correct for background and to ensure the components do not absorb at the wavelengths being measured.
9. If the emission spectra is off-scale with TMAO, the sensitivity of the spectrofluorometer may have to be adjusted from high to low sensitivity. All measurements will then have to be done using the same settings.
10. A shift of the peak ( $\lambda_{\text{max}}$ ) spectra to the left, toward lower wavelength values (blue-shift), with increasing amounts of TMAO corresponds to the tryptophan residue(s) becoming less solvent exposed and is consistent with folding and formation of secondary structure (**Fig. 1B**). While a shift of the peak spectra to the right, toward higher wavelength values (red shift), after the addition of a denaturant such as urea, results from the tryptophans becoming more solvent exposed and corresponds to unfolding or disruption of protein structure. These changes in the local environment of the aromatic amino acids can also lead to changes in the fluorescence intensity (*see Fig. 1B*).
11. The Stern-Volmer quenching constant,  $K_{\text{sv}}$ , is determined according to the following equation  $F_0/F = 1 + K_{\text{sv}} [Q]$  where  $F_0$  represents the fluorescence intensity ( $\lambda_{\text{max}}$ ) in the absence of acrylamide and  $F$  represents the fluorescence intensity ( $\lambda_{\text{max}}$ ) in the presence of the quencher (*16*).  $F_0/F$  is then calculated and plotted as a function of quencher concentration,  $[Q]$  to give a straight line from which  $K_{\text{sv}}$  can be calculated (**Fig. 2B, right panel**). The smaller the value for  $K_{\text{sv}}$  the more buried, inaccessible, the tryptophan. An upward curve is indicative of both static and dynamic quenching taking place, while for multiple tryptophan containing proteins a downward sloping curve suggests that one of the fluorophores is inaccessible to the quencher (*16*).

---

## Acknowledgments

We are grateful to Ms Esther Combe for the data shown in **Fig. 2B** and acknowledge project grant support from the Association for International Cancer Research, Biotechnology and Biological Sciences Research Council and the Royal Society.

## References

1. Kumar, R., Johnson, B. H., and Thompson, E. B. (2004) Overview of the Structural Basis for Transcription Regulation by Nuclear Hormone Receptors. *Essays Biochem.* **40**, 27–39.
2. Claessens, F., and Gewirth, D. T. (2004) DNA Recognition by Nuclear Receptors. *Essays Biochem.* **40**, 59–72.
3. Kumar, R., and Thompson, E. B. (2003) Transactivation Functions of the N-Terminal Domains of Nuclear Hormone Receptors: Protein Folding and Coactivator Interactions. *Mol. Endocrinol.* **17**, 1–10.
4. Lavery, D. N., and McEwan, I. J. (2005) Structure and Function of Steroid Receptor AF1 Transactivation Domains: Induction of Active Conformations. *Biochem. J.* **391**, 449–464.
5. McEwan, I. J., Lavery, D. N., Fischer, K., and Watt, K. (2007) Natural Disordered Sequences in the Amino Terminal Domain of Nuclear Receptors: Lessons from the Androgen and Glucocorticoid Receptors. *Nucl. Recept. Signal.* **5**, 1–6.
6. Acevedo, M. L., and Kraus, W. L. (2004) Transcriptional Activation by Nuclear Receptors. *Essays Biochem.* **40**, 73–88.
7. Rosenfeld, M. G., Lunyak, V. V., and Glass, C. K. (2006) Sensors and Signals: A coactivator/corepressor/epigenetic Code for Integrating Signal-Dependent Programs of Transcriptional Response. *Genes Dev.* **20**, 1405–1428.
8. Codina, A., Love, J. D., Li, Y., Lazar, M. A., Neuhaus, D., and Schwabe, J. W. (2005) Structural Insights into the Interaction and Activation of Histone Deacetylase 3 by Nuclear Receptor Corepressors. *Proc. Natl. Acad. Sci. USA* **102**, 6009–6014.
9. Demarest, S. J., Martinez-Yamout, M., Chung, J., Chen, H., Xu, W., Dyson, H. J., Evans, R. M., and Wright, P. E. (2002) Mutual Synergistic Folding in Recruitment of CBP/p300 by p160 Nuclear Receptor Coactivators. *Nature* **415**, 549–553.
10. Darimont, B. D., Wagner, R. L., Apriletti, J. W., Stallcup, M. R., Kushner, P. J., Baxter, J. D., Fletterick, R. J., and Yamamoto, K. R. (1998) Structure and Specificity of Nuclear Receptor-Coactivator Interactions. *Genes Dev.* **12**, 3343–3356.
11. He, B., Gampe, R. T., Jr, Kole, A. J., Hnat, A. T., Stanley, T. B., An, G., Stewart, E. L., Kalman, R. I., Mingos, J. T., and Wilson, E. M. (2004) Structural Basis for Androgen Receptor Interdomain and Coactivator Interactions Suggests a Transition in Nuclear Receptor Activation Function Dominance. *Mol. Cell.* **16**, 425–438.
12. Estebanez-Perpina, E., Arnold, L. A., Nguyen, P., Rodrigues, E. D., Mar, E., Bateman, R., Pallai, P., Shokat, K. M., Baxter, J. D., Guy, R. K., Webb, P., and Fletterick, R. J. (2007) A Surface on the Androgen Receptor that Allosterically Regulates Coactivator Binding. *Proc. Natl. Acad. Sci. USA* **104**, 16074–16079.
13. Baskakov, I. V., Kumar, R., Srinivasan, G., Ji, Y. S., Bolen, D. W., and Thompson, E. B. (1999) Trimethylamine N-Oxide-Induced Cooperative Folding of an Intrinsically Unfolded Transcription-Activating Fragment of Human Glucocorticoid Receptor. *J. Biol. Chem.* **274**, 10693–10696.
14. Kumar, R., Lee, J. C., Bolen, D. W., and Thompson, E. B. (2001) The Conformation of the Glucocorticoid Receptor aF1/taul Domain Induced by Osmolyte Binds Co-Regulatory Proteins. *J. Biol. Chem.* **276**, 18146–18152.
15. Reid, J., Kelly, S. M., Watt, K., Price, N. C., and McEwan, I. J. (2002) Conformational Analysis of the Androgen Receptor Amino-Terminal Domain Involved in Transactivation. Influence of Structure-Stabilizing Solutes and Protein-Protein Interactions. *J. Biol. Chem.* **277**, 20079–20086.
16. Eftink, M. R., and Ghiron, C. A. (1976) Exposure of Tryptophanyl Residues in Proteins. Quantitative Determination by Fluorescence Quenching Studies. *Biochemistry* **15**, 672–680.
17. Kumar, R., Betney, R., Li, J., Thompson, E. B., and McEwan, I. J. (2004) Induced Alpha-Helix Structure in AF1 of the Androgen Receptor upon Binding Transcription Factor TFIIF. *Biochemistry* **43**, 3008–3013.
18. Brodie, J., and McEwan, I. J. (2005) Intra-Domain Communication between the N-Terminal and DNA-Binding Domains of the Androgen Receptor: Modulation of Androgen Response Element DNA Binding. *J. Mol. Endocrinol.* **34**, 603–615.
19. Greenfield, N., Vijayanathan, V., Thomas, T. J., Gallo, M. A., and Thomas, T. (2001) Increase in the Stability and Helical Content of Estrogen Receptor Alpha in the Presence of the Estrogen Response Element: Analysis by Circular Dichroism Spectroscopy. *Biochemistry* **40**, 6646–6652.
20. Warnmark, A., Wikstrom, A., Wright, A. P., Gustafsson, J. A., and Hard, T. (2001) The N-Terminal Regions of Estrogen Receptor Alpha and Beta are Unstructured in Vitro and show Different TBP Binding Properties. *J. Biol. Chem.* **276**, 45939–45944.



21. Nair, S. K., Thomas, T. J., Greenfield, N. J., Chen, A., He, H., and Thomas, T. (2005) Conformational Dynamics of Estrogen Receptors Alpha and Beta as Revealed by Intrinsic Tryptophan Fluorescence and Circular Dichroism. *J. Mol. Endocrinol.* **35**, 211–223.
22. Dahlman-Wright, K., Baumann, H., McEwan, I. J., Almlof, T., Wright, A. P., Gustafsson, J. A., and Hard, T. (1995) Structural Characterization of a Minimal Functional Transactivation Domain from the Human Glucocorticoid Receptor. *Proc. Natl. Acad. Sci. USA* **92**, 1699–1703.
23. Kumar, R., Volk, D. E., Li, J., Lee, J. C., Gorenstein, D. G., and Thompson, E. B. (2004) TATA Box Binding Protein Induces Structure in the Recombinant Glucocorticoid Receptor AF1 Domain. *Proc. Natl. Acad. Sci. USA* **101**, 16425–16430.
24. Wardell, S. E., Kwok, S. C., Sherman, L., Hodges, R. S., and Edwards, D. P. (2005) Regulation of the Amino-Terminal Transcription Activation Domain of Progesterone Receptor by a Cofactor-Induced Protein Folding Mechanism. *Mol. Cell. Biol.* **25**, 8792–8808.
25. Hi, R., Osada, S., Yumoto, N., and Osumi, T. (1999) Characterization of the Amino-Terminal Activation Domain of Peroxisome Proliferator-Activated Receptor Alpha. Importance of Alpha-Helical Structure in the Transactivating Function. *J. Biol. Chem.* **274**, 35152–35158.

# Chapter 13

## Development of Phosphorylation Site-Specific Antibodies to Nuclear Receptors

Inés Pineda Torra, Julia A. Staverosky, Susan Ha, Susan K. Logan, and Michael J. Garabedian

### Abstract

Protein phosphorylation is a versatile posttranslational modification that can regulate nuclear receptor function. Although the precise role of receptor phosphorylation is not fully understood, it appears that it functions to direct or refine receptor activity in response to particular physiological requirements.

Identifying and characterizing specific nuclear receptor phosphorylation sites is an important step in elucidating the role(s) receptor phosphorylation plays in function. Although traditional methods of metabolic labeling and in vitro protein phosphorylation have been informative, receptor phosphorylation site-specific antibodies are simple and reliable tools to study receptor phosphorylation. This chapter will discuss how to develop nuclear receptor phosphorylation site-specific antibodies to elucidate function.

**Key words:** Phosphorylation, Phosphorylation site-specific antibodies, Nuclear receptors.

---

### 1. Introduction

Phosphorylation is an important modulator of nuclear receptor function (1). Protein phosphorylation affords rapid changes in protein activity without requiring new protein synthesis. The study of protein phosphorylation in general, and nuclear receptor phosphorylation in particular, has been hindered by the lack of simple assays to detect changes in receptor phosphorylation. Although certain proteins display a shift in their electrophoretic mobility on a one-dimensional SDS polyacrylamide gel in response to phosphorylation, this is not the case for most steroid and nuclear receptors (2). The traditional analysis of receptor

phosphorylation was a multistep process that required metabolic labeling of the receptor with large amounts of  $^{32}\text{P}$ , receptor isolation, protease digestion, separation, and evaluation of the resulting phosphopeptide by HPLC or thin layer chromatography (3). Although informative, these studies have been limited to cultured cells and may not accurately reflect receptor phosphorylation in a given tissue or in response to a particular stimulus in an intact organism. Thus, phosphorylation site-specific antibodies provide the means to evaluate phosphorylation during development, differentiation, or pathophysiological processes using simple immunohistochemical and immunoblotting procedures (4–10). Receptor-specific phospho antibodies have been used successfully in the following applications:

1. Immunoblotting from tissues and cell lines (5, 6, 9, 10).
2. Immunoprecipitation from cultured cell lines (11).
3. Immunofluorescence (tissue culture cells and paraffin-embedded tissue specimens) (7, 9).
4. Immunohistochemistry (paraffin-embedded and frozen sections) (7, 8, 12).
5. Chromatin immunoprecipitation assays (13).

This chapter provides a guide to the development and production of phosphorylation site-specific antibodies to nuclear receptors.

---

## 2. Materials

### **2.1. Phosphorylation Site-Specific Antibody Production**

#### *2.1.1. Immunization*

1. Synthesis of phosphopeptide immunogen.
2. New Zealand white rabbits.
3. Freund's complete adjuvant: antigen solution emulsified in mineral oil and mixed with dried mycobacteria.
4. Freund's incomplete adjuvant: antigen solution emulsified in mineral oil only.

#### *2.1.2. ELISA*

Performed by the company producing the antisera.

#### *2.1.3. Affinity Purification*

Performed by the company producing the antisera.

### **2.2. Analysis of Antibody Specificity**

1. Suitable cell line(s) (e.g., HEK293, LNCaP, RAW264.7).
2. Dulbecco's Modified Eagle Medium (DMEM) (Invitrogen; Mediatech).
3. Phenol red free DMEM (Invitrogen; Mediatech).

4. Fetal bovine serum (FBS) (Hyclone; Atlanta Biologicals).
5. Charcoal/Dextran Treated FBS (Hyclone).
6. Cationic lipid transfection reagent [e.g. Lipofectamine (Invitrogen), Effectene (Qiagen); FuGENE (Roche)].
7. Site-directed mutagenesis kit [e.g. QuikChange (Stratagene)].
8. R1881 (Methyltrienolone; Perkin-Elmer; 10  $\mu$ M stock in 100% ethanol; store in aliquots at  $-20^{\circ}\text{C}$  in the dark).
9. T0901317 (Sigma): 1mM stock in DMSO; store in aliquots at  $-20^{\circ}\text{C}$  in the dark.
10. Phorbol-12-myristate-13-acetate (PMA, Sigma): 8 mM stock in DMSO; store in aliquots at  $-20^{\circ}\text{C}$ .
11. Forskolin (FSK; Sigma): 10 mM stock in DMSO; store in aliquots at  $-20^{\circ}\text{C}$ .
12. Cell Lysis Buffer: 20 mM Tris-HCl, pH 7.5, 150 mM NaCl, 1 mM EDTA, 1 mM EGTA, 1% (w/v) Triton X-100, 2.5 mM sodium pyrophosphate (Sigma; 221368), 1.0 mM  $\beta$ -glycerolphosphate (Sigma; G6251), 30 mM sodium fluoride (Sigma; S6521) (*see Note 1*). Heat to  $65^{\circ}\text{C}$  for 5–10 min to completely dissolve the Triton. Cool and store at  $4^{\circ}\text{C}$  (good for several months).
13. Colorimetric Protein Concentration Reagents [e.g. Bio-Rad protein assay kit; BCA Protein Assay Reagent Kit (Pierce)].
14. Sodium orthovanadate (Sigma): 0.2 M stock (*see Note 2*).
15. Calyculin A (Cell Signaling): 10  $\mu$ M stock in DMSO (*see Note 1*).
16. Phosphatase Buffer: 50 mM Tris-HCl, pH 7.5, 100 mM NaCl, 2 mM dithiothreitol, 0.1 mM EGTA, 2 mM  $\text{MnCl}_2$ .
17. Lambda phosphatase enzyme (Upstate Biotechnology or New England Biolabs).

---

### 3. Methods

#### 3.1. Phosphorylation Site-Specific Antibody Production

Once the phosphorylation site has been identified, there are three main steps in developing and validating phosphorylation site-specific antibodies (**Fig. 1**):

1. Synthesis of the phosphopeptide immunogen (**Subheading 3.1**).
2. Immunization with the phosphopeptide immunogen (**Subheading 3.2.1**), ELISA (**Subheading 3.2.2**), and affinity purification (**Subheading 3.2.3**).
3. Analysis of phospho-antibody specificity (**Subheading 3.3**).

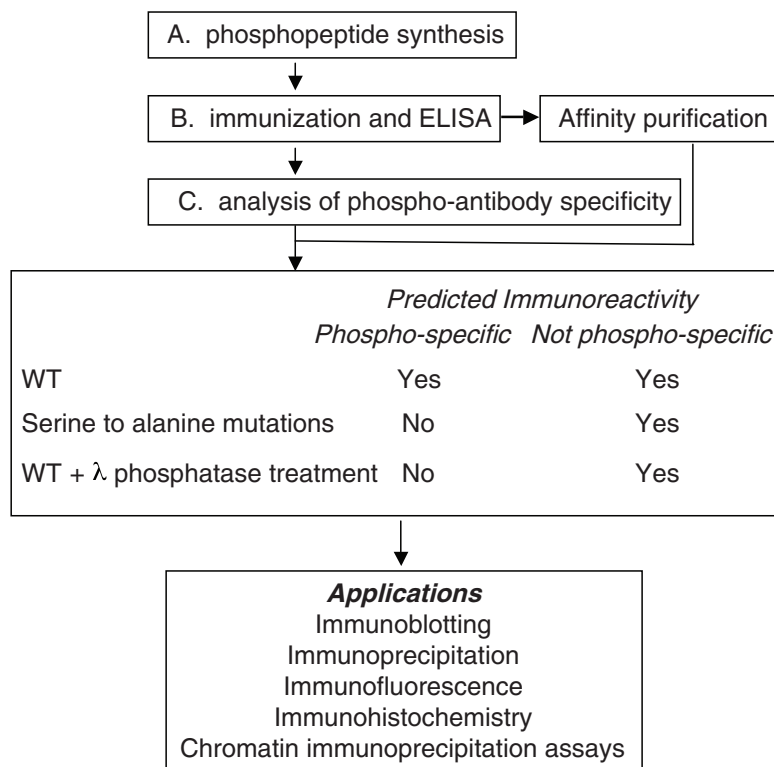


Fig. 1. Phosphorylation site-specific antibody production and applications. Shown is a flow chart of the step in phospho-antibody production and validation including (a) phosphopeptide synthesis, (b) immunization of rabbits, ELISA of the serum, and affinity purification are done most easily through commercial sources. (c) Analysis of phosphospecificity is performed in the investigator's laboratory. This entails analyzing immunoreactivity of the WT vs. serine to alanine phosphorylation site mutation by immunoblotting, and also through treating the WT receptor with lambda phosphatase and assessing immunoreactivity. A criterion for phosphospecificity is shown as positive (yes) or negative (no) immunoreactivity. Published applications of receptor phosphorylation site-specific antibodies are shown.

### 3.2. Phosphopeptide Synthesis

The phosphopeptide immunogens used to successfully generate phosphorylation site-specific antibodies to the glucocorticoid receptor (GR)(9), androgen receptor (AR) (7), and liver X receptor alpha (LXR)(8) range between 15 and 17 amino acids in length (Table 1). In each case, the peptide was run through a BLAST search for short nearly identical peptide sequences to rule out the possibility that the antibody will cross react with other eukaryotic proteins. Given that most laboratories do not have phosphopeptide synthesis capabilities, commercial vendors

**Table 1**  
**Phosphopeptide immunogens**

Receptor	Sequence	Length
<i>Glucocorticoid receptor</i>		
GR S203P	C <sub>194</sub> LQDLEFSSG(pS)PGKE <sub>207</sub>	16
GR S211P	C <sub>202</sub> GSPGKETNE(pS)PWRS <sub>215</sub>	15
GR S226P	C <sub>218</sub> LLIDENLL(pS)PLAG <sub>230</sub>	14
<i>Androgen receptor</i>		
AR S213P	C <sub>202</sub> EGSSSGRAREAA(pS)GAPTS <sub>218</sub>	17
AR S650P	C <sub>642</sub> EGEASSTT(pS)PTEETT <sub>656</sub>	15
<i>Liver X Receptor alpha</i>		
LXR alpha S198P	C <sub>189</sub> ATSLPPRAS(pS)PPQI <sub>202</sub>	15

are enlisted for custom phosphopeptide synthesis. A number of companies synthesize high quality and custom phosphopeptide (see **Note 3**). Typically 20 mg of the phosphopeptide is synthesized and purified to >90% homogeneity: 10 mg is used for the immunization, boosting, and ELISA testing and 10 mg is used for subsequent analysis and/or affinity purification of the antibody. The phosphorylation site is placed asymmetrically toward the C-terminal portion of the peptide, although the influence of location of the phosphorylated residue within the peptide on antibody production has not been systematically examined. An additional cysteine residue is added to the N-terminus of the peptide to facilitate chemical cross-linking to common carrier proteins, such as keyhole limpet hemocyanin (KLH), that are utilized to enhance phosphopeptide immunogenicity.

### 3.2.1. Immunization

The KLH-coupled phosphopeptide is used to immunize New Zealand white rabbits using a standard immunization and boosting protocols (see later) (see **Note 4**). This standard protocol takes 118 days to complete, although the initial test bleeds are available after 52 days. Because of biological variation and to ensure at least one rabbit elicits a robust immune response to the phosphopeptide, six rabbits are typically immunized per phosphopeptide antigen (see **Note 5**). Mouse monoclonal phospho-specific antibodies against steroid receptor phosphorylation sites have also been generated (5). We do not have experience with this approach, and therefore this approach will not be presented.

1. Day 0 Pre-bleed New Zealand White Rabbits (~5 mL serum).

2. Inject primary subcutaneous (SQ) injection with 500 mg of KLH coupled phosphopeptide with Freund's Complete Adjuvant (FCA) (No more than 0.1 mL is injected per site).
3. Day 21 Boost SQ with 500 mg of KLH coupled phosphopeptide with Freund's Incomplete Adjuvant (FIA).
4. Day 42 Boost SQ with 250 mg of KLH coupled phosphopeptide with FIA.
5. Day 52 Test Bleed: ELISA titer assay of bleed and examine test bleed by immunoblotting (see below).
6. Day 63 Boost SQ with 250 mg of KLH coupled phosphopeptide with FIA.
7. Day 73 Production bleed.
8. Day 84 Boost SQ with 250 mg of KLH coupled phosphopeptide with FIA.
9. Day 94 Production bleed: ELISA titer assay of bleed and examine test bleed by immunoblotting (see below).
10. Day 105 Boost SQ with 250 mg of KLH coupled phosphopeptide with FIA.
11. Production bleed (~20 mL serum).
12. Terminal bleed (~50 mL serum)

### 3.2.2. ELISA

Sera from immunized rabbits are tested for antibody titer by enzyme-linked immunosorbent assay (ELISA) for preferential binding to the specific phosphopeptide when compared with the unphosphorylated peptide (*see Note 6*).

High titer antibodies showing preference for the phosphorylated immunogen are further tested on receptor proteins expressed in cultured cells by immunoblotting (**Fig. 1**). In principle, a phosphospecific antibody should recognize the protein in a phosphorylated but not unphosphorylated state (see section below on specificity). In practice this is rarely the case. Therefore, validating specificity of phospho-antibodies is largely empirical. In addition, some sites may require receptor ligand or activation of signaling pathways to induce phosphorylation and detection with a phospho-antibody (**Fig. 2**).

### 3.2.3. Affinity Purification

In most instances, the crude serum itself contains high titer and specific phospho-antibodies sufficient for applications such as immunoblotting where the background bands (if any) can be distinguished from the receptor by molecular weight and intensity of the signal (*see Note 7*). However, applications such as immunohistochemistry or immunofluorescence frequently require affinity purification of the phosphospecific antibody.

Even with a robust immune response, the antibodies directed against the immunogen reflect only a small percentage of the total



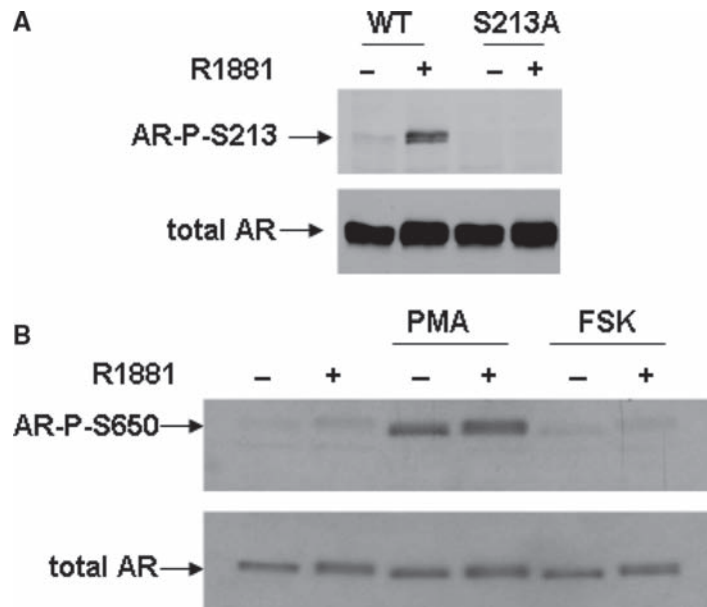


Fig. 2. Androgen and PMA-induced phosphorylation of the androgen receptor. **(A)** 293T cells were transfected with AR wild-type (WT) and serine-to-alanine mutant (S213A). Cells were treated for 2 h with 10 nM R1881, protein extracts prepared and blotted with AR S213-phospho-specific antibody, or an antibody that recognizes total AR. **(B)** LNCaP cells were steroid starved and treated for 2 h with 10 nM R1881 (a synthetic androgen receptor ligand) (lanes 2, 4, and 6), 1 mM phorbol 12-myristate 13-acetate (PMA; an activator of protein kinase C) (lanes 3 and 4) or 50 mM forskolin (FSK; an activator of protein kinase A) (lanes 5 and 6). Protein extracts were blotted and probed with the AR S650-phospho-specific antibody, or an antibody that recognizes total AR. Note that AR phosphorylation at S213 is androgen-dependent, whereas phosphorylation at S650 is PMA-dependent, and androgen-independent.

antibody complement present in the rabbit serum. These endogenous rabbit antibodies can lead to nonspecific background. Affinity purification of the phospho-specific antibody can eliminate the nonspecific antibodies not directed against the phosphopeptide immunogen and enrich specific phospho-antibody species. The simplest method is to purify the antibody using the phosphopeptide immunogen (*see Note 8*).

### 3.3. Analysis of Phospho-Antibody Specificity

#### 3.3.1. Validation of Phospho-Specific Antibodies Using Cell Culture Assays

The most straightforward method to examine specificity is to compare immunoreactivity between the wild type phosphorylated receptor vs. a non-phosphorylatable serine-to-alanine version (**Fig. 1**). Typically, a cell line with high transfection efficiency (e.g., HEK293 cells) are transfected with wild type and a serine-to-alanine variant of the receptor. Cell lysates are prepared followed by immunoblot analysis with the phosphorylation site-specific antibody (**Figs. 2a, 3b, and 4a**). To guard against

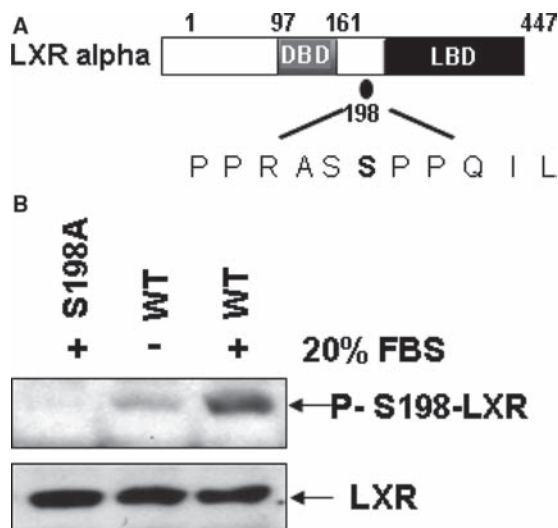


Fig. 3. Generation of LXR alpha phospho specific antibodies. (a) Domain structure of human LXR alpha with S198 phosphorylation site is depicted. (b) Phospho-S198 (P-S198) specific antibody. HEK 293T cells were transfected with FLAG-tagged LXR alpha wild type and serine to alanine mutant (S198A), incubated for 24 h in serum-free medium and activated overnight with 20% FBS. Protein extracts were blotted and probed with the S198-phospho-specific antibody. Membranes were then stripped and reblotted with the FLAG antibody to detect total LXR alpha proteins.

dephosphorylation reaction occurring during extract preparation, phosphatase inhibitors are routinely included in cell lysis buffer (see [Notes 1 and 2](#)). The phospho-immunoreactivity should be largely eliminated by the mutation (see [Note 9](#)).

Although phospho-antibodies bind more avidly to the phosphorylated form of the protein, most phospho-antibodies react to some extent with the nonphosphorylated protein. This may reflect a mixture of antibodies against the phospho and non-phospho portions of the immunogen that were generated during multiple rounds of immunization, or to antibodies recognizing an epitope encompassing both the phosphorylation site and the neighboring nonphosphorylated residues. The ability of the phospho-antibody to selectively detect the antigen must be determined empirically by titrating the antibody from dilutions of 1:1,000 to 1:10,000.

Transfection of Cultured Cells with Wild-Type Receptor and Phosphorylation Site-Mutants

1. Plate HEK293 cells ( $\sim 0.5\text{--}1 \times 10^7$  cells per 10 cm dish) in DMEM + 10% FBS without antibiotics. *Cells should be 50–95% confluent on the day of transfection.*
2. Transfect 5  $\mu\text{g}$  of the wild-type receptor expression vector (e.g., pCDNA-3-hAR) or 5  $\mu\text{g}$  of the phosphorylation site

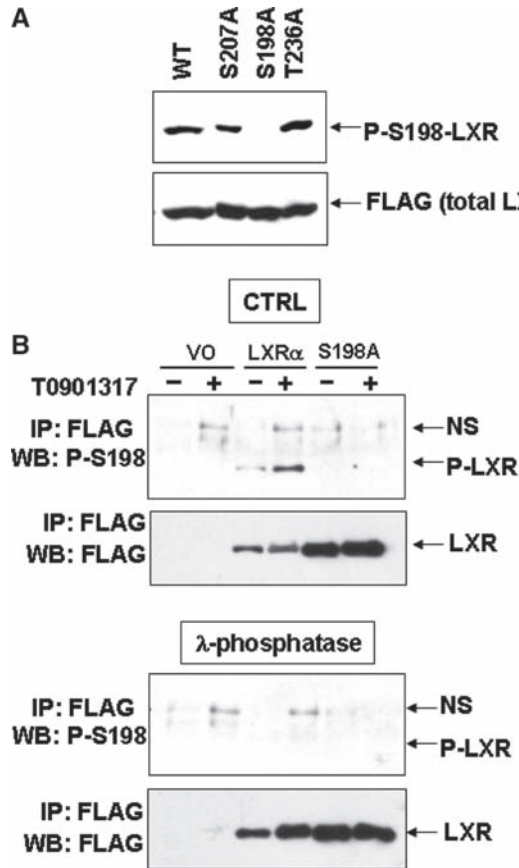


Fig. 4. Specificity of LXR alpha S198 phosphorylation site-specific antibody. **(A)** HEK 293T cells were transfected with FLAG-tagged LXR alpha wild-type (WT) and serine or threonine to alanine mutants (S198A, S207A, and T236A). Cells were incubated for 24 h in serum-free medium and activated overnight with 20% FBS. Protein extracts were blotted and probed with the S198-phospho-specific antibody, and reblotted with the FLAG antibody to detect total LXR alpha proteins. **(B)** RAW 264.7 cells infected with a retroviral vector only (VO), or stably expressing WT or S198A, were treated with vehicle (-) or T0901317 ligand for 2 h. FLAG-immunoprecipitated LXR alpha proteins were separated transferred, and membranes were incubated either in phosphatase buffer alone (CTRL) or in buffer containing 400 units of lambda phosphatase ( $\lambda$ -phosphatase). Membranes were probed with the phospho-S198 specific antibody to detect phosphorylated LXR alpha at S198, and then stripped and reprobed with a polyclonal antibody against FLAG to detect total LXR alpha. NS, nonspecific bands.

mutant receptor (e.g., pCDNA-3-hAR S213A) using cationic lipid transfection reagent. *The receptor phosphorylation site mutations are most easily generated using Stratagene's QuikChange mutagenesis kit.*

3. After the transfection, remove the media and replace it with phenol red free DMEM + 10% charcoal-treated FBS. *Charcoal-treated FBS reduces the levels of hormones in the serum and can result in lower basal and higher ligand-dependent levels of phosphorylation. Phenol-red is a weak agonist for some nuclear receptors and therefore is omitted to reduce activation in the absence of ligand treatment.*
4. After 12–18 h, re-feed the cells with phenol red-free DMEM + 10% charcoal-treated FBS with the appropriate ligand (e.g., 10 nM R1881 for AR; 5  $\mu$ M T0901317 for LXR), kinase activator (20 nM PMA; 10 nM FSK) or an equal volume of the vehicle (ethanol or DMSO) and incubate for 2–12 h. *It is wise to perform a time course to determine the appropriate length of ligand incubation for maximal phosphorylation.*
5. Cells are rinsed twice with ice-cold PBS and removed by aspiration.
6. Place the tissue culture plate on ice.
7. Add 0.2–0.5 mL lysis buffer to the confluent 100-mm dish ( $2 \times 10^7$  cells). *For other plate sizes, adjust volume of lysis buffer according to the surface area of the plate.*
8. Scrape the cells off the plate, and transfer the suspension to a 1.5-mL conical microcentrifuge tube. Vortex gently for 3–5 s and keep tubes on ice for 15 min.
9. Centrifuge 15 min at  $16,000 \times g$  (maximum speed), 4°C.
10. Determine protein concentration using colorimetric protein concentration reagent.
11. Normalize protein concentration among samples.
12. Transfer an appropriate amount of the lysate to a fresh microcentrifuge tube and when necessary adjust the volume to 50  $\mu$ L with lysis buffer.
13. Add 10  $\mu$ L of 5 $\times$  SDS buffer, boil for 5 min.
14. Run 10–20  $\mu$ L of the protein sample on a SDS polyacrylamide gel and analyze by immunoblotting.

Transfer the supernatant to a fresh microcentrifuge tube. Cell extracts can be frozen at  $-70^{\circ}\text{C}$  until used for immunoblotting.

### 3.3.2. In Vitro Phosphatase Assay

An additional and perhaps more stringent test of antibody phosphospecificity is to generate dephosphorylated receptor in vitro and then see if there is diminished phospho-antibody reactivity toward the receptor.

1. The dephosphorylation reaction is most easily accomplished by incubating protein transferred membranes in phosphatase buffer without or with 400 units of lambda phosphatase at 4°C for 16 h. Lambda phosphatase is an  $\text{Mn}^{2+}$ -dependent, dual specificity protein phosphatase

with activity toward phosphorylated serine, threonine, and tyrosine residues.

2. After treatment, the membrane is probed with the phospho-antibody, and then stripped and reprobed with an antibody that recognizes total protein. The immunoreactivity of the protein toward the phospho-antibody should be diminished in the lambda phosphatase-treated membrane, but not the untreated membrane, whereas the total protein should be unchanged (**Fig. 4b**) (*see Note 10*).

### 3.3.3. Immunoprecipitation of Nuclear Receptors

Enrichment of receptors by immunoprecipitation with a receptor-specific antibody prior to immunoblotting with the phospho-antibody can be performed if the phosphorylated receptor species is low or the phospho-antibody has a low signal-to-noise ratio. The receptor is immunoprecipitated for a few hours and then blotted for the phosphospecific form. An example of this is shown for hormone-dependent LXR phosphorylation at S198 using mouse RAW264.7 cells ectopically expressing an N-terminal FLAG-epitope tagged human LXR alpha (8). In this typical example, LXR is immunoprecipitated with a FLAG-M2 mouse monoclonal antibody, eluted and immunoblotted with LXR phospho-specific and total LXR antibodies. The result shows detectable hormone-dependent phosphorylation of LXR (**Fig. 4b**; top panel).

All solutions should be ice cold and procedures should be carried out at 4°C or on ice

1. Rinse cells attached to a tissue culture plate twice with ice-cold PBS and remove by aspiration.
2. Place the tissue culture plate on ice.
3. Add 0.5–1.0 mL lysis buffer to the confluent 100-mm dish (1–2 × 10<sup>7</sup> cells). *For other plate sizes, adjust volume of lysis buffer according to the surface area of the plate.*
4. Scrape the cells off the plate, and transfer the suspension to a 1.5-mL conical microcentrifuge tube. Vortex gently for 3–5 s and keep tubes on ice for 15 min.
5. Centrifuge 15 min at 16,000 × *g* (maximum speed), 4°C.
6. Transfer the supernatant to a fresh microcentrifuge tube. *Leave the last 20–40 μL of supernatant in the tube to ensure that none on the sedimented material is transferred, which can increase background. Cell extracts can be frozen at –70°C until used for immunoprecipitation.*
7. Preparation of the FLAG M2 antibody-agarose conjugated beads:
  - a. In a 1.5-mL conical microcentrifuge tube, combine 30 μL of the FLAG M2 antibody-agarose slurry per IP and mark with pen on the tube the amount of beads.

- b. Add 0.5 mL of ice-cold TBS, and centrifuge 5 s at 16,000  $\times g$ .
- c. Remove supernatant.
- d. Repeat step c.
- e. Remove supernatant to the mark on the tube.
- f. Resuspend beads by flicking the tube.
- g. Store at 4°C until use.
8. In a microcentrifuge tube, combine 0.5–1.0 mL cell lysate (from **step 6**) and 30  $\mu$ L of the 50% FLAG-M2 agarose slurry (from **step 7**).
9. Incubate 1–2 h at 4°C with rocking. *Samples can also be incubated overnight.*
10. Microcentrifuge 5 s at 16,000  $\times g$  (maximum speed), 4°C.
11. Aspirate the supernatant (containing unbound proteins).
12. Add 0.5–1 mL ice-cold lysis buffer (with phosphatase inhibitors) and resuspend the beads by inverting the tube 3 or 4 times.
13. Microcentrifuge 2–5 s at 16,000  $\times g$  (maximum speed), 4°C.
14. Aspirate the supernatant, leaving 20  $\mu$ L supernatant on top of the beads.
15. Wash beads in TBS with phosphatase inhibitors three more times.
16. Remove all possible TBS after last wash.

#### FLAG Peptide Elution

17. Add 30  $\mu$ L TBS to the beads.
18. Add 2  $\mu$ L of 3 $\times$  FLAG peptide at 5  $\mu$ g/ $\mu$ L (final [FLAG-peptide] 300 ng/mL).
19. Incubate for 30 min at 4°C to elute protein from antibody.
20. Microcentrifuge 30 s at 16,000  $\times g$ , 4°C.
21. Remove 25  $\mu$ L of the eluted proteins.
22. Add 5  $\mu$ L of 5 $\times$  SDS buffer, boil for 5 min.
23. Analyze immunoprecipitates by immunoblotting.

---

## 4. Notes

1. Sodium pyrophosphate,  $\beta$ -glycerolphosphate, and sodium fluoride are general phosphatase inhibitors. Sodium vanadate is a tyrosine phosphatase inhibitor, whereas Calyculin A

is a potent inhibitor of the serine-threonine protein phosphatases PP1 and PP2A. *Calyculin A is toxic, so gloves should be worn when handling this agent.*

2. Vanadate needs to be depolymerized to convert it into a potent protein tyrosine phosphatase inhibitor. This is accomplished through a series of pH titration and heating steps. To prepare 50 mL of a 1200 mM sodium vanadate stock: Dissolve 1.84 g of sodium orthovanadate in 45 mL in dH<sub>2</sub>O and adjust to pH 10 with 1N HCl (should turn yellow). Boil until the solution turns clear (a few minutes) and let it cool to room temperature. Readjust to pH 10, and repeat this cycle until the solution remains colorless and the pH remains at 10. Adjust volume to 50 mL and store the activated vanadate in 1 mL aliquots at -20°C.
3. There are a number of vendors that provide custom peptide synthesis services (<http://www.biocompare.com/matrix/118/Peptide-Synthesis.html>). We use Anaspec Inc., (San Jose, CA), for our custom phosphopeptide synthesis.
4. Although a number of companies will perform custom polyclonal antibody production services, we use Covance, Inc (Denver, PA) for the production of rabbit polyclonal antibodies to receptor phosphopeptides. They also perform coupling of the immunogen to KLH, as well as ELISA and affinity purification services.
5. Fewer than six rabbits can be used; however, it is our experience that only one or two rabbits out of six yield high affinity antisera against the phosphopeptide. Although it may seem wasteful and expensive to use six rabbits, it is often useful since the additional animals mount an immune response to a portion of the peptide that does not include the phosphorylation site. This generates an antibody that recognizes the protein of interest *independent* of phosphorylation, and is an ideal control antibody for subsequent studies.
6. Initially we performed ELISA comparing antibody titers of the phosphopeptide *and* nonphosphopeptide immunogens. This necessitated synthesis of the cognate nonphosphopeptide, which increases cost. In principle, this should have revealed which serum contained antibodies that reacted selectively with the phosphorylated immunogen. In practice, we found that a better measure of phosphorylation site reactivity and specificity was high titers toward the phosphopeptide. Therefore, we now perform ELISAs only against the phosphopeptides and characterize the serum with the highest titer antibodies. Additionally, since the cost of inoculating six rabbits is high, some investigators skip ELISA assays altogether and test each bleed for immunoreactivity toward wild type vs. mutant receptor as shown in [Fig. 3a](#).



7. We have performed affinity purification of the antibodies in our laboratory. However, unless this is being done on a routine basis, we found that it is faster and ultimately more cost effective to have the company that did the immunization perform the affinity purification.
8. It should be noted that affinity purification can be problematic, since the highest titer antibodies may bind very tightly (or irreversibly) to the column and therefore be extremely difficult to elute. Occasionally, we have had a more robust phospho-reactivity of the crude serum when compared with the affinity-purified antibody. Therefore, if affinity purification is warranted, then a small test batch should be purified and tested prior to committing to a large-scale purification. Covance offers a “safety net” protocol where a small test batch of serum is affinity purified, and sent back to the investigator for analysis prior to full-scale purification.
9. The appropriate antibody dilution must be determined empirically using serial dilutions of the antibody by immunoblot analysis. We have found that some require dilution as high as 1:10,000 to eliminate nonspecific reactivity with the phosphorylation site mutant receptor.
10. In the analysis of receptor phosphorylation using phospho-specific antibodies, it is important to blot with the phospho-antibody first, since it is more labile, followed by stripping the blot and reprobing with an antibody that will detect the total receptor levels. This rules out background due to up regulation of the protein as opposed to recognition of the phosphorylation site.

## References

1. Weigel, N.L. and N.L. Moore (2007) *Steroid receptor phosphorylation: a key modulator of multiple receptor functions*. *Mol Endocrinol*, **21** (10): p. 2311–9.
2. Zhang, Y., C.A. Beck, A. Poletti, D.P. Edwards, and N.L. Weigel (1995) *Identification of a group of Ser-Pro motif hormone-inducible phosphorylation sites in the human progesterone receptor*. *Mol Endocrinol*, **9** (8): p. 1029–40.
3. Krstic, M.D., I. Rogatsky, K.R. Yamamoto, and M.J. Garabedian (1997) *Mitogen-activated and cyclin-dependent protein kinases selectively and differentially modulate transcriptional enhancement by the glucocorticoid receptor*. *Mol Cell Biol*, **17** (7): p. 3947–54.
4. Al-Dhaheri, M.H. and B.G. Rowan (2006) *Application of phosphorylation site-specific antibodies to measure nuclear receptor signaling: characterization of novel phosphoantibodies for estrogen receptor alpha*. *Nucl Recept Signal*, **4**: p. e007.
5. Clemm, D.L., L. Sherman, V. Boonyaratankornkit, W.T. Schrader, N.L. Weigel, and D.P. Edwards (2000) *Differential hormone-dependent phosphorylation of progesterone receptor A and B forms revealed by a phosphoserine site-specific monoclonal antibody*. *Mol Endocrinol*, **14** (1): p. 52–65.
6. Gioeli, D., S.B. Ficarro, J.J. Kwiek, D. Aaronson, M. Hancock, A.D. Catling, F.M. White, R.E. Christian, R.E. Settlage, J. Shabanowitz, D.F. Hunt, and M.J. Weber (2002) *Androgen receptor phosphorylation. Regulation and identification of the phosphorylation sites*. *J Biol Chem*, **277** (32): p. 29304–14.
7. Taneja, S.S., S. Ha, N.K. Swenson, H.Y. Huang, P. Lee, J. Melamed, E. Shapiro, M.J.

- Garabedian, and S.K. Logan (2005) *Cell-specific regulation of androgen receptor phosphorylation in vivo*. J Biol Chem, **280** (49): p. 40916–24.
8. Torra, I.P., N. Ismaili, J.E. Feig, C.F. Xu, C. Cavasotto, R. Pancratov, I. Rogatsky, T.A. Neubert, E.A. Fisher, and M.J. Garabedian (2008) *Phosphorylation of LXR alpha Selectively Regulates Target Gene Expression in Macrophages*. Mol Cell Biol.
  9. Wang, Z., J. Frederick, and M.J. Garabedian (2002) *Deciphering the phosphorylation "code" of the glucocorticoid receptor in vivo*. J Biol Chem, **277** (29): p. 26573–80.
  10. Yang, C.S., M.J. Vitto, S.A. Busby, B.A. Garcia, C.T. Kesler, D. Gioeli, J. Shabanowitz, D.F. Hunt, K. Rundell, D.L. Brautigan, and B.M. Paschal (2005) *Simian virus 40 small t antigen mediates conformation-dependent transfer of protein phosphatase 2A onto the androgen receptor*. Mol Cell Biol, **25** (4): p. 1298–308.
  11. Wang, Z., W. Chen, E. Kono, T. Dang, and M.J. Garabedian (2007) *Modulation of glucocorticoid receptor phosphorylation and transcriptional activity by a C-terminal-associated protein phosphatase*. Mol Endocrinol, **21** (3): p. 625–34.
  12. Lee, M.J., Z. Wang, H. Yee, Y. Ma, N. Swenson, L. Yang, S.S. Kadner, R.N. Baergen, S.K. Logan, M.J. Garabedian, and S. Guller (2005) *Expression and regulation of glucocorticoid receptor in human placental villous fibroblasts*. Endocrinology, **146** (11): p. 4619–26.
  13. Blind, R.D. and M.J. Garabedian (2008) *Differential recruitment of glucocorticoid receptor phospho-isoforms to glucocorticoid-induced genes*. J Steroid Biochem Mol Biol, **109** (1–2): p. 150–7.

# Chapter 14

## Tissue-Selective Knockouts of Steroid Receptors: A Novel Paradigm in the Study of Steroid Action

Karel De Gendt and Guido Verhoeven

### Abstract

The use of tissue-selective rather than ubiquitous knockouts of steroid receptors allows a more refined study of the mechanism of steroid action in defined target tissues and circumvents problems such as early lethality or major developmental defects precluding studies in affected organs. In this chapter, we describe the main steps involved in the development of tissue-selective steroid receptor knockouts by *Cre/loxP* technology. Problems in the development of a mouse strain with a floxed receptor allele, the selection of a suitable *Cre* expressing mouse strain, the generation of cell-selective knockouts by crossbreeding of the mentioned mouse strains, and the control of appropriate receptor inactivation are discussed taking the generation of mice with a Sertoli cell-selective ablation of the androgen receptor as an example.

**Key words:** Androgen receptor, Estrogen receptor, Glucocorticoid receptor, Mineralocorticoid receptor, Vitamin D<sub>3</sub> receptor, *Cre/loxP* technology, ES cells, Gene targeting, Testis, Sertoli cell.

---

### 1. Introduction

The finding that homologous recombination can be used to target specific genes in mammalian cells and the application of this approach to embryonic stem cells (ES) has paved the way to modify or silence virtually any desired gene in mice. The 2007 Nobel prize in Physiology or Medicine duly rewards the invaluable contributions of Mario Capecchi, Oliver Smithies, and Martin Evans to the development of this technology (1). By now at least 11,000 genes have been knocked out including the genes encoding steroid hormone receptors.

However, it soon became evident that mice models in which genes (including steroid receptor genes) are inactivated ubiquitously display inherent limitations. Inactivation of genes that are expressed early during development, for instance, may result in a lethal phenotype (as illustrated by the glucocorticoid receptor (GR) knockout) or may result in major developmental defects that preclude the study of the role of the targeted gene in affected organs or systems (as exemplified by the inability to study the role of the androgen receptor (AR) in the control of spermatogenesis in mice with an AR knockout because of the cryptorchid position of the testis) (2, 3). Moreover, ubiquitous ablation of a gene may result in adaptive and compensatory changes that obscure interpretation of the role of that particular gene in defined cells or tissues (4).

These problems can often be bypassed by the generation of conditional knockouts that allow tissue-selective and/or temporally controlled gene inactivation. The advent of the Cre/*loxP* recombination technology and the creation of modified inducible Cre recombinases have provided the tools to achieve virtually any desired conditional knockout (5, 6). This strategy is used ever more in the analysis of the effects of steroid hormone receptors. In the present chapter, we will provide a detailed account of the use of this approach in the study of the role of the AR in Sertoli cells (3, 7–9). Where relevant we will refer to other steroid hormone receptors to illustrate the potential and the problems involved in the use of these techniques (see the **Notes** section).

---

## 2. Materials

1. DNA manipulations: Amplification of DNA fragments was performed using Taq DNA polymerase and nucleotides (Invitrogen, Merelbeke, Belgium). DNA was purified from agarose gels using Qiagen gel extraction kit (Qiagen, Hilden, Germany). Restriction enzymes and appropriate restriction buffers (Promega Madison, WI, USA, or Invitrogen, Carlsbad, CA, USA). Radio-active labeling of DNA was performed using <sup>32</sup>P-dCTP (250 μCi/25 μL, 3,000 Ci/mmol, Amersham Biosciences, Arlington Heights, IL, USA). Hybridisation was performed using Rapid-hyb buffer (Amersham Biosciences). All constructs were transformed and grown in Epicurian Coli<sup>®</sup> XL10-Gold<sup>™</sup> ultracompetent cells (Stratagene, La Jolla, CA, USA). All oligonucleotides were synthesised by Eurogentec (Sar-Tilman, Belgium).
2. The plasmids pPNTlox2 and pOG231 were kindly provided by Prof. P. Carmeliet, Centre of Transgene Technology and

Gene Therapy (CTG), Flanders Interuniversity Institute for Biotechnology (VIB), Leuven, Belgium.

3. The BAC clone 138d19 (Genome systems Inc. St. Louis, MO, USA) containing AR exon 2 was obtained after PCR clone selection with primers mARex2-/mARex2+ (**Table 1**).
4. The pGEM-T<sup>®</sup> Vector System I kit and pGEM-7 vector (Promega).
5. Mitomycin C (Duchefa Biochemie B.V. Haarlem, The Netherlands).

**Table 1**  
**Sequences of oligonucleotides used for the generation and characterisation of the AR<sup>lox</sup> mouse strain and for *Rhox5* measurements by quantitative RT-PCR**

Primer name	Sequence
mAR7	5'AGCCACCAAGCACCAGCTGGG3'
mAR8	5'CAGGATTCAAAGTGTCCATAGG3'
mAR14	5' <i>CTCGAGCAGCTGGGACCACCTACATCACC3'</i>
mAR15	5' <i>CTCGAGGTACCATAACTTCGTATAGCATA</i> CATTATACGAAGT-TATGAGCAATCCATAGAATAGTCACTTGG3'
mAR20	5'ACTATGTAGATTGAGCTAGCCC3'
mAR23	5'CTTGGAGGTTACATAGCTCC3'
mAR24	5'GGCCGCGCTAGCAA3'
mAR25	5'GGCCTTGCTAGCGC3'
mAR28	5'AGCCTGTATACTCAGTTGGGG3'
mAR29	5'AATGCATCACATTAAGTTGATACC3'
mAR34	5' <i>CTAGTCTAGACTAG3'</i>
CreCDSfw	5'GCGATTATCTTCTATATCTTCAGG3'
CreCDSrev	5'GCCAATATGGATTAACATTCTCCC3'
mARex2-	5'TTTGAAGAAGACCTTGCAGC3'
mARex2+	5'AGGGACCATGTTTTGCCCA3'
Rhox5fw	5'TCATCATTGATCCTATTGAGGGTATG3'
Rhox5rev	5'CTCTCCAGCCTGGAAGAAAGC3'
Rhox5probe	FAM-5' <i>CTCGGAAGAACAGCATGATGTGAAAGCA3'</i> -TAMRA
Luci-fw	5'GCCCTGGTTCCTGGAACAA3'
Luci-rev	5'TCGAAGTATCCGCGTACGTG3'

The *loxP* site in primer mAR15 is shown in bold. Restriction sites are shown in italics

6. Cell culture reagents: Geneticin (Invitrogen); Gancyclovir (G418, Sigma-Aldrich St. Louis, MO, USA); Thromb-X medium (RESGRO, Millipore, Brussels, Belgium). ES medium: Dulbecco's modified Eagle's medium (DMEM) (Invitrogen) supplemented with 100 mM nonessential amino acids (Invitrogen), 15% (v/v) heat-inactivated fetal calf serum (Hyclone Logan, UT, USA), 0.001% (v/v)  $\beta$ -mercapto-ethanol (Sigma-Aldrich), 1 mM sodium-pyruvate (Invitrogen), 2 mM L-glutamine (Invitrogen), 100 IU/mL penicillin (Invitrogen), 100  $\mu$ g/mL streptomycin (Invitrogen) and 10 ng/mL Leukemia Inhibitory Factor (LIF) (Biognost, Heule, Belgium).
7. The R1 ES cell line was derived from 129Sv x 129cX/Sv by Andras Nagy (Samuel Lunenfeld Research Institute, Mount Sinai Hospital, Toronto, Ontario, Canada) and was available through the CTG.
8. Blastocyst injection: M2 medium, M16 medium (Eurogentec, Seraing, Belgium); pregnant mare serum gonadotropin (Sigma); human chorionic gonadotropin (Pregnyl, Organon; Oss, The Netherlands)
9. Genomic DNA for genotyping was prepared using phenol/chloroform/isoamylalcohol (25:24:1; v/v) (Invitrogen).
10. PGK-Cre animals were generated in the laboratory of Dr. P. Lonai (Weizmann Institute of Science, Rehovot, Israel) and were available through the CTG.
11. The AMH-Cre animals were kindly provided by Dr. F. Guillou (Institut National de la Recherche Agronomique (INRA), Nouzilly, France).
12. Swiss Webster mice (Charles River Laboratories L'Arbescle, France) and C57Bl/6N and CD1 wild-type mice (Janvier Le Genest Saint Isle, France) were used for maintenance of the strains or for backcrossing to specific backgrounds.
13. Immunohistochemistry reagents: Bouins fluid (for 105 mL: 75 mL saturated picric acid (Vel, Haasrode Belgium), 25 mL formaldehyde 37% (v/v) (Fluka, Buchs, Switzerland), 5 mL glacial acetic acid (Sigma-Aldrich)). Citric acid and bovine serum albumin (BSA) (Sigma-Aldrich). H<sub>2</sub>O<sub>2</sub>, ethanol, and methanol (BDH, Poole, United Kingdom). Tris-buffered saline (TBS, 0.05 M Tris-HCl, pH 7.4, 0.85% (v/v) NaCl (Sigma-Aldrich)). Normal swine serum (Diagnostics Scotland, Carlisle, Lanarkshire, United Kingdom). Rabbit anti-human AR (N-20) polyclonal antibody (sc-816, Santa Cruz Biotechnology, Santa Cruz, CA, USA). Swine anti-rabbit biotinylated second antibody (E0353), 3,3'-diaminobenzidine tetra-hydrochloride chromogenic substrate (K3468, Liquid DAB+ kit) (DAKO, Cambridge, United Kingdom).

Ready-to-use VECTASTAIN® Elite ABC-HRP reagent (PK-7,100, Vector Laboratories). Haematoxylin and pertex (Cellpath, Newtown Powys, United Kingdom).

14. Quantitative RT-PCR reagents: RNeasy midi kit and on-column DNaseI-treatment (Qiagen, Hilden, Germany). Luciferase mRNA (Promega). Superscript II RNaseH<sup>-</sup> reverse transcription kit, RNaseOUT<sup>®</sup>, random primer hexamers, MgCl<sub>2</sub>, dNTPs, Sybr<sup>®</sup>green (Invitrogen). Buffer A and Amplitaq Gold enzyme (Applied Biosystems, Foster City, CA, USA).

---

### 3. Methods

All the presently available tissue-selective knockouts of steroid receptors have been made using Cre/*loxP* technology. The Cre recombinase of the P1 bacteriophage is a site-specific recombinase of the integrase family that efficiently promotes recombination between specific 34 bp recognition sequences, called *loxP* sites. *LoxP* recognition sequences comprise two 13 bp inverted repeats flanking an 8 bp spacer region, which confers directionality. Intramolecular recombination between two *loxP* sites oriented in the same direction results in excision of the intervening (“floxed”) DNA. Recombination between *loxP* sites oriented in opposite direction results in reversible inversion of the intervening DNA (5, 6, 10). To generate a tissue-selective knockout, a first mouse strain in which a functionally critical part of the steroid receptor gene is floxed has to be crossed with a second mouse strain that expresses the Cre recombinase under the control of a lineage/cell type-specific promoter. An appropriate breeding strategy will result in the generation of progeny carrying the floxed allele (or alleles) of the steroid receptor in all cells and expressing the Cre recombinase in the selected lineage or cell type only, resulting in a lineage/cell-type-selective excision of the critical DNA fragment and inactivation of the targeted steroid receptor (*see Note 1*).

As an example of the application of this type of conditional knockout approach in the study of steroid receptor function, we will describe the generation of mice with a selective knockout of the AR in Sertoli cells (*see Note 2*). In a first part, we will give a detailed account of the procedure involved in the generation of mice with a “floxed” androgen receptor allele (AR<sup>lox</sup>). In a second part, criteria for the selection of an appropriate Cre-expressing mouse strain will be outlined. Finally, we will briefly discuss the phenotyping of animals with cell-selective knockouts and the procedures involved in checking the efficiency and selectivity of the recombination process.



### 3.1. Development of a Mouse with a “Floxed” Androgen Receptor Allele

The generation of a mouse strain with a floxed AR allele (AR<sup>flox</sup>) involves: selection of a crucial region in the AR gene that, when excised, will result in receptor silencing; construction of a targeting vector that allows flanking this region with correctly oriented *loxP* sites by homologous recombination in ES cells; and screening for properly recombined ES clones and generation of mice transmitting the AR<sup>flox</sup> allele via the germline.

#### 3.1.1. Selection of the Exon to Be Floxed and Position of the *LoxP*s Sites

In the case of the AR, we decided to flox exon 2. The rationale for this choice was that exon 2 encodes the first zinc finger of the DNA-binding domain, which is essential for the recognition of androgen response elements. Moreover, excision of exon 2 causes a frame-shift mutation resulting in the formation of a premature termination codon. In the human, the loss of exon 2 by a point mutation on the donor splice site at the end of the exon causes a complete androgen insensitivity syndrome with extremely low levels of the (inactive) AR transcript and protein (11). These observations could be confirmed also in the mouse (3, 9, 12, 13).

*LoxP* sites should be inserted in such a way that they do not interfere with the functionality of the floxed allele. To avoid interference with splicing processes, insertion within 100 bp of the intron-exon boundary should be avoided. When floxing the first exon, *loxP* sites should be positioned outside known regulatory sequences (see Note 3).

#### 3.1.2. Preparation of the Targeting Construct

The design of a targeting vector for homologous recombination in ES cells implies four major steps: detailed mapping of the targeted region of the steroid receptor gene (in this case the region encompassing exon 2 of the AR); introduction of 2 *loxP* sites flanking the selected exon; introduction of both positive and negative selection markers for screening purposes; and introduction of 2 “homology arms” for efficient homologous recombination with the ES genome.

1. Obtain a detailed map of the gene to be targeted. For the AR exon 2 genomic region, a 120 kbp genomic *HindIII*-fragment of the mouse AR containing exons 1 and 2 was isolated from a mouse ES129/SvJ BAC library (BAC clone No. 138d19), after PCR identification with specific primers for AR exon 2 (mARex2<sup>-</sup> and mARex2<sup>+</sup>, Table 1). The identity of the fragment was confirmed by Southern blotting with a probe for AR exon 2 and by sequencing. A Southern blot of a *NheI*, *XbaI*, *KpnI*, *EcoRV*, and *EcoRI* restriction digest was performed and hybridised with a <sup>32</sup>P-labeled probe for the mouse AR exon 2. The identified fragments were isolated and ligated into an appropriately digested pGEM-7 vector. In this way, five different but overlapping subclones containing AR exon 2 were obtained, and these were further mapped by restriction digests with a selection of restriction enzymes

(all with six-base recognition sites). A restriction map spanning about 15.6 kbp around AR exon 2 was constructed and used as a basis for the design of an appropriate targeting vector (Fig. 1a).

2. Introduce the required *loxP* sites into the target gene. The pNTlox2 plasmid, derived from the original pNT vector (14), was used as a tool to introduce the required *loxP* sites into the AR gene. This plasmid contains a neomycin resistance gene (neomycin phosphotransferase, *neo*), driven by the phosphoglycerate kinase-1 (*pgk*) promoter (*pgk-neo*) and flanked by *loxP* sites, for positive selection. In addition, it contains a *pgk* promoter-driven Herpes simplex virus thymidine kinase gene

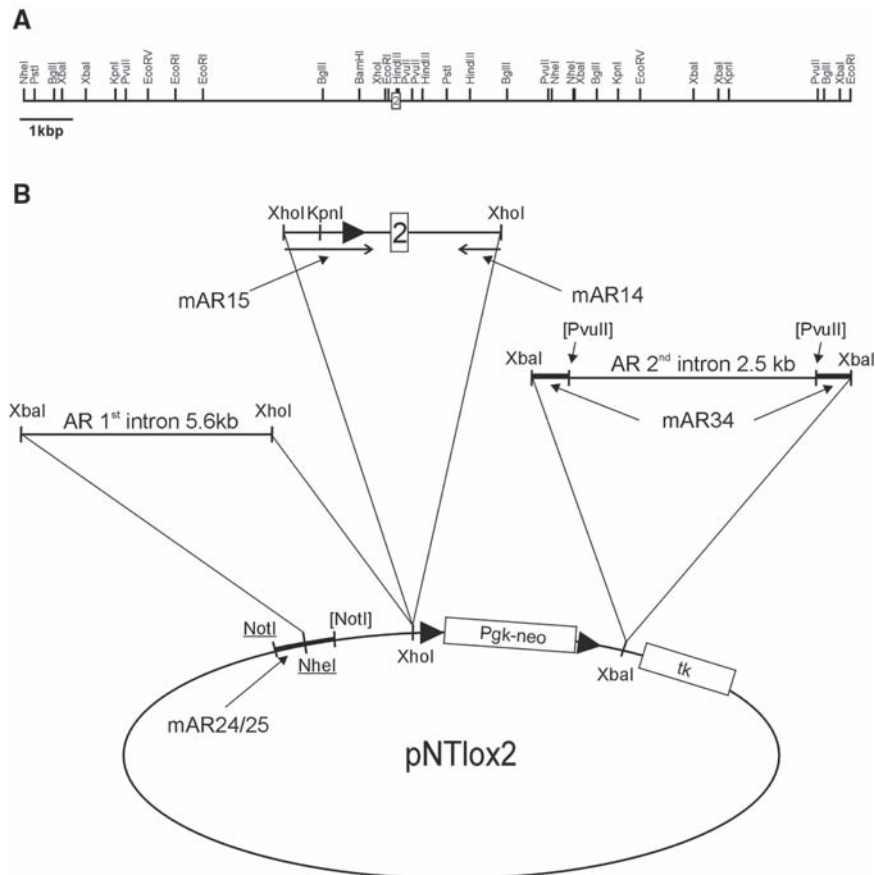


Fig. 1. Restriction map of the genomic region encompassing the mouse AR exon 2 and assembly map of the targeting vector. **(A)** Consensus restriction map for the exon 2 region based on alignment of the 5 genomic fragments subcloned from the BAC clone 138d19. Exon 2 is shown as a *box*. The figure is drawn to scale. This map was used as a base for all further cloning strategies. **(B)** Map outlining the strategy for the assembly of the targeting vector. *LoxP* sites are indicated as *triangles*. Not drawn to scale. Details of the assembly are described in the text. The unique *NheI* and *NotI* restriction sites are underlined and the PCR primers mAR14 and mAR15 are shown as *arrows* flanking Exon 2 (*box*). Destroyed restriction sites are shown between *square brackets*.

(*tk*) for negative selection and appropriate multiple cloning sites (MCS). The detailed strategy for the assembly of the entire vector is outlined in [Fig. 1B](#).

Before the introduction of different DNA-fragments, the 5' MCS of the vector pNTlox2 was modified to allow insertion of different fragments in a logical order. The modified vector was obtained by incorporation of a set of double-stranded oligonucleotides (mAR24/25, [Table 1](#)) into the *NotI* restriction site of the MCS, resulting in a unique *NheI* restriction site 3' of the *NotI* restriction site and 5' of the *loxP* sequence preceding the neo cassette. The modification resulted in the destruction of the *NotI* restriction site 3' of the *NheI* site. This modification was necessary to clone the different fragments in the correct order and to maintain a unique restriction site (*NotI*) for the linearisation of the construct prior to electroporation in ES cells.

Subsequently, the 5' genomic region for homologous recombination was inserted as a 5.6 kbp *XbaI* – *XhoI* fragment. In a separate step, a modified AR exon 2 was constructed by PCR so that a *loxP* site was introduced 132 bp 5' from AR exon 2, immediately 3' from the *XhoI* restriction site. In the forward primer (mAR15), a *KpnI* restriction site was inserted between the *XhoI* site and the *loxP* sequence for subsequent screening of transgenic animals. The reverse primer (mAR14) contained an extra *XhoI* site, positioned 223 bp downstream of AR exon 2. The PCR fragment was cloned into the pGEM-T vector and its sequence was verified. The modified AR exon 2 was then again excised from the plasmid by means of *XhoI* digestion and inserted in the *XhoI*-digested targeting vector. Sequencing was used to verify the orientation of the fragment and all three *loxP* sites.

Ultimately, a 2.5 kbp genomic fragment from the second intron of the AR gene adjacent to exon 2 was excised from a genomic subclone by *PvuII* digestion, to serve as a second homology arm (*see Note 4*). 5' phosphorylated adapters (mAR34) containing an *XbaI* restriction site were ligated to the fragment, and the ligation reaction was subjected to *XbaI* digestion. The gel-purified fragment was then ligated in the *XbaI*-digested targeting vector. Again, orientation was verified by sequencing. The final targeting vector was used for electroporation after linearisation by *NotI* digestion. All fragments were chosen and designed to minimize the differences between the “floxed” AR exon 2 locus in the targeting vector and the corresponding region in the original wild-type (WT) AR gene.

### 3.1.3. Homologous Recombination in Embryonic Stem Cells (ES)

1. The embryonic stem (ES) cell line R1 was used for generation of transgenic ES cells. This ES cell line shows high efficiency in colonising the germline of the 129 mouse strain (15). R1 ES cells were cultured on mitomycin C-treated (Duchefa Biochemie) embryonic fibroblasts in ES medium (as described

in the Materials section). Six million ES cells were electroporated (Biorad Gene pulser, 250V, 500mF) with 20µg of *NotI*-linearized targeting vector in Dulbecco's modified Eagle's medium supplemented with 20% fetal calf serum and 2000 units/mL Leukemia Inhibitory Factor (15) and seeded onto mitomycin C-treated neomycin-resistant embryonic fibroblasts in 0.1% gelatin coated 10 cm dishes.

2. Twenty-four hours after electroporation, the medium was replaced with medium containing active G418 (0.2mg/mL Geneticin) to select clones containing the *neo* selection marker. Gancyclovir (2µM) selection was applied approximately 4 days later to select for the clones that had lost the *tk*-cassette. About eight days later, surviving individual colonies were expanded into 48-well plates and grown in duplicate, one for genomic DNA extraction and one for storage at -80°C.
3. Two DNA probes external to the targeting vector (probes A and B) were used to screen for correct homologous recombination by Southern blotting as shown in Fig. 2. Panel A demonstrates the genomic organisation before and after homologous recombination. Panel B shows Southern blot analysis of *EcoRV*-digested DNA from ES cells transfected with the targeting vector using probe A. The presence of a 4.6 kbp fragment of the recombined allele ( $AR^{Ex2-neo}/Y$ ) when compared to a WT band of 9.3 kbp ( $AR^+/Y$ ) revealed correct homologous recombination. In the same way, probe B was used to detect correct recombination at the 5' site of the construct using a *NheI* digest (band shift from 10 to 12 kbp, not shown). Additionally, hybridisation with an internal probe (C) after *NheI* digestion excluded the presence of randomly integrated targeting vectors (see Note 5). Probes A and C were generated as PCR fragments using primer pairs mAR20/23 and mAR7/8, respectively, and cloned into the pGEM-T vector. Probe B was generated from a 447 bp *XbaI* fragment located 3' from AR exon 2 that was cloned in an appropriately digested pGEM-7 vector. <sup>32</sup>P-labelling of the probes was performed by PCR using the same primers (probe A and C) or by random primed labeling (probe B) on a template obtained by digestion from the vector containing the probe.

Out of 158 individual ES clones surviving the G418/Gancyclovir selection, 9 were found to have undergone correct homologous recombination without further random integration ( $AR^{Ex2-neo}/Y$ , Fig. 2). One of these clones was then further expanded to allow removal of the *neo* selection cassette. Recombination efficiencies reported in the literature vary from 0.5 up to 78%, depending on the size of the recombination arms and the origin of the genomic DNA used (see Note 4).

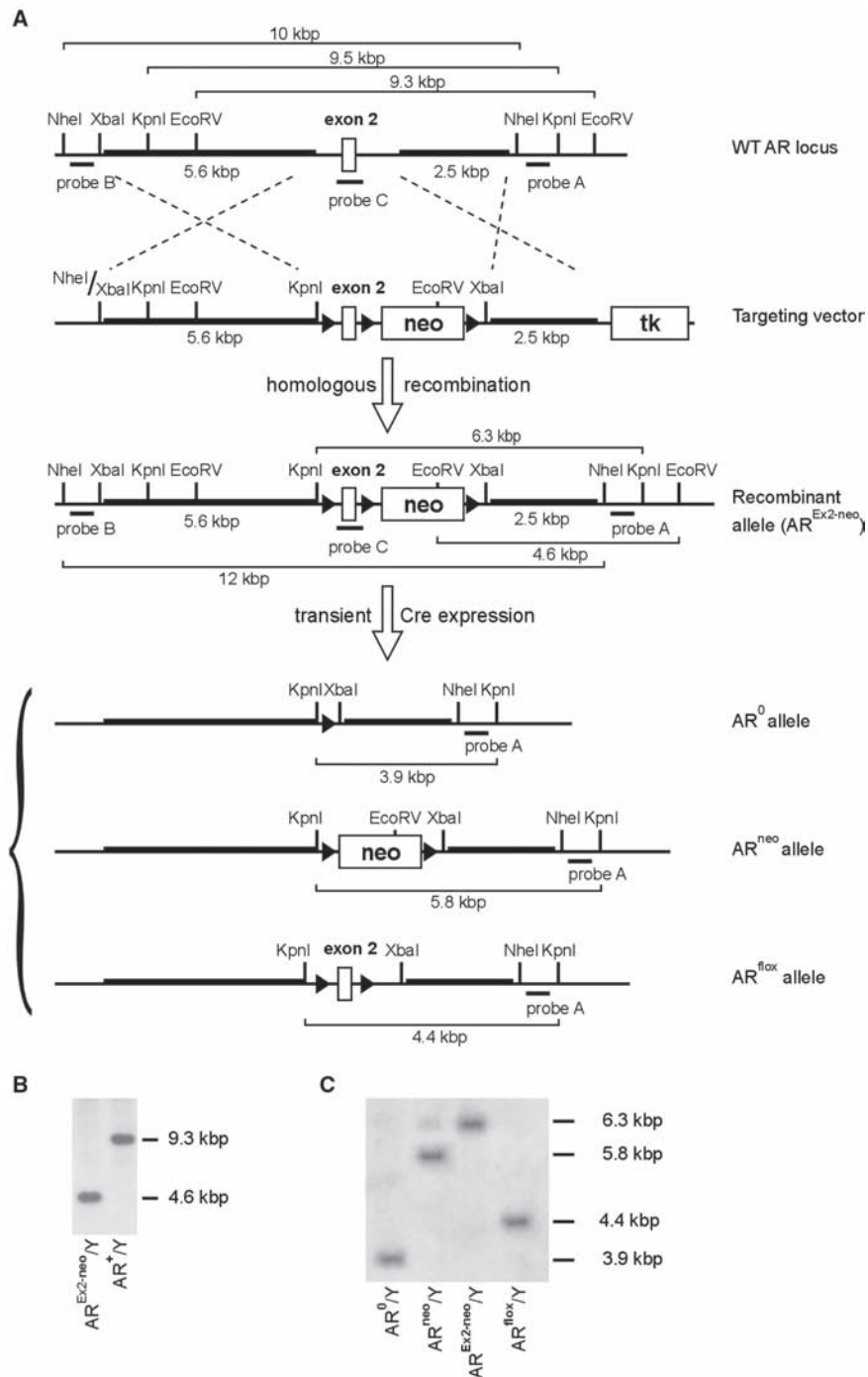


Fig. 2. Generation of an AR allele with a floxed exon 2. See text for detailed explanation, *LoxP* sites are indicated by *triangles*. **(A)** Homologous recombination of the WT AR locus with the targeting vector leads to the formation of a recombinant allele in ES cells. After transient Cre-expression in these ES cells, three possible recombination events can be distinguished. **(B)** Southern blot analysis of *EcoRV*-digested DNA from ES cells transfected with the targeting vector using probe A. The presence of a 4.6 kbp fragment of the recombined allele ( $AR^{Ex2-neo}/Y$ ) vs. a WT band of 9.3 kbp ( $AR^+/Y$ ) revealed correct homologous recombination. **(C)** Southern blot analysis of DNA isolated from pOG231 transfected recombinant ES cells. DNA was digested with *KpnI* and hybridised with probe A. All possible recombinations are shown: complete excision ( $AR^0/Y$ ), 3.9 kbp; excision of exon 2 only ( $AR^{neo}/Y$ ), 5.8 kbp; no excision ( $AR^{Ex2-neo}/Y$ ), 6.3 kbp and the desired excision of the neo cassette only ( $AR^{lox}/Y$ ) showing a 4.4 kbp fragment.

### 3.1.4. Removal of Selection Cassettes

After the selection of a correctly recombined ES clone, the neo cassette was excised by transient transfection of a Cre expression plasmid (*see Note 6*). Targeted ES cells were transiently transfected by electroporation (250 V, 500 mF) with the Cre-expressing plasmid pOG231 (*16*) and plated on feeder cells without selection. The resulting colonies were expanded, and genomic DNA was prepared for Southern blot analysis. DNA was digested with *KpnI*, blotted, and hybridised with probe A (**Fig. 2c**). All possible recombinations were observed: complete excision of exon 2 and neo cassette, resulting in a 3.9 kbp fragment (AR<sup>0</sup>/Y); excision of exon 2 only, resulting in a 5.8 kbp fragment (AR<sup>neo</sup>/Y); no excision (AR<sup>Ex2-neo</sup>/Y), 6.3 kbp and the intended excision of the neo cassette only resulting in a 4.4 kbp fragment (AR<sup>lox</sup>/Y). Most of the studied clones showed complete excision. Only 1 correctly excised ES clone carrying a floxed AR exon 2 and no neo selection cassette (AR<sup>lox</sup>/Y) could be picked up out of 216 clones tested. This clone was expanded in “Thromb-X medium” to optimize subsequent germline transfer (*17*) and used for blastocyst injection.

### 3.1.5. Blastocyst Injection

The targeted ES cell clones selected by genotyping were injected into the inner cell mass of 3.5-day-old blastocysts (8–12 cells per blastocyst), isolated from the uteri of superovulated 129 Swiss females by flushing with M2 medium. Superovulation was induced by injection of 7.5 IU pregnant mare serum gonadotropin followed by injection of 7.5 IU human chorionic gonadotropin after a 48-h interval. Injected blastocysts were left to recover 2–3 h at 37°C (5% CO<sub>2</sub>) in M16 medium and subsequently reimplanted into pseudopregnant (2.5 days postcoitum) females (20 embryos per female) to proceed to term. Chimeric progeny were identified by the agouti contribution of the ES cells to the coat color. From the blastocyst injections, one female (20% chimerism) and 7 male chimeric mice (3 with 5%, 3 with 50% and one with 60% chimerism) were obtained. As an alternative to this technique, morula aggregation can be performed (*see Note 7*).

### 3.1.6. Germline Transmission and Genotyping

Chimeric males were mated to 129 Swiss females to test germline transmission. Transgenic founders were identified again by scoring coat and eye color. Two of the 50% chimeric males displayed 100% germline transmission as judged by coat color. The 60% chimera produced only 1 litter containing transgenic pups. One of the 50% chimeras with 100% germline transmission was used as founder strain.

Initially, genotyping of the offspring was performed by Southern blotting of a *KpnI* digest and hybridisation with probe A. The appearance of a 4.4 kb band (due to the presence of an extra *KpnI* restriction site introduced via oligonucleotide mAR15) confirmed the presence of the floxed AR exon 2 in comparison with a 9.5 kb



WT AR band. In a later stage, genotyping was done by PCR on genomic DNA with a primer pair (mAR28 & mAR29, [Table 1](#)) carefully chosen to amplify different band sizes for the floxed, the WT and the excised (knockout) AR allele. This primer pair allows the simultaneous detection of different AR alleles in one PCR reaction (*see* [Note 8](#)).

### 3.1.7. Maintenance of the “Floxed” Mouse Strain

The AR<sup>flox</sup> mouse strain was initially bred on a mixed 129/Swiss background. In general, AR<sup>flox/+</sup> females were mated to WT males and heterozygous females were selected from the progeny, either for further maintenance of the strain or for generation of cell-selective knockouts. In a later stage, backcrossings were initiated to transfer the mutated allele to a C57Bl/6N or a CD1 background. Six generations of backcrossing resulted in a 98% C57Bl/6N and a 98% CD1 AR<sup>flox</sup> strain, respectively (*see* [Note 9](#)).

### 3.2. Selection of a Suitable Cre-Expressing Mouse Strain

The selection of an appropriate Cre expressing mouse line is a second crucial step in the process of generating a lineage/cell type-selective knockout model. Expression of the recombinase in the tissue of interest determines the specificity and the completeness and as such the success of the new transgenic mouse model. Three criteria need to be considered when selecting a Cre mouse line:

1. Tissue and/or cell-selectivity of Cre expression.
2. Timing and duration of Cre expression.
3. Level of Cre expression.

For the Sertoli cell (SC)-selective excision of the floxed exon 2 allele, we selected an AMH-Cre line, kindly provided by Dr. F. Guillou (Tours, France). This mouse strain carries a transgene in which the Cre recombinase is placed under the control of a 3.6 kbp promoter fragment of the human Anti-Müllerian Hormone (*AMH*) gene on a C57Bl/6SJL background (*18*). The construct was randomly integrated in the genome by pronuclear zygote injection. In male mice, the endogenous *AMH* gene is expressed, selectively in testicular SC, as early as 12 days post-coitum (dpc) and reaches maximum levels by 15 dpc. Thereafter, expression progressively declines to a very low level by day 12 of postnatal life (*9*). As the expression of the AR in SC starts around day 3–5 of postnatal life (*19*), excision of the floxed exon 2 is expected to occur long before the AR is expressed. Moreover, as AMH is a relatively abundant secreted protein, the AMH promoter is expected to drive Cre expression strongly enough to obtain SC Cre protein levels that can efficiently recombine the *loxP* sites. Finally the suitability of the AMH-Cre strain was nicely demonstrated by crossing this strain with a “reporter strain” (*18*) (*see* [Note 10](#)). In this reporter strain (R26R) (*20*), excision of a floxed STOP cassette induces the expression of the *LacZ* gene as can be shown by X-gal staining. The authors demonstrate that



Cre activity is limited to the SC in the testis and can be detected from 15.5 dpc on. Moreover, X-gal staining is observed in virtually every SC, reflecting not only SC-selective Cre expression, but also highly efficient recombination (3). The latter is an important feature, as an ablation of the AR in only part of the SC would heavily confound the interpretation of the phenotype. For these reasons, the AMH-Cre strain from the laboratory of Dr. Guillou was considered a very promising tool to generate a SC-selective AR knockout.

It should be mentioned that alternatives for the use of relatively short promoter fragments have recently been developed to drive site-specific Cre expression in a reliable way. These alternatives have successfully been applied to create tissue-selective inactivation of the GR and the mineralocorticoid receptor (MR) (*see* **Note 11**). Furthermore, the development of modified Cre recombinases that become only active in the presence of an exogenously administered pharmacological compound has made it possible to control steroid receptor gene inactivation not only spatially but also temporally (*see* **Note 12**).

A database of tissue-specific Cre-expressing mouse strains is available from <http://nagy.mshri.on.ca/cre>.

Despite the fact that detailed studies are lacking, there are many indications that (as is the case for the floxed mouse lines) genetic background may influence Cre expression level, pattern and timing (*see* **Note 13**). Additionally, ectopic expression of the Cre recombinase in germ cells and/or early embryo's may lead to unforeseen problems in the generation of tissue-selective knockouts (*see* **Note 14**).

### **3.3. Control of Appropriate Receptor Ablation**

After the generation (or selection) of an appropriate floxed mouse strain and an appropriate Cre-expressing mouse strain, intercrossing can be initiated to generate the intended animals with a tissue-selective knockout. The complexity of the breeding scheme depends on the fact whether the parent strains are homozygous/heterozygous or hemizygous for the floxed receptor allele or for the promoter-Cre construct. In our case of a cell-selective knockout of the AR in male animals, for instance, the breeding scheme is facilitated by the fact that male mice carry only one AR allele located on the X-chromosome. The genetic constitution of the progeny can be verified by genetic analysis (Southern blotting and PCR reaction on the tail DNA). Phenotypic analysis should be as complete as possible to avoid that unexpected characteristics are missed. The analysis of the phenotype can often already give a good indication of the selectivity and efficiency of the intended knockout. In the case of the Sertoli cell-selective knockout of the AR (SCARKO), for instance, the characteristics of the animals were markedly different from those of a ubiquitous AR knockout (external phenotype male instead of female, normal internal genitalia

rather than absence of all Wolffian duct-derived structures, normally descended instead of intra-abdominal testes). Moreover, the small size of the testes and the meiotic block on histological examination reflected a disturbance in Sertoli cell function. Nonetheless, it remained to be demonstrated that this phenotype was related to the intended Sertoli cell-selective knockout. The fact that the AMH-Cre strain used in these experiments induces Sertoli cell-selective activation of a reporter gene in the R26R reporter strain can be considered as a suggestive indirect argument for a successful experiment ([Subheading 3.2.](#)) but AR inactivation needs to be confirmed in a more direct way at the DNA (Southern blotting and PCR), mRNA (northern blotting and in situ hybridisation) or at the protein level (*see* [Note 15](#)). In this particular case, PCR on testicular DNA confirmed the presence of a floxed AR allele and an allele with excision of exon 2 (as a consequence of the fact that SC are not the only AR containing cells in the testis). Moreover, immunohistochemistry confirmed the complete absence of AR staining in Sertoli cells whereas staining was normal in peritubular myoid and Leydig cells (*see* [Note 16](#)) (3, 9). Finally, to confirm functional ablation of the AR, expression of *Rbmx5*, a gene known to show an approximately 50-fold induction in testicular Sertoli cells under the influence of androgens (21), was studied and found to be virtually absent in the SCARKO testis (*see* [Note 17](#)) (3, 9).

#### **3.4. Selection of Appropriate Control Animals**

One of the underestimated problems in many studies with tissue-selective knockout models is the selection of an appropriate control to use as a reference for further studies with the tissue selective knockout animals. When breeding is performed with female mice that are heterozygous for the AR<sup>fllox</sup> allele and males that are heterozygous for the AMH-Cre, for instance, three types of control male littermates are generated: WT males, males carrying the AR<sup>fllox</sup> allele (but not the AMH-Cre), and males carrying AMH-Cre (but not the AR<sup>fllox</sup>). It cannot a priori be excluded that even the relatively subtle genetic modifications resulting from the introduction of the *loxP* sites (in the AR<sup>fllox</sup> strain) or the AMH-Cre construct (in the AMH-Cre strain) may induce phenotypic consequences that may confound the interpretation of the results (we have already discussed the possibility of the creation of hypomorphic alleles in [Note 6](#)). Accordingly, careful phenotyping of all possible controls for all the characteristics studied is absolutely required. If no significant differences are observed, all possible controls can eventually be combined. If significant differences are observed, it is important to report those to allow correct interpretation of the data and to caution other investigators using the same or comparable mouse strains. The same comparisons are needed when changing the genetic background of one of the mice strains used.

In the SCARKO studies, we did not observe any differences when comparing the reproductive phenotype of the mentioned control groups with their WT littermates. However, while using the same AR<sup>lox</sup> mouse strain, on a C57Bl/6 background, to generate ubiquitous AR knockouts (ARKO) using a PGK-Cre mouse strain, limited but significant weight differences were observed between WT male littermates and littermates carrying the AR<sup>lox</sup>.

---

## 4. Notes

1. A similar approach can be used to generate mice with a ubiquitous steroid receptor knockout. In this case, the mouse strain carrying the floxed receptor allele(s) should be crossbred with a strain expressing Cre ubiquitously, for example, under the control of a CMV promoter (22), a  $\beta$ -actin promoter (23) or a phosphoglycerate kinase-1 promoter (24).
2. Comparable techniques as those described here have in the meantime been used to generate selective knockouts of the AR in other testicular cells (25, 26), prostate epithelial cells (27), and osteoblasts (28).
3. The most straightforward approach to obtain a complete knockout might be to flank the entire gene with *loxP* sites. However, in most cases this is technically not feasible. An alternative option is to target the exon containing the translational start site. In this case, care should be taken that the introduction of a 5' *loxP* site does not disturb crucial regulatory sequences of the gene. The majority of the studies on conditional steroid receptor knockouts have used mutated receptor alleles causing excision of the first or second zinc finger (Table 2).
4. The optimal length of the homology arms required to allow homologous recombination varies greatly depending on the genetic structure of the targeted region. As a general rule, either arm should be at least 2 kbp long. Upper limits of the arm lengths are usually determined by the cloning efficiency of the targeting vector and experiments have shown that the efficiency of recombination reaches a plateau when the combined homology flank length reaches 8 kbp (29). It should be noted that the use of isogenic DNA (DNA from the same strain of mice as the ES cells that will be used for electroporation) is extremely important as it has a major beneficial influence on recombination efficiency (30).
5. The use of both external and internal probes in this screening procedure is essential to exclude multiple (random) integration

**Table 2**  
**List of published mouse lines with “floxed”steroid receptor genes**

Steroid receptor gene	Floxed exon	Encoded receptor fragment	Reference
Androgen receptor	Exon 1	N-terminal domain	(48, 49, 31)
	Exon 2	1st zinc finger	(3, 12)
	Exon 3	2nd zinc finger	(46)
Vitamin D <sub>3</sub> receptor	Exon 2	1st zinc finger	(50, 51)
Estrogen receptor $\alpha$	Exon 3	1st zinc finger	(52)
Estrogen receptor $\beta$	Exon 3	1st zinc finger	(52)
Glucocorticoid receptor	Exon 3	1st zinc finger	(53)
Mineralocorticoid receptor	Exon 3	1st zinc finger	(39)

into the genome and to verify correct homologous recombination. In the case of the AR, the screening of the ES cells was facilitated by the fact that the ES cells used are of a male origin and accordingly carry only one copy of the X chromosome and the AR gene.

- In general, it is advisable to remove the selection cassette used to allow identification of ES cells that have integrated the target vector by homologous recombination (e.g., neo-cassette). The presence of such a cassette in a noncoding/intronic region of the targeted gene may lead to a knock-down or hypomorphic allele that results in reduced expression levels of the relevant gene already in the floxed mouse strain (6). Although such hypomorphic phenotypes may be informative as such (31), they are unwanted when one aims to create a cell-selective knockout. The hypomorphic state of the gene in the entire animal obscures the interpretation of the phenotype when such a floxed mouse strain is crossed with a Cre expressing strain (6, 31).

To allow removal of the selection cassette, the cassette is usually floxed in the targeting construct. Alternatively, the Flp recombinase system can be used to permit removal of selectable markers (32). When *loxP* sites are used both to allow excision of a functionally critical region of the targeted gene and to allow removal of a selection cassette, one ends up with ES cells in which the mutated allele contains at least 3 *loxP* sites in a row (Fig. 2). Selective removal of the selection cassette can be achieved by transient transfection of the ES cells with a Cre expressing vector (as in our description of the floxed AR). A disadvantage of this approach is that additional in vitro manipulation may affect the capacity of the ES cells to contribute to the germline in chimeric mice (33). The alternative is to remove the selection marker in vivo for

instance by crossing the floxed strain, still carrying the selection cassette, with “deleter” Cre expressing strains such as *MeuCre40* that generate partial mosaic *Cre/loxP* recombination patterns in the early embryo that are transmitted to the germline (34). In both procedures, cells or animals need to be identified carrying the desired mutated allele in which only the cassette has been removed. Such correct recombinations tend to be rare.

7. As an alternative to blastocyst injection, morula aggregation can be used to obtain chimeric progeny (35). In short, ES cells and Swiss Webster morula-stage embryonic cells are brought together in conic wells and left to reaggregate. The resulting morulas are then reimplanted in pseudopregnant females. Alternative techniques using tetraploid morula cells allow the generation of progeny that is derived 100% from the ES cells as the 4n morula cells can only give rise to the extraembryonic tissues (35).
8. It is possible to detect the presence of all forms of the targeted allele in a single PCR reaction. For this purpose, the forward primer (in our case: mAR28, **Table 1**) is selected 5' from the floxed sequence, the reverse primer 3' (mAR29, **Table 1**) from the floxed fragment. A PCR reaction can then be optimized using freshly prepared genomic DNA. We have experienced that the purity of the genomic DNA is critical for the success of this PCR reaction designed to detect the three possible AR alleles: after the initial precipitation of the tail lysate with isopropanol, a phenol/chloroform/isoamyl alcohol (25:24:1, v/v) extraction step is required, followed by a second isopropanol precipitation and a 70% ethanol wash. The products of the PCR reaction are then separated on an agarose gel. The practicability of this technique is highly dependent on the resolution of the WT and the floxed PCR band in the gel, as the insertion of both *loxP* sites adds only 68 bp to the WT allele. Alternatively, multiple PCRs can be performed with primer pairs selected inside the floxed region.
9. During these backcrossings, it is important to cross successively heterozygous  $AR^{\text{floxed}/+}$  females and WT C57Bl/6N males to allow also crossing over events between the X-chromosomes (the hemizygous state of the AR allele in the male prevents this). An inevitable drawback of breeding with heterozygous parents and backcrossing with heterozygous  $AR^{\text{floxed}/+}$  females is the possibility that crossing over occurs within the floxed AR allele, resulting in the loss of one *loxP* site from the genome. Therefore, control experiments should be performed on a regular basis to check the integrity/functionality of the floxed allele. This can be done either by sequencing of the PCR-product obtained in

the genotyping reaction or (more elaborately) by the generation of knockout animals and demonstration of the presence of the knockout allele in their DNA.

10. The specificity and efficiency of newly generated Cre expressing mouse strains should be evaluated by cross-breeding with a “reporter strain.” The latter strains usually carry a reporter gene, separated from a strong promoter by a floxed STOP-cassette (usually a repeated poly-adenylation (**pA**) sequence). Cre-mediated excision of the cassette activates the reporter gene that is subsequently expressed. Several reporter strains have been generated. One of the most widely used is the ROSA26 (R26R) strain (20). In this strain, excision of the STOP cassette results in the expression of  $\beta$ -galactosidase that can easily be detected by X-gal staining.

A second generation of “double reporter mice” express different reporters before and after recombination. In these animals, the pA sequences in the STOP-cassette are preceded by a second reporter (Green fluorescent protein (GFP) or alkaline phosphatase (AP)) (36, 37). The latter is then driven by the ubiquitous promoter as long as the construct is intact. Recombination removes both this reporter and the pA signals and switches on the second reporter (mostly *LacZ*). This approach allows assessment of the prerecombination expression levels of the strong promoter in the tissue of interest. Since the genetic background may affect Cre expression, reporter mice should ideally be bred on the same background as that used for the floxed mice in the intended tissue-selective knockout.

11. The use of relatively short promoter fragments to drive Cre expression sometimes results in mosaic and ectopic expression patterns. Recent data show that these problems can often be overcome by the use of BAC (bacterial artificial chromosome) or YAC (yeast artificial chromosome)-derived transgenes in which Cre is inserted at the ATG of a gene chosen to drive Cre expression. The advantage of these BAC or YAC vectors is that they harbor large genomic regions encompassing almost all the regulatory elements of the selected gene locus. Moreover, expression of Cre can nicely be controlled by increasing the number of transgene copies in the Cre expressing mouse strain (38). This technique has successfully been applied, for instance to inactivate the GR and MR in specific regions of the brain (38, 39). The presence of more regulatory elements in the BAC constructs may also lead to unexpected events. Expression may be observed in organs or cell types where it has not been observed previously. Moreover, the insertion of large BAC constructs in the genome may also import other genes and their regulatory sequences. The effect of the amplification of

these genes on the phenotype needs to be carefully evaluated in appropriate control mice (*see Subheading 3.4*).

12. To achieve not only spatially but also temporally-controlled Cre-induced gene inactivation, a number of fusion constructs have been developed in which the Cre recombinase is linked to the mutated ligand-binding domain (LBD) of a steroid hormone receptor to allow ligand-dependent Cre activation. The Cre-ER<sup>T2</sup> recombinase, for instance, is a fusion protein of a mutated LBD of the human estradiol receptor and the Cre recombinase, the activity of which can be induced by 4-hydroxy-tamoxifen but not by estradiol. It displays low leakiness and highly efficient induction (38, 40, 41). An analogous fusion protein has been developed containing a mutated LBD of the human progesterone receptor, inducible by the synthetic steroid RU486 (4).
13. Several investigators communicate (unpublished) difficulties in maintaining cell-selective and efficient knockout models during prolonged breeding and particularly when changing the genetic background of the floxed or Cre-expressing mouse strains. During an attempt to transfer our AR<sup>fllox</sup> strain (originally on a 129/Swiss background) onto a C57BL/6N background, we also observed important variation in the testicular phenotype when the floxed (C57BL/6N) animals were crossed with the original AMH-Cre mice. Some animals displayed a SC-selective and complete inactivation of the AR, while others displayed intermediary phenotypes with persistent expression of the AR in a variable fraction of the SC. Surprisingly, when the same floxed mice were crossed with a strain expressing Cre ubiquitously (under control of the phosphoglycerate kinase-1 promoter), a complete androgen insensitivity phenotype was observed indicating that exon 2 could still be excised. The mechanism of the decreased efficiency of exon 2 excision in the crossings with AMH-Cre mice could not be identified but the problem disappeared when the AR<sup>fllox</sup> strain was transferred to a 98% CD1 background.
14. Crossing of a mouse strain carrying a floxed allele with a strain expressing the Cre recombinase under the control of a cell-selective promoter may unexpectedly result in the generation of animals in which the conditional allele is rearranged regardless of the inheritance of the Cre recombinase transgene. Problems of this kind have been observed, for instance, in the generation of mice with conditional knockouts of the vitamin D<sub>3</sub> receptor (G. Carmeliet, personal communication). This type of event can probably be explained by the fact that even gametes from heterozygous Cre carrying parents that do not harbor the Cre transgene may contain sufficient amounts of Cre mRNA or protein in their



cytoplasm to cause Cre-mediated rearrangement at or after the two cell stage of zygote development (24, 42). Ectopic and mosaic recombination may also be observed with promoter-Cre constructs that cause transient Cre expression in the early embryo (43). In all these cases, both mice with a cell-specific and mice with ectopic recombination may be produced and the genotype needs to be carefully checked in each individual animal.

15. Cre-mediated excision of an exon does not necessarily result in complete gene inactivation. Some steroid receptor alleles lacking an exon may still give rise to the production of truncated transcripts and proteins, or proteins originating from alternative translational start codons. A vitamin D<sub>3</sub> receptor (VDR) allele that lacks exon 2, for instance, allows the synthesis of a protein that originates from an alternative ATG codon in exon 3 (44, 45). This protein is still able to bind 1 $\alpha$ , 25-dihydroxyvitamin D<sub>3</sub>. It is unclear whether this truncated protein has any remaining function. In the case of the AR, a mouse line harboring a floxed exon 3 was generated, in which a mutant AR protein lacking the second zinc finger can still be found after recombination of the *loxP* sites (46). The authors are using this model to search for effects of the AR that do not depend on binding to androgen responsive elements. Effects that do not depend on glucocorticoid response element binding have in fact been described, for instance for the GR (47).
16. Immunohistochemical studies on expression of the AR were routinely performed on testes derived from 50-day-old mice. Testes were fixed in Bouins fluid for 4–6 h at room temperature and stored in 70% (v/v) ethanol at 4°C prior to further processing into paraffin blocks. Paraffin blocks were sectioned at 5  $\mu$ m thickness. Immunohistochemistry was performed on dewaxed sections in conjunction with heat-induced antigen retrieval for 5 min in 0.01 M citrate buffer, pH 6.0, using a pressure cooker. This was followed by endogenous peroxidase blocking (3% (v/v) H<sub>2</sub>O<sub>2</sub> in methanol) for 30 min at room temperature. Sections were washed with tap water for 5 min followed by a 5 min wash in Tris-buffered saline (TBS). Between all antibody or reagent incubations, two washes for 5 min at room temperature in TBS were performed. Tissue sections were subsequently blocked for 30 min in TBS containing normal swine serum (1:4) and 5% (w/v) bovine serum albumin. The rabbit anti-AR polyclonal primary antibody was diluted 1:200 in the same blocking buffer and incubated overnight with the sections at 4°C. A swine anti-rabbit biotinylated second antibody was used in conjunction, diluted 1:500 in the same blocking serum, and

incubated at room temperature for 30 min. Bound antibodies were visualized by incubating the sections with Ready-To-Use VECTASTAIN® Elite ABC-HRP reagent for 30 min followed by color development with 3,3'-diaminobenzidine tetra-hydrochloride chromogenic substrate, monitored microscopically. Sections were counterstained with haematoxylin, dehydrated, and mounted with pertex. Images were captured using an Olympus Provis microscope (Olympus Optical Co., London, United Kingdom) equipped with a Kodak DCS330 camera (Eastman Kodak Co., Rochester, NY, USA). Captured images were stored on a Macintosh G4 computer and compiled using Photoshop 7.0 (Adobe, Mountain View, CA, USA). To enable comparative evaluation of the immunostaining, sections of tissues from control and knockout animals were processed in parallel on at least three occasions to ensure reproducibility of results; on each occasion tissue sections from 4 to 6 animals in each group were run. To ensure direct comparability of staining intensities, one section each from control, ARKO and SCARKO mice were mounted on the same slide.

17. Quantitative RT-PCR for the *Rbox5* gene was performed on testes derived from 50-day-old animals, snap-frozen into liquid nitrogen and weighed. After homogenisation in a Dounce homogenizer, RNA was isolated with the Qiagen RNeasy midi kit according to the manufacturers' instructions, encompassing an on-column DNaseI-treatment. To allow specific mRNA levels to be expressed per testis and to control for the efficiency of RNA extraction, RNA degradation and the RT step, an external standard was used. The external standard was luciferase mRNA, and 10 ng was added to each testis at the start of the RNA extraction procedure. cDNA was prepared by reverse transcription, using the Superscript II RnaseH<sup>-</sup> reverse transcription kit including RNaseOUT<sup>™</sup>, according to the manufacturers instructions, starting from 2 µg of total RNA and using 150 ng of random primers per reaction. All samples were reverse transcribed simultaneously. For sample cDNA quantification, the ABI Prism 7,700 sequence detector PCR detection system (Applied Biosystems, Foster City, CA, USA) was used. The quantitative PCR two-step protocol was 10 min at 95°C, 40 cycles of 15 s at 95°C and 1 min at 60°C. Components for real-time PCR were obtained from Applied Biosystems, apart from primers and probes (Eurogentec) and Sybr<sup>®</sup>green (Invitrogen). For the luciferase external standard, each 25-µL real-time PCR reaction contained 1× buffer A, 5 mM MgCl<sub>2</sub>, 400 µM dNTPs, 200 nM of each primer (lucif-w, lucif-rev; see [Table 1](#)), 0.4 x Sybr<sup>®</sup>green I and 0.025 U/µL Amplitaq Gold enzyme. For the *Rbox5* gene, a labeled probe was

used (Rhox5probe; see **Table 1**): in this case, 100 nM of each primer (Rhox5fw, Rhox5rev; see **Table 1**), 400 nM probe and no Sybr<sup>®</sup>green I were added to the reaction. Subsequent quantitative PCR was performed on 5  $\mu$ L of a 1/10 dilution of the cDNA reaction. For luciferase, uniqueness of the amplicon was checked by polyacrylamide gel electrophoresis.

To create standards for the quantitative PCR, gene-specific cDNAs were generated by RT-PCR. The fragments were then cloned into pGEM-T Easy, sequenced to confirm their identity, and quantified by spectrophotometry. Primer pairs were designed according to the published cDNA sequences and, where possible, spanned an intron to avoid amplification of genomic DNA. To allow specific mRNA levels to be expressed per testis and to correct for differences in the efficiency of RNA extraction, RNA degradation and the reverse transcription reaction, gene expression data were expressed as a ratio to luciferase mRNA. All samples and standard curves were run in triplicate.

---

## Acknowledgments

This work was supported by a Concerted Research Action (Research Fund, Katholieke Universiteit Leuven) and the Fund for Scientific Research Flanders (Belgium). Karel De Gendt is a postdoctoral fellow of the Research Foundation Flanders (FWO). We thank Dr. F. Guillou (Tours France) for the AMH-Cre mice and Prof. J. Swinnen, F. Claessens, L. Schoonjans, M. Dewerchin, G. Carmeliet and P. Carmeliet (K.U.Leuven, Belgium) for helpful discussions and advice in creating the transgenic animals.

## References

1. Vogel, G. (2007) Nobel prizes – A knock-out award in medicine. *Science*, **318**, 178–179.
2. Schmid, W., Cole, T.J., Blendy, J.A., and Schutz, G. (1995) Molecular genetic analysis of glucocorticoid signalling in development. *Journal of Steroid Biochemistry and Molecular Biology*, **53**, 33–35.
3. De Gendt, K., Swinnen, J.V., Saunders, P.T.K., Schoonjans, L., Dewerchin, M., Devos, A., Tan, K., Atanassova, N., Claessens, F., Lecureuil, C., Heyns, W., Carmeliet, P., Guillou, F., Sharpe, R.M., and Verhoeven, G. (2004) A Sertoli cell-selective knockout of the androgen receptor causes spermatogenic arrest in meiosis. *Proceedings of the National Academy of Sciences USA*, **101**, 1327–1332.
4. Kellendonk, C., Tronche, F., Casanova, E., Anlag, K., Opherk, C., and Schutz, G. (1999) Inducible site-specific recombination in the brain. *Journal of Molecular Biology*, **285**, 175–182.
5. Sauer, B. (1998) Inducible gene targeting in mice using the Cre/lox system. *Methods—A Companion to Methods in Enzymology*, **14**, 381–392.
6. Nagy, A. (2000) Cre recombinase: The universal reagent for genome tailoring. *Genesis*, **26**, 99–109.

7. De Gendt, K., Atanassova, N., Tan, K.A.L., de Franca, L.R., Parreira, G.G., Mckinnell, C., Sharpe, R.M., Saunders, P.T.K., Mason, J.I., Hartung, S., Ivell, R., Denolet, E., and Verhoeven, G. (2005) Development and function of the adult generation of Leydig cells in mice with Sertoli cell-selective or total ablation of the androgen receptor. *Endocrinology*, **146**, 4117–4126.
8. Denolet, E., De Gendt, K., Allemeersch, J., Engelen, K., Marchal, K., Van Hummelen, P., Tan, K.A.L., Sharpe, R.M., Saunders, P.T.K., Swinnen, J.V., and Verhoeven, G. (2006) The effect of a Sertoli cell-selective knockout of the androgen receptor on testicular gene expression in prepubertal mice. *Molecular Endocrinology*, **20**, 321–334.
9. Tan, K.A.L., De Gendt, K., Atanassova, N., Walker, M., Sharpe, R.M., Saunders, P.T.K., Denolet, E., and Verhoeven, G. (2005) The role of androgens in Sertoli cell proliferation and functional maturation: Studies in mice with total or Sertoli cell-selective ablation of the androgen receptor. *Endocrinology*, **146**, 2674–2683.
10. Sauer, B. and Henderson, N. (1988) Site-specific DNA recombination in mammalian-cells by the Cre recombinase of bacteriophage-P1. *Proc.Natl.Acad. Sci.U.S.A.*, **85**, 5166–5170.
11. Hellwinkel, O.J.C., Bull, K., Holterhus, P.M., Homburg, N., Struve, D., and Hiort, O. (1999) Complete androgen insensitivity caused by a splice donor site mutation in intron 2 of the human androgen receptor gene resulting in an exon 2-lacking transcript with premature stop-codon and reduced expression. *Journal of Steroid Biochemistry and Molecular Biology*, **68**, 1–9.
12. Yeh, S.Y., Tsai, M.Y., Xu, Q.Q., Mu, X.M., Lardy, H., Huang, K.E., Lin, H., Yeh, S.D., Altuwaijri, S., Zhou, X.C., Xing, L.P., Boyce, B.F., Hung, M.C., Zhang, S., Gan, L., and Chang, C.S. (2002) Generation and characterization of androgen receptor knockout (ARKO) mice: An in vivo model for the study of androgen functions in selective tissues. *Proceedings of the National Academy of Sciences USA*, **99**, 13498–13503.
13. De Gendt, K., Atanassova, N., Tan, K.A.L., de Franca, L.R., Parreira, G.G., Mckinnell, C., Sharpe, R.M., Saunders, P.T.K., Mason, J.I., Hartung, S., Ivell, R., Denolet, E., and Verhoeven, G. (2005) Development and function of the adult generation of Leydig cells in mice with Sertoli cell-selective or total ablation of the androgen receptor. *Endocrinology*, **146**, 4117–4126.
14. Tybulewicz, V.L.J., Crawford, C.E., Jackson, P.K., Bronson, R.T., and Mulligan, R.C. (1991) Neonatal lethality and lymphopenia in mice with a homozygous disruption of the C-Abl protooncogene. *Cell*, **65**, 1153–1163.
15. Nagy, A., Rossant, J., Nagy, R., Abramow-Newerly, W., and Roder, J.C. (1993) Derivation of completely cell culture-derived mice from early-passage embryonic stem-cells. *Proceedings of the National Academy of Sciences USA*, **90**, 8424–8428.
16. O’Gorman, S., Dagenais, N.A., Qian, M., and Marchuk, Y. (1997) Protamine-Cre recombinase transgenes efficiently recombine target sequences in the male germ line of mice, but not in embryonic stem cells. *Proceedings of the National Academy of Sciences USA*, **94**, 14602–14607.
17. Schoonjans, L., Kreemers, V., Danloy, S., Moreadith, R.W., Laroche, Y., and Collen, D. (2003) Improved generation of germline-competent embryonic stem cell lines from inbred mouse strains. *Stem Cells*, **21**, 90–97.
18. Lecureuil, C., Fontaine, I., Crepieux, P., and Guillou, F. (2002) Sertoli and granulosa cell-specific Cre recombinase activity in transgenic mice. *Genesis*, **33**, 114–118.
19. Bremner, W.J., Millar, M.R., Sharpe, R.M., and Saunders, P.T.K. (1994) Immunohistochemical Localization of Androgen Receptors in the Rat Testis – Evidence for Stage-Dependent Expression and Regulation by Androgens. *Endocrinology*, **135**, 1227–1234.
20. Soriano, P. (1999) Generalized lacZ expression with the ROSA26 Cre reporter strain. *Nature Genetics*, **21**, 70–71.
21. Lindsey, J.S. and Wilkinson, M.F. (1996) Pem: A testosterone- and LH-regulated homeobox gene expressed in mouse Sertoli cells and epididymis. *Developmental Biology*, **179**, 471–484.
22. Schwenk, F., Baron, U., and Rajewsky, K. (1995) A cre-transgenic mouse strain for the ubiquitous deletion of loxP-flanked gene segments including deletion in germ cells. *Nucleic Acids Research*, **23**, 5080–5081.
23. Lewandoski, M. and Martin, G.R. (1997) Cre-mediated chromosome loss in mice. *Nature Genetics*, **17**, 223–225.
24. Lallemand, Y., Luria, V., Haffner-Krausz, R., and Lonai, P. (1998) Maternally expressed PGK-Cre transgene as a tool for early and uniform activation of the Cre site-specific recombinase. *Transgenic Research*, **7**, 105–112.

25. Tsai, M.Y., Yeh, S.D., Wang, R.S., Yeh, S., Zhang, C., Lin, H.Y., Tzeng, C.R., and Chang, C. (2006) Differential effects of spermatogenesis and fertility in mice lacking androgen receptor in individual testis cells. *Proceedings of the National Academy of Sciences USA*, **103**, 18975–18980.
26. Zhang, C.X., Yeh, S.Y., Chen, Y.T., Wu, C.C., Chuang, K.H., Lin, H.Y., Wang, R.S., Chang, Y.J., Mendis-Handagama, C., Hu, L.Q., Lardy, H., and Chang, C.S. (2006) Oligozoospermia with normal fertility in male mice lacking the androgen receptor in testis peritubular myoid cells. *Proceedings of the National Academy of Sciences USA*, **103**, 17718–17723.
27. Simanainen, U., Allan, C.M., Lim, P., McPherson, S., Jimenez, M., Zajac, J.D., Davey, R.A., and Handelsman, D.J. (2007) Disruption of prostate epithelial androgen receptor impedes prostate lobe-specific growth and function. *Endocrinology*, **148**, 2264–2272.
28. Notini, A.J., McManus, J.F., Moore, A., Bouxsein, M., Jimenez, M., Chiu, W.S.M., Glatt, V., Kream, B.E., Handelsman, D.J., Morris, H.A., Zajac, J.D., and Davey, R.A. (2007) Osteoblast deletion of exon 3 of the androgen receptor gene results in trabecular bone loss in adult male mice. *Journal of Bone and Mineral Research*, **22**, 347–356.
29. Deng, C.X. and Capecchi, M.R. (1992) Reexamination of gene targeting frequency as a function of the extent of homology between the targeting vector and the target locus. *Molecular and Cellular Biology*, **12**, 3365–3371.
30. Te Riele, H., Maandag, E.R., and Berns, A. (1992) Highly efficient gene targeting in embryonic stem-cells through homologous recombination with isogenic dna constructs. *Proceedings of the National Academy of Sciences USA*, **89**, 5128–5132.
31. Holdcraft, R.W. and Braun, R.E. (2004) Androgen receptor function is required in Sertoli cells for the terminal differentiation of haploid spermatids. *Development*, **131**, 459–467.
32. Meyers, E.N., Lewandoski, M., and Martin, G.R. (1998) An Fgf8 mutant allelic series generated by Cre- and Flp-mediated recombination. *Nature Genetics*, **18**, 136–141.
33. Fedorov, L.M., HaegelKronenberger, H., and Hirschhain, J. (1997) A comparison of the germline potential of differently aged ES cell lines and their transfected descendants. *Transgenic Research*, **6**, 223–231.
34. Leneuve, P., Colnot, S., Hamard, G., Francis, F., Niwa-Kawakita, M., Giovannini, M., and Holzenberger, M. (2003) Cre-mediated germline mosaicism: a new transgenic mouse for the selective removal of residual markers from tri-ox conditional alleles. *Nucleic Acids Research*, **31**.
35. Tanaka, M., Hadjantonakis, A.K., and Nagy, A. (2001) Aggregation chimeras. Combining ES cells, diploid and tetraploid embryos. *Methods in Molecular Biology*, **158**, 135–154.
36. Lobe, C.G., Koop, K.E., Kreppner, W., Lomeli, H., Gertsenstein, M., and Nagy, A. (1999) Z/AP, a double reporter for Cre-mediated recombination. *Developmental Biology*, **208**, 281–292.
37. Novak, A., Guo, C.Y., Yang, W.Y., Nagy, A., and Lobe, C.G. (2000) Z/EG, a double reporter mouse line that expresses enhanced green fluorescent protein upon Cre-mediated excision. *Genesis*, **28**, 147–155.
38. Erdmann, G., Schutz, G., and Berger, S. (2007) Inducible gene inactivation in neurons of the adult mouse forebrain. *BMC Neuroscience*, **8**.
39. Berger, S., Wolfer, D.P., Selbach, O., Alter, H., Erdmann, G., Reichardt, H.M., Chepkova, A.N., Welzl, H., Haas, H.L., Lipp, H.P., and Schutz, G. (2006) Loss of the limbic mineralocorticoid receptor impairs behavioral plasticity. *Proceedings of the National Academy of Sciences USA*, **103**, 195–200.
40. Indra, A.K., Warot, X., Brocard, J., Bornert, J.M., Xiao, J.H., Chambon, P., and Metzger, D. (1999) Temporally-controlled site-specific mutagenesis in the basal layer of the epidermis: comparison of the recombinase activity of the tamoxifen-inducible Cre-ERT and Cre-ERT2 recombinases. *Nucleic Acids Research*, **27**, 4324–4327.
41. Hayashi, S. and McMahon, A.P. (2002) Efficient recombination in diverse tissues by a tamoxifen-inducible form of Cre: A tool for temporally regulated gene activation/inactivation in the mouse. *Developmental Biology*, **244**, 305–318.
42. Cochrane, R.L., Clark, S.H., Harris, A., and Kream, B.E. (2007) Rearrangement of a conditional allele regardless of inheritance of a cre recombinase transgene. *Genesis*, **45**, 17–20.
43. Eckardt, D., Theis, M., Doring, B., Speidel, D., Willecke, K., and Ott, T. (2004) Spontaneous ectopic recombination in cell-type-specific Cre mice removes loxP-flanked marker cassettes in vivo. *Genesis*, **38**, 159–165.



44. Bula, C.M., Huhtakangas, J., Olivera, C., Bishop, J.E., Norman, A.W., and Henry, H.L. (2005) Presence of a truncated form of the vitamin D receptor (VDR) in a strain of VDR-knockout mice. *Endocrinology*, **146**, 5581–5586.
45. Erben, R.G., Soegiarto, D.W., Weber, K., Zeitz, U., Lieberherr, M., Gniadecki, R., Moller, G., Adamski, J., and Balling, R. (2002) Deletion of deoxyribonucleic acid binding domain of the vitamin D receptor abrogates genomic and nongenomic functions of vitamin D. *Mol.Endocrinol.*, **16**, 1524–1537.
46. Notini, A.J., Davey, R.A., McManus, J.F., Bate, K.L., and Zajac, J.D. (2005) Genomic actions of the androgen receptor are required for normal male sexual differentiation in a mouse model. *J.Mol.Endocrinol.*, **35**, 547–555.
47. Reichardt, H.M., Kaestner, K.H., Tucker-mann, J., Kretz, O., Wessely, O., Bock, R., Gass, P., Schmid, W., Herrlich, P., Angel, P., and Schutz, G. (1998) DNA binding of the glucocorticoid receptor is not essential for survival. *Cell*, **93**, 531–541.
48. Matsumoto, T., Takeyama, K.I., Sato, T., and Kato, S. (2003) Androgen receptor functions from reverse genetic models. *Journal of Steroid Biochemistry and Molecular Biology*, **85**, 95–99.
49. Sato, T., Matsumoto, T., Kawano, H., Watanabe, T., Uematsu, Y., Sekine, K., Fukuda, T., Aihara, K.I., Krust, A., Yamada, T., Nakamichi, Y., Yamamoto, Y., Nakamura, T., Yoshimura, K., Yoshizawa, T., Metzger, D., Chambon, P., and Kato, S. (2004) Brain masculinization requires androgen receptor function. *Proceedings of the National Academy of Sciences USA*, **101**, 1673–1678.
50. Van Cromphaut, S.J., Dewerchin, M., Hoenderop, J.G.J., Stockmans, I., Van Herck, E., Kato, S., Bindels, R.J.M., Col-len, D., Carmeliet, P., Bouillon, R., and Carmeliet, G. (2001) Duodenal calcium absorption in vitamin D receptor-knockout mice: Functional and molecular aspects. *Proceedings of the National Academy of Sciences USA*, **98**, 13324–13329.
51. Masuyama, R., Stockmans, I., Torrekens, S., Van Looveren, R., Maes, C., Carmeliet, P., Bouillon, R., and Carmeliet, G. (2006) Vitamin D receptor in chondrocytes promotes osteoclastogenesis and regulates FGF23 production in osteoblasts. *Journal of Clinical Investigation*, **116**, 3150–3159.
52. Dupont, S., Krust, A., Gansmuller, A., Dierich, A., Chambon, P., and Mark, M. (2000) Effect of single and compound knockouts of estrogen receptors alpha (ER alpha) and beta (ER beta) on mouse reproductive phenotypes. *Development*, **127**, 4277–4291.
53. Tronche, F., Kellendonk, C., Kretz, O., Gass, P., Anlag, K., Orban, P.C., Bock, R., Klein, R., and Schutz, G. (1999) Disruption of the glucocorticoid receptor gene in the nervous system results in reduced anxiety. *Nature Genetics*, **23**, 99–103.

# Chapter 15

## Methods for Identifying and Studying Genetic Alterations in Hormone-Dependent Cancers

Outi R. Saramäki, Kati K. Waltering, and Tapio Visakorpi

### Abstract

Genetic alterations underlying the development of cancer include large chromosomal aberrations, such as amplifications, deletions and translocations as well as small changes in sequence, i.e. mutations. Thus, different methods are needed to reveal various types of genetic changes. Fluorescence in situ hybridisation (FISH) is a versatile technique for detecting chromosomal alterations either in cultured cells or even in formalin-fixed paraffin-embedded tissue. For screening mutations, denaturing high-performance liquid chromatography (DHPLC) provides a relatively fast, cheap and sensitive option. The only special requirement is the HPLC equipment suitable for the analysis. As a screening tool, it does not reveal the actual base pair change, which in the end needs to be done by sequencing. FISH and DHPLC can both be utilized in research as well as in clinical diagnostic laboratories.

**Key words:** Fluorescence in situ hybridisation; Sequencing; Denaturing high-performance liquid chromatography; Cancer; Genetic alterations

---

### 1. Introduction

Genetic alterations underlie the development of cancers, including hormone-dependent ones. Several types of genetic aberrations can be detected in malignant cells. These include copy number alterations, such as deletions and amplifications. Rearrangements that do not necessarily alter the copy number, such as translocations, can also be found. In addition to these large chromosomal aberrations affecting the whole gene or genes, also base pair changes, i.e. mutations are often detected in cancers. These, most often somatic, genetic changes activate oncogenes and inactivate



tumour suppressor genes. Examples of copy number alterations in hormone-dependent carcinomas include amplification of *ERBB2* gene in breast cancer (1) and amplification of *AR* gene in prostate cancer (2). Translocations, which were thought to be rare in carcinomas, have also now been found in solid tumours. Especially, the rearrangement leading to *TMPRSS2:ERG* fusion seems to be common, found in 30–60% of prostate cancers (3). Examples of point mutations found in hormone-dependent carcinomas are common inactivating missense mutations in *TP53* tumour suppressor gene in breast cancer (4), and activating point mutations in the androgen receptor (*AR*) gene in antiandrogen-treated prostate cancers (5).

Different methods are needed to detect various types of genetic aberrations in cancer tissue. Fluorescence in situ hybridisation (FISH) enables the visualisation of both copy number alterations as well as other types of chromosomal rearrangements, including translocations (Fig. 1). FISH can be performed on cultured cells, but most importantly also from tissues including archival formalin-fixed paraffin-embedded (FFPE) tumour samples. Previously, the FISH analysis on FFPE specimens required isolation of nuclei prior to the hybridisation (6). However, today the analysis can equally well be performed on tissue sections without the disruption of tissue architecture allowing the identification of malignant and non-malignant cells in the specimen (7). The development of FISH was originally dependent on the emergence of recombinant plasmids that were able to carry large DNA inserts. The first FISH probes were cosmids, subsequently PIs (bacteriophage PI), YACs (yeast artificial chromosomes) and PACs (PI-derived artificial chromosome) became available. Today, the most com-

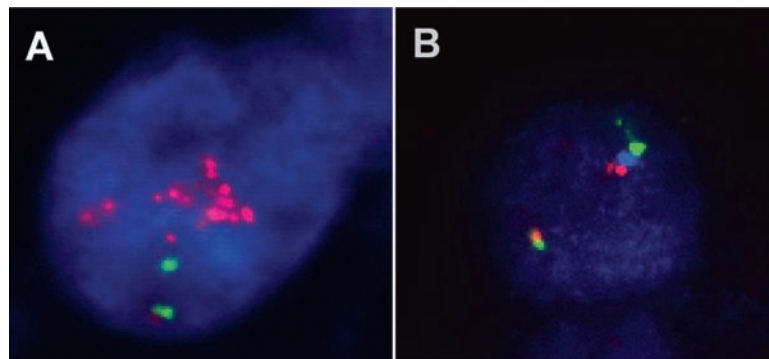


Fig. 1. FISH analysis of prostate cancer xenograft samples. (A) AR amplification (*red*) in a prostate cancer xenograft LuCaP69 sample. Centromere X probe (*green*) is used as a control and the chromosome appears to have been duplicated prior to AR amplification. (B) Fusion of *TMPRSS2* (*red*) and *ERG* (*green*) in a prostate cancer xenograft sample. The *blue* probe, which is normally located between the two genes (see wildtype chromosome), has been deleted from the abnormal chromosome and the *red* and *green* signals are fused (see *Color Plates*).

monly used probes for FISH are bacterial artificial chromosome (BAC) clones. It is now possible to select a BAC clone for almost any gene of choice just by browsing the genome databases by using e.g., NCBI Map Viewer (<http://www.ncbi.nlm.nih.gov/mapview/>), UCSC Genome Browser ([genome.ucsc.edu/](http://genome.ucsc.edu/)) or Ensembl Genome Server (<http://www.ensembl.org/index.html>). The average size of the BAC inserts is 120–140 kb, providing a strong signal. For the most studied oncogenes and tumour suppressor genes, also labelled ready-to-use FISH probes can be purchased from several vendors. In FISH, the probe DNA is first extracted, labelled, denatured and then hybridised to denatured samples on microscope slides, stained when necessary and visualised with an epifluorescence microscope. The most expensive and a key-part of the FISH analysis is the microscope, which needs to be equipped with high quality fluorescence filters. The FISH signals are, even under optimal conditions, quite weak.

Only genetic alterations that affect thousands of base pairs of DNA can be detected by FISH. Thus, other methods are needed for the analysis of smaller alterations. There are a number of methods for screening base pair changes. The most straightforward is direct sequencing. A shortcoming of sequencing is that it is laborious and slow if large fragments (e.g., whole coding region of a gene) need to be analyzed. However, new sequencing technologies, such as massively parallel sequencing will facilitate large scale sequencing (8). Unfortunately, the price of these methods is also very high. A major problem in direct sequencing of cancer tissues is that typically the samples contain not only malignant cells, but also normal cells. Thus, mutations can be masked by the sequence derived from the normal cells. There are two solutions for this problem: (1) one can microdissect malignant cells from the sample, which, however, is very time consuming, or (2) one can use methods that are sensitive enough to detect a mutation even in a small fraction of cells. There are several mutation screening methods that can be used for mixed cell population. These include single-strand conformational polymorphism (SSCP) assay, conformation sensitive capillary electrophoresis (CSCE), and denaturing gradient gel electrophoresis (DGGE) (9–11).

One relatively new mutation screening technique is a heteroduplex analysis with denaturing high-performance liquid chromatography (DHPLC). It is a very sensitive and cost effective method for screening unknown mutations from a large number of samples. There is no need to label or otherwise modify the PCR fragments to be run in DHPLC making the procedure simple and cheap. In DHPLC, normal DNA and sample DNA are PCR amplified separately and then mixed, denatured and allowed to slowly renature. If a mutation is present, some of the reannealed fragments will have mismatches, which form bubbles in the DNA

double strand. The DNA is bound to a column with triethylammonium acetate (TEAA) and then eluted with a gradient of acetonitrile under partially denaturing conditions. The heteroduplexes with the bubbles elute earlier than perfectly matched homoduplexes and can be seen as additional peaks on an electropherogram (Fig. 2). Sensitivity and specificity of DHPLC has been reported to be as high as 96–98% even for single base pair changes (12). Thus DHPLC is as sensitive for detecting point mutations as sequencing. However, to confirm and characterise the sequence alteration, the sample has to be subsequently sequenced. Depending on the structure of the gene of interest, mutation screening can be performed from cDNA or DNA. Generally, it is easier and faster when using cDNA. However, often RNA (and hence cDNA) is not available from the sample. Mutations may also affect the stability of the transcript, and thus the mutated transcript might be underrepresented in the cDNA pool. Therefore, in most cases the analysis is done using genomic DNA. In this chapter, we provide details for both FISH and DHPLC analysis of chromosomal defects.

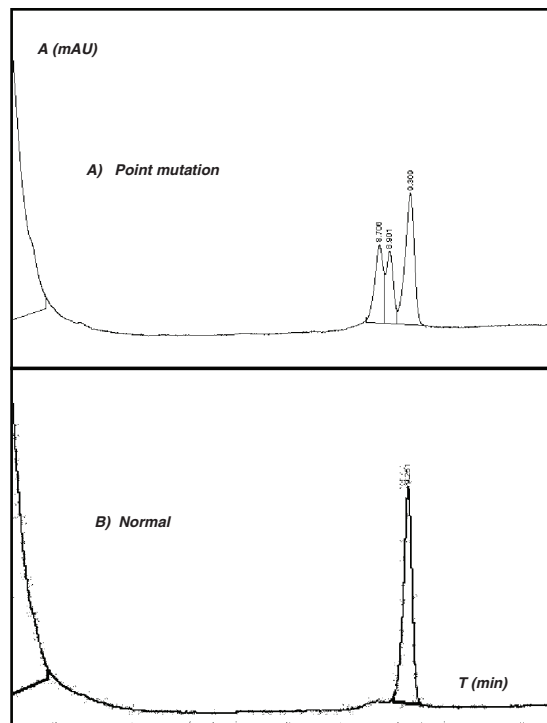


Fig. 2. DHPLC analysis of normal DNA sample and a prostate cancer cell line carrying a point mutation. (A) Prostate cancer cell line (LAPC4) carrying T > G single base mutation in the same region compared with negative control (13). (B) Negative control carrying no mutations in AR promoter region.

## 2. Materials

### 2.1. Fluorescence In Situ Hybridisation

#### 2.1.1. Labelling of Probes by Nick Translation

1. Double-stranded DNA extracted from a bacterial clone containing the desired genomic sequence. (*see Note 1*).
2. 10× A4 (dNTP) mix: 0.2 mM dATP, dCTP and dGTP, 500 mM Tris-HCl, pH 7.8, 50 mM MgCl<sub>2</sub>, 100 mM β-mercaptoethanol, 100 μL/mL bovine serum albumin (BSA).
3. FITC-12-dUTP (DuPont), TexasRed-6-dUTP (DuPont), AlexaFluor594-5-dUTP, (Molecular Probes), digoxigenin-11-dUTP (Roche Diagnostics), biotin-16-dUTP (Boehringer Mannheim) or other labelled dUTP (*see Note 2*).
4. Enzyme mix: 500 U/mL DNA Polymerase I, (e.g., Promega or Fermentas), 1 U/mL DNase I, (from bovine pancreas grade I, 10,000 U, Roche), 100 μg/mL BSA (nuclease free), (50 mg/mL stock (Gibco BR)) in a buffer containing 50 mM Tris-HCl (pH 7.5), 5 mM magnesium acetate, 1 mM β-mercaptoethanol, 50% (v/v) glycerol. The enzyme mix is prepared as follows (*all steps on ice*): (1) 5–10 mL Buffer (excess stored in freezer for later use): 50 mM Tris-HCl (pH 7.5), 5 mM magnesium acetate, 50% (v/v) glycerol, 1 mM β-mercaptoethanol. (add β-mercaptoethanol after autoclaving). (2) BSA-stock: add 2 μL BSA (50 mg/mL) to 1 mL buffer. (3) DNase-stock: add 1 mg (=3,000 U) DNase I to 300 μL BSA-stock (its activity will be 3,000 U/300 μL = 10 000 U/mL) and aliquot (e.g. 6 × 50 μL) and store in freezer for later use. Working solution prepared by diluting 1:100 with BSA-stock (activity will be 100 U/mL). (4) Enzyme-mix: Dilute DNase-stock again 1:100 in the BSA-stock and add 50 U DNA Polymerase I (e.g., 1 μL DNase-stock + 5–5.5 μL DNA Polymerase I + BSA-stock a.d.100 μL). Store in -20°C (*see Note 3*).

#### 2.1.2. Agarose Gel Electrophoresis

1. Agarose.
2. TBE buffer (0.5×): 45 mM Tris, 45 mM boric acid, 1 mM EDTA, pH 8.0.
3. Loading buffer: 15% Ficoll 400, 0.25% bromophenol blue, 0.35% xylencyanoid.
4. DNA-ladder.

#### 2.1.3. Hybridisation

1. Carnoy fixative: 1/3 acetic acid glacial/methanol.
2. Xylene.
3. Methanol.
4. 1M NaSCN.
5. 0.9% (w/v) NaCl, pH 1.5.
6. Ethanol: 100%, 85%, 70%.

7. MM 1.0 solution (50% formamide, 10% dextran sulphate, 1× SSC, pH 7): 1 g dextran sulphate (MW 500,000), 5 mL formamide (high-grade), 1 mL 20× SSC (3 M sodium chloride–0.3 M sodium citrate buffer). Warm at +70°C until the dextran has dissolved, adjust the pH to 7. Adjust the volume to 7 mL by H<sub>2</sub>O. Store at –20°C (*see Note 4*).
8. Cot-1 DNA, (Gibco BRL).
9. Denaturation solution: 70% formamide/2× SSC, pH 7. Store in 4°C (*see Note 4*).
10. Pepsin (Sigma): 67 mg in 40 mL of 0.9% (w/v) NaCl, pH 1.5.
11. Rubber cement (Fixogum, Marabu).

#### 2.1.4. Post-Hybridisation Washes and Staining

1. 50% formamide/2× SSC, stored in 4°C (*see Note 4*).
2. 4× SSC/0.05% (v/v) Tween, store in RT.
3. 4× SSC, store in RT.
4. 4× SSC/1% (w/v) BSA, stored in –20°C.
5. 5 µg/mL avidin-FITC, 10 µg/mL streptavidin-PacificBlue, 2 µg/mL anti-digoxigenin- FITC (or – rhodamine) diluted in 4× SSC/ 1% BSA.
6. 4× SSC/0.1% Triton-X, store in RT.
7. Phosphate buffer with NP-40 (PN-buffer): 0.1 M NaH<sub>2</sub>PO<sub>4</sub>, 0.1 M Na<sub>2</sub>HPO<sub>4</sub>/0.1% NP-40, pH 8.0) Preparation: solution A: 13.8 g NaH<sub>2</sub>PO<sub>4</sub> ad 1,000 mL H<sub>2</sub>O, solution B: 89 g Na<sub>2</sub>HPO<sub>4</sub> ad 5,000 mL H<sub>2</sub>O. Adjust the pH of solution B to pH 8 with solution A. Mix 5 mL NP-40 gently into 4,950 mL buffer. Store in RT.
8. 5 µg/mL biotinylated anti-avidin, 2.5 µg/mL biotinylated anti-streptavidin diluted in 4× SSC/1% (w/v) BSA.
9. Diamidino-2-phenylindole (DAPI, Molecular Probes).
10. Vectashield antifade solution (Vector Laboratories).

## 2.2. DHPLC (Denaturing High Performance Liquid Chromatography)

### 2.2.1. PCR

1. Platinum-Taq (Invitrogen) or other suitable PCR-kit.
2. dNTP mixture (10 µM).
3. MgCl<sub>2</sub>-buffer 0.5–3.0 mM.
4. Agarose gel (1.5% (w/v)).
5. TBE-buffer (0.5×).

### 2.2.2. DHPLC

1. Triethylammonium acetate buffer (2%) (Helix™ Buffer A for DHPLC).
2. Acetonitrile (25%); 1% triethylammonium acetate buffer (Helix™ Buffer B for DHPLC).
3. Helix Analytical Column (Varian).

**2.3. Sequencing**

1. Qiagen or other PCR-purification kit.
2. BigDye Terminator v3.1 Cycle Sequencing Kit.
3. Sodium (or potassium) acetate (3.0 M).
4. Absolute ethanol.
5. Ethanol (70%).

---

**3. Methods****3.1. Fluorescence  
In Situ Hybridisation***3.1.1. Labelling of  
Probes by Nick  
Translation*

1. Mix in a dark microcentrifuge tube, starting with water and then in indicated order: (1.) add 50  $\mu\text{L}$   $\text{H}_2\text{O}$ , (2.) 5  $\mu\text{L}$  10 $\times$  A4, (3.) 1  $\mu\text{g}$  dsDNA extracted from BAC-clone, (4.) 1  $\mu\text{L}$  labelled nucleotide, (5.) 1  $\mu\text{L}$  DNA polymerase I, (6.) 4  $\mu\text{L}$  enzyme-mix.
2. Vortex and spin briefly.
3. Incubate 40–60 min at 15°C.
4. Stop reaction by incubating 15 min at 70°C.
5. Check probe fragment size by agarose gel electrophoresis (appropriate size is 200–500 bp). The nicking reaction may be permanently stopped by adding 3  $\mu\text{L}$  of 0.5 M EDTA (*see Note 5*).
6. Do a test hybridisation on normal lymphocyte metaphase spreads to ensure that the probes hybridise to the correct region in the correct chromosome. Use a centromeric probe for the chromosome in question as reference.
7. Store at –20°C.

*3.1.2. Agarose Gel  
Electrophoresis*

1. Weigh 0.6 g of agarose and dissolve it in 60 mL of 0.5 $\times$  TBE buffer by heating the solution in a microwave oven until it boils. Mix well. Cool the agarose to about 50°C. Add 2  $\mu\text{L}$  ethidium-bromide, mix well and pour the gel into a gel holder. Leave the gel for 30 min in RT (or 10 min in the fridge) (*see Note 6*).
2. Prepare the samples: 4  $\mu\text{L}$  sample, 2  $\mu\text{L}$  loading buffer, 6  $\mu\text{L}$  of 0.5 $\times$  TBE.
3. Pipet 4  $\mu\text{L}$  ready-to-use 100 bp DNA ladder into the first (and last) well of the gel. Pipet the samples into the other wells.
4. Run the gel in 0.5 $\times$  TBE running buffer for 30–50 min at 150 V.
5. Check the DNA fragment length on a UV illuminator. A smear of DNA should be visible. The optimal fragment length for labelled centromere probes is 250–400 bp and 300–600 bp for locus-specific probes (*see Note 5*).

*3.1.3. Hybridisation*Preparation of  
Hybridisation Mixture

1. Pipet into a dark eppendorf tube, on ice: 1  $\mu$ L Cot-1 DNA (125–1,000 ng/ $\mu$ L), 0.5  $\mu$ L labelled centromeric probe, 1.5  $\mu$ L labelled locus-specific probe, and 7  $\mu$ L master mix (MM 1.0) (*see* [Notes 7–9](#)).
2. Mix well and centrifuge briefly in a microcentrifuge.
3. Denature at 75°C (water bath) for 5 min, spin down quickly and place on ice to wait for hybridisation.

Preparation of Samples  
(Metaphase or Interphase  
Nuclei)

All incubations and dehydrations are done in Coplin jars.

1. Warm up the denaturation solution to 72–75°C in a water bath (*see* [Note 10](#)).
2. Mark the area of slide containing the sample with a diamond pen.
3. Denature prewarmed slides in denaturation solution for 2–3 min (*see* [Note 10](#)).
4. Dehydrate in an ethanol series (70, 85, 100%, 2 min each) and air dry.
5. Transfer slides onto a 37°C warming plate.

Preparation of Samples  
(Freshly Frozen Tissue  
Sections)

1. Carnoy fix the tissues: 10 min in 50% Carnoy fixative, 10 min in 75% Carnoy fixative, and 2  $\times$  10 min 100% Carnoy fixative. Air dry.
2. Denature and dehydrate like the cell preparations above.

Preparation of Samples  
(Formalin Fixed, Paraffin-  
Embedded Tissue Samples  
(5–10  $\mu$ M Sections))

All incubations and dehydrations are done in Coplin jars.

1. Removal of paraffin: 2  $\times$  15 min in 100% xylene at room temperature (RT).
2. Removal of xylene: 2  $\times$  5 min in 100% methanol at RT.
3. Pretreatment: 10 min in 1 M NaSCN at 80°C.
4. Removal of NaSCN: 3  $\times$  2 min in ddH<sub>2</sub>O at RT.
5. Digestion of proteins: 5–20 min pepsin (67 mg in 40 mL of 0.9% NaCl, pH 1.5) at 37°C (*see* [Notes 11 and 12](#)).
6. Removal of excess pepsin: dip in ddH<sub>2</sub>O.
7. Washing of pepsin: 2 min 2 $\times$  SSC at RT.
8. Dehydration: 2 min each in 70, 85, and 100% ethanol.
9. Air dry.

## Hybridisation

1. Pipet 10  $\mu$ L of hybridisation mixture on slides.
2. Cover with a cover slip of appropriate size (*see* [Note 8](#)) and seal with rubber cement (Fixogum, Marabu). For FFPE samples: Denature the probes and sample together on the slide at 80°C for 6–10 min. This can be done in a hybridisation oven or on a heat block. It is advisable to apply extra fixogum after denaturation.



- Hybridise in a humid chamber at 37°C for 1–2 nights (*see Note 13*).

### 3.1.4. Hybridisation Washes and Staining for Biotinylated and Digoxi- genin-Labelled Probes

All washes are done in Coplin jars with mild shaking, preblocks and incubations under a 24 mm × 60 mm cover slip. **Protect the slides from light!**

- Remove rubber cement and the cover slip.
- Wash at 45°C for 2 × 5 min in 50% formamide/2× SSC (*see Note 14*).
- Wash at RT for 2 × 5 min in 4× SSC/0.05% Tween.
- Wash at RT in 4× SSC for 5 min (*see Note 15*).
- Preblock: Pipet 100 μL of 4× SSC/1% BSA on the slide, cover with a cover slip and incubate at RT for 5 min.
- Remove the cover slip and excess preblock solution. Pipet 100 μL of 5 μg/mL avidin-FITC (for biotin-labelled probes) and/or 2 μg/mL anti-digoxigenin – rhodamine (for digoxigenin-labelled probes) in 4× SSC/1% BSA. Cover with a cover slip and incubate for 20 min at RT (*see Note 16*).
- If using biotin-labelled probes, continue as follows, otherwise proceed to **step 13**. Wash once in 4× SSC for 10 min, once in 4× SSC/0.1% Triton-X for 10 min, once in 4× SSC for 10 min, and once in PN for 5 min.
- Preblock as in **step 5**.
- Incubate in 100 μL of 5 μg/mL biotinylated anti-avidin in 4× SSC/1% BSA under a cover slip for 20 min (*see Note 16*).
- Wash three times in PN for 10 min each.
- Preblock as in **step 5**.
- Incubate in 100 μL of 5 μg/mL avidin-FITC in 4× SSC/1% BSA under a cover slip for 20 min (*see Note 16*).
- Wash three times in PN for 10 min each.
- Let the slides dry a little but not completely. Counterstain with 0.01–0.001 μM DAPI in Vectashield anti-fade solution (*see Note 17*).

### 3.2. DHPLC (Denaturing High Performance Liquid Chromatography)

#### 3.2.1 PCR

- Design your primers with ex. Primer3-program ([http://frodo.wi.mit.edu/cgi-bin/primer3/primer3\\_www.cgi](http://frodo.wi.mit.edu/cgi-bin/primer3/primer3_www.cgi)) freely available in the internet. Design each amplicon to be approximately 300–600 bp in length, with 20 bp primers and 60°C Primer T<sub>m</sub> as a default primer picking conditions. Make sure that adjacent amplicons overlap each other at least over the primer annealing region (*see Notes 18 and 19*).
- Calculate the needed volume (the amount of samples, positive control, and negative control) and pipette 24 μL of the following MasterMix to each 0.5-mL microcentrifuge tube or each well in 96-well plate:

MasterMix Components: Final concentration Volume:

10× PCR-buffer: 1 × 2.5 μL

10 mM dNTP: 0.2 mM each 0.5 μL

25 mM MgCl<sub>2</sub>: 1.5 mM 1.5 μL

Forward-primer (25 μM): 0.2 μM 0.2 μL

Reverse-primer (25 μM): 0.2 μM 0.2 μL

Platinum® *Taq* DNA polymerase: 0.02 U/μL 0.1 μL

Autoclaved, distilled water: to 24 μL 19.0 μL

3. Add 1.0 μL of template DNAs (50 ng/μL) or autoclaved, distilled water as a negative control to the tubes.
4. Mix the contents of the tubes, cap the tubes carefully and spin briefly.
5. Perform the 25–35 cycles of PCR as follow:
  - Step1: (initial activation): 95°C 1.0 min
  - Step2: (cycle denaturation): 94°C 30 s
  - Step3: (annealing): 57°C 30 s
  - Step4: (extension): 72°C 1.0 min
  - Step5: (cycles): Go to step2 34 times
  - Step6: (end extension) 72°C 5°min
  - Step7: (cooling) 4.0°C for ever
6. Check that size of each sample for each amplicon is correct and specific with 1.5% agarose gel electrophoresis (1.5 mA for 45 min) and detect with UV-detector. Adjust the reaction conditions if necessary by titration of MgCl<sub>2</sub>-concentration and/or annealing temperature (*see* **Notes 20 and 21**).

### 3.2.2. DHPLC

1. Design your DHPLC running conditions for each PCR amplicon (*see* the above **Subheading 3.2.1 PCR**) with DHPLC-melt programme (<http://insertion.stanford.edu/melt.html>) freely available on the internet. Note: Use only detergent free PCR buffers for DHPLC.
2. Mix each sample amplicon (PCR-product) with same reference amplicon (known to have unchanged sequence) in 96-well plate.
3. Denature mixture in PCR-machine at 95°C for 5 min.
4. Renaturate sample-reference mixture with –1°C/min temperature slope from 95 to 65°C in 30 min. Cool samples to +4°C.
5. Run the ready samples like recommended in DHPLC-melt program for each amplicon in different temperatures in recommended Buffer B gradient. Adjust the running conditions if necessary (*see* **Notes 22 and 23**). Read carefully and familiarize yourself intimately with the user guide of the instrument. See **Fig. 2** as an example of a DHPLC electropherogram.

6. Sequence (look under **Subheading 3.3 Sequencing**) the samples that were detected to carry a mismatch.

### 3.3. Sequencing

1. Purify your PCR-products with Qiagen PCR purification kit (or with other suitable PCR-purification kit) and dilute them to 30.0  $\mu\text{L}$  of water prior for sequencing reaction.
2. Calculate the needed volume (the amount of samples) and pipette 9  $\mu\text{L}$  of the following MasterMix to 96-well plate. Make separate reactions for forward and reverse primers.  
MasterMix Components: 1  $\times$  reaction:  
Big Dye Termination ready Reaction Mix: 1.0  $\mu\text{L}$   
5  $\times$  Sequencing Buffer: 1.5  $\mu\text{L}$   
Primer (5.0  $\mu\text{M}$ ): 1.0  $\mu\text{L}$   
Autoclaved, distilled water: 5.5  $\mu\text{L}$
3. Add 1.0  $\mu\text{L}$  of sample (purified PCR-product) to each well.
4. Mix the contents of the tubes, cap the tubes carefully and spin briefly.
5. Perform the 25 cycles of sequencing reaction as follow:  
Step1: 95°C 3.0 min  
Step2: 98°C 45 s  
Step3: 50°C 10 s  
Step4: 60°C 4.0 min  
Step5: 98°C 15 s  
Step6: 50°C 10 s  
Step7: 60°C 4.0 min  
Step8: GO to Step5 24 times  
Step9: 4.0°C for ever
6. Purify the sequencing reaction with normal ethanol-salt purification:
7. Add 2.5 volume of absolute ethanol (25  $\mu\text{L}$ ) and 1/10 volume of 3 M Sodium acetate (1.0  $\mu\text{L}$ ) to each sequencing reaction.
8. Incubate in RT for 15 min.
9. Centrifuge in RT, at 2,000  $\times g$  for 45 min (*see Note 24*).
10. Open the caps, place the plates immediately bottom up in centrifuge on cellophane and spin gently for 1 min at 700  $\times g$ .
11. Pipette 125  $\mu\text{L}$  of 70% ethanol in each well.
12. Centrifuge in RT, at 2,000  $\times g$  for 15 min (*see Note 24*).
13. Open the caps, place the plates immediately bottom up in centrifuge on cellophane and spin gently for 1 min at 700  $\times g$ .

14. Pipette 10  $\mu$ L of HiDi™ (Applied Biosystems) formamide (or other high quality pure formamide) into all wells, close the caps and spin.
15. Denature samples at 95°C for 3.0 min.
16. Run the denatured samples with ABI 3700 sequencer. Read carefully and familiarize yourself intimately with the user guide of the instrument.

---

## 4. Notes

1. The DNA should be of high molecular weight and quality. The concentration of P1, PAC or BAC clones cannot be measured by spectrophotometry (A260), since spectrophotometry may exaggerate the concentration thousands-fold. Thus, fluorometry needs to be used.
2. The label can be either a fluorescent label directly conjugated to the nucleotide or a conjugate that is stained fluorescently after hybridisation (indirectly conjugated). The colour of the directly conjugated label is determined by itself, whereas indirect labels can be stained by a variety of colours, depending on application and the microscope filters at hand. Indirect labelling also allows for amplification of the signal intensity, if more than one layer of staining is used. This is useful when the target region is small or otherwise difficult to see. Directly fluorescent labels are best suited for centromeric and telomeric probes, which cover a longer stretch of the genome than locus (gene) specific probes. Please note that all fluorochromes are light-sensitive and should be stored and used in dark containers or otherwise protected from light.
3. Check activity of enzymes from the tubes, as it varies. Do a test nick translation when using a new batch of enzyme mix. If after nicking the fragments are too short, the enzyme mix can be further diluted 1:2 or 1:3 in the BSA-stock. Test again.
4. All solutions containing formamide should be used under a hood. Only use highest grade formamide. The formamide stock should be kept frozen and the solutions containing formamide should be kept refrigerated and protected from light.
5. Shorter probes (200–300 bp) are better for detection of centromeric and telomeric regions. When using tissue sections as samples, shorter probes may penetrate the matrix of the tissue better than longer probes. If the probes are too long after nicking, the reaction can be restarted unless EDTA has been added. It may be necessary to add 1–2  $\mu$ L enzyme mix. Additional nicking times should not exceed 20 min. Run a new gel after

nicking. Sometimes the probes cannot be seen in the gel. This does not necessarily mean the probe is useless. Test it.

6. You can add ethidiumbromide in the running buffer, if you forget to add it in the gel. Note: Ethidiumbromide is a known mutagen/carcinogen and caution should be taken when handling stock and waste solutions; always wear gloves. Waste solution should be disposed of according to local/national rules.
7. If you wish to use two locus-specific probes, pipet 1.2  $\mu\text{L}$  each in the hybridisation mix and leave the centromeric probe out. If using three locus-specific probes, 1  $\mu\text{L}$  of each can be used.
8. Make sure that different probes in the same hybridisation are labelled with different labels. Biotin-labelled and digoxigenin-labelled probes may be stained with different fluorochromes and used in the same hybridisation.
9. The volume of the hybridisation mix should be adjusted according to the area of the cover slip needed to cover the sample. 10  $\mu\text{L}$  is enough for cover slips up to 22  $\times$  22  $\text{mm}^2$ .
10. The given temperatures should be measured from inside of the Coplin jar. Some cell preparations denature more easily than others. If the nuclei look very fuzzy in the microscope after hybridisation and staining, use a lower denaturation temperature or shorten the denaturation time.
11. Pepsin is inactivated quickly in solution, so it is best to keep appropriate sized lots ready in the freezer and solubilise them in 37°C 0.9% NaCl, pH 1.5 just before use.
12. The success of FISH on FFPE samples is dependent on the way that the tissues are fixed. Longer fixing times or higher concentration of formalin fixes the tissues better, and harder pretreatment may be required. The amount of pepsin may be increased or the incubation time prolonged. Harder fixing also affects the denaturability of the samples, and higher temperatures or longer denaturation times may be necessary for well fixed samples. In contrast, if the morphology of the samples seems to suffer from the advised pretreatments, pepsin treatment, and denaturation may be eased. Sometimes nothing helps. On tissue microarrays, the samples are rarely uniform enough to get all of them successfully hybridised at once. Several hybridisations with adjusted pretreatments may be needed.
13. Longer hybridisation time may be needed for tissue samples compared with cell preparations.
14. To avoid toxic fumes from formamide solutions, alternative washes may be used when using cell line preparations: wash at 72°C in Wash Solution 1 (0.4 $\times$  SSC/0.3% NP-40) for

- 2 min and then wash at RT in Wash Solution 2 (2× SSC/0.1% NP-40) for 5 min. Follow the protocol from **step 3** as stated.
15. When using only directly labelled probes, the staining **steps** from 5 to 13 should be replaced by 5 min in distilled water at RT.
  16. Instead of fluorescently conjugated avidin and anti-avidin, you may use fluorescently conjugated streptavidin and anti-streptavidin.
  17. DAPI fluoresces also at the wavelength used for e.g. Pacific-Blue and can block the signals. Use the more dilute DAPI for applications with blue signals.
  18. The size of each amplicon should be as big as possible, but still detectable. Normally amplicons up to 600 bp are easy to sequence or run in DHPLC.
  19. Same primers can be use for DHPLC and sequencing reactions.
  20. No PCR-product: lower the annealing temperature to 55–60°C and increase MgCl<sub>2</sub>-condition up to 4.5 mM. Add more cycles and more template to PCR-reaction.
  21. PCR-reaction is too unspecific: Perform for each primer pair with titration of the annealing temperature (55–60°C) and MgCl<sub>2</sub>-conditions (0.5–3.0 mM). Check the end product for each amplicon with 1.5% agarose gel electrophoresis.
  22. First test the running conditions recommended in the DHPLC melt programme to obtain the best sensitivity for each amplicon and adjust the running conditions to half denaturing form for the each PCR amplicon. Use known SNPs of the gene (if known) as positive controls.
  23. DHPLC; Normally two degrees lower and one degree higher running conditions compared with DHPLC melt program are needed extra to increase the sensitivity and specificity of DHPLC for unknown mutations.
  24. To prevent pellet detachment, do not leave your samples in the centrifuge.

## References

1. Slamon DJ, Clark GM, Wong SG, Levin WJ, Ullrich A, McGuire WL. (1987) Human breast cancer: correlation of relapse and survival with amplification of the HER-2/neu oncogene. *Science* 235:177–182.
2. Visakorpi T, Hyytinen E, Koivisto P, et al. (1995) In vivo amplification of the androgen receptor gene and progression of human prostate cancer. *Nat Genet* 9:401–406.
3. Tomlins SA, Rhodes DR, Perner S, et al. (2005) Recurrent fusion of TMPRSS2 and ETS transcription factor genes in prostate cancer. *Science* 310:644–648.

4. Hollstein M, Sidransky D, Vogelstein B, Harris CC. (1991) p53 mutations in human cancers. *Science* 253:49–53.
5. Taplin ME, Bubley GJ, Shuster TD, et al. (1995) Mutation of the androgen-receptor gene in metastatic androgen-independent prostate cancer. *N Engl J Med* 332:1393–1398.
6. Hyytinen E, Visakorpi T, Kallioniemi A, Kallioniemi OP, Isola J. (1994) Improved technique for analysis of formalin fixed paraffin embedded tumors by fluorescence in situ hybridization. *Cytometry* 16:93–99.
7. Saramäki O, Willi N, Bratt O, et al. (2001) Amplification of EIF3S3 gene is associated with advanced stage in prostate cancer. *Am J Pathol* 159:2089–2094.
8. Thomas RK, Nickerson E, Simons JF, et al. (2006) Sensitive mutation detection in heterogeneous cancer specimens by massively parallel picoliter reactor sequencing. *Nat Med* 12:852–855.
9. Ainsworth PJ, Rodenhiser DI. (1994) A nonradioactive method for the detection of single-strand conformational polymorphisms (SSCP). *Methods Mol Biol* 31:205–210.
10. Ren J. (2000) High-throughput single-strand conformation polymorphism analysis by capillary electrophoresis. *J Chromatogr B Biomed Sci Appl* 741(2):115–128.
11. Fodde R, Losekoot M. (1994) Mutation detection by denaturing gradient gel electrophoresis (DGGE). *Hum Mutat* 3(2):83–94.
12. Xiao W, Oefner PJ. (2001) Denaturing high-performance liquid chromatography: A review. *Hum Mutat* 17:439–474.
13. Waltering KK, Wallén MJ, Tammela TL, Vessella RL, Visakorpi T. (2006) Mutation screening of the androgen receptor promoter and untranslated regions in prostate cancer. *Prostate* 66(15):1585–1591.



# INDEX

## A

- Acetylation ..... 3, 5, 11, 12, 207
- Activation function 1 (AF1) ..... 5, 9, 10, 171, 172, 179, 181, 182, 206–208, 210, 213
- Activation function 2 (AF2) ..... 8–10, 22, 28, 60, 171, 172
- ACTR ..... 159, 160, 168
- Affinity chromatography
  - glutathione agarose ..... 99, 110, 111, 157–161, 163–166, 183, 215
  - Ni-NTA/ Sepharose ..... 53, 56, 57, 59, 61, 98, 110, 174, 176, 177, 183, 208–211, 215, 216
- Agonist(s) ..... 6, 7, 13, 14, 31, 51, 61, 63, 73–75, 159, 168, 172, 230
- Antagonist(s) ..... 6, 14, 22, 31, 51, 61–63, 74, 75, 172,  $\alpha$ -helix ..... 6–9, 60, 78, 205, 209
- Androgen receptor (AR) ..... 9, 10, 12, 13, 21–23, 25–28, 30, 31, 37, 38, 41, 42, 46, 69–84, 86–90, 97–99, 103, 105–111, 116, 118, 123, 124, 126, 127, 129, 132, 135, 141–147, 149, 151–153, 172, 178, 179, 182, 205, 206, 208, 210, 213, 224, 225, 227–230, 237–239, 241–253, 255, 256, 264, 266
- Androgen response element (ARE) ..... 70, 90, 103, 106–108, 242, 256
- Androgen insensitivity syndrome ..... 23, 28, 242, 255

## B

- Bile acids ..... 3, 4
- Binding kinetics
  - association ..... 176, 181, 182
  - dissociation ..... 21–28, 30, 31, 131, 171, 176, 181, 182
- Bradford assay ..... 61, 179, 209, 211
- Buffers
  - HEPES ..... 98–100, 161, 175, 184, 188, 189, 216
  - Phosphate ..... 24, 37, 64, 98, 99, 110, 126, 210, 268
  - Tris buffered saline (TBS) ..... 24, 26, 28, 159, 161–163, 232, 240, 256
  - Tris-borate-EDTA (TBE) ..... 100, 102, 113, 115, 117, 118, 126, 267–269
  - Tris-HCl ..... 24, 53, 54, 56, 58, 126, 130, 132, 144, 145, 159, 162, 174, 175, 177, 189, 190, 208, 209, 215, 223, 240, 267

## C

- Cancer
  - Breast ..... 191, 193, 264
  - Prostate ..... 12, 23, 30, 70, 98, 109, 127, 264, 266

- CBP (CREB-binding protein) ..... 10, 12, 171
- Charge clamp ..... 6, 8
- Cholesterol ..... 4
- Chromatin ..... 10, 11, 70, 73, 123–125, 127–129, 131, 134, 136, 158, 207
- Chromatin immunoprecipitation (ChIP) ..... 10, 14, 74, 123–136, 222, 224
- Circular dichroism ..... 9, 205, 206
- Coactivator(s) *see also* ACTR, CBP, LxxLL, P/CAF, SRC-1, TIF2 ..... 6, 10–12, 51, 63, 158, 168, 171, 172, 205, 207, 209, 210
- Confocal microscopy ..... 64, 74, 76, 80, 81, 83–87, 90
- Corepressor(s) *see also* SMRT ..... 11, 51, 63, 157, 158, 168, 171
- Cortisol ..... 4
- Cre recombinase ..... 249–256
- Cyan fluorescent protein (CFP) ..... 70, 76–83, 86–92

## D

- DEAE-dextran *see also* transfection ..... 24, 26, 28, 31
- Detergents
  - NP-40 ..... 24, 189, 268, 275, 276
  - SDS ..... 24, 25, 27, 30, 54, 56–58, 60, 61, 99–101, 109–111, 126, 145, 151, 159–163, 165–169, 175, 177–179, 183, 184, 189, 190, 193, 194, 211, 215, 221, 230, 232
  - Triton X-100 ..... 99, 111, 126, 159, 161, 162, 223, 268, 271
  - Tween 20 ..... 99, 111, 190, 268, 271
- Dihydrotestosterone (DHT) ..... 21, 22, 24–26, 31, 135, 144, 147, 152
- Dimerization ..... 5, 7, 9, 69, 79
- DHPLC (Denaturing high performance liquid chromatography) ..... 263, 265, 266, 268, 271, 272, 276
- DNA
  - binding domain (DBD) ..... 5–9, 14, 70, 73, 75, 98, 99, 103, 106–110, 116, 118, 205–208, 242
  - binding kinetics ..... 69
  - half sites ..... 7–9, 107
  - heteroduplexes ..... 265, 266
  - major groove ..... 8, 9, 103
  - minor groove ..... 9, 103
- Dounce homogenizer ..... 99, 112, 257

**E**

- Embryonic stem cells (ES) .....237, 240,  
242, 244–247, 251–253  
17 $\beta$ -estradiol (E2) .....53, 54, 56–58,  
172, 191, 196, 255  
Electrophoretic mobility shift assay (EMSA)..... 97–105,  
109, 112, 115, 117, 118, 120, 121  
Estrogen receptor (ER) .....7–12, 31, 52–62, 64, 69, 75,  
76, 79, 123, 124, 132, 134, 135, 172, 191, 196–199,  
206, 237, 252, 255  
Estrogen response element (ERE) ..... 7

**F**

- Farnesyl X receptor (FXR) ..... 4, 8  
Fluorescein isothiocyanate (FITC) .....38, 40–43,  
46, 215, 267, 268, 271  
Fluorescence  
in situ hybridization (FISH).....263–266, 275  
loss in photobleaching (FLIP)..... 14, 69,  
71, 73, 74, 82, 85, 86  
recovery after photobleaching (FRAP).....14, 69–76,  
79–92  
resonance transfer (FRET).....69–71, 75–83, 86–92  
steady state emission *see tryptophan*  
Flow cytometry.....35, 36, 38, 40,  
41, 45, 47–49  
FKBP51 ..... 142–144, 146, 147, 149  
FKBP52 ..... 150, 152  
Footprinting  
DNase I ..... 97–99, 101, 103–106, 113,  
115, 116, 120  
methylation interference..... 97–99, 102–105, 107, 113,  
116, 117, 119  
methylation protection .97, 99, 102–105, 108, 113, 116,  
118, 121  
FxxLF..... 22, 26, 78, 79

**G**

- Gene Expression..... 8, 11, 14, 98, 134,  
145, 146, 149, 187, 188, 191, 200, 202, 207, 258  
Glucocorticoid receptor (GR) ..... 3, 4, 9–11, 37, 38,  
41, 42, 45–47, 69, 75, 124, 151, 206, 224, 225, 237,  
238, 249, 252, 254, 256  
Glucocorticoid response element (GRE) ..... 10  
Glutathione S-transferase (GST).....99, 106,  
107, 109, 110, 111, 157–166, 168, 169, 172, 184  
Green fluorescent protein (GFP) ..... 36, 71,  
72, 74, 76, 79, 81–86, 90, 254

**H**

- Histone acetyl transferase (HAT)..... 10, 12  
Hinge (domain)..... 5, 12

- Hormone response element (HRE) *see also ARE, ERE,*  
*GRE and Half sites* .....10, 21, 144  
Hsp90 73, 141, 142

**K**

- Kinase  
Cdk7 *see also TFIIH*..... 11  
MAP ..... 11  
PKA..... 227  
PKC..... 227  
T4 polynucleotide.....100, 112, 113  
thymidine ..... 243

**L**

- Labelling  
antibodies ..... 40–42  
DNA..... 100, 112, 113, 119, 127,  
131, 133, 136, 238, 245, 267, 269, 274  
protein ..... 24, 27, 32, 221, 222  
Ligand  
binding domain (LBD) ..5–9, 13, 14, 51–65, 70, 73, 75,  
78, 79, 99, 205, 207, 208, 255  
binding pocket..... 6, 8  
dissociation.....21–28, 30, 31  
Liver receptor homologue (LRH-1)..... 6, 7, 9  
Liver X receptor (LXR)..... 4, 8, 224, 225, 228–231  
LoxP..... 237–239, 241–244, 246,  
248, 250–253, 256  
LxxLL..... 6, 7, 63, 78, 209

**M**

- Mammalian Cell lines  
COS ..... 22, 23, 25, 26, 28, 30–32  
CV-1..... 30  
HEK 293T ..... 30, 31, 222, 227–229  
HeLa ..... 105, 111  
Hep3B ..... 74, 78, 80, 83, 84, 86, 87, 90  
LAPC4..... 266  
LNCaP..... 30, 99, 109, 111,  
127, 128, 222, 227  
MCF-7..... 191, 193, 196, 199  
RAW 264.7 ..... 222, 229, 231  
Methyltrienolone.....24, 80, 223  
Mouse Mammary Tumour Virus (MMTV) ..... 75

**N**

- N-terminal domain (NTD).....5, 9–12, 14,  
70, 75, 78, 172, 205–210  
Nuclear magnetic resonance (NMR).....8, 9, 205, 206  
Nur-related protein 1 (Nurr1) ..... 7, 13  
Nuclear Extract  
preparation.....97, 99, 105, 109, 111, 115, 120

**O**

O-GlcNAc ..... 11, 12  
Osmolyte *see* TMAO

**P**

P/CAF ..... 10, 12  
Polymerase chain reaction

PCR ..... 58, 81, 83, 100, 113,  
123, 129, 130–134, 136, 239, 242–246, 249, 250,  
253, 265, 268, 269, 271–273, 276

real time ..... 15, 127, 129–132, 187,  
190, 191, 198–201, 203, 239, 241, 257, 258

Peroxisome proliferator activated receptor  
(PPAR) ..... 4, 9, 13, 206

Phosphatase

alkaline ..... 254  
inhibitors ..... 232, 233  
lamda ..... 223, 224, 228–231  
PP1/2 ..... 233  
tyrosine ..... 233

Phosphorylation ..... 3, 5, 11, 12, 15, 221–231, 233, 234

Pregnane X receptor (PXR) ..... 6

Progesterone receptor (PR) ..... 7, 9, 37, 38, 41,  
42, 46, 47, 69, 75, 151, 196–198, 206

Protein concentration *see* Bradford

Protein expression

bacterial cells ..... 10, 109, 110, 158,  
161, 163, 168, 176, 178, 184, 207  
mammalian cells ..... 26, 28, 35, 36, 38,  
40, 161, 163, 187, 201

Protein-protein interactions ..... 8–11, 75, 76, 157, 158,  
171–173, 176, 180

Protease inhibitors

cocktail ..... 24, 53, 99, 126, 128, 145, 150,  
154, 161, 174, 176, 183, 211  
PMSF ..... 99, 174, 176, 183, 207, 208

**R**

Recognition helix *see also* DNA-binding domain ..... 8

Reporter genes

$\beta$ -galactosidase ..... 141, 142, 144–146, 149, 254  
luciferase ..... 30, 90, 193, 200, 241, 257, 258

Retinoic acid ..... 4, 8, 159

Retinoic acid receptor (RAR) ..... 3, 4, 8, 159–161

Retinoid X receptor (RXR) ..... 7–9

RNA interference (RNAi) *see* siRNA

**S**

Small interfering RNA (siRNA) ..... 15, 135,  
172, 187–189, 191–193, 196–203

SMRT ..... 159, 168, 171

Stern-Volmer constant ..... 209, 216

Steroid

factor 1 (SF1) ..... 7

hormone *see also* cortisol, estradiol, testosterone,  
vitamin D<sub>3</sub> ..... 3, 4, 21, 35, 36, 41, 42, 46,  
47, 97, 141, 151, 152, 188, 205, 237, 238, 255

receptor ..... 3, 5, 7–9,  
11, 12, 14, 15, 21, 23, 46, 69, 70, 73, 78, 97, 98, 205,  
207, 225, 237, 238, 241, 242, 249, 251, 252, 256

Sumoylation ..... 3, 5, 11, 12

Surface plasmon resonance (SPR) ..... 172, 175, 179, 184

**T**

TATA-binding protein (TBP) ..... 11, 172

Testosterone ..... 21, 22, 30, 73, 86, 152

TFIIB ..... 11

TFIIF ..... 11, 171, 172

TFIIH ..... 11, 171

Thyroid hormone receptor (TR) ..... 8, 13, 159, 172

TIF2 ..... 78, 172

Tip60 ..... 10, 12

TMPRSS2 gene ..... 264

Transfection

transient ..... 22, 23, 26, 31, 32,  
80, 81, 83, 84, 188, 189, 191, 192, 200, 223,  
227–230, 247, 252

Transgenic ..... 12, 244, 247, 248, 258

Trimethylamine N-oxide (TMAO) ..... 9, 208, 210,  
212–216

Tryptophan (emission spectrum) ..... 15, 205,  
208–212, 214–216

**V**

Vitamin D<sub>3</sub> ..... 4, 13, 256

Vitamin D receptor (VDR) ..... 4, 237, 252, 255, 256

**W**

Western blotting ..... 145, 149–152, 154, 187, 190, 191, 193,  
194, 196, 198

**X**

X-ray crystallography ..... 6, 8, 14, 51, 64, 205

**Y**

Yeast

DNA transformation ..... 144, 146, 147, 153

Yellow fluorescent protein (YFP) ..... 70, 76–83, 86–92

**Z**

Zinc

finger (module) ..... 8, 73, 242, 251,  
252, 256

ion ..... 8, 64